BERGISCHE
UNIVERSITÄT
WUPPERTAL

Effect of concrete technological aspects on hot- and residual-strength of concrete subjected to cyclic high temperatures

Dissertation

zur Erlangung des Grades eines
Doktor-Ingenieurs (Dr.-Ing.)

in der
Fakultät für Architektur und Bauingenieurwesen
der
Bergischen Universität Wuppertal

vorgelegt von

Ahmad Iravani Mohammadabadi

aus Esfahan, Iran

Wuppertal, April 2025

Gutachter: Univ.-Prof. Dr.-Ing. Steffen Anders
Zweitgutachter: Univ.-Prof. Dr.-Ing. Wolfram Klingsch

Veröffentlicht als Heft 34 in der Schriftenreihe des
Instituts für Konstruktiven Ingenieurbau
Fakultät für Architektur und Bauingenieurwesen
Bergische Universität Wuppertal

Herausgeber

Der Geschäftsführende Direktor
Institut für Konstruktiven Ingenieurbau
Bergische Universität Wuppertal

Fachgebiet

Werkstoffe im Bauwesen
Univ.-Prof. Dr.-Ing. Steffen Anders
Univ.-Prof. em. Dr.-Ing. Wolfram Klingsch
Fakultät für Architektur und Bauingenieurwesen
Bergische Universität Wuppertal

Organisation und Verwaltung

Institut für Konstruktiven Ingenieurbau
Bergische Universität Wuppertal
Pauluskirchstraße 11
42285 Wuppertal
Telefon: (0202) 439-4039

ISBN 978-3-940795-33-5

Abstract

The construction industry is a major contributor to global CO_2 emissions. To support the EU's climate goals, developing sustainable concrete with enhanced durability and a reduced carbon footprint is essential. This dissertation investigates the use of byproducts from high-temperature industrial processes, primarily blast furnace slag (BFS) and slag sand, to create stable, thermally resistant, and sustainable concrete alternatives. The study focused on improving concrete durability during and after one-time or repeated thermal exposures.

The influence of slag sand as a supplementary cementitious material was assessed by comparing hot and residual compressive strength of concretes made with CEM III/A, CEM III/B, and ordinary Portland cement (CEM I) upon or following exposure to various thermal loads (different number of cycles with various maximum temperatures). These were also compared to limestone-based CEM II/A-LL. Additionally, the performance of BFS, slag sand, and other non-standard metallurgical slags as aggregates was evaluated against conventional aggregates like quartzite, basalt, and limestone.

Based on over 1800 experimental data points, obtained in a collaborative project between the University of Wuppertal and "Institut für Baustoff-Forschung e.V." (FEhS), BFS and slag sand significantly improved residual compressive strength. While slag sand slightly reduced hot compressive strength, it markedly enhanced residual compressive strength, especially after cooling and following humid storage. Higher slag content in cement correlated with improved post-exposure mechanical properties. Temperature profile modeling of a 30 cm-thick wall revealed that slag and basalt aggregates lowered internal temperatures more effectively than quartzite during heating and cooling. Reduced thermal conductivity and internal stress translated into higher estimated residual load-bearing capacity, slightly better with slag than basalt aggregates during cooling.

Concrete made of slag-rich cements (CEM III/A) with BFS aggregates showed the best residual strength, highlighting the importance of cement-aggregate interaction. Preliminary tests with other industrial slags also showed promise, suggesting further research potential. This work provides a robust framework and practical guidance for designing durable, thermally stable, and environmentally sustainable concrete.

Table of content

List of Figures

List of Tables

List of Abbreviations, Symbols

ASCE = American Society of Civil Engineering

BFS = Blast furnace slag

ca. = circa

Cu-slag = copper slag

EAF = Electric arc furnace

EC2 = EN 1992-1-2

EC4 = EN 1994-1-2

Ef-slag = electric arc furnace slag

e.g. = for example

et al. = et alii

ETK = standard temperature-time curve

HPC = high performance concrete

LD = Linz-Donawitz

LD-slag = Linz-Donawitz process slag

max. = maximum

min. = minimum

NPC = normal strength concrete

no. = number

OPC = ordinary Portland cement, CEM I

RABT-ZTV = Richtlinien für die Ausstattung und den Betrieb von Straßentunneln

RILEM = the International Union of Testing and Research Laboratories for Materials and Structures

SCM = supplementary cementitious materials

Slag sand = ground granulated blast furnace slag

UHPC = ultra-high performance concrete

vs. = versus

Acknowledgements

This dissertation has been compiled at the Department of Construction Materials, Faculty of Architect and Civil Engineering at Bergische University of Wuppertal under the supervision of Univ.-Prof. Dr.-Ing. Steffen Anders. The experimental part of this work was carried out using the facilities available at the "Institute Konstruktiver Ingenieurbau" (IKIB) at the University Wuppertal. Being carried out in the context of research and academic work, it has been submitted to obtain the Dr.-Ing degree in Civil Engineering. Though the cover only holds my name, there are many people who directly or indirectly contributed to the completion of the submitted dissertation. I would like to seize this opportunity to express my deepest thanks to all who played a role, major or minor, to the completion of this work.

First, I would like to thank Univ.-Prof. Dr.-Ing. Steffen Anders for the supervision of this dissertation, for his constant guidance, encouragement and support, and for the facilities provided to complete the practical part of this research. I would also like to thank all my collogues at IKIB at the University Wuppertal, since without their help, the conduction of this study could not be possible. My special thanks goes to Dr.-Ing Volkert Feldrappe from "Institut für Baustoff-Forschung e.V." (FEhS) for the technical discussions during the assessment the results. I also would like to warmly thank Dr.-Ing. Stefan Zwolinski from "Güteschutz Beton Nordrhein-Westfalen Beton- und Fertigteilwerke e. V." for his encouragement and technical advice, and Dieter Heller, for his support during my work at "Bundesverband Leichtbeton e.V.".

Furthermore, I would like to thank my best friend, my tireless companion, my faithful love and my dear wife, Dr. Pharm D. Maryam Shetab Boushehri, who provided the best support to this job and much more to my life. I am also indebted to my dear family, my father, mother, brother (Hamed Iravani), and sister (Mina Iravani), who have not stopped supporting and encouraging me for a single moment. I would also wish to express my gratitude to my colleagues, my friends who have contributed to the completion of this dissertation with their constant support.

I also wish to seize this opportunity to acknowledge the association of "Arbeitsgemeinschaft industrieller Forschungsvereinigungen e.V. (AiF)" and the organisation of "Industrielle Gemeinschaftsforschung (IGF)" of "Bundesministerium für Wirtschaft und Klimaschutz (BMWK)" in Germany for supporting the collaborative project carried out by the University of Wuppertal and "Institut für Baustoff-Forschung e.V." (FEhS) (Verwendung von Eisenhüttenschlacken zur Steigerung des Hochtemperaturwiderstands ze-mentgebundener Bauprodukte; project No. 20318N), part of which has been presented within the context of the present dissertation.

Wuppertal, October 2025

نیست بر لوح دلم جز الف قامت دوست

چه کنم، حرف دگر یاد نداد استادم (پدرم)

حافظ

1 Introduction and objectives

1.1 Background and Motivation

Enhancing the sustainability of concrete is of paramount importance, particularly since construction and building industry is one of the largest contributors to global carbon dioxide (CO_2) burden. Globally, the industry is responsible for about 37 % of total carbon emissions, with cement production alone responsible for approximately 8 % of CO_2 emissions [1]. To achieve the European Union's target of 55 % reduction in greenhouse gas emissions by 2030, new constructions need to be associated with lower carbon footprint and, more importantly, the concrete industry needs to be more sustainable. To mitigate this impact, recent decades have witnessed a significant increase in efforts in terms of improving concrete sustainability and reducing the associated carbon footprint. Since a major part of CO_2 emission in concrete production originates from cement manufacturing, modifying concrete's composition to maintain or improve concrete properties while reducing the amount of required cement has been an important approach to improve its environmental friendliness. Key strategies within this context involve the substitution of ordinary Portland cement (OPC; CEM I) with supplementary cementitious materials (SCMs) with pozzolanic effect, such as natural pozzolans (trass) or industrial pozzolans (fly ash and slag), which not only reduce the amount of required clinker, but also improve certain durability aspects of the concrete. The use of recycled aggregates, innovative low carbon cements, and optimization of the concrete mix design are amongst other approaches used to enhance sustainability. In addition to lowering the clinker consumption, sustainability can be also sought after by increasing the service life of the concrete, particularly upon exposure to different stress conditions. Increasing the service life of concrete will reduce the need for renewing concrete constructions, thus lowering the demand for raw materials, minimizing energy consumption, and reducing construction waste. This contributes to decreased CO_2 emissions associated with cement production and transportation while also conserving natural resources. Additionally, extended service life enhances structural reliability, reduces maintenance costs, and supports more sustainable urban development by decreasing the environmental footprint of infrastructure projects. Of course, this requires the design of concrete formulations with higher durability and better stability under normal and stress conditions.

Modification of concrete composition, e.g. through partial replacement of the conventional cement or incorporation of more sustainable aggregates might have significant unprecedented impact upon its properties such as strength, durability, and long-term stability, particularly when exposed to extreme conditions such as elevated temperatures, e.g. in case of fires or in high-heat industrial settings. In general, sustainability approaches often involve introducing new materials into the concrete mix, either in the cement or as aggregates. It is now well established that exposure of concrete, even when composed of conventional, well-established

components, to high temperatures can negatively influence, if not completely degrade its mechanical properties. Considering the different thermal conductivity of these new materials compared to those used in conventional concrete, the thermal conductivity of the more sustainable concretes might be affected, influencing thereby the temperature-induced thermal gradients and internal stresses, and hence the rate of microcrack formation and the concrete's ability to maintain structural integrity during exposure to thermal loads. On the other hand, some more sustainable components are byproducts of high temperature industrial processes and might improve the behavior of the concrete under such conditions. Accordingly, it is essential to thoroughly investigate and understand how sustainability-driven modifications to concrete affect its performance under high-temperature conditions. On the other hand, it is highly beneficial to develop stable concrete alternatives using sustainable materials that can also improve its thermal performance. In any case, the change in the physical and mechanical properties of the more sustainable concretes post exposure to thermal loads is yet to be established. This is particularly essential should these concretes be used in structures that are repeatedly exposed to heating and cooling cycles, which is common in many industrial settings. In such cases, the residual physical and mechanical properties of the concretes immediately, and long after cooling might have changed. Depending on the properties of the materials used, this change can be for the better or for the worse. In case of certain materials, the mechanical properties after cooling might further deteriorate as a result of ongoing physico-chemical processes. Other materials, particularly those used in the cement, might enable partial strength regain. Hence, investigation of the impact of such cement components upon the thermal behavior of concrete is essential to ensure that the thermal resistance of critical structural elements, in normal concrete structures or those designed to withstand extreme conditions, is not compromised, but maintained or even ameliorated. Additionally, the development of concretes with higher thermal resistance can contribute to sustainability by increasing the durability and longevity of concrete constructions, particularly those regularly exposed to thermal loads in their service life.

Blast furnace slag (BFS), a byproduct of iron and steel industry, is widely used as an alternative material for natural aggregates in road and concrete construction industries. Depending on the cooling process, BFS can be available in two different forms; the rapidly cooled granulated BFS with amorphous structure (> 90 %) and a glassy granular appearance, which is then dried and ground to form the ground granulated BFS, which is henceforth referred to as slag sand, and the slowly cooled BFS with more crystalline, rock-like structure, creating air-cooled BFS, which from hereon in, will be referred to as BFS. Hence, in this work, BFS is either used as an abbreviation for the umbrella term "blast furnace slag" or to refer to "air-cooled blast furnace slag", while the ground granulated blast furnace slag is specifically referred to as "slag sand". In general, when used as aggregates, BFS is characterized by a long service life, high load-bearing capacity, frost and heat resistance and very good adhesion. Additionally, due to pozzolanic and latent hydraulic properties, the ground granulated form of BFS (slag sand) can

be also used in concrete as a supplementary cementitious material (SCM), improving the mechanical properties of the concrete while reducing the required amount of CEM I in concrete. In this case, factors such as particle size, reactivity, CEM I substitution ratio, and curing conditions can impact the mechanical properties of the developed concrete, under normal conditions and particularly during and after exposure to high thermal loads. In this work, we sought to develop more stable and thus sustainable concrete alternatives with improved thermal resistance, both during and after a one time and repetitive exposure to high temperatures, using sustainable components derived from high temperature industrial processes. To this end, on one hand, the effect of partial substitution of the CEM I with different amounts of slag sand upon the thermal and mechanical properties of the concrete during and after exposure to thermal loads with different maximum temperatures has been investigated. On the other hand, the influence of BFS and other industrial slags as aggregates has been examined. Resistance to extreme temperatures is a crucial property for structural safety, particularly in public buildings and industrial infrastructures, and improving the high temperature performance of concrete helps prevent many catastrophic scenarios. As the industry continues to develop more and more innovative approaches towards sustainable concrete mixes, a rigorous assessment of their behavior at elevated temperatures is critical to ensure that the benefits of these materials do not come at the expense of reduced safety and structural integrity but even improve the mechanical properties of constructions both during and after single or multiple high temperature exposure. This necessitates not only laboratory testing, but also the development of predictive models that can accurately capture the long-term behavior of modified concretes in extreme environments.

All construction standards prescribe investigating concrete mechanical properties upon exposure to high temperatures based on the available national and international regulations, such as ISO 834, ASTM E119, BS 8110, etc. In Europe, EN 1992-1-2 (EC2) for fire design of (reinforced) concrete structures and EN 1994-1-2 (EC4) for fire design of composite steel and concrete structures prescribe the use of standard temperature-time profile to ensure the integrity, stability and insulation of structural elements during exposure to elevated temperatures, with fire being only one scenario of attention. However, these standards, (except for a small part in the Appendix B of EC4) do not set any requirements for the structural design once the fire is extinguished. Accordingly, the mechanical properties of the concrete at longer time-points after cooling is not included. EC2 and EC4 also give limited attention to cases in which structural elements are exposed to repetitive cycles of heating and cooling. Under such circumstances, not only the effect of repeated heating on concrete's mechanical properties under hot conditions, but also the residual properties after each cycle should be fully investigated. Hence, a further goal of this work is to formulate a general approach to investigate the performance of concrete during, immediately after, and at different time points following exposure to repetitive cycles of heating and cooling, and thus to fill in the existing gap in the standard in this regard.

1.2 Identified research gaps in need of investigation

A comprehensive review of existing literature (presented in Chapter 2) reveals several key gaps in the understanding of concrete behavior under high-temperature exposure, particularly regarding the use of alternative and sustainable materials. While various studies have investigated the thermal and mechanical properties of conventional concrete, there remains a lack of systematic evaluation in critical areas. These gaps include:

- **The effect of industrial by-product as SCMs or aggregates on thermal stability:** While the effect of slag sand and BFS on the thermal stability of concrete has been investigated, the results are highly controversial. In case slag sand is used to partially substitute CEM I, the reported optimum substitution ratio to obtain optimal thermal performance has been very different. There is a need for a more systematic investigation of the effect of slag sand and its content (using standard cements) upon the thermal stability of concrete. The effect of slag sand or BFS as aggregates has been much less investigated, while the impact of alternative industrial aggregates such as steelworks slags from Linz-Donawitz (LD) and electric furnace processes, as well as copper slag, remains even more underexplored. Literature also lacks a systematic comparison of these materials against conventional aggregates such as quartzite and basalt. Investigating the interaction between cement and aggregates is crucial for determining the thermal resistance of concrete, as their combined behavior influences key properties such as thermal expansion, strength retention, and microstructural stability under high temperatures. Differences in thermal expansion between cement paste and aggregates can lead to internal stresses and microcracking, affecting durability. Additionally, chemical reactions between cementitious phases and aggregate components at elevated temperatures may alter the overall stability of the concrete matrix, further impacting its thermal resistance.
- **Simultaneous evaluation of hot and residual compressive strength:** Studies often focus either on the immediate mechanical behavior of concrete at elevated temperatures or on its residual properties after cooling. In many cases, only residual properties have been investigated. However, a combined assessment of hot and residual compressive strength on the same material is still missing.
- **The influence of slag sand content on post-thermal strength recovery:** While slag sand is well recognized as an SCM, its role in aiding strength recovery after thermal stress has not been comprehensively investigated. Moreover, a systematic investigation of the effect of slag sand content of the cement (using standard industrially available cements) upon the strength recovery post-thermal exposure is missing.
- **Systematic investigation of thermal cycling stability:** The long-term stability of concrete (with or without slag sand as SCM and slag sand and/or BFS as aggregates) subjected to repeated heating and cooling cycles remains an area requiring further study.

Existing research often examines single exposure events rather than assessing the impact of multiple cycles on both strength retention and microstructural integrity.

- **The combined effect of BFS aggregates and natural aggregates:** While slag sand/ BFS aggregates are known to improve certain mechanical and durability properties, their effectiveness in combination with conventional aggregates such as quartz and basalt in improving the thermal resistance of concrete requires further systematic study.
- **The role of limestone in high-temperature performance:** Both as a component in cement and as an aggregate, limestone has a significant impact on thermal behavior, yet studies systematically comparing its performance against slag sand/ BFS remain limited.

Addressing these gaps is crucial for developing more durable and sustainable high-temperature-resistant concrete solutions.

1.3 Research objectives

In line with the previously mentioned research gaps, the overall aim of the current work is triple:

1- To formulate a general approach to investigate the performance of concrete during, immediately after, and at different time points following exposure to repetitive cycles of heating and cooling, and to fill in the existing gap in the standard in this regard.
2- To investigate the thermal and mechanical stability of concretes made of more sustainable cements and aggregates during, immediately after and long after exposure to one or repeated cycles of heating and cooling.
3- To use the obtained data for the development of a more stable concrete alternative with improved thermal resistance and durability, both during and after one time and repetitive exposure to high temperatures, using sustainable components derived from high temperature industrial processes.

To fulfill the abovementioned goals, the present dissertation sets up ground practice to compose temperature concrete and seeks to investigate the effect of the following parameters:

1) Factors related to the compositions (Table 3.4):

- Systematic investigation of the effect of slag sand content upon the improvement of the thermal stability of the concrete in terms of hot and residual compressive strength as well as the recovery of the thermally induced loss of concrete strength immediately or within the course of days following exposure to thermal stress,
- Systematic investigation of the effect of slag sand and BFS aggregates the improvement of the thermal stability of the concrete in terms of hot and residual compressive strength as well as the thermal conductivity of the specimens when compared to quartzite and basalt aggregates,

- Investigation of the effect of slag sand source upon the improvement of the thermal stability of the concrete considering their different reactivity,
- Investigation of the effect of different non-standard industrial aggregates (a treated steelwork slag from a Linz-Donawitz processes, two steelwork slags from the electric furnace process and a copper slag) upon the improvement of the thermal stability of the concrete in terms of hot and residual compressive strength as well as the thermal conductivity of the specimens when compared to natural aggregates such as quartz and basalt,
- Investigation of the effect of BFS aggregates when used in mixture with quartz or basalt aggregates upon the improvement of the thermal stability of the concrete in terms of hot and residual compressive strength compared to the use of each aggregate alone,
- Investigation of the effect of limestone as a part of the cement and as added aggregates upon the thermal stability of the concrete in terms of hot and residual compressive strength when compared to slag sand

2) Effect of factors related to the thermal load and the recovery time:

- Systematic investigation of the effect of peak temperature upon the thermal stability of the concrete specimens in terms of hot and residual compressive strength prepared without or with different contents of slag sand, and with BFS, quartz and basalt aggregates,
- Systematic investigation of the effect of number of heating cycles upon the thermal stability (in terms of hot and residual compressive strength) of the concrete specimens prepared without or with different contents of slag sand, along with BFS, quartz and basalt aggregates,
- Systematic investigation of the post-thermal load storage duration and conditions upon the strength recovery of the concrete specimens prepared without or with different contents of slag sand, along with BFS, quartz and basalt aggregates,

3) Factors related to the mechanical properties of the specimens:

- Investigation of the impact of cold compressive strength upon the thermal stability (in terms of hot and residual compressive strength) of different concrete specimens,

To achieve the aforementioned research goals, a comprehensive study design was developed, leveraging prior preliminary work, existing literature reports, and two fundamental hypotheses: *i)* addition of slag sand as an SCM can improve the mechanical strength of the concrete upon and after exposure to thermal loads, *ii)* Industrial aggregates obtained during processes involving high temperatures, including but not limited to BFS aggregates, can improve concrete stability upon and after exposure to thermal loads. This work program was structured around

the significance of key variables, allowing for the identification of generalizable results. Furthermore, it facilitated a systematic expansion of the range of raw materials used to enhance the thermal resistance of concrete. This study not only sought to validate the proposed hypotheses, but also to establish a robust framework for improving concrete performance under thermal stress.

1.4 Structure of the dissertation

Adjunct to the introduction, the dissertation consists of 7 further chapters: literature review and state of the art, material and methods, results and discussion, from laboratory to large scale, technological design guidelines, summary and conclusions and finally, outlook and perspectives.

Chapter 2 seeks to provide a thorough review of the state of the art and the result of the studies that bear to the topic of this dissertation. In chapter 3, an overview of the used materials and their properties, along with the experimental design, the rationale behind it and the experimental methodologies will be explained. Chapter 4 has been dedicated to the description and report of the fundamental results of the experiments introduced in Chapter 3. Within this chapter, these results and their implications will be further discussed and compared with the reports available in the literature. In Chapter 5 a model development will be introduced, which enables the transfer of the findings from the material level to the structural element level. Based on the results of the study, Chapter 6 proposes technological design guidelines towards more sustainable and more heat-resistant concretes. Finally, Chapter 7 will bring the findings of the thesis to a conclusion, providing a summary of the main findings of the research work, which Chapter 8 provides a brief outlook to the future of this topic.

2 State of the art and literature review

2.1 Concrete and high temperature exposure

Concrete structures frequently encounter high temperatures in diverse scenarios, each presenting unique challenges to the structures' integrity and performance. These scenarios predominantly include exposure to fires and/or repetitive cycles of heating and cooling, the latter of which is commonly observed in both industrial and environmental contexts. Understanding the impact of these thermal exposures is critical for ensuring safety, durability, and integrity of concrete structures.

2.1.1 Exposure to fire

In urban settings, concrete buildings, bridges, and tunnels are often exposed to fire incidents. These incidents arise from different factors such as electrical faults, human error, natural disasters, or industrial accidents. The prevalence of such incidents is considerable. In the United States, the National Fire Protection Association (NFPA) reported approximately 1.4 million fires in 2020 alone, many of which affected concrete structures [2]. According to the European Fire Safety Alliance (EFSA), around 5000 lives are lost annually due to fire incidents [3]. It is worth noting that a significant number of fire-related deaths are due to asphyxiation or smoke inhalation [3]. Globally, financial damages arising from fires are estimated to be around billions of dollars each year [2]. This includes the extensive repair costs for damaged concrete elements and highlights the need for continued development of fire-resistant materials and construction techniques for such structures.

While the rate of the temperature rise during fire varies depending on the source and the properties of the construction, often three distinct phases can be identified in the process:

i. The initial stage, which involves the slow growth of the fire, with temperatures rising gradually from ambient levels to around 300 °C [4].
ii. The growth phase, where the fire spreads rapidly, with temperatures typically reaching 800 °C to 1200 °C within minutes. Temperatures over 1000 °C are particularly reached in confined spaces such as tunnels, where the heat buildup and lack of ventilation exacerbates the situation [4].
iii. The decay phase occurs as the fire burns out. This phase is associated with a gradual decrease of the temperature, though it can remain above 600 °C for an extended period of time depending on the fire load and ventilation [5].

While concrete is generally more resistant to fire when compared to other construction materials such as steel or wood, it can still get damaged upon exposure to such high temperatures [6]. The mechanisms underlying this damage depends on a variety of factors such as the temperature to which the concrete is exposed, the composition of the concrete and the type of additives (e.g.

aggregates) used in the concrete mix. The damage to concrete structure can lead to loss of strength, and in extreme cases spalling. The latter refers to the breaking off or flaking of concrete surfaces when subjected to high temperatures. It can be explosive, where pieces are violently ejected, or more gradual, where the surface layers peel away [7]. The most paramount examples within this frame are the fire incidents in the Mont Blanc Tunnel in 1999, and the more recent fire incident in Grenfell Tower in 2017, both of which led to significant damages to concrete elements or layers, necessitating significant repair costs [8],[9],[10].

2.1.2 Exposure to cyclic thermal loads

Another important case of concrete exposure to high thermal loads is the issue of constructions exposed to repetitive cycles of heating and cooling. This can happen naturally, where concrete infrastructures are exposed to climates with high temperature fluctuations, but even more so in case of industrial sites such as power plants, steel mills, cement plants, refineries and chemical processing units, furnaces in glass manufacturing plants, incineration plants, foundries and oil and gas facilities. A good example of concrete exposure to natural temperature fluctuation are structures such as concrete pavements and bridges, which are subjected to diurnal and seasonal temperature variations, with cycles ranging from -20 °C to 40 °C. In case of the industrial sites, concrete constructions can get exposed to very high temperatures, depending on the industrial process, and then cooled down, with the cycle of heating and cooling repeating over and over again. For instance, concrete structures near furnaces, kilns, or reactors, or those used in of solar thermal power plants experience daily thermal cycles with temperatures fluctuating from ambient conditions to as high as 300 °C to 600 °C [11],[12]. These repetitive thermal cycles can damage the mesoscale concrete structure through repetitive calcic dehydration and rehydration as well as the repetitive differential thermal expansion and contraction of the cement paste and aggregates, leading to microcracking, decrease in concrete strength, structural fatigue, decrease in the module of elasticity, and even in cases of high temperature levels, chemical reactions in the concrete structure and even surface spalling [13]. This can of course negatively impact, or even fully deteriorate the performance of the concrete in construction level. Of course, within this context, not only the exposed temperature but also the number of the heating and cooling cycles plays a critical role.

A good example of real-life failure of a reinforced concrete construction exposed to repetitive cycles of heating and cooling is an industrial reinforced concrete quenching tower in a Fujian steel mill, located in Southeastern China, built in 1987. Hot coke, with a temperature around 1000 °C was transported to the quenching tower by train. The quenching was done rapidly by spraying cold water in the tower, through which the temperature was reduced to below 250 °C in about 10 min. The tower was exposed to more than 40 quenching cycles on a daily basis. The exposure of the tower to repetitive cycles of heating and cooling as well as wetting and drying made the structure fail after 34 years. In situ investigations revealed severe durability damage, such as a large-scale cracking of the concrete, the peeling of the concrete covers, and

the fracture of rebars [14]. These real-life examples highlight the importance of testing concrete properties upon exposure to not only one time, but repeated thermal cycles, and the essentiality of establishing standard guidelines for testing these.

2.1.3 Laboratory-scale methods to evaluate concrete's thermal resistance

General information on testing steps:

Evaluating the thermal resistance of concrete is essential for understanding its performance and durability under high-temperature conditions. Laboratory-scale methods provide controlled environments to simulate thermal loads and analyze the resulting effects on concrete's thermal, mechanical, microstructural, and mineralogical properties. By replicating conditions such as rapid heating, sustained high temperatures, and cooling cycles, researchers can examine key factors like compressive strength retention, cracking behavior, and thermal conductivity. This knowledge plays a pivotal role in the development of thermally resistant concrete mixes and in designing structures with enhanced fire safety and longevity. When conducting laboratory-based tests to investigate the thermal resistance of concrete, it is essential to distinguish between material-level tests and structural-level tests. Material-level tests focus on analyzing the intrinsic thermal and mechanical behavior of concrete at the material point, isolating specific properties such as thermal conductivity, heat capacity, and high-temperature compressive strength. These tests aim to exclude temperature gradients, ensuring that the results reflect the fundamental properties of the concrete itself, rather than the effects of heat transfer across a structural element. In contrast, structural-level tests evaluate the thermal performance of entire concrete components, where temperature gradients, thermal stresses, and interactions between different materials play a crucial role. These tests more accurately simulate real-world exposure conditions, making them essential for assessing structural integrity, fire resistance, and long-term performance in practical applications. Understanding the distinction between these two testing approaches is critical for accurately interpreting results and applying them to concrete design and performance optimization.

In general, all laboratory-scale thermal resistance tests comprise similar steps. The first step is the sample preparation, where specimens to be tested are prepared in standardized dimensions. This is followed by the exposure of the specimens to controlled heating conditions to simulate thermal loads (temperature-time curves). Depending on the requirements, this step can be carried out under stressed or unstressed conditions [15],[16]. In stressed method, the concrete specimen is subjected to both thermal loads (heating) and mechanical loads (stress) simultaneously. The mechanical load (usually around 20 to 40 % of the room temperature compressive strength) is applied prior to thermal exposure and maintained throughout. The goal is to investigate the load bearing capacity of the concrete structure in hot conditions. In unstressed test method, the specimen is exposed to thermal loads (e.g., heating) without any mechanical stress applied. This method focuses purely on the thermal effects on concrete, such as changes in microstructure, cracking, or spalling. In both methods, the hot mechanical

properties are measured [17]. There is a third method of testing, known as the unstressed residual property test [16]. This is carried out as a normal unstressed test, but the specimen is permitted to cool down before the residual mechanical properties are measured [15],[17]. A schematic overview of the evolution of temperature and stress versus time in these tests is shown in Figure 2.1. In stressed testing, a constant load (approx. 20 - 40 % of room temperature compressive strength) is applied to the test specimen until time point t, while the specimen is heated up to the temperature T, and then is stabilized in T from the time point t_0 to t, at which point the load is increased until the specimen fails. In unstressed testing, specimen is heated up to the temperature T without any load, and then is stabilized in T from the time point t_0 to t, at which point the load is applied and increased until the specimen fails. In case of residual property testing, specimen is heated up to the temperature T without any load, and then is stabilized in T from the time point t_0 to t_1, and is then cooled down to room temperature by time point t, at which point the load is applied and increased until the specimen fails.

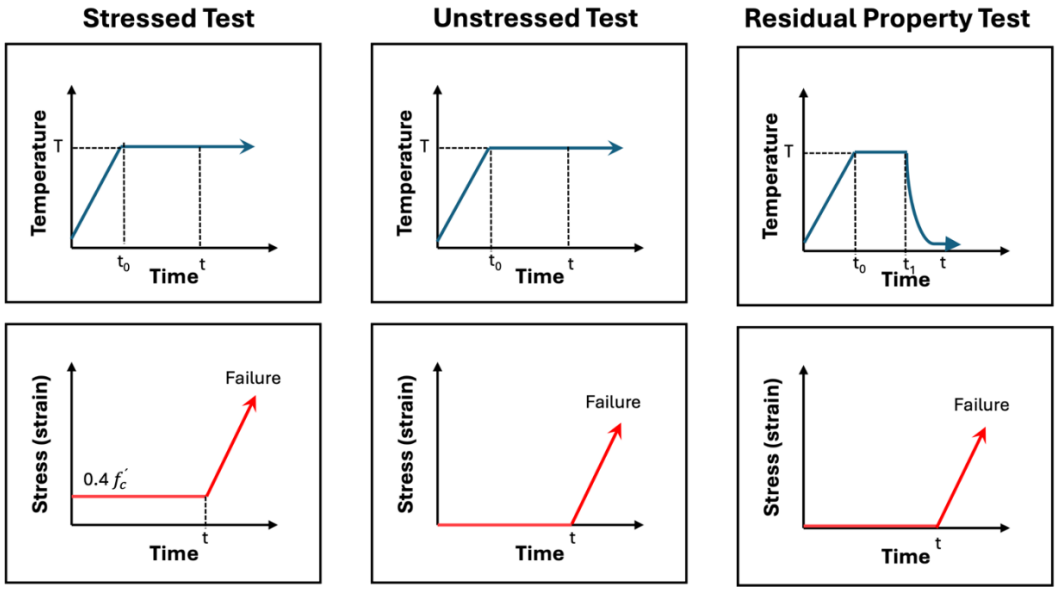

Figure 2.1 Schematic of temperature (up) and load (down) profiles for laboratory-based tests to evaluate concrete's thermal resistance. Figure is produced based on [17]

Thermal load simulation:

Simulation of the thermal load exposure can be carried out through a variety of methods. A comparative view of these is shown in Figure 2.2. The most commonly used method is the standard temperature-time curve (also known as ETK). It constitutes a very common temperature-time profile in various national and international standards, such as ISO 834, BS 476: part 20, DIN 4102 and ASTM E119.

This curve models the temperature rise during a compartment fire scenario, where the temperature inside a building rises rapidly due to combustion. The time-temperature relationship is defined by the following formula:

$$T = 345\log(8t + 1) + T_0 \quad \text{(Equation 2.1)}$$

Where, T is the furnace temperature in °C at time t, t is time in min, and T_0 is the initial furnace temperature, typically 20 °C.

The standard temperature-time curve is the most suitable for testing the fire resistance of materials exposed to fire hazards based on the burning rate of common combustible building materials and contents, such as timber, paper, and fabric. As such, it is ideal for assessing the fire resistance of fire protection systems in typical buildings, but it can also be used for fire testing of tunnel linings. [18],[19],[20]. Even though the standard temperature-time curve has been a standard for many years, it became evident that the burning rates of certain materials, such as petrol, gas, and chemicals, significantly exceed those of materials like timber. Consequently, an alternative approach was needed to conduct tests on structures and materials used in the petrochemical industry, leading to the development of the Hydrocarbon curve, which was originally developed for the petrochemical and offshore industries, and later adopted for tunnels as fire incidents in this context is associated with the burning of petroleum and chemicals. This model is also more representative of fires in closed tunnels, due to the limited ventilation conditions therein. It has been used in several standards such as DIN EN 1363-2 [21]. The temperature development of the Hydrocarbon fire curve is described by Equation 2.2:

$$T = 20 + 1080\ (1 - 0.325e^{-0.167t}) \quad \text{(Equation 2.2)}$$

Where, T is the furnace temperature in °C at time t and t is time in min [21],[22],[23],[24].

Based on the Hydrocarbon curve, French regulations require a more intense version known as the Modified Hydrocarbon curve, due to the rapid increase in temperature observed in Mont Blanc and Tauern tunnel fires [24],[25]. Additionally, after the fire incident in the Velsar tunnel, the TNO Center for Fire Safety in the Netherlands introduced the RWS (Rijkswaterstaat) fire curve. In tunnel design, the RWS curve depicts a more severe scenario of fire, with temperatures rising higher and the exposure duration being longer. The rate of temperature increase in this curve was determined experimentally, and its accuracy was confirmed in full scale tests conducted Runehamar tunnel in Norway [24],[26].

The RABT-ZTV (Richtlinien für die Ausstattung und den Betrieb von Straßentunneln) temperature-time curves, developed by the Ministry of Transport in Germany, feature a rapid temperature rise from 15 °C to 1200 °C within just 5 min. However, the exposure duration at 1200 °C is shorter compared to other curves. For car fires, the temperature begins to decline after 30 min, whereas for train fires, the drop-off starts at 60 min. Both fire scenarios include a 110 min cooling period back to 15 °C [24],[26],[27]. Unlike the hitherto described open temperature profiles, these two profiles represent closed temperature curves, in which mechanical properties are tested after complete cooling in form of residual mechanical properties.

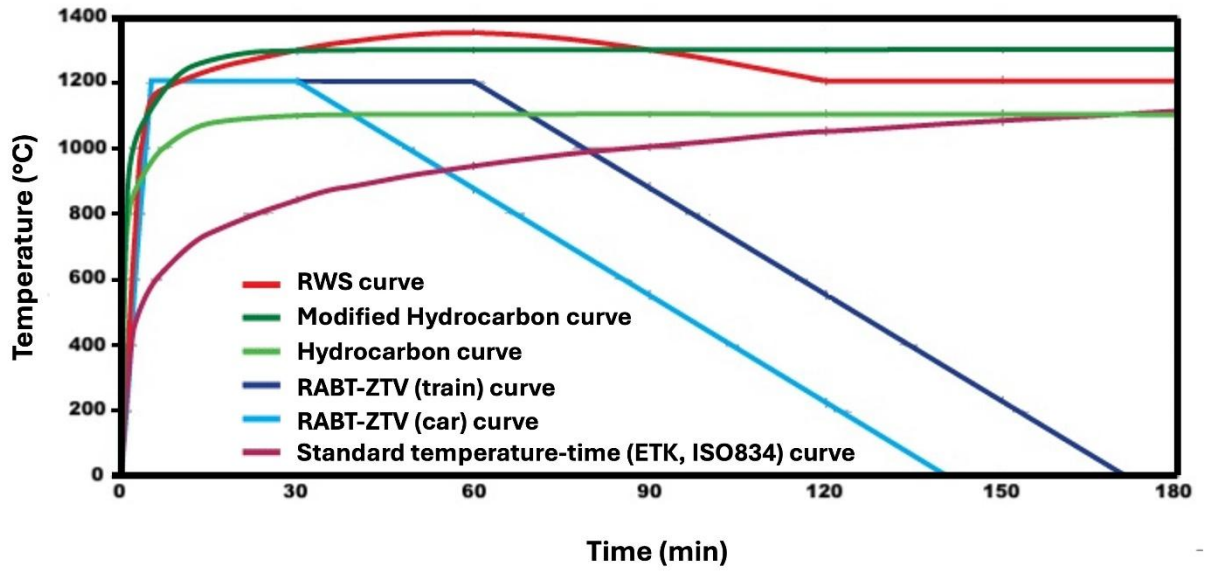

Figure 2.2 Different temperature-time curves for laboratory testing of concrete fire resistant [24]

2.1.4 Effect of high temperatures on concrete properties

It is well-known that exposure of concrete to high temperatures leads to a significant loss of its mechanical properties, mainly owing to the chemical and physical changes both in the aggregates and the cement paste [28]. At high temperatures, concrete undergoes various physical (such as phase expansion, condensation, evaporation, and vapor diffusion), chemical (including thermochemical damage and dehydration), and mechanical (such as thermomechanical damage, spalling, and cracking) processes, all of which contribute to the deterioration of its properties [29]. The change in the mechanical properties is often manifested in the form of a significant reduction of the flexural and compressive strengths [30], tensile strength [31],[32] and modulus of elasticity [28]. Due to increased brittleness and the development of microcracks, concrete's tensile strength and modulus of elasticity degrade more rapidly than compressive strength [4],[33]. In addition to the concrete composition, the decrease in compressive strength of the concrete depends on the maximum exposure temperature [30], the heating duration [34], and the number of thermal cycles to which concrete is exposed [35].

Normally, the mechanisms involved in the loss of concrete mechanical properties are multiple and temperature dependent. The thermal damage results from a variety of factors, such as the differential expansion between the aggregates and the cement paste [36],[37], the decomposition of hydrates as a result of $Ca(OH)_2$ and C-S-H decomposition [38], the growth of the pore structure due to the loss of bound water [39], and crack development owing to the rehydration of lime during cooling [40].

In the following, temperature induced physicochemical, and mineralogical changes in the concrete and their effect on the properties of the concrete will be elaborated on.

2.1.5 Temperature induced physicochemical and mineralogical changes in concrete structure

With an increase in temperature, complex changes happen within the concrete structure, a summary of which are presented in Figure 2.3. Starting from lower temperatures (ca. 80 °C) up to middle high temperature ranges of 300 °C - 400 °C, concrete loses its physically and most part of its chemically bound water. The loss of free water initiates in the temperature range of 20 - 80 °C as a result of expansion. The free water in the concrete matrix evaporates at around 100 °C, while the dehydration of C-S-H at around 300 °C - 400 °C leads to the partial release of the chemically bound water in the concrete structure, which ultimately weakens the concrete matrix [41]. According to the results of thermogravimetry and high temperature X-ray diffraction analyses by Song et al., the first dehydration of the C-S-H gel occurs in the temperature range of 80 °C to 240 °C [42]. As a result of the release and evaporation of the water, steam pressure builds up in the concrete, potentially leading to the spalling of denser concrete mixtures such as high-performance concrete (HPC) and UHPC (the moisture clog effect) [43]. This is further exacerbated by the more rapid buildup of thermal gradients and higher thermal expansion in case of high-performance concretes [43]. Due to the more porous structure, normal concrete can experience less damage at this temperature range, since vapor can leave the concrete microstructure more easily [44]. However, high heating rates or else repetitive exposure to such high temperatures can increase the chances of spalling even in normal concrete [45]. In general, concrete experiences significant loss of compressive strength in the temperature range of 300 °C - 400 °C. This particularly results from the structural changes in C-S-H phase, including the decrease in the interlayer distance, structural disordering, and increase in porosity, which renders the concrete's microstructure increasingly brittle [46].

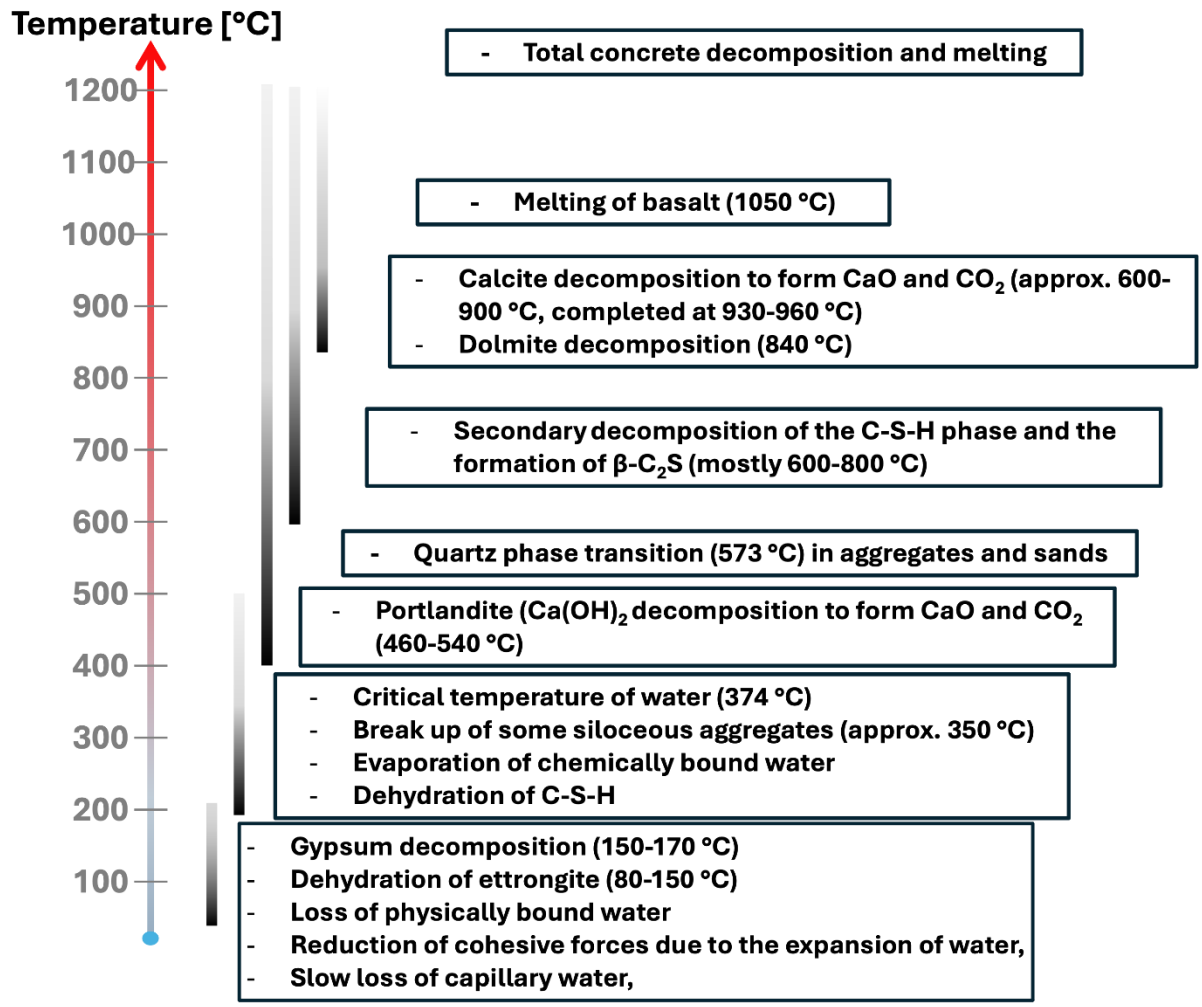

Figure 2.3 Effect of increase in temperature on concrete structure, generated based on [47]

The temperature induced chemical changes in the C-S-H paste have been the subject of extensive research over the years. Various models have been developed to describe the structure of C-S-H. The most important are the Powers-Brunauer model and the Feldman-Sereda model. The Powers-Brunauer model describes C-S-H as a layered structure with an extensive surface area, estimated to range between 100 and 700 m^2/g. The mechanical strength of this structure is believed to stem from van der Waals interactions [48]. On the other hand, the Feldman-Sereda model portrays C-S-H as a series of irregular and randomly arranged layers, creating interlayer spaces with dimensions varying from 5 to 25 Å. Studies on CEM I have revealed that the nanoscale structure of C-S-H is responsible for the strength of cement mortar [48]. However, this nanostructure undergoes significant alterations when exposed to elevated temperatures. These alterations begin at temperatures as low as 80 °C, where, based on the in situ neutron diffraction experiments conducted by Castellote et al., ettringite loses its crystalline form [49] and is later converted to meta-ettringite at around 120 °C [50]. As a result of this transformation along with evaporation of the physically bound water, this stage has been generally reported to be associated with a slight decrease of concrete's compressive strength [51]. Nevertheless, some reports on the change of concrete strength in the range of 105 °C to 200 °C deviate from

this general context, where few studies report an increase in the compressive strength at this temperature range [51], while others report the value to remain constant or negligibly decrease [52]. Lim, who has reported an increase in strength, attributed this to an internal autoclaving effect or a change in the local mechanical properties of the C-S-H confirmed through a detected increase in hardness in statistical nanoindentation tests [51]. It seems that the water to cement ratio plays an important part in this scenario, as Gong has reported more noticeable decrease of strength in this temperature range for specimens with higher ratios [52]. The decrease in concrete strength becomes once more visible above 300 °C, where using atomic force microscopic (AFM) analysis, Lim has demonstrated a change of the concrete nanostructure towards a more globular structure, that can be an indicator of the C-S-H shrinkage [51]. Using synchrotron radiation, Shaw et al. demonstrated that tobermorite transforms to wollastonite ($CaSiO_3$) [53], while Rodriguez et al. showed that the temperature at which this chemical transformation occurs depends on the Ca/Si ratio of the specimen, with higher Ca/Si ratios being associated with transformation at lower temperatures [54]. In the CEM I, which is associated with a Ca/Si ratio between 1.5 to 2, this has been shown to occur around 400 °C [49]. This combined with the shrinkage of the C-S-H above 300 °C can explain the reduction of strength above 300 °C. It has been shown that decomposition of C-S-H phase continues even further beyond, and continues up to a temperature of 1000 °C. The calculated activation energy for this decomposition has been shown to vary from 83.69 to 371.93 kJ/mol, which signifies the dehydration of C-S-H is a multi-step reaction because of its complex structure [55]. Peng et al. investigated kinetics of C-S-H decomposition in temperatures between 400 °C to 800 °C using X-ray diffraction on HPC specimens. The detected decomposition products were mainly tricalcium silicate (C_3S) and beta-dicalcium silicate (β-C_2S). They reported that the decomposition started around 560 °C, but it only became significant at temperatures above 600 °C, and enhanced dramatically with increase of temperature, both in terms of the extent and the rate of decomposition. They attributed the strength loss of HPC below 600 °C to the enlargement of the matrix pores [56]. While these data cannot be directly extrapolated to the normal strength concrete, they still shed light on the decomposition of the C-S-H phase and the effect of temperature thereupon.

When exposed to temperatures higher than 400 °C and up to 900 °C, complex changes within the concrete occur, which further decrease its strength. Some of these changes originate from the changes in the cement paste, while others depend on the aggregates used for concrete production. Between 400 °C and 540 °C, $Ca(OH)_2$ is decomposed to form CaO and water vapor. Unlike the decomposition of the C-S-H gel, this is a single step process [55]. The decomposition of $Ca(OH)_2$ not only increases the internal vapor pressure, but also results in volumetric changes and additional microcracking, as CaO has different properties compared to $Ca(OH)_2$.

The temperature range of 400 °C - 900 °C is also associated with the transformation of aggregates, which, depending on their mineralogical properties, undergo thermal expansion and

potential phase changes. A well-known example within this frame is the phase transition of quartz-based aggregates (a siliceous aggregate) at around 573 °C [57]. The difference in the thermal expansion coefficient of the aggregates and the cement paste (Figure 2.4) leads to increased internal stresses and further microcracking and can, even in cases, lead to spalling. According to Reiners et al., larger C-S-H phases in general lead to temperature-induced alterations in the microstructure of the hardened cement paste, e.g. greater differences between the thermal expansion of the concrete layers at different distances from the heated surface. This in turn contributes to concrete spalling [58]

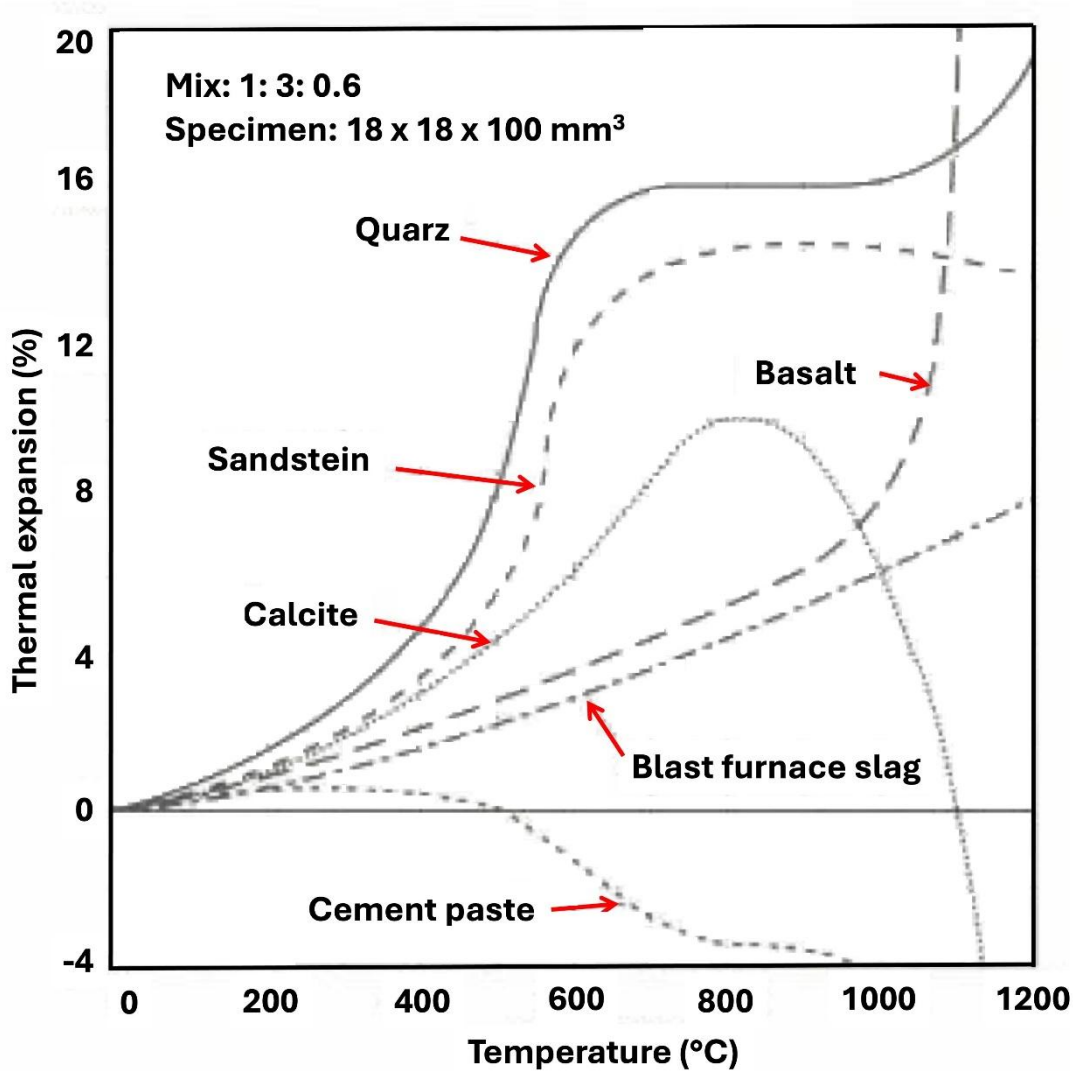

Figure 2.4 Thermal expansion of CEM I cement paste and different types of aggregates at elevated temperatures, slightly modified from [28]

Considering that aggregates usually comprise 65-75 % of the concrete volume, their effect on the thermal behavior of the concrete is significant. In general, it has been demonstrated that using non-siliceous aggregates can improve the thermal behavior of concrete, as they often have higher specific heat capacities [57]. Most non-siliceous aggregates are stable up to a temperature of 600 °C. Above this temperature, however, calcareous ($CaCO_3$), magnesite

($MgCO_3$) and composite aggregates thereof (dolomite aggregates) break down through an endothermic reaction, the products of which are CaO/MgO and CO_2 [59]. In the temperature range of 600 °C to 900 °C, decomposition of calcite ($CaCO_3$) present in the cement paste and limestone aggregates occurs [60]. The major part of this process, however, occurs at temperatures above 850 °C with the highest rate at 900 °C, leading to the release of CO_2 and the formation of CaO, culminating in volume reduction, increased porosity, and further weakening the concrete structure [28],[47],[61] As a result of the aforementioned changes, both compressive strength and elastic modulus significantly decrease. Concrete dehydration and decomposition reactions lead to the progressive development of microcracks and increase in concrete porosity. The microcracks then further connect with each other, leading to a reduction in mechanical integrity and durability.

2.1.6 Concrete properties post-exposure to thermal loads

The performance of concrete after exposure to elevated temperatures depends on how the thermal load has affected the concrete's mechanical, physical, and chemical properties. These effects are critical for assessing the structural integrity and serviceability of concrete elements in post-fire scenarios, but it is also of vital importance for the continued serviceability of the structures exposed to repetitive cycles of heating and cooling. In fact, the residual properties after exposure to elevated temperatures, be it a one-time or regular exposure, are of great importance for determining the minimum load-bearing capacity of concrete constructions [62].

In general, the retained mechanical properties of concrete after cooling down referred to as residual mechanical properties. The residual mechanical properties of the concrete are often measured based on the residual compressive, flexural and splitting tensile strengths as well as the residual module of elasticity (see section 1.3.8). In fact, residual compressive strength is usually 10-15 % lower than the hot compressive strength [62],[63]. This is due to the formation and propagation of cracks during cooling, particularly in the interfacial transition zone between the aggregate and the paste [64]. The concrete's modulus of elasticity, which represents the stiffness of concrete, also undergoes a significant reduction post thermal exposure. Even after cooling, the modulus of elasticity remains low due to permanent structural changes [64]. In general, the porosity and permeability of concrete post-heated remains higher than the pre-heated state [65]. The increased porosity arises from the loss of hydration products and microcracking, which do not heal during cooling [66]. Moreover, thermal exposure often results in permanent drying shrinkage and thermal cracking [67]. During cooling, differential thermal contraction between aggregates and the cement matrix exacerbates cracking [68].

While mechanical properties of concrete often exacerbate after cooling, there might be still chances of (partial) strength recovery. The most important is the maximum temperature to which the concrete has been exposed. When exposed to temperatures up to 300 °C, dehydration of C-S-H gel and microcracking cause moderate strength reduction. Residual strength recovery is typically higher because damage remains reversible to some extent [62],[69],[70]. Between

300 °C and 600 °C, $Ca(OH)_2$ decomposition and aggregate thermal expansion result in significant loss of strength, with lower recovery potential under normal conditions due to permanent chemical and microstructural changes. Depending on the peak temperature in the range and the post-cooling curing conditions, however, some degrees of strength recovery is possible [70]. Exposure to temperatures beyond 750-800 °C, on the other hand, often leads to irreversible damage as a result of the decarbonation of $CaCO_3$ and severe aggregate-matrix debonding, greatly reducing strength recovery [69],[71]. Other factors affecting the strength recovery are the duration of exposure [34],[72],[73], heating rate [69],[74], cooling rate [66],[75],[76],[77] (particularly when concrete is heated to higher temperatures) [76],[77], and post-exposure environment and curing conditions (relative humidity [78],[79], curing in water [78],[80], CO_2 curing [71], and the number of thermal cycles, to which concrete has been exposed [81]. This factor will be elaborated on in section 1.3.9. Usually, a combination of these factors can determine the chances of concrete rehabilitation of post-thermal load exposure.

Other than external conditions, concrete composition can also affect the extent of strength recovery. Among this, the composition of the cement paste has been shown to play a part. For instance, high-alumina cements or cements with pozzolanic additives (such as slag sand) exhibit improved thermal stability compared to CEM I, as they retain more hydration products and experience less microstructural damage, facilitating strength recovery [82],[83],[84]. Similarly, SCMs are expected to improve the thermal stability of the matrix by reducing porosity and enhancing the bond between cement paste and aggregates, which can result in better strength retention and recovery [85],[86]. Another factor is the water to cement ratio. In general, a low water-cement ratio is believed to be beneficial for the recovery, as it improves initial concrete strength and reduces porosity, which can limit damage during heating [87]. However, it should be also considered that denser concrete structures are more prone to spalling [88]. Furthermore, higher water to cement ratio has been shown beneficial for concrete rehabilitation through post-exposure carbonation curing, as the lower matrix density improves CO_2 penetration in the damaged concrete microstructure [89]. In addition to the above mentioned, type of the aggregates also plays an essential part [90]. For instance, quartz aggregates undergo a phase transformation at approximately 573 °C (α-β transition), causing expansion and microcracking [91]. On the contrary, limestone and dolomite aggregates exhibit better thermal stability above 600 °C and contribute to higher residual strength and recovery, as they undergo less thermal expansion and cracking [92]. Furthermore, some industrial aggregates, such as slag-based aggregates, have better thermal resistance [93], reduce the thermal conductivity of the concrete [94]. The weight of the aggregates is another influential factor on concrete rehabilitation. Within this context, light weight aggregates have been shown to perform superior to their normal weight counterparts, mainly due to the smaller density and lower thermal expansion coefficient of the concrete product [90]. Obviously, the extent and distribution of microcracks developed during heating strongly dictates the strength recovery. Furthermore, strong bonding

between the cement paste and aggregates is critical for recovery, as severe thermal stress and debonding hamper strength regain [95].

It should be however highlighted that while the residual mechanical properties are important in case of concrete exposure to fire, they are essential to heed in case of concrete construction exposed to repetitive cycles of heating and cooling. Usually, structures exposed to repetitive cycles of heating and cooling are air cooled, with the slow rate of cooling being in favor of mitigating the damage and regaining strength. In such cases, repetitive thermal cycles can deteriorate concrete structures through repeated cycles of calcic dehydration and rehydration, as well as differential thermal expansion and contraction between the cement paste and aggregates. This process results in microcracking, a reduction in concrete strength, structural fatigue, a decrease in the modulus of elasticity, and even chemical reactions within the concrete. [35],[96],[97].

2.1.7 Temperature-induced changes in concrete's thermal properties

The thermal properties that influence temperature distribution in a structural element include thermal conductivity, specific heat, thermal expansion, and mass loss. The test procedures outlined in current standards for measuring concrete's thermal properties are primarily designed for room temperature conditions. Standardized methods for evaluating thermal properties at elevated temperatures are limited and only partially established (as summarized in Table A.1.1 in Appendix A.1). In the following, we will provide an overview of the concrete's thermal properties and the influence of increasing temperatures thereupon:

Thermal conductivity: Thermal conductivity quantifies a material's ability to conduct heat and is defined as the amount of heat (in watts) that passes through a unit area of the material under unit temperature gradient. The type and amount of moisture present in concrete significantly affects its thermal conductivity [98],[99]. At room temperature, the thermal conductivity of conventional normal-strength concrete typically ranges from 1.4 to 3.6 W/mK on average [4]. The thermal conductivity of concrete decreases with an increase in temperature, mainly due to the evaporation of the physically and chemically bound water, with the reduction, according to Nguyen et al., reaching approximately 23 % when the temperature increases to 800 °C [100]. Figure 2.5, reported by Kodur et al., shows the decrease of concrete thermal conductivity as a function of increase in temperature. The figure shows both the upper and lower bound values of thermal conductivity based on EC2, which is applicable to all aggregate types, the reduction of concrete's thermal conductivity per ASCE (American Society of Civil Engineering) relations, which is applicable for concrete with carbonate aggregates, and the variation in measured test data depicted as shaded area. The observed variation in reported data has been mainly attributed to the differences in the moisture content of the specimens, type of the aggregates, test conditions, and the measurement techniques [4].

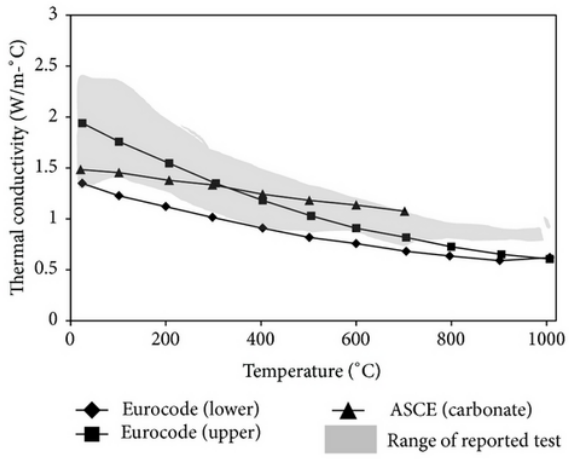

Figure 2.5 Decrease in the thermal conductivity of normal strength concrete as a function of temperature, including both the upper and lower bound values based on EC2, the reduction based on ASCE for specimens with carbonate aggregates, and the variation in the reported data shown as gray shade [4]

Specific heat: Concrete's specific heat is the amount of heat energy required to raise the temperature of a unit mass of concrete by one degree Celsius (or Kelvin) [101]. The specific heat of concrete at room temperature varies between 840 J/kg·K and 1800 J/kg·K, depending on the type of aggregates used. Up to 400 °C, the specific heat of concrete remains nearly constant, followed by an increase up to around 700 °C, after which it stabilizes in the 700-800 °C range [4]. Among the factors affecting specific heat, aggregate type plays a critical role. Concrete made with carbonate aggregates exhibits higher specific heat within the 600-800 °C range due to an endothermic reaction associated with the decomposition of dolomite, which absorbs a significant amount of energy [102].

Thermal expansion: Thermal expansion describes the extent to which concrete expands or contracts in response to the change in temperature and is defined as the change in unit length per degree of temperature change. [103]. Figure 2.6 shows the thermal expansion behavior of normal strength concrete as a function of temperature based on the EC2 (for carbonate and siliceous aggregates) [104] and ASCE [105], with the shaded region representing the range of test data reported by various researchers compiled by Kodur et al [4]. Thermal expansion begins at 0 % at room temperature and rises to approximately 1.3 % by 700 °C, after which it remains relatively constant up to 1000 °C. The significant increase observed between 20 °C and 700 °C is primarily attributed to the thermal expansion of the aggregates and cement paste [4].

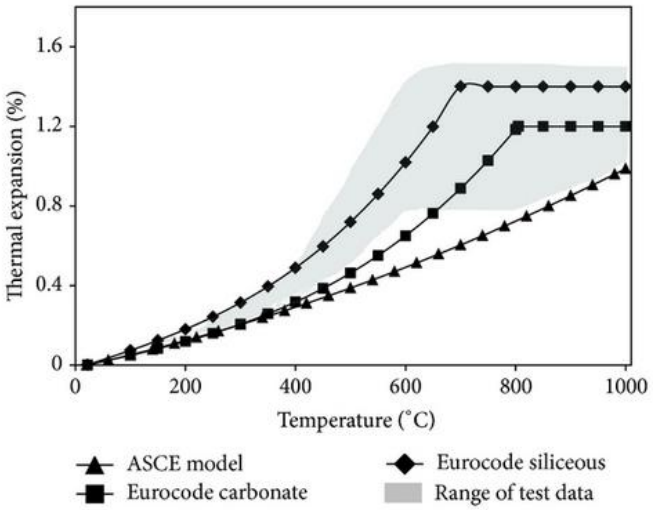

Figure 2.6 Temperature-dependent thermal expansion of normal strength concrete [4]

Mass loss: Mass loss represents the reduction of the concrete mass, mainly resulting from the high temperature-induced water evaporation and/or CO_2 release. In general, concrete mass is reduced by increasing temperature due to the evaporation of the physically and chemically bound water at lower temperature and the decomposition of $CaCO_3$ at higher temperatures. According to Hager, the decrease of concrete mass can be divided into four phases. The mass loss between the ambient temperature and 100 °C is rather low, as it corresponds to the evaporation of the physically bound water in the concrete capillary pores. The mass loss increases in the range of 100 - 300 °C to around 5.6 %, mainly due to the simultaneous evaporation of the capillary and gel water. The third phase involves the temperature range of 300 °C and 500 °C, where the mass loss decreases due to the significant evaporation of all physically and chemically bound water. Finally, above 500 °C, the rate of mass loss increases due to the decomposition of $CaCO_3$ and the release of CO_2 [47],[106]. Kodur et al. have reported a different pattern for the mass loss of normal strength concrete, which is mainly dictated by the type of aggregates. They reported that the mass loss for specimens with both carbonate and siliceous aggregate concrete remains minimal up to approximately 600 °C. Beyond this temperature, the type of aggregate significantly impacts mass loss, where unlike concretes with siliceous aggregate, which show negligible mass loss, specimens with carbonate aggregates experience a 20-30 % loss of initial mass. This increased mass loss in carbonate aggregate concrete is primarily due to the dissociation of dolomite ($CaMg(CO_3)_2$) at around 600 °C [4],[102].

The thermal properties of the concrete are important determinants of the temperature profile inside the concrete structural elements. The available building codes focus on ensuring adequate resilience in case of fire. In structures built with normal-strength concrete, structural elements are designed to obtain a fire resistance rating (FRR) in the range of 1 to 4 h. The structural elements are not made of pure concrete, but concrete with reinforcement (e.g. steel). Hence, one of the most important parameters setting the FRR is the depth of the concrete coverage,

which protects the incorporated reinforcement from thermal damage. Depending on the exposure temperature and duration of the thermal load, the temperature in different internal layers of the concrete might eventually increase. The temperature field development plays a significant role on the component level in the event of fire and must be calculated numerically if simplified table methods are not used [108].

2.1.8 Temperature induced changes of concrete's mechanical properties

The mechanical properties that affect the strength and stiffness of a structural component include the compressive strength, tensile strength, stress-strain behavior, and modulus of elasticity. Detailed test procedures for assessing the mechanical properties of concrete at ambient temperature are given in the European Standards DIN EN 12390-3 for compressive strength [109] and DIN EN 12390-6 for tensile strength [110] as well as the American standards such as ASTM C39 for compressive strength [111] and ASTM C496 for tensile strength [112]. However, neither ASTM nor European Standards provide guidance for evaluating the mechanical properties of concrete at elevated temperatures. RILEM (the International Union of Testing and Research Laboratories for Materials and Structures) offers test procedures for assessing the mechanical properties of concrete in the temperature range of 20 - 750 °C [113] (Table 1.3). However, building codes such as DIN EN 1992-1-2 (EC2) for fire design of (reinforced) concrete structures [104] and DIN EN 1994-1-2 (EC4) for fire design of composite steel and concrete structures [114] prescribe the use of standard temperature-time profile as described under ISO 834 to ensure the integrity, stability and insulation of structural elements during exposure to elevated temperatures, with fire being the center of attention. In the following, we will provide an overview of the most important measures of concrete's mechanical properties and the influence of increasing temperatures thereupon.

Compressive strength: compressive strength gives the uniaxial compressive stress at which the material completely fails, regardless of whether signs of failure are visible or not. Compressive strength can be measured during the exposure of the specimen to thermal loads (hot compressive strength) or once the specimen is cooled down to ambient temperature (residual compressive strength). Different building codes have certain requirements for the reduction of the compressive strength of structural elements at elevated temperatures. In Figure 2.7.a, the change in the relative compressive strength of the normal strength concrete according to DIN EN 1992-1-2 (for concrete with carbonate and siliceous aggregates) [104], ASCE relations [105] and the range of data reported in the literature are shown according to Kodur et al. [4]. The diagram shows a large but uniform variation of the compiled test data for normal strength concrete within a temperature range of 20 °C to 800 °C. In Figure 2.7.b, the decline of the relative compressive strength of normal strength concrete in the temperature range of 20 °C to 1000 °C reported by 46 studies and complied by Ma et al. has been presented. The figure depicts a similar trend for the reported results, but with the reported values in two studies being slightly lower than the general range [115]. This is perhaps due to the fact that the data collected by

Kodur et al. [4] comprises both the hot and residual compressive strengths, whereas the data collected by Ma et al. [115] only contains values on the residual compressive strength, which are generally lower. Figures 2.7.c and 2.7.d present the data reported in a more recent article by Shahraki et al, which has collected the residual compressive strength of the concretes with siliceous (c) and calcareous (d) aggregates from 59 different studies. The graphs also include the EC2 reduction factors for the compressive strength of concrete at high temperatures as well as the EC4 recommended reduction factors for residual strength. As observed, the normalized residual compressive strength for concretes with both aggregate types are associated with large variations at different temperatures. However, while the median of the data for concretes with siliceous aggregate is slightly higher than the EC4 recommendation, it falls below the EC4 recommendations in case of concretes with calcareous aggregates. It should be however noted that a smaller number of data points have been available for analysis in case of the latter [116].

In general, all studies indicate that the compressive strength of concrete remains almost constant or even slightly increase in the range of ambient temperature and up to 300 °C. From 300 °C up to 800 °C, the compressive strength decreases dramatically, so that at temperatures above 800 °C, all the concrete's compressive strength is almost lost [115].

The water to cement ratio is another parameter influencing the compressive strength of the concrete post-thermal exposure. Shahraki et al. compiled and analyzed the normalized residual compressive strength reported 59 different studies based on the water to cement ratio (w/c) and suggested that a water to cement ratio higher than 0.5 has a positive effect on the residual compressive strength of the concrete with calcareous aggregates, but not the concrete with siliceous aggregates [116].

Aggregate type has been also shown to significantly impact the reduction of concrete's compressive strength. Ma et al. have presented the reduction of relative compressive strength of the concretes prepared with natural aggregates (dolomite, limestone, gravel, granite and basalt) based on the data compiled from 40 research papers [115]. The obtained regression curves have demonstrated that concrete with dolomite and gravel aggregates have shown the lowest and highest decrease in the relative compressive strength, while specimens with limestone, granite and basalt have performed almost similar and in between.

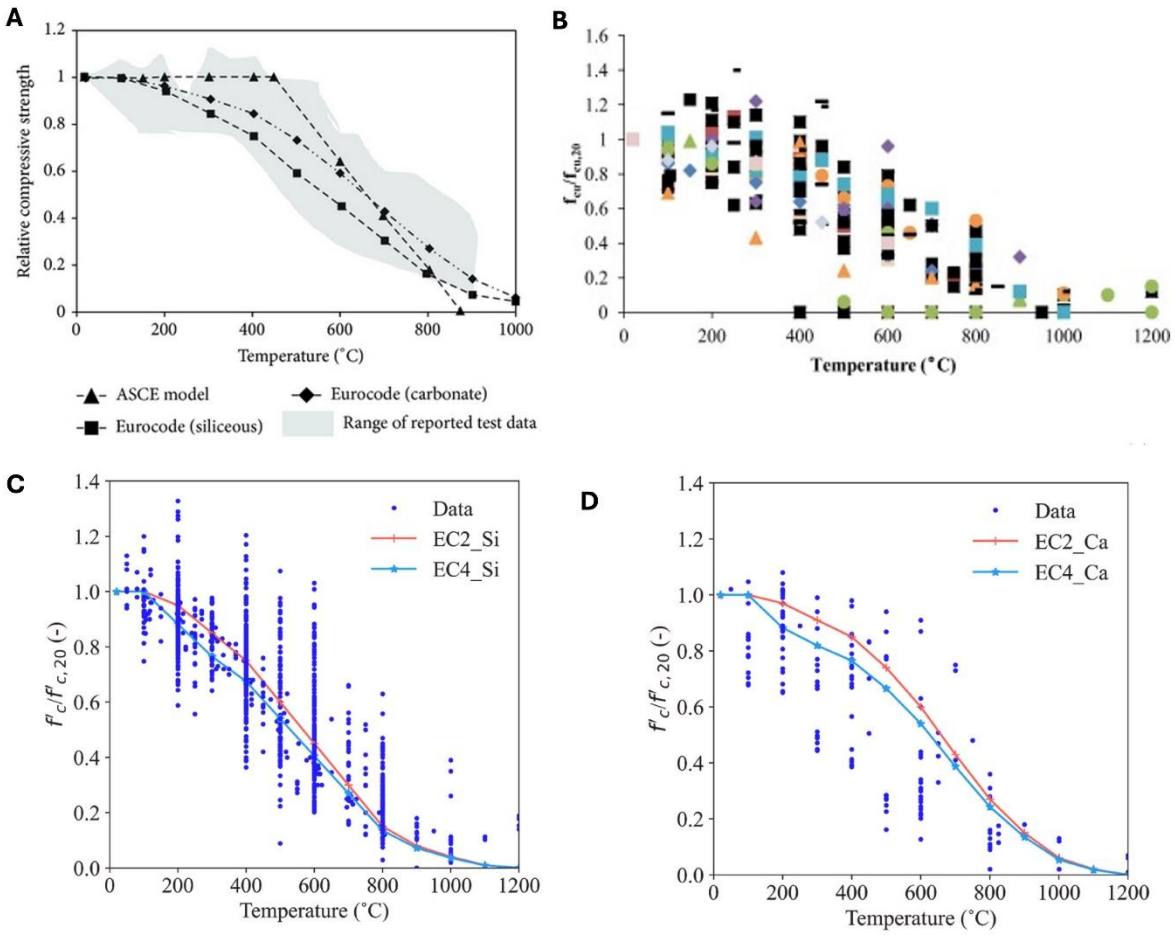

Figure 2.7 A) The change in the relative compressive strength of the normal strength concrete according to DIN EN 1992-1-2 (EC2; for concrete with carbonate and siliceous aggregates), ASCE relations, and the range of data reported in the literature according to Kodur et al [4], including both the hot and residual compressive strength values , B) the decline of the relative residual compressive strength of normal strength concrete in the temperature range of 20 °C to 1000 °C reported by 46 studies and complied by Ma et al. [115], C and C) the change in the relative residual compressive strength of concrete with siliceous (C) and calcareous (D) aggregates in the temperature range of 80 °C to 1200 °C collected by Shahraki et al, complied from the reports of 59 different studies [116]. It is worth to note that the wide distribution of the data is the result of the differences in the concrete composition and the experimental conditions used in different studies.

Another factor that significantly impacts residual compressive strength is the duration of exposure to thermal loads. Prolonged exposure exacerbates chemical decomposition, microcracking, and aggregate-matrix debonding, decreasing compressive strength and reducing the likelihood of strength recovery. Shorter exposure times allow for better preservation of the material's original properties [34],[72]. Longer exposure times, on the other hand, allow a larger portion of the specimen to achieve thermal equilibrium with the furnace environment, significantly influencing its residual compressive strength [116]. Shahraki et al. have compiled and analyzed the residual compressive strength of the concretes exposed to different elevated temperatures reported in 59 different studies based on the duration of heating. They found a

minimum 2 h retaining at the elevated temperature time to be necessary for lowering the standard deviation of normalized concrete strength. In the case of concrete with siliceous aggregates, medians of the data for a retaining time of over 2 h better matched the EC4 recommendations, whereas for specimens with calcareous aggregates, those with less than 2 h of retaining time were better matched. The authors concluded that the data suggests that the EC4 recommendation may underestimate the safety margin for concrete containing calcareous aggregates, though they believed further analysis to be necessary [116].

The final determining factor within the context of the residual compressive strength is the cooling rate. Shahraki et al. also had a look at collective data on the effect of cooling rate upon the residual compressive strength of the concrete heated to different maximum temperatures. For concrete with the calcareous aggregates, all studies had measured the residual compressive strength after air cooling. For concrete with silicious aggregates, most studies report lower values of residual compressive strength following water cooling. Nonetheless, Shahraki et al. found the identified pattern not to be significant when comparing all datapoints [116].

Tensile strength: Depending on the measurement method, three different types of tensile strength can be defined. Direct tensile strength represents the required force to pull apart a cylindrical or prismatic concrete specimen along its longitudinal axis [117]. Flexural tensile strength is a measure of an unreinforced concrete specimen to resist failure in bending [118]. Splitting tensile strength is the force required to split a cylindrical concrete specimen across the vertical diameter [119]. Similar to compressive strength, tensile strength of the concrete decreases with increasing temperature, though it is more affected as the latter, due to increased brittleness and the development of micro-cracks [120]. Ma et al. have summarized the reduction of the relative flexural (Figure 2.8.a) and splitting (Figure 2.8.b) tensile strength of normal strength concrete due to exposure to different elevated temperatures based on the data presented in 11 research works. These results confirm the more rapid decrease of tensile strength compared to the compressive strength as a result of increase in temperature [115].

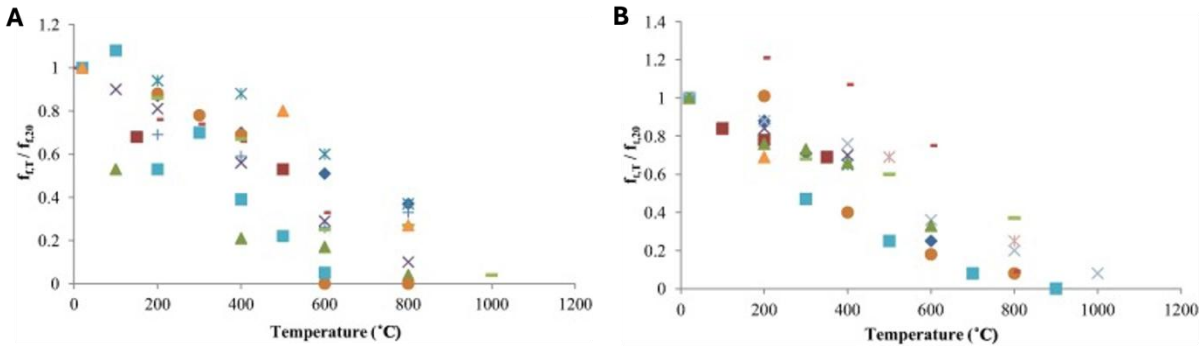

Figure 2.8 Reduction of the relative residual flexural (a) and splitting (b) tensile strength of normal strength concrete due to exposure to different elevated temperatures based on the data presented in 11 research work compiled by Ma et al. [115]

Stress-strain behavior: The stress–strain response of a material describes the measured stress when subjected to continuously increasing deformation. It serves as input data for mathematical

models used to assess the fire resistance of concrete structural elements. As temperature rises, the compressive strength of concrete diminishes, and its ductility increases, resulting in a reduced slope of the stress-strain curve (Figure 2.9) [4],[121]. While the diagram represents the stress-strain curve, the stress-strength curves under hot conditions are expected to follow a similar trend.

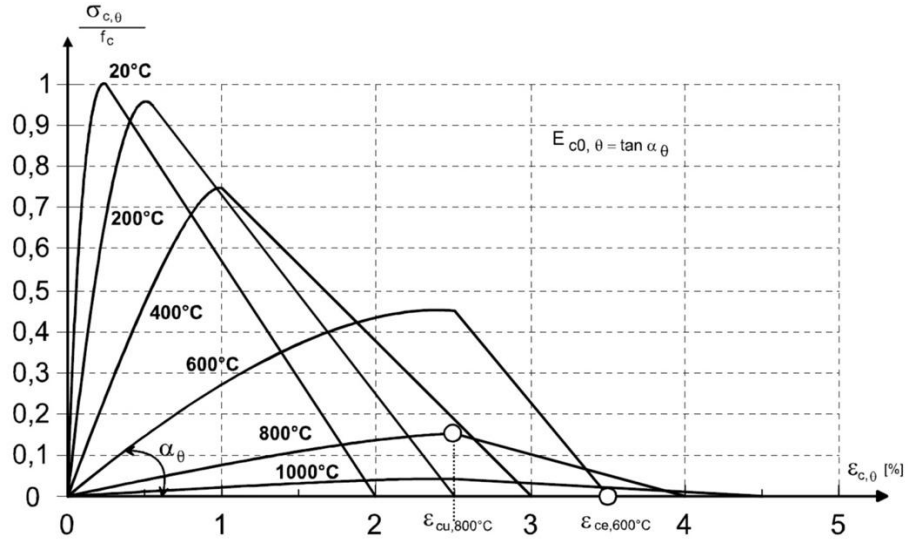

Figure 2.9 Stress-Strain diagram for normal strength concrete with quartzite aggregates exposed to different peak temperatures along with linear downwards sloping branch. The recommended Values for $\varepsilon_{cu,\theta}$ and $\varepsilon_{ce,\theta}$ according to DIN EN 1994-1-2 (EC4) [114]

Modulus of elasticity: For concrete, the modulus of elasticity defines how much the concrete will deform when a load is applied. It is defined as the ratio of normal stress to the corresponding strain when tensile or compressive stresses are applied, provided that they are below the material's proportional limit [122]. In general, concrete's modulus of elasticity decreases with the increase in temperature with almost a linear trend and remains low even when the concrete has cooled down [64]. Compared to compressive strength, modulus of elasticity is more strongly affected by thermal loads [4],[33].

2.1.9 Effect of repetitive heating and cooling cycles on the properties of concrete

Repetitive heating and cooling cycles significantly impact the properties of concrete, primarily due to the internal strains induced by both expansion and contraction of the cement pastes and aggregates [123], but also due to thermo-hygric process such as "water clog" as well as thermal fatigue [124]. The expansion-induce strains include thermal expansion, cracking expansion and chemically induced expansion, whereas the contraction-induced strains pertain to drying shrinkage, load-induced thermal strain both during heating and at constant temperature, and time-dependent creep [123]. Thermomechanical and thermo-hygric damage from cyclic thermal stress/strain and pore pressure fluctuations can progressively degrade the concrete matrix. Thermo-hygric damage, caused by periodic pore pressure changes, accelerates

coarsening and crack development. However, temperatures below 200 °C may not create detectable microcracks in the cement matrix. Over time, high-cycle thermal fatigue compounds these effects, resulting in irreversible defects and cracks that impair the material's macro properties. This degradation compromises matrix integrity and reduces concrete's strength [124].

The magnitude of the thermal cycle-induced strains depends on a variety of factors, among the peak temperature to which the concrete is exposed is paramount [123],[125]. Khoury has proposed the concept of 'concrete-specific critical temperature', up to which a second thermal cycle would not lead to significant additional damage. Above this temperature, however, thermal cycling, especially in unloaded concrete, tends to induce significant progressive cracking, the onset of which as well as the degree of induced damage is primarily detected by the type of aggregates and to a lower extent by the composition of the cement paste [123]. Khan et al. have reported the residual compressive strength of the concretes exposed to repetitive thermal cycles with the peak temperature of 100 - 300 °C to be higher than the strength at ambient temperature [126], [127]. Similarly, Boquera et al. reported the preservation of the CEM I concrete mechanical properties after exposure to 25 cycles with peak temperatures in the range of 20 - 300 °C, despite the formation of microcracks. The authors attributed the observed strength recovery to the rehydration of the cement paste during slow cooling to ambient temperature. However, when the peak temperature increased to 600 °C and above, CEM I cement demonstrated a fragmentation status after 25 cycles [128]. Combined, these results confirm the concept of "concrete specific critical temperature" suggested by Khoury [123]. As moderate temperature cycles do not lead to the decomposition of chemically bound water and cement hydration products, strength recovery post cooling is still possible. However, significant increase in the number of heating cycles seems to deteriorate the mechanical properties of the concrete even at lower temperature levels. For instance, exposing concrete to repetitive thermal cycles with a maximum temperature of 60 °C, Tao et al. reported the compressive strength to initially increased up to a number of 60 thermal cycles, following which a decrease in compressive strength was observed, with the value reaching the initial compressive strength after 120 cycles. The decline in compressive strength continued with further thermal cycles, so that a 19.4 % reduction compared to the initial strength was reached after 300 cycles [129]. Investigating the effect of thermal cycles with maximum temperatures of 40 °C, 60 °C and 80 °C, Li et al. found a slow decrease of strength within the first 100 cycles, followed by a faster decrease up to 200 cycles, and a reduced rate of decrease above 200 cycles [33].

In addition to the temperature gradient and number of cycles, other factors, such as type of aggregates and composition of the cement paste, water to cement ratio and the heating and cooling rate can affect the properties of the concrete exposed to cyclic thermal loads. As mentioned under section 2.1.5, aggregate type can significantly impact the performance of concrete upon exposure to elevated temperatures. In general, light weight aggregates are

believed to perform superior to their medium weight counterparts upon exposure to thermal cycles. Hossain et al. investigated the effect of different lightweight coarse aggregates, including pumice, perlite, lytag (sintered fly ash), and crushed brick upon the performance of concrete exposed to repetitive cycles of heating and cooling. Amongst these, specimens with lytag and brick aggregates were associated with higher residual compressive strengths compared to those with other aggregate types and similar to the control specimen. Perlite and pumice concrete specimens exhibited superior thermal performance compared to lytag and brick aggregate concrete samples, attributed to their porous microstructures. Basalt aggregates, on the other hand, led to significantly higher cracking levels in the cement paste and aggregates at elevated temperatures due to their low porosity, which hindered the vapor from being rapidly released from the concrete microstructure [130]. Type of the cement can be influential, as different cement produce matrices with different contents of C-S-H phase and different rehydration behaviors, different pore structures, and different pore coarsening and cracking tendencies [131]. The water to cement ratio plays an important part as well. Pastes with higher water to cement ratio have stronger resistance to the change of vapor pressure and better thermal fatigue performance. However, the lower initial strength of the concrete pores and matrix makes these undergo relatively severer thermal damage [124]. Last but not least, both the heating and cooling rate play a significant part, with faster heating and cooling rates leading to higher stress induction and greater damage to the concrete structure [66],[75],[76],[77],[132].

Many of the standard laboratory test settings, the details of which are presented under section 2.1.8, seek to determine the hot and residual properties of the concrete with the goal to investigate thermal resistance upon a one time exposure to thermal loads, e.g. in case of the fire, and provide the needed information to determine what can be saved after such incidents. However, with a few exceptions, standard methods to determine the residual properties of concrete at sustained or cyclical high temperatures is in great parts missing [121]. There has been, however, an increasing demand for obtaining such information for two main reasons. First, advanced industrial applications, particularly in nuclear reactors, demand a deeper understanding of the properties of different types of concrete under complex, sustained, or repetitive mechanical and thermal stresses at moderately high temperatures. Second, the development of new concrete mixtures and proportions continues to expand, which necessitates investigating the properties of these upon exposure to one time or repeated heating cycles depending on the intended use [35]. Fortunately, many building codes require testing the performance of concrete specimens (or even elements) during exposure to thermal loads. These prescribe testing conditions based on national and international standards for concrete fire resistance (temperature-time regimens). As the name suggests, these testing conditions are mostly to simulate one time exposure to fire, and do not consider (with a few exceptions) exposure to repetitive heating and cooling cycles, and the effect upon the residual physical and mechanical properties. In the next section, we will discuss how thermal resistance/performance of concrete is tested on the laboratory scale. We will begin with different temperature-time

profiles used for the simulation of thermal load exposure and describe the parameters that are measured in order to reflect the concrete's mechanical properties both during and after exposure to thermal loads. We will then briefly debate the limitations of these testing methods and address the areas where there is a need for further improvement.

2.2 Candidate materials for the design of sustainable thermal-resistant concrete

2.2.1 Slag sand and BFS

BFS is the main by-product of the iron and steel manufacturing process (approximately 90 % by mass), specifically the reduction stage, in which iron ore is converted into pig iron. During this process, the raw materials (iron ore, coke, and limestone) react at high temperatures. Reacting with the flux (limestone), the impurities in the iron ore form a molten slag on top of the molten iron [133]. Production of each ton of pig iron leads to the formation of around 200 - 300 kg of BFS (umbrella term referring to both air-cooled and granulated blast furnace slag) [134]. In Germany, about 11.4 million tons of iron mill slag were produced in 2020, of which 7.3 million tons were BFS [135]. This molten slag is then separated and can be cooled either rapidly (quenched) with water or slowly with air. The rapid cooling of BFS (e.g. water quenching) leads to the formation of granulated BFS with amorphous structure (> 90 %) and a glassy granular appearance, which is then dried and ground to form the ground granulated BFS, which is henceforth referred to as slag sand. This is often further ground and used to substitute CEM I as an SCM. Alternatively, the slow cooling of the molten slag allows for the formation of a more crystalline, rock-like structure, creating air-cooled BFS, which from hereon in, will be referred to as BFS. The dominant crystalline structure (> 50 %) of BFS prevents the slag to exhibit cementitious (latent hydraulic) properties, and the material is therefore used as aggregates [136]. Of the 7.3 million tons of BFS produced in 2020, more than 90 % was in the form of slag sand, which is used as SCM in concrete industry [135]. Both slag sand and BFS are composed of oxides of calcium (CaO; 29-50 %), silicon (SiO_2; 30-40 %), aluminum (Al_2O_3; 7-19 %), and magnesium (MgO; 0-21 %), as well as other materials (less than 10 %) [133],[137]. However, the smaller particle size of slag sand [138] (Blaine surface area around 300 - 600 m²/kg) [139] along with higher amorphous content [140] significantly increases its reactivity. Slag sand usually has a white to off-white color. Concrete containing slag sand can initially display a blue or green hue in the early days after placement, which generally fades with exposure to air and sunlight. The off-white color of the slag sand then enhances the whiteness and brightness of the concrete structure, which is often seen as an aesthetic benefit.

Slag sand is commonly used as an SCM and specified to use in concrete according to DIN EN 15167-1 [141],[142]. As previously mentioned, the development of mechanical properties in traditional concrete with CEM I clinker is due to the hydration of CaO, the production of which is associated with significant CO_2 emissions. Hence, improving concrete

sustainability can be achieved by using other materials that can produce strength forming phases through alternative pathways, such as SCMs. SCMs comprise a variety of natural pozzolans or industrial byproducts that can form additional C-S-H through pozzolanic and in cases hydraulic reactions [143],[144]. Materials with hydraulic activity are those that impulse $Ca(OH)_2$ to react with water and form cementitious compounds (C-S-H), while pozzolanic activity refers to the reaction with calcium hydroxide ($Ca(OH)_2$) in the presence of water to form additional cementitious compounds C-S-H. When mixed with water and $Ca(OH)_2$ (produced during the hydration of CaO in CEM I), SCMs form additional C-S-H through participation in pozzolanic reactions. C-S-H can in turn enhance the strength and durability of the concrete, reducing thereby the need for CEM I and decreasing the CO_2 production. SCMs are often used to replace a portion of the clinker in the cement to obtain optimal mechanical properties, reducing the amount of clinker required per ton of cement [143],[144]. Particularly replacing parts of the clinker with the industrial byproduct and different types of waste will help recycle these and thus further contribute to the improvement of concrete sustainability. Figure 2.10 illustrates a schematic presentation of the composition of the most commonly used SCMs, including slag sand (shown as SL) within the context of a $CaO\text{-}AL_2O_3\text{-}SiO_2$ ternary diagram.

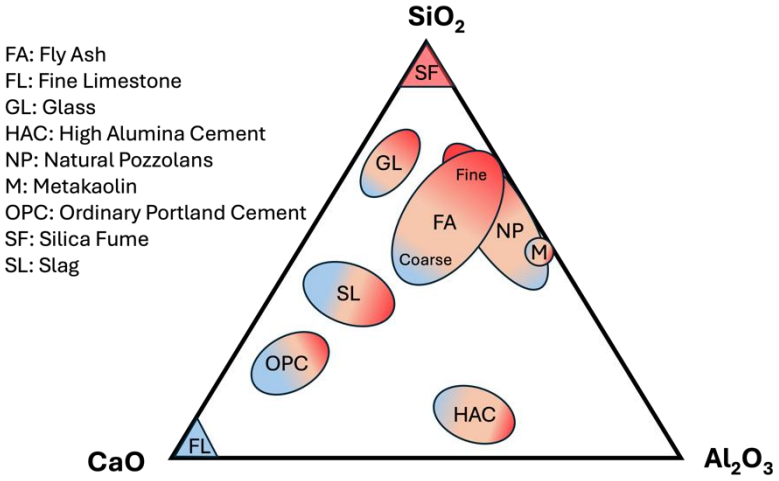

Figure 2.10 A CaO-AL2O3-SiO2 ternary diagram schematically presenting the composition of the commonly used SCMs including slag sand (shown as SL); Modified from [145]

The European Standard EN 197-1 introduces three types of Portland blast furnace cement, in which part of the clinker has been substituted by the slag sand. These include CEM III/A with 35 % - 64 % slag sand content, CEM III/B with 65 % - 80 % slag sand content, and CEM III/C with 81 % - 95 % slag sand content. Despite being defined in EN 197-1, however, the last type, CEM III/C is considered a specialty cement and is barely used for normal construction. EN 197-1 also introduces CEM II/B-S cement as a type of Portland-composite cement that contains 21 - 35 % slag sand [146].

Slag sand has latent hydraulic properties. This means that following activation by alkalis (such as those available in the (hydrated) cement paste, e.g. sodium oxide (Na_2O), potassium oxide (K_2O), calcium hydroxide ($Ca(OH)_2$), sodium carbonate (Na_2CO_3) and potassium carbonate

(K_2CO_3)), slag sand can get hydrated and form cementitious compounds [147]. These products are also referred to as “primary C-S-H”, which further contributes to the strength and durability of concrete on the long run. Other hydration products include calcium hydroxide ($Ca(OH)_2$), ettringite, AFm (alumina, ferric oxide, monosubstituted) phases and a hydrotalcite-like phase [148].

$$2(3CaO \cdot SiO_2) + 6H_2O \rightarrow 3CaO \cdot 2SiO_2 \cdot 3H_2O + 3Ca(OH)_2 \text{ (Primary C-S-H)} \quad \text{(Equation 2.3)}$$

[149]

Since the mechanism of slag sand’s hydration is different from that of the Portland clinker, it comes as no surprise that the rate of the reaction is also different. In general, the hydraulic reaction of the slag sand is much slower, for the addition of slag sand increases the stability of ettringite, which delays the hydration of the cement and the production of $Ca(OH)_2$ [150]. It has been shown that in the initial phases of hydration, the reaction is mainly with the alkali hydroxides, while at later stages, reaction with $Ca(OH)_2$ becomes more dominant [151].

To define the hydraulic activity of the slag sand, many different indices have been proposed. These include a variety of the chemical indices, which exploit the chemical composition of the slag sand to predict its hydraulic activity [152], the slag reactivity index introduced by the American standard ASTM C989 and the French standard NF P 18 - 506 (1992) [151],[152], and the hydraulic index (HI) defined by Keil et al, based on the compressive strength of the 70:30 slag sand: CEM I mortars [151],[153].

From a chemical standpoint, the hydraulic activity of slag sand depends on several factors, such as the basicity of slag, which is defined as CaO/SiO_2 ratio [154], the hydration temperature, water to cement content, replacement ratio and the tricalcium aluminate (C_3A) levels of the cement [140],[155].

In addition to the hydraulic reactions, slag sand can also lead to the formation of secondary C-S-H through further pozzolanic reactions with $Ca(OH)_2$ [156]:

$$3Ca(OH)_2 + 2SiO_2 + H_2O \rightarrow 3CaO \cdot 2SiO_2 \cdot 3H_2O + 3Ca(OH)_2 \text{ (Secondary C-S-H)} \quad \text{(Equation 2.4)}$$

[149]

The rate of pozzolanic reactions depends on many factors, including the source and chemical composition of the slag sand [157], the fineness of the slag sand (67 % faster reaction rates for ultrafine slag sand compared to ordinary slag sand) [158], the curing temperature (70 % at room temperature vs. over 90 % in the temperature range of 90 - 200 °C) [159], and the alkali involved in the reaction [140]. Figure 2.11. shows the modified changes in hydrated CEM I when blended with slag sand assuming a complete reaction of the former and 75 % reaction of the latter as reported by Lothenbach et al. [145] .

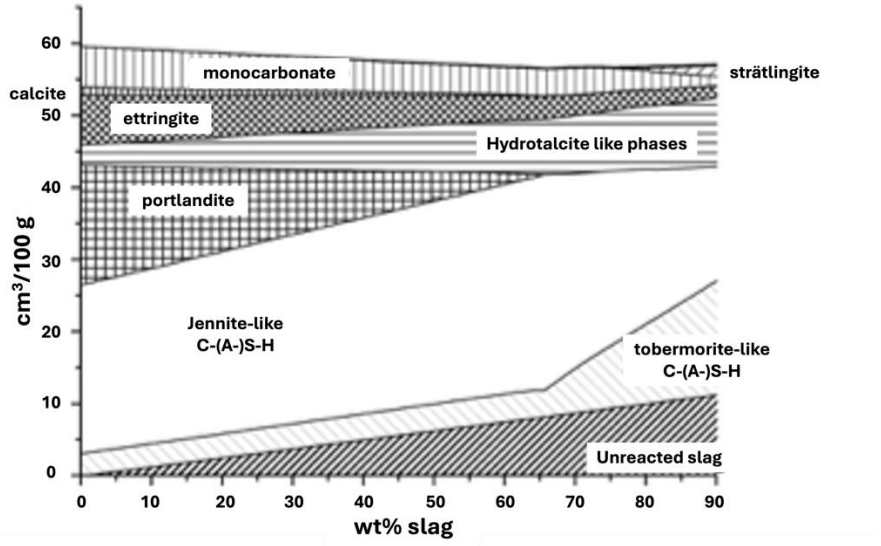

Figure 2.11 Changes in hydrated CEM I when blended with slag sand modeled by Lothenbach et al., assuming complete reaction of the CEM I (CaO 60, SiO2 22, Al2O3 4.6,Fe2O3 2.7, MgO 1.9, Na2O 0.3, K2O 1.0, SO3 3.2, and CO2 3 wt.%) and 75 % reaction of slag sand (CaO_3 9, SiO_2 38, Al_2O_3 11, Fe_2O_3 1, MgO 10, K_2O 0.3, and S 1wt.%).Al/Si in C–S–H=0.1 [145]

As a result of the latent hydraulic and pozzolanic reactions, slag sand can partially substitute part of the CEM I in the concrete structure, reducing thereby the carbon footprint of concrete through decreasing the CO_2 emission and recycling of industrial waste. For instance, substituting 50 % of the clinker by slag sand has been shown to reduce the CO_2 emission by 40 % [160]. Slag sand can also lead to an increase in the durability properties of the concrete. On one hand, since the hydraulic and pozzolanic reactions have a rather slow rate, they continue overtime which leads to an increase in the strength as the concrete ages [161]. On the other, compared to CEM I, slag sand generates less heat during hydration, reducing thereby the risk of thermal cracking in massive concrete members such as dams [162]. In general, slag sand has been shown to improve the resistance of concrete not only under normal conditions, but also to harsh environments and freeze-thaw cycles [163]. Due to creating a denser microstructure, slag sand decreases concrete permeability and thereby its resistance to sulfate attacks, chloride ion penetration and alkali-silica reactions (ASR) [164]. Furthermore, slag sand improves the workability of the fresh concrete and aesthetics of the resultant structures by virtue of its fine particle size and smooth texture [165]. Finally, the use of slag sand in the concrete industry helps recycling a waste product of another industrial process, further contributing to the sustainability perspective.

With all the mentioned benefits, the use of slag sand as an SCM is also associated with certain limitations. For one thing, it requires adequate alkalis presence in the concrete mix to ensure the activation of the hydraulic reactions. For another, the produced specimens have slower development of initial compressive strengths as it takes more time for enough C-S-H to be produced through hydraulic and pozzolanic reactions. In general, adding slag sand to concrete reduces the rate of hydraulic reactions, as it increases the stability of ettringite, which delays

the cement hydration and $Ca(OH)_2$ production. The slower production of $Ca(OH)_2$, a major player in pozzolanic reactions, reduces the rate of secondary C-S-H formation [150]. Hence, the degree to which clinker can be substituted by ground slag sand is limited. Most studies report that clinker substitution with slag sand leads to a delayed increase of compressive strength up to a certain slag content, following which the compressive strength is negatively affected. The defined optimum slag content has been different depending on the properties of concrete formulation. In general, however, the limit seems to be around 50 % [155],[162], [165],[166].

Unlike slag sand, air-cooled crystalline slag (BFS) has been often used as fine or coarse aggregates for asphaltic paving, road bases and sub-bases, railway ballast, and concrete production. The main benefits of using BFS as aggregates is mainly resource conservation by reducing the need for natural aggregates as well as waste reduction [167],[168]. Similar to slag sand, 95 % of the BFS chemical composition consists of CaO, SiO_2, Al_2O_3, and MgO. However, the physical properties are rather different as they are highly affected by the cooling conditions. Major chemical concerns in case of air-cooled BFS are; i) iron unsoundness, a rare phenomenon originating from the oxidization of the partially reduced iron oxides in BFS leading to expansion induced particle disintegration, ii) dicalcium silicate unsoundness, which occurs when a phase transition from the beta form to the gamma form takes place during cooling, leading to volume expansion and damage to aggregate structure (a.k.a. “falling,") iii) calcium sulfide content, which, according to DIN EN 12620 should be kept under 2 %, as higher values might contribute to changes in concrete microstructure, permeability and strength due to ettringite-mediated void filling, initiation of internal sulfate attacks, and formation of Thomasite [167], [169],[170].

The color of BFS aggregates typically ranges from light to dark gray, depending on its chemical composition, though occasional blue, green, or pink stains may appear in smaller areas. The aggregate particles exhibit a highly rough texture due to their vesicular structure, which results from gases trapped therein during cooling. While it is generally believed that the pores in BFS particles are not interconnected, thus making “vesicular” a more accurate description than “porous”, the internal voids may be accessible to liquids and gases from the particle's exterior [167]. Compared to natural aggregates, BFS aggregates possess higher angularity and lower specific density, which All these can influence the mix proportioning, the workability and the early-age shrinkage. BFS coarse aggregates have lower abrasion resistance than natural aggregates and are highly vesicular with low fracture energy/toughness. These characteristics impact the mechanical load transfer behavior at joints and cracks and account for a poorer aggregate interlock therein [167]. Indeed, reports on the mechanical performance of BFS aggregates have been quite mixed and depend on aggregate properties, particularly aggregate size [171],[172], aggregate content [173],[174],[175],[176]. The effect of these aggregates upon the performance of concrete at higher temperatures will be elaborated in section 2.2.2.2.

2.2.2 Effect of slag sand and BFS on the temperature resistance of concrete

In this section, the available information on the potential influence of slag sand and BFS used for the design of sustainable concrete alternative with improve thermal resistance will be debated. This section will be presented in two parts. The first part will focus on the effect of slag sand as an SCM and the second section will discuss the available literature on the use of slag sand and/or BFS as added aggregates.

2.2.2.1 Effect of slag sand as an SCM

As previously mentioned, slag sand and BFS are byproducts of high temperature processes in the iron industry. Hence, these are expected to be temperature resilient materials. However, when used as an SCM for the partial substitution of the CEM I, it is not the properties of the slag sand that determines the thermal and mechanical properties of the concrete at high temperatures, but rather the properties of the hydration products. In fact, slag sand as an SCM can enhance or reduce the high-temperature resistance of concrete depending on the replacement level, mix design, water to cement ratio and type of the aggregates. In general, CEM I substitution by ground slag sand is expected to affect the thermal resistance of the concrete as in the following:

i) Due to the lower $Ca(OH)_2$ content of the concretes in which part of the CEM I has been substituted by slag sand, the loss of concrete strength in the temperature range of 400 - 500 °C, which is associated with the decomposition of this hydration product, is expected to decrease [177],[178].

ii) Slag sand modifies the composition of the C-S-H gel, which, depending on the replacement level might increase the stability of the phase at high temperatures. According to Richerdson, the water content in C-S-H decreases with C/Si ratio. Slag sand promotes pozzolanic reactions and consume $Ca(OH)_2$ as well as free or even bound water, which forms additional (secondary) C-S-H with lower C/Si ratio than in pure CEM I. Due to the lower C/Si ratio, further pozzolanic reactions will involve a reaction process with water, making the water in specimens with slag sand to be more closely incorporated in the C-S-H structure. This makes it more difficult to dehydrate the C-S-H gel in the slag containing specimens [179],[180]. Hence, the stability of the concrete at high temperatures might be different from the concrete without slag sand.

iii) Presence of slag sand in concrete increases the proportion of fine pores, which improves concrete strength.

iv) Concrete containing slag sand has a denser microstructure [177]. This can improve the thermal resistance by reducing the permeability of the concrete, thereby limiting moisture migration upon rapid heating. On the downside, limiting the escape of water vapor can also increase the risk of explosive spalling.

v) Partial substitution of the CEM I by minerals such as ground slag sand has been shown to lower the thermal expansion coefficient of the concrete. This can reduce the thermal mismatch between the cement paste and the aggregates, thereby improving the performance of concrete at high temperatures [181].

vi) Partial substitution of the CEM I by ground slag sand reduces the amount of lime available for rehydration post-cooling, which mitigates the associated volume expansion and the resultant strength loss and crack development [182].

A number of studies have already been dedicated to comparing the thermal resistance of mortars/concrete made of CEM I and the slag sand containing cement CEM III/A. In the following, we will review the most important findings of these studies. Detailed information about the composition and development of the specimens used for these investigations are summarized in Table A.1.2.

Andiç-Çakır et al. investigated the residual compressive strength and residual flexural strength of the mortars made of CEM I and CEM III/A (with 45 % slag sand content) cast with siliceous standard sand aggregates. The specimens were exposed to temperatures of 150, 300, 450, 600 and 900 °C for 4 h and subsequently cooled down to room temperature for 24 h, following determination of the mechanical properties. The results demonstrated that specimens made of CEM III/A had higher residual compressive strength when heated to all temperatures except for 150 °C. The residual flexural strength of the specimens made of CEM III/A was higher than the mortars made of CEM I when exposed to 450 °C, the temperature associated with the decomposition of $Ca(OH)_2$, and almost similar when heated to 300, 600 and 900 °C. Similar to the residual compressive strength, the residual flexural strength of the CEM III/A mortars was lower when heated to 150 °C. Scanning electron microscopic imaging revealed that high temperature-induced cracks in CEM I paste microstructure were significantly larger than those observed in the CEM III/A paste (Figure 2.12). With the exception of 150 °C, the mass loss of CEM III/A containing mortars was always higher than specimens made of CEM I [183].

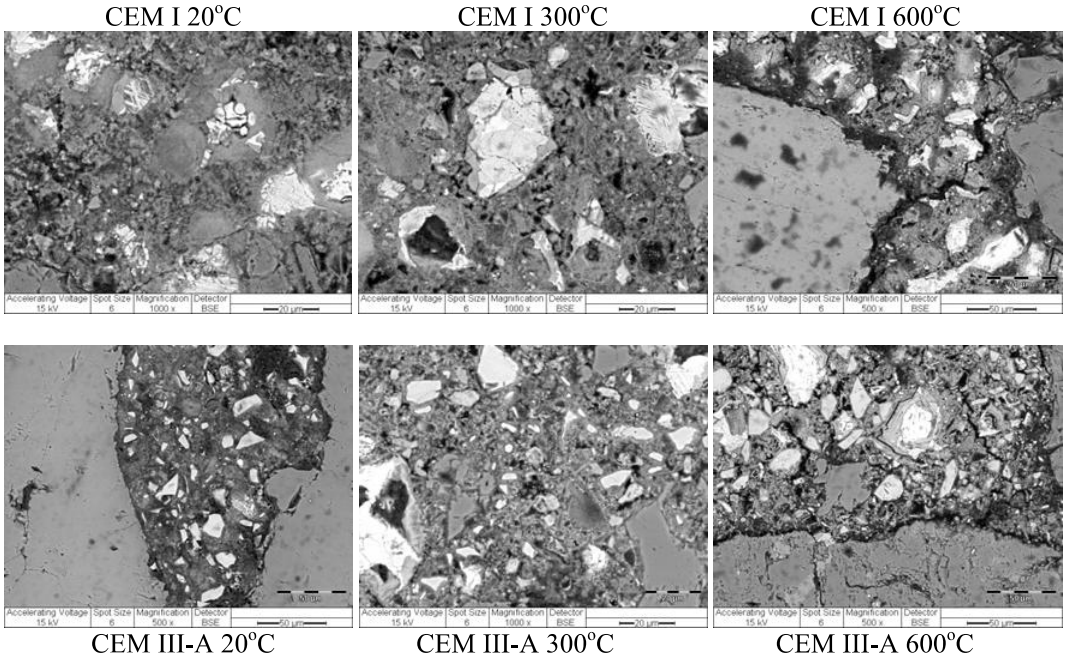

Figure 2.12 Scanning electron microscopic images showing temperature-induced crack sizes in cement paste of mortars made of CEM I and CEM III/A at 20, 300, and 600 °C [183]

Zemri et al. made a similar comparison between the concrete (hardened cement paste without aggregates) and mortars made of CEM I and CEM III/A. Specimens were heated to 160, 300, 400 or 650 °C with a heating rate of 1 K/min and a holding time of 1 h. Residual compressive strength as well as the residual modulus of elasticity were determined once the specimens were cooled to room temperature. Results demonstrated that concrete (hardened cement paste) specimens made of CEM I had slightly higher relative residual compressive strength after heating to all temperatures: 136 % vs. 120 % at 160 °C, 123 % vs 96 % at 300 °C, and 99 % vs. 90 % at 400 °C for specimens with CEM III/A and CEM I, respectively. When heated to 600 °C, however, concrete made of CEM I underwent spalling, whereas those made of CEM III/A retained 60 % of the initial compressive strength post cooling. In case of mortars, however, the relative residual compressive strength of specimens made of CEM III/A was significantly higher: 107 % vs. 114 % at 160 °C, 87 % vs. 110 % at 300 °C, 71 % vs. 79 % at 400 °C, and 23 % vs. 36 % at 650 °C for specimens made of CEM I and CEM III/A, respectively. The residual modulus of elasticity of both hardened cement paste and mortar specimens reduced by increasing temperature, but it was always higher for those made of CEM I (except for concrete heated to 650 °C). In general, the results demonstrated that specimens made of CEM III/A are significantly more resistant to higher temperatures (here 650 °C), as they partially retained their compressive strength after cooling, while both concrete and mortars made of CEM I showed significant cracking [184].

Hager et al. compared the residual compressive and splitting tensile strengths as well as residual modulus of elasticity of the concrete specimens made of CEM I and CEM III/A, either in combination with riverbed gravel or crushed basalt as coarse aggregates after heating to 200,

400, 600, 800, and 1000 °C. The specimens were heated to the target temperature with a rate of 0.5 K/min and were held at the maximum temperature for 3 h. Results showed a very slight and overall insignificant difference between the relative residual compressive and splitting tensile strengths and the residual modulus of elasticity of the concretes made of both cement types, regardless of the type of coarse aggregates used. Permeability measurements demonstrated that specimens made of CEM III/A were generally associated with only slightly lower values. It was concluded that it is more the type of aggregate, and not the type of the cement, that determines the mechanical properties of the concrete post thermal load exposure [185].

The thermal resistance of specimens made of slag sand has been also investigated upon long-term exposure. For instance, Carette et al. investigated the effect of 35 % slag sand in the cement upon the long-term thermal resistance of concrete. Specimens were subjected to 75, 150, 300, 450 and 600 °C for 1, 4 or 8 months. Measurement of the residual compressive strength demonstrated that addition of the slag sand as an SCM did not improve the residual mechanical properties of the concrete regardless of the temperature or water to cement ratio [186].

Other studies have sought out the optimal slag sand content for improved thermal resistance. Wang investigated the effect slag sand content in the cement (5, 10, 20, 50 and 80 %) upon the residual compressive strength of the concrete specimens with three different water to binder ratios (0.23, 0.47 and 0.71) after exposure to different elevated temperatures (105, 200, 440, 580, 800, and 1050 °C). The holding time was 2 h for 105 °C, 6 h for 200 °C and 440 °C and 4 h for the rest of the temperatures. In general, the results show that increasing the slag sand content to above 50 % improves the relative residual compressive strength of the concrete when heated to above 200 °C, with the effect of high slag sand content being more pronounced for the highest water to binder ratio (0.71; Figure 2.13.a). The positive effect of higher slag sand content upon the residual modulus of elasticity, however, is more pronounced for lower water to binder ratios. In general, it was concluded that increasing slag sand content of the concrete significantly improved the thermal resistance [187]. The positive effect of increasing the slag sand content has been also confirmed by Aydin, who compared the relative residual compressive strength of pumice mortars with 0, 20, 40, 60, and 80 % slag sand heated to different elevated temperatures with a rate of 10 K/min. He observed the most beneficial effect of the higher slag sand content at 900 °C, at which the mortars containing 80 % slag sand merely lost 25 % of the original compressive strength post air cooling, whereas those without slag sand lost 70 % [188]. With the water to cement ratio being around 0.7, these results are in accordance with the findings reported by Wang [187]. Similarly, Delhomme et al. reported an increase in the slag sand of the mortars to improve the relative residual compressive strength at all temperatures. Using X-ray diffractometry, the authors demonstrated that the reason for the slag sand mediated improved residual compressive strength above 500 °C is the ability of slag sand to react with lime, which limits the $Ca(OH)_2$ production. As the production of $Ca(OH)_2$ is associated with significant volume expansion, presence of slag sand lowers the risk of cracking that can occur as a result [182]. Sim et al. investigated the effect of slag sand in concrete (0 %,

20 % and 40 %) with water to cement ratio of 0.48 warmed up to 200, 400 and 600 °C and measured the value of hysteresis nonlinearity parameter, α as an indicator of the development of thermal damage induced microcracks in concrete. Based on this value, they concluded the 40 % slag sand content to be associated with the lowest thermal damage to the structure of the concrete [189]. Hosam et al. studied the effect of 10 % and 20 % slag sand in the concrete upon its thermal resilience and reported increased relative residual compressive strength at all temperatures; most notably 80 % vs. 64 % at 600 °C and 36 % vs. 32 % at 800 °C for concrete with and without slag, respectively. When heated to 400 °C, the relative residual compressive strength of the specimens with 20 % slag sand was higher than those with 10 % slag sand [190].

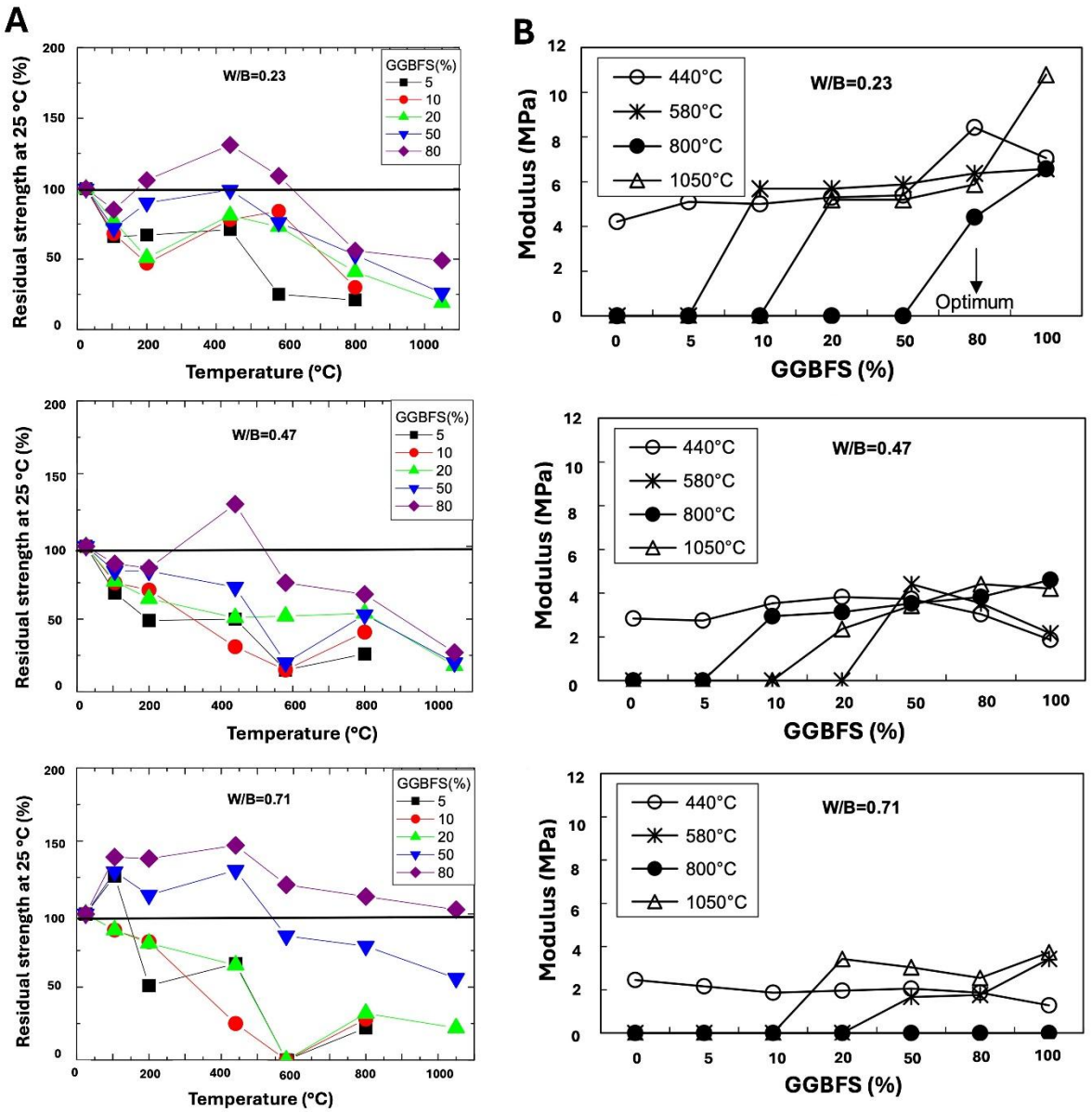

Figure 2.13 A) Relative residual compressive strength of the concretes with different slag sand (GGBFS) content following exposure to various elevated temperatures for concrete with different water to binder (WB) ratios and B) effect of slag sand (GGBFS) content upon the residual modulus of elasticity of the concrete with different WB ratios as reported by Wang [187]

Literature also holds reports that are to the contrary. For instance, Li et al. exposed concrete

mixtures with 0, 50, 60, and 70 % slag sand and crushed stone and river sand as coarse and fine aggregates to different elevated temperatures. Specimens were heated to 200, 300, 400, 500, 600 and 700 °C with a heating rate of 5 K/min and were kept at the mentioned maximum temperatures for 240, 200, 160, 140 and 90 min, respectively. The specimens were then water cooled for 30 min to reach the room temperature. The results demonstrated minor differences between the residual compressive strength and the residual module of elasticity of the specimens made of pure CEM I and those with 50 % slag sand content at different temperatures, while increasing the slag sand content above 50 % reduced the values of both parameters. Similarly, specimens with 60 % and 70 % slag sand content had slightly lower residual splitting tensile strength compared to concrete made of pure CEM I, whereas a slag sand content of 50 % slightly increased the residual splitting tensile strength of the specimens [191]. The authors found similar results in a different publication for concrete with 0, 10, 30 and 50 % slag sand content. They showed that increase of the slag sand content of the cement from 10 % to 30 and 50 % led to a significant reduction of the residual compressive strength when heated to 500 °C. Concrete with 50 % slag sand content showed the lowest residual compressive strength when heated to all temperatures above 300 °C. Moreover, the increase in the slag sand content of the cement resulted in a reduction of the modulus of elasticity. The authors also showed that increasing the slag sand content of the concrete led to the increase of the carbonation depth at all temperatures, with a temperature dependent trend being observed at for all concretes regardless of the presence or absence of the slag sand [192].

Mendes et al. demonstrated that the effect of slag sand on the residual compressive strength of concrete depends on the cooling rate. The authors compared the residual compressive strength of the specimens with 0, 35 and 50 % slag sand following exposure to 400 °C and 800 °C. The specimens were air or water cooled to room temperature. Measurements of the residual compressive strength demonstrated that while both the specimens with or without slag sand lost around 20 % additional residual compressive strength when water cooled, following exposure to 800 °C, specimens with slag sand only lost 5 % water cooling induced residual compressive strength versus the 14 % observed in case of concrete made of pure CEM I. Infrared analyses suggested that the higher strength loss in the specimens without slag is due to the accelerated CaO rehydration into $Ca(OH)_2$ in CEM I (Figure 2.14) [193].

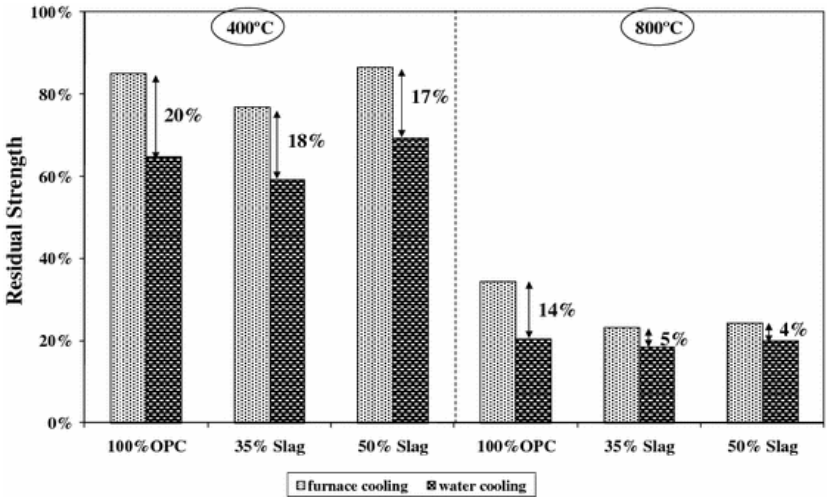

Figure 2.14 Effect of air and water cooling upon the residual compressive strength of concrete with different amounts of slag sand following exposure to 400 °C (left) and 800 °C (right) as reported by Mendens et al. [193]

Other studies report that the incorporation of the slag sand in the concrete can improve the residual mechanical properties up to a certain replacement ratio, above which the residual compressive strength either does not change or decreases. For instance, Siddique and Kaur showed the positive effect of slag sand as SCM upon the residual compressive and splitting tensile strengths as well as the residual modulus of elasticity. In addition to the cement mix with 0, 20, 40 and 60 % slag sand content, the investigated concrete specimens also contained silicious fine and coarse aggregates. The results demonstrated that while addition of the slag sand decreased the initial compressive and splitting tensile strength of the concrete, slag sand containing concretes had higher the relative residual compressive and splitting tensile strength of the concrete compared to the specimens made of pure CEM I. However, increasing the slag sand content beyond 20 % did not bring about any additional benefits [194]. Singh et al. developed concrete mixes with different contents of slag sand (0, 5, 10, 15, 20 and 25 %) and nanosilica (1-5 %) and investigated the fire resistance thereof using the ISO 834 standardized fire curve. Measurement of the residual compressive strength after air or water cooling revealed that regardless of the cooling rate, increasing the slag sand content of the concrete up to 20 % and the nano silica up to 4 % increased the relative residual compressive strength. Above this level, the value of the relative residual compressive strength decreased after exposure to all temperatures [195].

As observed, the results of the studies described above are rather controversial. Some studies report that the addition of slag sand does not much improve the residual mechanical properties while others report a significant improvement. Some report an optimum slag sand content above which the thermal resistance is not further enhanced, while others propose a “the less, the better” or “the more, the better” concept. In general, it can be concluded that based on the reviewed literature, the impact of slag sand on the thermal resilience of the concrete might depend on a variety of factors. First, the exposure temperature seems to be paramount. Many of the reviewed studies suggest a significant improvement of thermal resilience of slag sand

containing concrete exposed to higher, more extreme temperature (>800 °C) [184],[187],[193]. As this temperature is associated with the decomposition of the $CaCO_3$ in CEM I, improvement of the thermal resilience due to the partial replacement of CEM I with slag is to be expected. Second, the aggregate size seems to play a major part. In general, the effect of slag sand on the thermal properties of mortars seems to be more positive than the concrete [182],[187],[188]. The third factor is the water to cement ratio, where very high slag sand contents (60-80 %) seem to generally be more beneficial for specimens with higher water to binder ratio (0.7) [182],[187],[188]. Next is the strength of the concrete, which also depend on the water to cement ratio. Investigations made by Poon et al. and Xiao et al. have shown that incorporation of lower contents of slag sand (< 50 %) in the cement mix has a more positive impact on the thermal resilience of high strength concrete than it does on the normal strength concrete [82],[196]. The cooling rate seem to be also determining, as air cooling has shown to bring about the positive impact of slag sand more significantly than water quenching [193]. Last but not least, is the type of aggregates used in the preparation of the concrete, as the thermal performance is largely determined by the difference in the thermal expansion coefficient of the cement paste and the aggregates [185]. While these general assumptions can be made based on the findings of the reviewed literature, drawing certain conclusions requires a systematic investigation by using standardized cement and aggregates with standardized parameters to investigate the effect of each and every one of the mentioned parameters.

Another point to be heeded to is that all described experiments have focused on the investigation of the effect of slag sand upon the residual properties of the concrete. Merely an early study has been dedicated to the measurement of the compressive strength of the concrete with slag sand under hot conditions. In this study, Sullivan and Sharsar have demonstrated that upon exposure of firebrick concrete containing slag sand to different elevated temperatures (up to 600 °C), the hot compressive strength remains over 80 % of the value in cold conditions. In the absence of slag sand, the same concrete type undergoes as significant decrease of hot compressive strength above 300 °C, with the value reaching 50 % of the cold compressive strength at 600 °C. The authors reported the optimal slag content for achieving adequate thermal performance is 35 % [197].

2.2.2.2 Effect of slag sand and BFS as fine and coarse aggregates

Compared to the number of the studies, which have investigated the effect of slag sand as SCM upon the thermal resistance of concrete, fewer studies have been dedicated to the investigation of the effect of slag sand or BFS as aggregates. In this section, the results of these investigations will be summarized. Detailed information on the composition of the specimens as well as the properties of the used aggregates are shown in Table A.1.3.

Vaidya et al. investigated the effect of partial replacement of natural sand with slag sand as fine aggregates. To this end, 20, 40 or 60 % of the natural sand in the concrete was substituted by slag sand. Concretes also contained CEM I as cement, undefined coarse aggregates with a

diameter of 20 mm and 1 % steel fiber. Concretes were heated up to different elevated temperatures (200, 400, 600, 800 and 1000 °C) and after a holding time of 30, 60 or 90 min following which they were allowed to cool down naturally for 1 h. The residual compressive, splitting and flexural tensile strength were measured. The results demonstrated that partial substitution of natural sand by slag sand aggregates significantly improved the relative residual compressive strength of the concrete upon exposure to higher temperatures, namely 800 °C and 1000 °C for all exposure durations. As the exposure time lengthened, the increase in the slag sand content at these temperatures negatively affected the relative residual compressive strength, with the 20 % substitution ratio giving the best results when concrete was exposed to 800 °C and 1000 °C for 90 min. In general, specimens with 40 % slag sand were associated with the highest cold compressive, flexural and splitting tensile strengths and had acceptable performance upon exposure to higher temperatures. Hence, the authors proposed the 40 % slag sand aggregate content for optimal performance at room temperature and under thermal loads [198].

Yüksel et al. investigated the effect of substituting different amounts of the 0-3 mm river aggregates by non-ground granulated BFS, bottom ash or a combination of both with equal ratios upon the temperature resistance of concretes. 3-7 mm river aggregates were used as coarse aggregates. The authors prepared three different series of specimens. Series C comprised specimens with 10, 20, 30, 40 or 50 % nonground granulated BFS, series K with the same contents of bottom ash, and series CK with the same contents of a combination of the two aggregates in equal amounts. The specimens were heated to 800 °C with a rate of 6 K/min and the relative residual compressive strength was measured and calculated after cooling naturally to room temperature. The results demonstrated that substitution of 10 % and 20 % of the river aggregates by non-ground granulated BFS improved the residual compressive strength, with higher slag aggregate content improving the value. However, increasing the content of slag aggregates above 20 % reduced the residual compressive strength, though the values obtained for 30 % and 40 % were still similar to that of slag-free concrete. Only when the content of the slag aggregate was raised to 50 % did the residual compressive strength decreased by 2 % compared to the slag-free control. When mixed with bottom ash, the relative residual compressive strength further improved, though a similar trend in terms of replacement ratio was observed, where substitution ratios above 20 % lead to a content dependent decrease of the residual compressive strength [199].

Vaidya et al. have also studied the effect of BFS as coarse aggregates upon the mechanical properties of the concrete following exposure to thermal loads. The specimens were made with locally available coarse aggregates, part of which (0 %, 20 %, 40 % or 60 %) was substituted by BFS aggregates. They also contained 1 % steel fibers. Specimens were heated to different elevated temperatures (200, 400, 600, 800 or 1000 °C) and the residual compressive of the specimens were measured after cooling. The results show that while all concrete specimens containing BFS aggregates had higher cold compressive strength compared to their BFS-free

counterparts, increasing the BFS content above 20 % did not lead to an increase of the initial compressive strength, but very slightly reduced it. Furthermore, comparison of the relative residual compressive strength of the specimens revealed that substitution of 20 % of the coarse aggregated for BFS aggregates significantly improved the residual compressive strength at all temperatures (Figure 2.15). The difference is most significant when heated to 800 °C, where the relative values of the residual compressive strength were equal to 59.2 % and 73.1 % for specimens without BFS aggregates and those with 20 % BFS aggregates, respectively. However, increasing the BFS aggregate content above this level leads to a content dependent decrease of the relative residual compressive strength at all temperatures, with the values being lower than that calculated for BFS-free control [200].

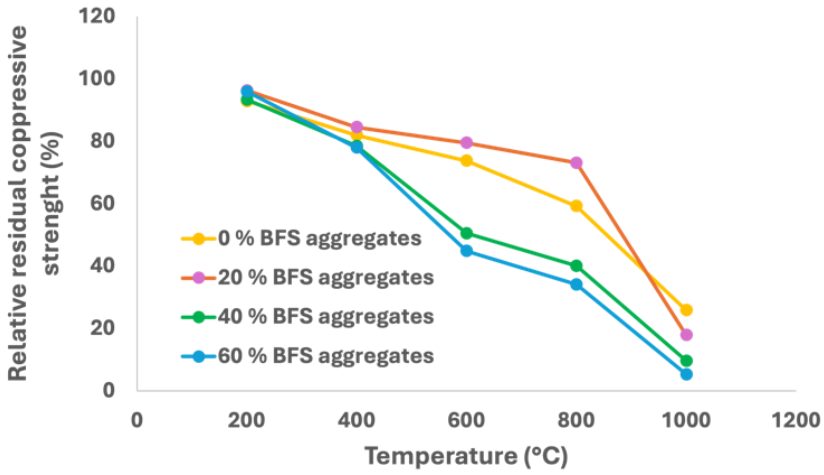

Figure 2.15 Relative residual compressive strength of concrete with different contents of slag sand as coarse aggregates upon exposure to different elevated temperatures. Values have been calculated based on the absolute residual compressive strengths reported by Vaidya et al. [200]

2.2.3 Other metallurgical slags

In addition to the slag sand, other metallurgical slags have been also examined for their potential to serve as SCMs. In general, metallurgical slags are classified as ferrous, non-ferrous, and red mud. Ferrous slags are byproducts of steel and iron production, while non-ferrous slags originate from other metal industries.

There are two general technological routes for steel production in steel mills; integrated plants, and semi-integrated plants [133]. Slag sand and BFS, which were elaborated on in the previous section, are byproducts of the first technology. Two of the most important slags obtained from non-integrated technologies are steel slags produced in the basic oxygen and electric arc furnaces during the refining stage.

Basic oxygen furnace steel slag (BOF slag) or LD-slag (in this dissertation) is a solid byproduct generated during the steelmaking process, specifically while refining of crude iron in a Linz-Donawitz oxygen converter [201]. BOF slag production is approximately 100-150 kg per 1 ton of steel, with global production reaching approximately 160-240 million tons annually

[202],[203]. The primary chemical components of BOF slag include CaO, Fe_2O_3, SiO_2, Al_2O_3, MnO, and Mg [204]. Due to its cementitious properties, BOF slag has been used as a construction material for many years [205].

Electric arc furnace (EAF) slag or Ef-slag (in this dissertation) is generated during the primary steelmaking process in EAF, with production rates ranging from 120 to 170 kg per ton of steel produced. The primary chemical constituents of EAF slag include iron oxides (FeO, Fe_2O_3), lime (CaO), silica (SiO_2), magnesia (MgO), and alumina (Al_2O_3). Additionally, trace amounts of chromium, manganese, and phosphorus oxides, as well as small quantities of free lime, are also present in the slag [206].

Ladle furnace (LF) slag and argon oxygen decarbonization converter (AOD) slag are other types of steel slags, produced during secondary refining process in LF and argon OAD converter, respectively [201],[206]. The secondary steelmaking process produces approximately 20-30 kg of LF slag [207] and 100–200 kg AOD slag [208] per ton of steel. The chemical and mineralogical properties of LF slag can vary greatly depending on its origin and the specific refinement process, as various alloys are added to the LF to achieve the desired steel grade [209]. The chemical composition of LF slag is thereby highly dependent upon the grade of produced steel [210]. Most sources report CaO and SiO_2 as the main components, followed by Al_2O_3 and to a lower extent Fe_2O_3. Other components include MgO, TiO_2 and MnO [211],[212]. AOD slag has a less variable composition and mainly comprises CaO and SiO_2, Al_2O_3, MgO, MnO, and low amounts of iron and chromium [213]. It naturally disintegrates during the cooling process, mainly owing to the β to γ dicalcium silicate (Ca_2S) phase transition [214].

Steel slags have been widely investigated as SCM and filler [215], as fine or coarse aggregates [216], and as alkali-activated binders [217] for the production of low carbon cements. Similar to BFS, steel slags can be cooled rapidly or slowly, which affects the crystallinity and thereby the reactivity [209],[218]. In general, the hydration reactivity of the steel slags is rather low. Accordingly, when used directly to substitute CEM I, the resulting specimens often possess low compressive strengths. Wang et al. investigated the effect of 5, 30 and 45 % CEM I substitution by BOS furnace steel slag upon the compressive strength of the concrete specimens. They found that when water to cement ratio was kept constant, increasing the steel slag substitution ratio reduced the compressive strength, in particular at early ages. For specimens with similar 28-day compressive strength, however, steel slag increased the late-stage compressive strength compared to the CEM I control [219]. Similar results have been reported for induction oven slag [220]. Fang et al. reported that CEM I replacement by LF slag up to 10 % could improve the mechanical properties of the concrete. On the contrary, substitution ratios of 10-30, though leading to strength gain at ultra early stages, led to strength loss in middle and late stages [221]. These results have been confirmed by Sultana et al. [211]. Araos et al. and Santamaria et al. reported that CEM I substitution by LF slag led to reduction of workability and decrease of the compressive strength [222],[212]. In addition to lowering the early compressive strength, steel

slags are also associated with the problem of swelling and expansion, which poses a great obstacle to their use in concrete constructions. Long-term storage in natural environment, supplementation with siliceous materials, mechanical grinding, water immersion treatment, and surface modification have been used to mitigate this issue [223].

When used as aggregates, steel slag, has been shown to increase the concrete's compressive strength up to a certain content (around 35 %) [224],[225]. A positive effect of steel slag aggregates on the concrete mechanical properties have been reported by other authors [226],[227],[228]. Unlike steel slag sand, the use of steel slag coarse aggregates can increase the fluidity of the mix [225],[227].

Non-ferrous slags, by-products of pyrometallurgical processing of non-ferrous metals (e.g. aluminum, copper, zinc, nickel and lead), have recently attracted interest in construction applications, particularly as SCMs, and to much lower degree, as aggregates in concrete. These slags differ from ferrous slags, such as steel slag or BFS in their chemical composition, physical properties and the metals from which they are derived. Compared to their ferrous counterpart, these have been less widely exploited in the concrete production industry. The pozzolanic activity of many non-ferrous slags such as copper slag [229], lead slag [230], nickel slag [231], and zinc slag [232] has been demonstrated. Nonetheless, non-ferrous slags have been less widely explored as SCMs compared to BFS and even steel slag. This lower interest can be attributed to the lower global production of non-ferrous slags [233] and the presence of sulphates, other anions and heavy metals in untreated non-ferrous slags, which can hamper the cement hydration process, while risking the release of contaminants to the environment on the long run [203],[233]. To increase the reactivity of non-ferrous slags and to reduce the heavy metal and anion content thereof, a secondary thermal treatment has been introduced. Additionally, rapid water cooling is often employed to prevent crystallization and to enhance slag reactivity. Additives like silica and limestone may be introduced as fluxes to lower the melting temperature, optimize viscosity, and increase reactivity as SCMs or in alkaline environments [233]. Similar to other types of slags, reduction of particle size through mechanical activation [229],[234],[235], as well as chemical activation, particularly using alkali [236] have been exploited to increase the reactivity of non-ferrous slags.

Non-ferrous slags are less suited for use as aggregates in concrete due to several reasons. For one, the significantly higher specific gravity of these aggregates leads to segregation of the paste or bleeding. For another, some metallurgical slags, e.g. lead and zinc slag, can reduce the fluidity or prolong the setting time of paste [203],[237].

Literature holds merely few studies, which have been dedicated to the investigation of the thermal resistance of concrete containing other metallurgical slags either as SCMs or as aggregates. One of these studies have been conducted by Boquera et al., who investigated the effect of steel slag aggregates upon the thermo-mechanical stability of concrete containing steel slag as aggregates following exposure to thermal cycles. The authors prepared concrete with

two different types of cement; CEM I and calcium aluminate cement (CAC) each in combination with either silico-calcareous aggregates or steel slag aggregates. Details on the composition of the specimens is shown in Table A.1.4. The specimens were exposed to 10 thermal cycles for a total duration of 185 h with temperatures in the range of 290 °C (minimum) to 700 °C (maximum). The macro-level visual inspection following thermal cycling revealed greater damage in concrete samples containing silico-calcareous aggregates, leading to fragmentation. In contrast, regardless of the cement type, samples incorporating steel slag aggregates maintained cohesion. However, micro-level analysis indicated a distinct separation at the interface between the cement paste matrix and the steel slag aggregates. The authors also found that in general and regardless of the cement type, specimens made of steel slag aggregates had lower thermal conductivity compared to their silico-calcareous aggregate containing counterparts. This pattern was still observed after exposure to thermal cycling, though the decrease in the thermal conductivity of the latter was more significant. The results for the residual compressive strength show, that use of steel slag aggregates in combination with both cement types led to a significant increase of the cold compressive strength, the residual compressive strength of these specimens after thermal cycling was significantly lower than the concrete with silico-calcareous aggregates. The authors linked the reduction in residual compressive strength and the high porosity observed in steel slag samples to detachment within the interfacial transition zone between the cement paste and the aggregates. However, significant degradation was observed in the silico-calcareous aggregates, leading to cracking in the coarse particles. It was generally concluded that the use of calcium aluminate cement and CEM I cement with steel slag aggregates lead to a limited concrete cohesion under the tested thermal cycling profile [238].

A second study within this context was carried out by Saha et al., who investigated the effect of ferronickel slag aggregates. To this end, 25, 50, 75 or 100 % of the natural siliceous sand was replaced by the ferronickel aggregates. The specimens were heated to different elevated temperatures (200, 400, 600 and 800 °C) with a heating rate of 5 K/min and were hold thereat for 2 h, following which they were free cooled to room temperature. It was demonstrated that substitution of sand for ferronickel aggregates increased the cold compressive strength up to 50 %, following which the compressive strength slightly reduced. The relative residual compressive strength, however, decreased by increasing the ferronickel slag content of the mortars. For specimens with 25 and 50 % substitution ratio, the content dependent reduction of residual compressive strength was only visible when heated to higher temperatures (600 and 800 °C). In case of higher substitution ratios, the effect was observed at all investigated temperatures [239].

2.2.4 Limestone

Limestone has been long since used to replace part of the CEM I, leading to the development of standard cements such as Portland-limestone cement (PLC) as classified under DIN EN 197-

1 [146]. The main objective of incorporating limestone has been to improve the properties of the concrete and to reduce the CO_2 burden. Today, PLC is sometimes classified as LCC (low carbon cement), mainly due to the fact that the use of ground limestone reduces the clinker content [240]. At low replacement levels, limestone powder not only promotes clinker hydration through providing nucleation sites (filler effect), but also, according to literature, interacts with C_3A in cement, forming minerals, which contributes to the development of compressive strength [241],[242]. Some sources even state that limestone functions as SCM when it is finely ground with clinker into the cement. It has been demonstrated that when finely ground, limestone can actively participate in the hydration process, forming crystallohydrates such as calcium monocarboaluminate [243].

The European Standard EN 197-1 allows a maximum substitution of 35 % of the CEM I by limestone (Type II/A-LL containing 6-20 % and Type II/B-LL containing 21-35 % limestone powder) [146]. It is generally believed that the beneficial effects of limestone substitution is limited to a maximum level of 10-15 %, above which the dilution of the CEM I leads to slower setting time and strength gain [244],[245]. It has been shown that replacing 10-15 % of the CEM I by limestone can reduce the CO_2 emissions by 10 % [244],[246]. In addition to its use in partial substitution of the CEM I, limestone can be also use as aggregates within the concrete.

The effect of elevated temperatures upon the properties of concrete and mortar comprising limestone in either form has been investigated in several studies. Here, we will first review the effect of limestone incorporation in the cement. Detailed information about the mix proportion and curing conditions for this and all further studies are presented in Table A.1.5. Klingsch et al. investigated the hot and residual compressive strength of the concretes made of CEM I and CEM II/A-LL with similar compositions heated to 300, 500 and 700 °C and kept at the maximum temperature for 2 h. For the specimens heated to 500 °C, compressive strength was also measured when the specimen temperature sank to 300 °C during air cooling. For those heated up to 700 °C, compressive strength was measured when the specimen temperature reached 500 and 300 °C during cooling. The relative compressive strength values for specimens with both cements is shown in Figure 2.16. As observed, regardless of the maximum temperature, specimens made of CEM II/A-LL are associated with slightly higher compressive strength values compared to those made of CEM I alone [247].

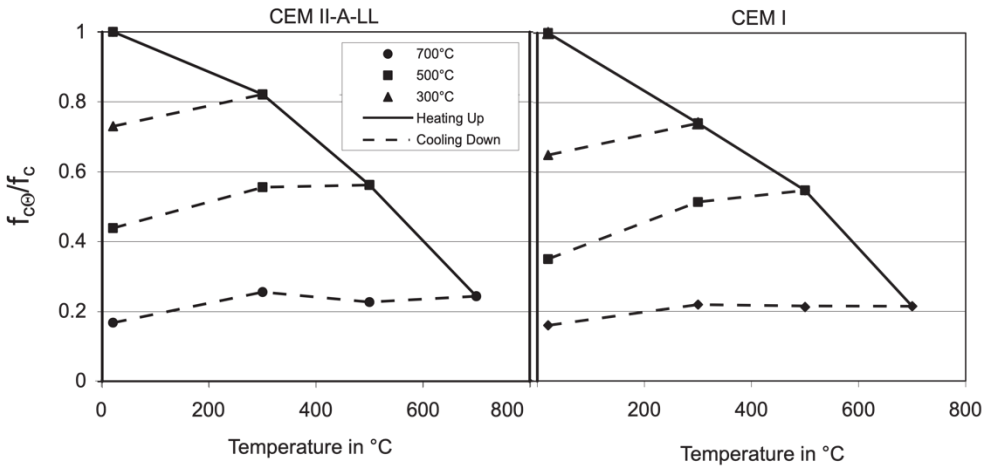

Figure 2.16 Compressive strength of the concrete made of CEM I or CEM II/A-LL at different temperatures during the heating and cooling phases as reported by Klingsch et al. [247]. The image has been slightly modified from its original form to fit the context of this dissertation

Adel Mohammed et al. prepared concretes in which 0, 10, 15, 20 or 25 % of the CEM I was substituted by limestone. Sand and gravel were used as aggregates. The specimens were heated to different elevated temperatures (200, 400 and 600 °C), at which they were kept for 1 h. Residual compressive and tensile strengths were measured after cooling. It was shown that substitution of 10 % of the CEM I with limestone could decrease the loss of compressive strength at all temperatures, with best results having been observed for 200 °C. Higher substitution ratios, however, led to higher levels of compressive strength loss when compared to concrete made of pure CEM I. The splitting tensile strength decreased more significantly when limestone was incorporated in the cement, with 10 % substitution accounting for lower reduction levels [248].

El-Kurdi et al. investigated the effect of 10 and 15 % CEM I substitution by limestone and the influence of adding 10 and 15 % additional limestone to the cement while keeping the CEM I mass content upon the mechanical properties of the concrete post-thermal exposure. Specimens were kept at 200, 400 or 600 °C for 2 h and the residual compressive and flexural strengths were measured. Results demonstrated that the use of limestone for partial CEM I substitution reduces the relative residual compressive strength, whereas the addition of limestone to the concrete while keeping the CEM I mass constant reduced the compressive strength loss [249]. While these results are in general in accordance with the findings of Adel Mohammed et al. [248], the slight improvement at 15 % replacement ratio has not been observed in this case.

Uygunoglu et al. studied the influence of substituting 10, 20 or 30 % of CEM I by limestone powder upon the residual compressive strength of the self-consolidating micro-concrete following exposure to different elevated temperatures (200, 400, 600, 800 and 1000 °C) for 2 h. They found that partial substitution of the cement in this type of concrete could improve the residual compressive strength at almost all temperatures, though the best results are obtained when only 10 % of the CEM I is replaced by limestone powder [250]. Perhaps the difference between the results reported by Uygunoglu et al. [250] and those reported by the previously

discussed studies [247],[248],[249] originates from the type of the concrete, namely self-consolidating micro-concrete, used in the former.

Literature also holds a few reports about the effect of limestone aggregates upon the thermal resistance of concrete. One of the earliest studies was carried out by Ahmed et al in 1992 [251]. In this study, the authors did not compare the thermal properties of concrete with and without limestone aggregates, but rather investigated the relative residual compressive strength as well as the bond strength of concrete with limestone aggregates following exposure to different elevated temperature, while examining the role of cement content, concrete age, holding time at the maximum temperature and cooling rate. The results showed an initial increase of the residual compressive strength (more noticeable for 7-day old concrete than 35-day old concrete) at 100 °C followed by a sharp drop above 150 °C, so that it reached almost half of the cold compressive strength at 600 °C. Surface cracks started to appear at 400 °C, becoming visible at 600 °C. 100 °C, bond strength slightly increased for young concrete, but following a sharp reduction around 150 °C, progressively deteriorated to reach 39-50 % of the original value at 600 °C. Cooling rate (air cooling vs water cooling) was found not to have a significant effect, while the exposure time was shown to influence the bond strength in case of older concrete, with a difference of 16 % being observed between the values obtained for 60 and 120 min holding periods [251].

The effect of cooling rate upon the residual mechanical properties of concrete with limestone aggregates has been also investigated by Bekam Kara [252]. The results confirm the findings of Ahmed et al [251]. until the 400 °C, where the cooling rate seems to minimally influence the residual mechanical properties of the concrete. Above 550 °C, however, Bekam Kara reports higher values for the residual compressive strength of the concrete after water cooling [252].

Tufail et al. compared the thermal performance of the concrete with granite, quartzite and limestone coarse aggregates. Specimens were subjected to different elevated temperatures in the range of 25 to 650 °C for 2 h, following which the residual compressive and splitting tensile strengths as well as the residual modulus of elasticity were measured. The results showed that the mechanical properties of concrete post-thermal exposure were largely dependent on the aggregate type and was the highest in case of concrete with granite aggregates. The residual compressive strength and modulus of elasticity of the concrete with limestone and quartzite aggregates decreased with an increase in temperature in a similar manner, while the residual splitting tensile strength of the former was slightly lower [253].

In general, these reports seem to point out that the partial substitution of the CEM I by limestone to a certain level (around 10 - 15 %) can improve the thermal performance, while higher substitution ratios are not beneficial. When used as coarse aggregates, concretes containing limestone aggregates can perform similar to those with quartzite aggregates in terms of maintaining their mechanical properties after exposure to elevated temperatures.

3 Materials and Methods

This chapter comprises three main sections; In the first section, the background for designing of experimental setup is introduced. The second section provides an overview of the materials used for concrete preparation and the concrete casting process. The last section provides a detailed explanation of the conducted experiments.

3.1 Design of the study

Based on the information presented in the literature review, the stability of concrete at high temperatures is affected by many factors including characteristics of high temperature exposure as well as characteristics of concrete decompositions. Here, the reasons behind the selected boundary conditions in terms of the thermal loads, the used materials, and the developed concrete specimens will be explained to show how the experimental parameters have been chosen to address the new perceptions associated with the material behavior.

3.1.1 Influential variables and key parameters

3.1.1.1 Thermal load

As previously detailed, exposure of concrete-based constructions to extensive thermal loads occurs under two different circumstances. First is the case of exposure to fire, where the concrete can be differently and unprecedently heated, and the outcome of inflicted thermal load can be singular. In such cases, the temperature often rises quickly and reaches even in cases above 1000 °C [254],[255]. Second, is the case of concrete constructions in the industrial areas, e.g. power plants, steel mills, cement plants, refineries and chemical processing units, etc. These constructions are often exposed to recurrent cycles of heating and cooling, mostly in temperatures in the range of 250-700 °C, or even higher [14]. Accordingly, the investigated thermal processes here were designed to expose the specimens to one or more cycles of heating and cooling with certain maximum temperatures.

The material behavior of concrete in case of natural fire is mostly studied based on standard temperature-time curve (ETK), which does not include any cooling phases. As we aim to study the behavior of concrete both at high temperature and after cooling (residual properties), and particularly after exposure to repeated heating cycles, a modified closed temperature-time curve according to RABT-ZTV was selected (see section 2.1.3). The curve was further modified based on the recommendations of RILEM [256]. Within this frame, the temperature increased slowly with the rate of circa 5 K/min to avoid a temperature difference between the concrete layers. This facilitates a smoother journey of the water molecules from the inner concrete layers towards the surface.

The maximum temperature levels selected for the experimental program was chosen based on the available information regarding the microstructural changes within the concrete (for

detailed information see section 2.1.4). These were also partially selected based on the results obtained during several preliminary studies focusing on concrete mass loss following exposure to thermal loads. These studies revealed that the decomposition of calcium hydroxide ($Ca(OH)_2$) in the concrete begins from 220 - 250 °C, which results in the first extensive water release in the concrete. Furthermore, measurement of the residual strength of the normal strength concrete after one heating cycle with maximum temperatures below 250 °C revealed only minimal changes [257]. Based on the findings of Saravanja et al., this temperature range (170 - 250 °C) is also associated with the beginning of microstructural changes as well as the risk of spalling in case of concretes with denser structure (without propylene fibers) [258]. Hence, the lowest maximum temperature used for the designed thermal program was set at 250 °C. According to literature, $Ca(OH)_2$ decomposition continues up to the temperature range of 400 - 500 °C, peaking at around 411 - 427 °C, with a significant reduction of the concrete strength being notable at this range as a result [42],[48],[259]. The second temperature level was thus selected as 500 °C, as it is associated with almost complete $Ca(OH)_2$ decomposition, yet it is still below around 573 °C, at which quartz, which is one the most widely used aggregates in the concrete industry, undergoes inversion [260]. Exposure of concrete to temperatures in the range of 600 - 700 °C leads to final destruction of the concrete structure due to the decomposition of the C-S-H phase [260]. Therefore, a maximum temperature of 700 °C was selected for the thermal programs used in the current investigation, as it is expected to have remarkable influence on concrete strength, particularly those composed of the widely used quartzite aggregates. Finally, the last maximum temperature was selected as 900 °C, as the rate of $CaCO_3$ decomposition is highest between 800 °C to 900 °C [115],[261]. Above 800 °C, all compressive strength of the concrete is depleted [13]. Thus, 900 °C is also a reasonable target temperature to investigate the re-hydration potential of the concrete specimens following almost full destruction and the potential influence of the used latent hydraulic materials.

Once heating reaches the maximum temperature, it is necessary to maintain it for a certain period of time to ensure achieving the same temperature throughout the specimen (hereafter referred to as the temperature homogenization phase). Based on preliminary experiments, maintaining the temperature for a minimum duration of 2 to 3 hours is necessary to achieve a homogenized temperature distribution inside the samples with the dimensions used in the current investigation (see section 3.3.1). Accordingly, a constant temperature phase of 4 h at maximum temperature was used within the experimental design. This also ensures the occurrence of all potential physical and chemical changes, as reviewed under section 2.1.5, the high temperature can bring about.

As previously debated, some concrete constructions within industrial areas are often subjected to repeated cycles of heating and cooling, which can influence their stability on the long run. Accordingly, we set to investigate the impact of exposure to multiple cycles of thermal loads with various previously introduced maximum temperatures. To this end, samples were heated for 5 / 8 or 20 / 24 cycles. As preliminarily studies had demonstrated a great part of the damage

to concrete structure to happen within the first 4 heating cycles, specimens were exposed to at least 5 (in some cases even 8) heating cycles prior to testing their residual strength. To simulate the long-term exposure, 20 (or in some cases 24) cycles were used. A schematic overview of the thermal cycles is shown in Figure 3.1.

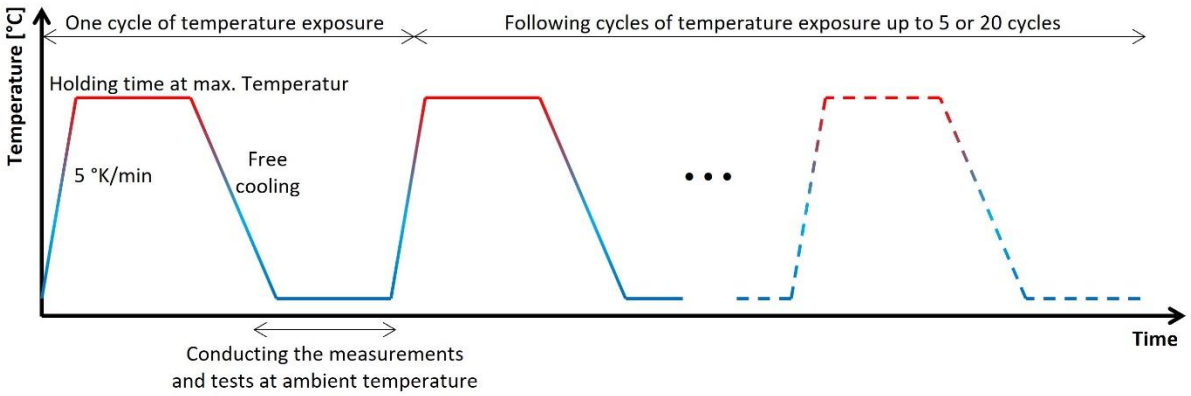

Figure 3.1 Schematic presentation of thermal cycles

Some research, including Hertz, have shown an additional reduction of the residual strength in case concrete specimens exposed to heat are rapidly cooled to ambient temperature [62],[76]. To avoid this, specimens were left in the heating chamber overnight to achieve a slow air-cooling process. The entire thermal load regime is described in detail in section 3.3.2.

3.1.1.2 Material selection

The goal of the current investigation has been to eventually develop a more stable concrete with higher resistance to one-time (e.g. in case of fire) and cyclic (e.g. in case of certain industrial constructions) thermal loads. Some potential concrete components such as basalt or blast furnace slag are inherently byproducts of physicochemical reactions at extremely high temperatures. As previously mentioned, basalt aggregates originate from the parent basalt rocks, which are natural and of volcanic origin [262]. Slag, on the other hand, is produced at high temperatures. Within this context, air-cooled combination of slag sand and BFS has been investigated as aggregates. As previously mentioned, slag sand contains a higher glassy amorphous content and is therefore more reactive than BFS [136]. To investigate the impact of slag sand as an SCM in the cement, various types of cements with different slag sand contents were explored. These included Portland cement (CEM I), Portland-slag cement (CEM II/B-S), blast-furnace cement A (CEM III/A) and blast-furnace cement B (CEM III / B), which contained 0 %, 30 %, 60 % and 80 % slag sand content according to the classification of DIN EN 197-1, respectively [146]. To investigate slag as an aggregate, slag sand (0/2 mm) as fine and BFS as coarse (2/4 mm or 2/8 mm) aggregate used.

In addition to the aforementioned materials, limestone was investigated as the literature reports its stability at high temperatures and favorable effect on improving the thermal resistance of

concrete [250]. Accordingly, Portland limestone cement (CEM II/A-LL) was used in supplementary investigations. Owing to the high calcite content of limestone, CEM II/A-LL, similar to CEM III possesses the potential to reserve water in the concrete matrix, providing slow hydration.

Last but not least, quartzite aggregates were used as these form the most common type of aggregates used in the concrete industry, though experience has demonstrated their limited temperature stability due to the quartz conversion at about 573 °C [57].

Based on the above mentioned, a comparison of standard natural aggregates for concrete production based on DIN EN 12620 [263] was carried out with the standard industrial aggregate BFS based on DIN EN 15167 [141],[142] and the non-standard industrial aggregates based on DIN 4301 [264] including electric arc furnace slag (Ef-slag), Linz-Donawitz process slag (LD-slag) and copper slag (Cu-slag) in terms of their influence on concrete stability at elevated temperatures. As iron and steel-based slags are byproducts of the reactions at hot conditions, their thermal behavior when used aggregates is also worth investigating. Furthermore, due to their large-scale production as industrial waste, they could provide economical alternatives to natural aggregates.

Further details about the aggregates and the relevant grain size distribution will be presented under section 3.2.2.

3.1.1.3 Concrete Formulation development

As mentioned under section 2.1.5, the strength, stability and durability of concrete depends on the type of materials used for concrete production, as well as the water to cement ratio, the ratio of coarse to fine aggregates, age of the concrete at the time of testing and curing conditions (temperature, relative humidity and duration). Accordingly, the formulation of the concretes was developed based on several conditions. First and foremost, the amount of cement paste was kept constant for all specimen series to enable a quantitative comparison thereof. Given the difference in the characteristics of aggregates, for instance chippy nature of the basalt and the superficial porosity of the BFS and Cu-slag, the amount of cement paste and its flowability had to be sufficient to enable the production of all concretes with the same amount of cement paste. Second, to maintain the fresh concrete properties and comparability, a stabilizer was used in case of the quartzite aggregates, and a superplasticizer was added in case of porous aggregates e.g. slags. This resulted in a relatively high cement content of 550 kg/m³ and a correspondingly high cement paste volume of 463 L (water to cement ratio of 0.52). The water to cement ratio of 0.52 was selected as it is sufficient to enable proper chemical reactions and leads to the formation of adequate capillary pores in the system that can balance the pressure and facilitate steam release during exposure to high temperatures, while ensuring sufficiently high compressive and flexural strengths of the concrete structure. On the other hand, as the study sought to investigate the influence of the slag sand as a component of cement upon the thermal stability of the concrete, this comparatively high cement content was thought to be beneficial.

Indeed, the effect of the slag sand content can be better investigated in case the cement content of the concrete is higher, for the influence of slag sand is expected to be more dominant due to the higher volume fraction. Third, efforts were made to maintain the initial strength of the produced custom concrete mixtures as similar as possible to those commonly used in constructions. Last but not least, the sequence and time of mixing, curing conditions as well as concrete age at testing were kept similar for all specimens in one experimental series.

In order to achieve practically appropriate moisture content in the test concretes and to avoid explosive spalling, a concept for hygric conditioning was developed. The aim was to achieve the normal moisture content of a concrete with an age of at least one year (about 3 - 4 % w/w). For most of the experiments investigating the exposure to high temperatures, this is usually achieved through the storage of the concrete for at least 90 days prior to testing [107]. The goal is to reduce the moisture content through moderate warming without inducing residual stresses. The concept of hygric conditioning developed here, however, enabled reducing the conditioning time to 46 days. Under such conditions, the average moisture content of the concrete specimens was reduced to approximately 3.5 % w/w (see section 3.3.1). In a different experimental series, the curing time was reduced to 28 days, as the goal was to compare the impact of the cold compressive strength of the specimens upon the thermal behavior of the concrete.

3.1.1.4 Type and interval of stability testing

The concrete thermal stability was evaluated based on measurements of the hot as well as residual compressive strengths. The strength of the concrete grows steadily for weeks or even months after casting. The initial compressive strength of the concrete is dependent upon a number of factors. These include the proportions of the concrete components, the type of the cement, the water to cement ratio, the quality, type and grade of aggregates, the mixing and placing method and the curing conditions. Upon exposure to high temperatures, the compressive strength of concrete is significantly reduced (see section 2.1.8). Accordingly, investigation of the concrete compressive strength under hot conditions is highly relevant to ensure the adequate load-bearing efficiency of the structure under such conditions. The detailed explanation of the methodology used for the measurements of the hot compressive strength of the concretes is presented under section 3.3.3. Briefly, the cylindrical specimens are warmed up to the selected high temperature, maintained thereat, and the related free strain is measured. This enabled the analysis of the thermal strain at different maximum temperature levels. The compressive strength and the related strain were also measured in last minutes of concrete maintenance at the maximum temperature and were plotted to analyze the stress-strain relationship. It is worth to note that no more experiments could be performed on these specimens, as they were destroyed after the strength measurements. The measurement of the one axial strength of the concrete upon exposure to a single cycle of heating could shed some light as to how the concrete stability would be like in case of fire. This would, of course, only

provide an insight and can by no means serve as an exact model for the fire scenario, for the fire results is an extremely fast rise of the temperature to significantly higher temperature levels, which are better reflected through standard temperature-time profiles described under section 2.1.3.

The measurement of the residual compressive strength of concrete is highly relevant in light of stability following exposure to thermal loads, as well as the potential strength recovery due to rehydration. This is even more relevant in case of the concrete constructions subjected to the repetitive cycles of heating and cooling, as it might influence the durability of these overtime. The experimental setup used for the measurement of residual compressive strength is detailed under section 3.3.2. The residual compressive strength was measured either immediately after exposure to the thermal loads (in cooled state) or at different time points during post-storage. In case of the immediate measurement of the residual compressive strength, the measurements were carried out directly after the concrete was cooled, by which, as previously mentioned, an overnight air-cooling of the concrete to ambient temperature in the turned off heating chamber is meant. Furthermore, some concretes were tested after 7 days of storage under standard conditions (20 °C and 65 % relative humidity; RH), while all were examined on day 28 post-storage. In addition to the measurements conducted after the storage of the concretes under the standard storage conditions for the given storage time, a part of the project sought to investigate the impact of post-thermal load storage time and conditions upon the residual compressive strength. In these cases, concretes were stored under conditions with three humidity levels; *i)* under dried air with no humidity exchange with the ambient air, *ii)* under the standard climate (20 °C and 65 % RH) and *iii)* under water. Measurement of the compressive strength was carried out after 28, 56, and 90 days of post-storage under each condition.

In addition to the measurements of the concrete compressive strength, changes of the concrete mass before and after the thermal load was registered. Concrete mass provides much information in respect with the internal changes in the concrete subjected to thermal load, and the recovery of the concrete afterwards, as it reflects primarily the change in the hydration of the concrete. Elevated temperatures result in the gradual loss of water from different hydration products, which is eventually mirrored by the mass loss. The preliminary studies preceding this work have also proven changes in the mass of concrete to be important for the explanation of certain chemical reactions during and after thermal exposure. Both the amount and the rate of mass loss have been shown highly relevant for defining concrete behavior during exposure to one or more cycles of thermal load. Changes in the mass of specimens were regularly monitored from the pre-curing step up to the end of the concrete storage post-thermal treatment [107].

3.1.2 Statistical design of experiments

3.1.2.1 Fundamentals of the design of experiments (DOE)

In general, concrete is produced using a wide range of materials, whose properties could potentially influence the behavior of the resulted product when exposed to high thermal loads. Therefore, a thorough investigation of the influence of every single potential concrete component on the thermal stability of the concrete specimen is not possible from a temporal perspective. On the other hand, not all materials might have equal degrees of influence on different concrete characteristics that describe its thermal stability. Accordingly, a part of the work used the concept of statistical design of experiments (DOE), with the goal of optimizing the test matrix and saving time without losing meaningful and influential parameters. Within this frame, DOE enables the selection of the most important concrete components for testing and allows for the identification of those with statistically significant impact upon the thermal stability of the concrete. It also enables the detection of meaningful interactions that can bring about statistically significant changes on the eventual outcome.

DOE is a practical data collection and analysis tool, enabling simultaneous investigation of the influence of multiple input parameters on multiple desired output responses. Through the simultaneous manipulation of several input parameters, DOE allows for the investigation of the impact of each parameter alone, and in combination with other investigated variables. As a result, the significance of the interaction between various input parameters can be also evaluated. Given the possibility to explore several variables and responses at the same time, DOE is often preferred over the conventional one-factor-at-a-time investigations, particularly in cases where the experimental matrix is large. Allowing strategic planning and execution of the experiments, DOE provides much more time, labor and cost saving alternative in such cases. This means that the DOE tool can provide more accurate information based on fewer number of experiments.

DOE comprises three different levels. In the first level, a screening design is developed to narrow down the field of input parameters under investigation. These parameters are often suspected to be influential based on experience or previous experimental work. In the second level, a full factorial experimental matrix is developed, which allows for the investigation of the effect of combination of each pair of input variables on all the experimental responses (outputs). The goal is to focus on a region of values, in which the process is close to optimization. The third level of DOE is a response surface design that enables the modeling of the response [265].

In the current work, full factorial designs were used to investigate the influence of cement and aggregate type as well as the maximum heated temperature, number of heating cycles and the post-storage on the residual compressive strength of the concrete (Table 3.1). Except for the type of used aggregates, which is a categorical variable, the rest of the investigated influencing parameters were in numeric form. First, the numerical parameters were used to generate a full

factorial experimental design. Among these, optimal experiments were then selected. To this end, methods of sequential optimization were used, and terms up to the second order were taken into account. The respective experimental plans were then used for the specimens with all five aggregate combinations (Table 3.2). The variables mentioned and their respective levels are shown in Table 3.1. It is worth noting that the DOE used in this work and the subsequent data analysis was conducted by FEhS-Research Institute for Construction Materials [266].

Table 3.1 Parameters investigated in terms of their influence upon the residual compressive strength along with their levels

Parameter	Unit	Variations	Abbreviation
1: Slag sand content of the cement	% (W/W)	0 (CEM I), 30 (CEM II/B-S), 60 (CEM III/A)	slag
2: Maximum temperature	°C	250, 500, 700	T
3: Number of heating cycles	-	1, 5, 20	C
4: Duration of post-storage	days	1, 28	P
5: Aggregate type	-	Quartz, Basalt, BFS	-

Identification of the variables and their interactions with significant influence on the experimental readouts at different experimental time points was achieved through statistical evaluation of the results using multiple regression and analysis of variance (ANOVA) and were only given for the regressions whose coefficient of determination (R^2) was greater than 0.50.

Table 3.2 The general optimized test plan used for the investigation of the impact of cement, maximum temperature, number of cycles, post-storage duration and the aggregate type upon the residual compressive strength of aggregates

No.	Slag sand content of the cement % (W/W)	Maximum temperature °C	Number of the heating cycles -	Duration of the post-storage d	Aggregate type fine/coarse
1	0	250	1	28	basalt/basalt slag sand/basalt slag sand/BFS quartz/BFS quartz/quartz
2	0	250	5	1	
3	0	250	20	1	
4	0	250	20	28	
5	30	250	1	1	
6	30	250	5	1	
7	30	250	20	28	
8	60	250	1	1	
9	60	250	1	28	
10	60	250	5	28	
11	60	250	20	1	
12	0	500	1	28	
13	0	500	5	28	
14	0	500	20	1	
15	30	500	1	1	
16	30	500	5	28	
17	30	500	20	1	
18	60	500	1	1	
19	60	500	5	1	
20	60	500	20	28	
21	0	700	1	1	
22	0	700	5	28	
23	0	700	20	28	
24	30	700	1	28	
25	30	700	5	1	
26	30	700	20	1	
27	60	700	1	28	
28	60	700	5	1	
29	60	700	20	1	
30	60	700	20	28	

Slag sand content of the cement: 0 % = CEM I, 30 % = CEM II/B-S, 60 % = CEM III/A

Experiments presented in each line have been conducted on three specimens.

Experiments on slag sand/basalt, slag sand/BFS and quartz/BFS have been carried out by FEhS-Research Institute for Construction Materials.

3.2 Materials

3.2.1 Cement

3.2.1.1 Industrial cement

The main study was performed using commercially available cement from the same manufacturing plant. To investigate the effect of different slag sand content of the cement, various cement types with increasing amount of slag sand were used. Based on the classification of DIN EN 197-1 [146], the used cements included the Portland-slag cement (CEM II/B-S; 30 % slag sand), the blast furnace cement A (CEM III/A; 60 % slag sand) and the blast furnace cement B (CEM III/B; 80 % slag sand). For the purpose of comparison, reference concretes were always made out of CEM I (CEM I; 0 % slag sand). The physical properties of the cements are given in Table A.2.1, while their chemical analyses are presented in Table A.2.2.

In addition to the effect of slag sand, the impact of limestone in the cement paste was also investigated. To this end, in another set of experiments, the thermal stability of the concretes made of Portland limestone cement (CEM II/A-LL) was compared to the reference specimens made of CEM I. CEM II/A-LL has a similar composition to CEM I, but with ca. 15 % of the Portland clinker substituted with limestone powder.

3.2.1.2 Laboratory cements

As the slag sand available from different suppliers has different origins, composition and reactivity, a part of the current work sough to explore as to whether the results obtained with the commercially available slag sand-containing cements can be generalized to cements containing slag sand of other origins. To this end, two different types of slag, which fulfill the requirements of DIN EN 15167-1 [142], were purchased from different suppliers and used to produce custom laboratory cements with compositions corresponding to CEM III/A according to the requirements of DIN EN 197-1 [142]. The selected slags represent the slag sands typically occurring in Central Europe, and were chosen as previous experience has shown that they have different reactivity. These are henceforth referred to as “Slag 2” and “Slag 3” (Tables A.2.1 and A.2.2).

For the production of the laboratory cements, 60 % of the pure Portland clinker (CEM I) from the manufacturing plant that provided the industrial cements was replaced by one of the slag sands previously introduced. they were first ground in a 10 kg laboratory ball mill to a typical Blaine fineness of approx. 4200 g/cm². It should be noted that this part of the experiments was carried out in collaboration with FEhS-Research Institute for Construction Materials, the details of which has been reported in [266].

Figure 3.2. shows the appearance of the two different slag sands used for the preparation of laboratory cements.

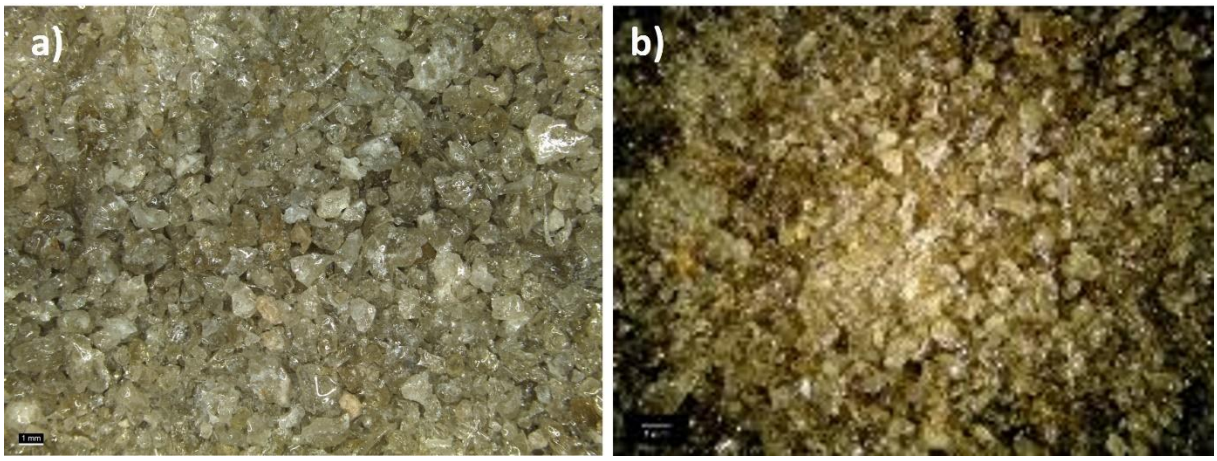

Figure 3.2 Visual presentation of the two blast furnace slags (Slag 2 and Slag 3) used for the preparation of the laboratory cements

3.2.2 Aggregates

3.2.2.1 Natural aggregates

As mentioned under the previous section, the natural aggregates investigated in the current work were basalt and quartz. The used grain size for mixing the aggregates according to standard grading curve were 0/2 mm, 2/4 mm, and 2/8 mm. The grain size distributions of the fractions are shown in Table 3.3 as well as Figure 3.5. Quartz was obtained as local fine (sand) and coarse (gravel) aggregates. Basalt aggregates were also used in the form of fine crushed sand and coarse chippings. Both aggregates had almost no surface moisture at the time of concrete production. The aggregates used met the technical requirements of DIN 1045-2 [267] for aggregates according to DIN EN 12620 [169]. Figure 3.3 shows the appearance of the two natural aggregates, quartz (a) and basalt (b), used in the mixes.

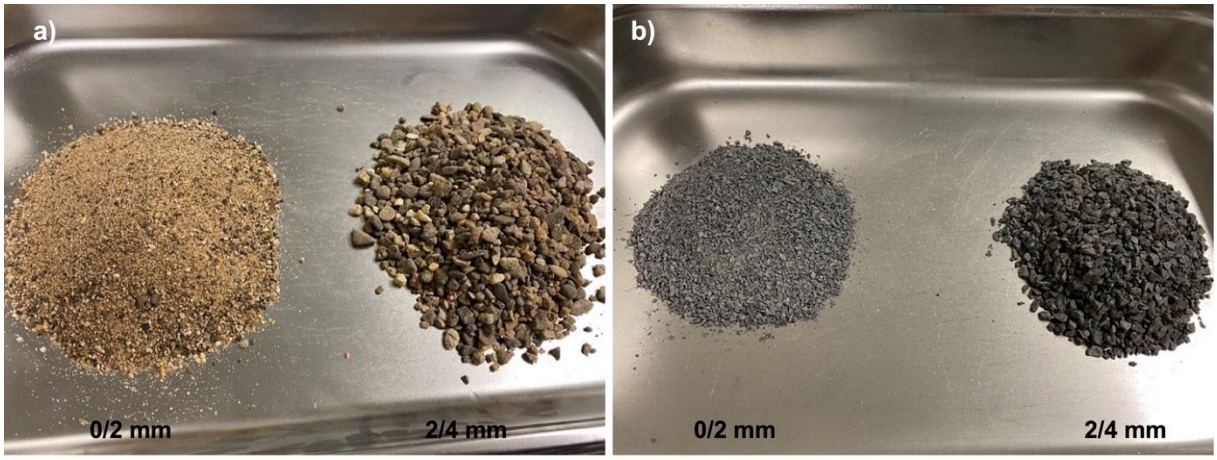

Figure 3.3 Visual presentation of the quartz (a) and basalt (b) used for the mixes

Table 3.3 Grain size distribution of the aggregates

		Passage through sieve with mesh or hole size (values in % (w/w))										Density
		0.125	0.25	0.5	1	2	4	8	16	31.5	63	[kg/dm³]
Fine aggregates (sand)	Quartz 0/2	1.0	10.9	48.4	79.1	94.6	100.0	100.0	100.0	100.0	100.0	2.64
	Basalt 0/2	0.5	2.3	15.6	54.0	93.7	100.0	100.0	100.0	100.0	100.0	2.90
	Slag 0/2	10.0	28.7	77.5	98.9	100.0	100.0	100.0	100.0	100.0	100.0	2.84
	Ef-Slag 1 0/5	4.7	7.4	13.5	23.6	44.8	81.8	100.0	100.0	100.0	100.0	3.98
	Ef-slag 2 0/5	1.0	1.5	4.1	17.3	52.1	97.9	99.8	100.0	100.0	100.0	3.88
	LD-slag 0/5	2.3	2.9	3.4	5.4	15.9	47.0	99.4	100.0	100.0	100.0	3.47
Coarse aggregates	Quartz 2/4	0.0	0.0	1.3	2.0	5.4	98.0	100.0	100.0	100.0	100.0	2.64
	Quartz 4/8	0.0	0.0	0.0	0.0	0.4	36.8	93.1	100.0	100.0	100.0	2.64
	Quartz 8/16	0.0	0.0	0.0	0.0	0.0	0.6	5.6	91.1	100.0	100.0	2.60
	Basalt 2/4	0.0	0.0	0.0	0.2	1.8	99.1	100.0	100.0	100.0	100.0	2.94
	Slag 2/4	0.0	0.0	0.0	3.2	17.4	93.1	100.0	100.0	100.0	100.0	2.83
	Ef-Slag 1 5/8	0.0	0.0	0.0	0.9	0.9	1.3	92.7	100.0	100.0	100.0	3.43
	Ef-Slag 2 5/8	0.0	0.0	0.0	0.4	0.4	2.8	96.9	100.0	100.0	100.0	3.78
	LD-Slag 5/8	0.0	0.0	0.0	1.1	1.1	1.1	96.7	100.0	100.0	100.0	3.87
	CU-Slag 0/8	6.4	9.6	15.6	27.7	49.7	75.7	99.6	100.0	100.0	100.0	3.79

3.2.2.2 Industrial aggregates

The industrial aggregates used in the study were blast furnace slag as fine (0/2 mm; slag sand) and coarse aggregates (2/8 mm; BFS) aggregates. The aggregates used met the technical requirements of DIN 1045-2 [267] for aggregates according to DIN EN 12620 [169]. The grain size distributions of the fractions are shown in Table 3.5. According to DIN 1045-2 [267], these aggregates can be used in concrete production in a manner similar to the natural aggregates. Accordingly, together with the natural aggregates, they are henceforth addressed as “standard aggregates”. Figure 3.4 shows the appearance of the 0/2 mm slag sand (left) and 2/4 mm BFS coarse aggregates (right) used in the mixes.

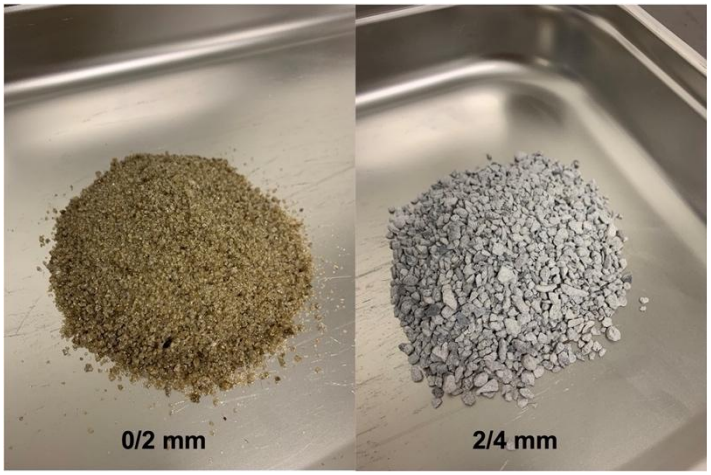

Figure 3.4 Visual presentation of the slag sand 2/4 mm fine aggregates (left) and 2/4 mm BFS coarse aggregates (right)

In addition to these, a treated steel work slag from a Linz-Donawitz processes (LD-Slag) with reduced free lime content (< 0.5 %), and two steel work slags from the electric furnace process (Ef-Slag 1 and 2) were investigated as fine (crushed sand) and coarse (crushed grain) aggregates. Finally, concretes were also made with a copper slag (Cu-Slag), which was available in the grain fraction of 0/8 mm. Although of all the industrial aggregates, only BFS is currently used practically in concrete production in accordance with DIN 1045-2 [267], others also meet the technical requirements defined thereby. Table 3.4 summarizes the grain size distributions of the individual fractions of the industrial aggregates used in this work.

3.2.2.3 Aggregate mixtures

In most cases, concretes were produced using mixtures of various individual aggregate fractions. In such cases, grading curve range of A/B 4 for most of the concretes or A/B 8 for concretes containing industrial aggregates were sought after. In case of the steel work and Cu-Slag aggregates with a maximum aggregate grain size of 8 mm, a grading curve in the range of A/B 8 was sought after. Some concretes were also prepared only using the 0/2 mm fraction of aggregates. The grading curves are depicted in Figure 3.5. Although concretes with this grain size are sometimes recognized as cement mortars, they will be addressed as concrete in this work for the ease of expression. In reality, however, these are categorized as fine concrete.

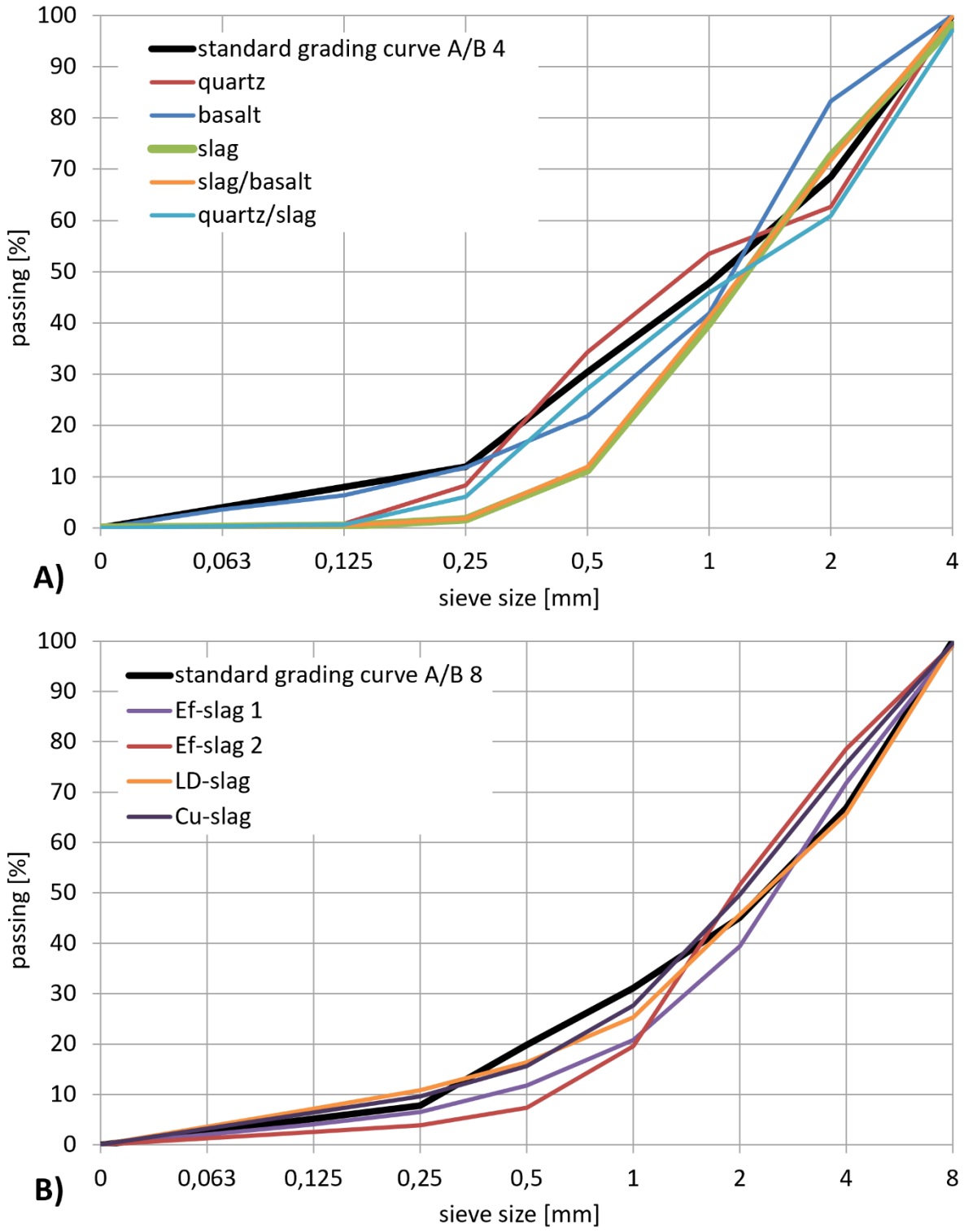

Figure 3.5 Grading curves of the used aggregates to produce concretes: A) standard aggregates and B) non-standard industrial aggregates

The largest grain of the grading curve was chosen to exclude test artifacts due to individual large aggregates in the concrete with the test body geometries used (standard prisms in a size of 40 x 40 x 160 mm³ and cylinders with an approximate diameter of 60 mm and an approximate length of 120 mm). The cylindrical concrete samples were primarily used to

determine the hot compressive strength, whereas the prisms were primarily used for experiments on the residual compressive strength.

In addition, to explore the influence of the largest grain size of the aggregate on the temperature stability of the concrete, limited concrete mixtures containing quartz or basalt with maximum grain size of 16 mm were cast. To maintain the comparability of the mixtures, the cement paste content of the formulations was kept constant.

3.2.3 Concrete formulation

Table 3.4 provides detailed information regarding the composition of the concrete specimens investigated within the scope of the current study.

Table 3.4 Composition of the specimens used within the context of the current study

a) Composition of the concretes with standard aggregates used for the investigation of the hot and residual compressive strength						
Composition	Units	Basalt/Basalt	Quartz/Quartz	Slag/Slag	Quartz/Slag	Slag/Basalt
Water/ Cement	[-]	0.52	0.52	0.52	0.52	0.52
Water	[l/m³]	286.0	286.0	286.0	286.0	286.0
CEM I/ CEM II/B-S/ CEM III/A	[kg/m³]	550.0	550.0	550.0	550.0	550.0
Basalt 0/2 mm		1426.5	-	-	-	-
Basalt 2/4 mm		107.6	-	-	-	378.0
Quartz 0/2 mm		-	868.8	-	1177.0	-
Quartz 2/4 mm		-	484.8		-	-
slag sand 0/2 mm		-	-	799.0	-	1162.0
BFS 2/4 mm		-	-	665.0	420.0	-
Stabilizer and superplasticizer when needed						

b) Composition of the concretes with standard aggregates used for the investigation of the residual compressive strength as well as mass loss						
Composition	Units	CEM I + Quartz	CEM III/B + Quartz	CEM III/B + Slag	CEM II/A-LL + Quartz	CEM II/A-LL + Quartz/ Limestone
Water/ Cement	[-]	0.52	0.52	0.52	0.52	0.52
Water	[l/m³]	264	264	264	264	264
CEM I 42.5 N	[kg/m³]	510.0	-	-	-	-
CEM II/A-LL 32.5 N		-	-	-	510.0	510.0
CEM III/B 42.5 N		-	510.0	510.0	-	-

Quartz 0/2 mm		1468.0	1461.0	-	1461.0	1371.0
slag sand 0/2 mm		-	-	1373.0	-	-
Limestone powder		-	-	-	-	100.0
Stabilizer and superplasticizer when needed						

c) Composition of the concretes with other types of slags from the steel and copper industries used for the investigation of the hot and residual compressive strength

Composition	Units	Ef-Slag 1	Ef-Slag 2	LD-Slag	Cu-Slag
Water/ Cement	[-]	0.52	0.52	0.52	0.52
Water	[l/m³]	286.0	286.0	286.0	286.0
CEM I/ CEM III/A	[kg/m³]	550.0	550.0	550.0	550.
Ef-Slag 1 0/8 mm		2057.0	-	-	-
Ef-Slag 1 0/8 mm		-	2041.0	-	-
LD-Slag 0/8 mm		-	-	1842.0	-
Cu-Slag 0/8 mm		-	-	-	1989.0
Stabilizer and superplasticizer when needed					

d) Composition of the concretes used for the investigation of the influence of aggregate largest grain size upon the residual compressive strength

Composition	Units	Quartz 0/2 mm	Quartz 0/4 mm	Quartz 0/8 mm	Quartz 0/16 mm	Basalt 0/2 mm	Basalt 0/4 mm	Basalt 0/8 mm
Water/cement	[-]	0.52	0.52	0.52	0.52	0.52	0.52	0.52
Water	[l/m³]	286	286	286	286	286	286	286
CEM II/B-S 42.5 N	[kg/m³]	550	550	550	550	550	550	550
Quartz 0/2 mm		1337.0	865.1	699.3	480.0	-	-	-
Quartz 2/4 mm		-	472.0	-	-	-	-	-
Quartz 2/8 mm		-	-	637.8	435.9	-	-	-
Quartz 8/16 mm		-	-	-	421.2	-	-	-
Basalt 0/2 mm		-	-	-	-	1515.3	1417.2	1094.6
Basalt 2/4 mm		-	-	-	-	-	98.0	-
Basalt 2/5 mm		-	-	-	-	-	-	97.0
Basalt 5/8 mm		-	-	-	-	-	-	324.3
Stabilizer and superplasticizer when needed								

e) Composition of the specimens used for investigation of the temperature-dependent maximum evaporable water

Composition	Unit	CEM I + Quartz	CEM II/A-LL + Quartz	CEM III/B + Quartz	CEM III/B + Slag	CEM III/B + Basalt
Water/ Cement	[-]	0.52	0.52	0.52	0.52	0.52
Water	[l/m³]	264	264	264	264	264
CEM I	[kg/m³]	510	-	-	-	-
CEM II/A-LL 32.5 N		-	510	-	-	-
CEM III/B 42.5 N		-	-	510	510	510
Quartz 0/2 mm		1468	1461	1461	-	-
slag sand 0/2 mm		-	-	-	1373	-
basalt 0/2 mm		-	-	-	-	1597
Stabilizer and superplasticizer when needed						

3.3 Experimental works

3.3.1 Concrete production and pre-curing

To produce concrete, standard mortar mixers or else concrete mixers were used. First, aggregates and cement were mixed, following which water was added to the mixture to produce the fresh slump concrete. The fresh concrete was characterized in terms of temperature, density and workability according to standards of DIN EN 12350 series [268]. The characterization was performed 10 minutes after the addition of water.

The concretes were then cast in standard prismatic molds (40 x 40 x 160 mm³) for the investigation of the residual compressive strength and in cylinder forms with an approximate diameter of 60 mm and an approximate length of 120 mm for the measurement of the hot compressive strength (similar to the standard diameter to height ratio). Due to the used specimen dimensions, an aggregate size of 0-4 mm was used. The selected specimen dimension was decided upon due to the large number of specimens to be tested in each experiment. The molds were first filled up to half with fresh concrete and shook on a vibrator. This was followed by completely filling up the molds and a second vibration step. Finally, the surface of the molded concrete was flattened, and the mold was covered and kept at room temperature for 24 h.

The following day, the molds were dismantled, and the specimens were released. The prismatic specimens were then stored in water. The cylindrical specimens were further modified prior to the storage in water. The modifications included the adjustment of the specimen height as well as grinding to obtain a parallel and smooth surface. The latter serves to ensure that both the top and bottom surfaces of the specimens are parallel, so that it does not affect the measured break

load during strength measurement test. Once the modification was completed, the specimens were stored in water.

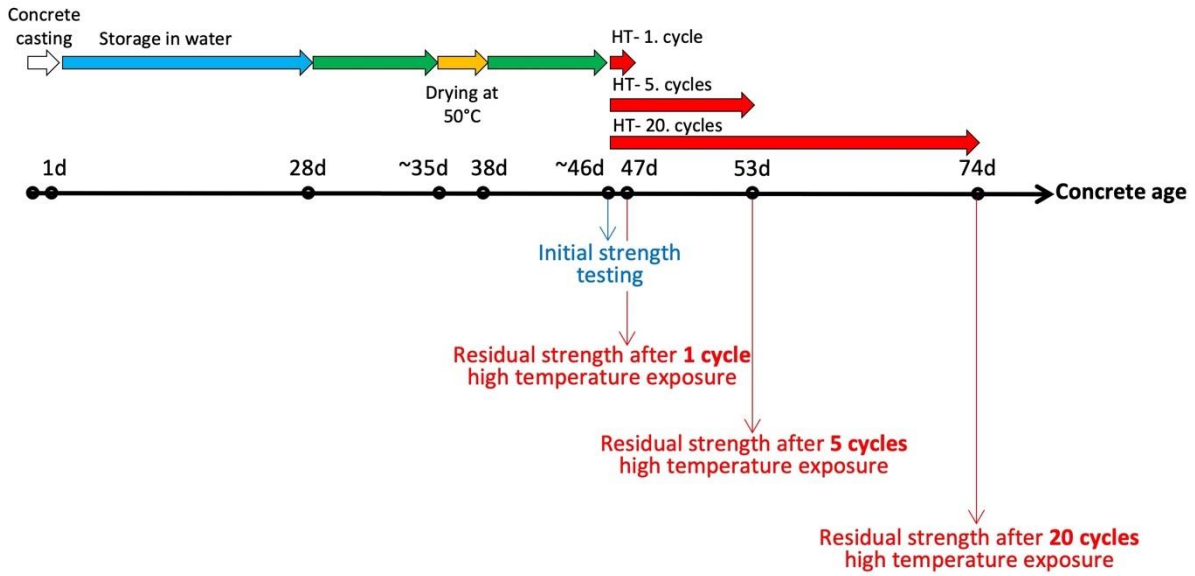

Figure 3.6 Schematic presentation of storage and conditioning of the concrete for all specimens with normal conditioning

Unless otherwise indicated, concretes were stored under water for 28 days to harden. This was followed by storage in a standard climate for 7 days, after which they were moderately dried at 50 °C for 3 days. For hygric homogenization, samples were further stored in standard climate (20 °C, 65% RH) for an additional 6 days before exposure to the high-temperature cycles. This gives a total concrete specimen age of 44 days, which due to additional over the weekend often was extended to 46 days. Under such conditions, the average moisture content of the concrete specimens was reduced to approximately 3.5 % w/w. As elaborated under section 3.1.1.3, this value corresponded to the normal moisture content of a concrete with an age of at least one year. The goal is to reduce the moisture content through moderate warming without inducing residual stresses [107]. This would help for the test specimen to have practically appropriate moisture content and to avoid explosive spalling. Additionally, the resulted concrete will have similar moisture contents to that of aged concretes in real life. As previously mentioned, production, storage and conditioning took a total of around 46 days (44-46 days), and combined with the subsequent high-temperature cycles, the total duration of the experiments including the casting, conditioning, and testing reached a maximum of 74 days in case of 20 heating cycles (Figure 3.6). The high temperature loading is described further in section 3.3.2 The conditioning process is shown schematically in Figure 3.6.

For a series of concrete specimens, the conditioning phase was kept shorter, as these were supposed to have a lower cold compressive strength. These specimens, which are indicated in Table 4.1, were stored under water for 7 days, followed by a further 21 day-long storage under standard climate (20 °C, 65% RH).

3.3.2 Thermal load profile

Concrete specimens were exposed to a temperature-time profile modified from RABT-ZTV and RILEM [256] as previously presented in [107] . The thermal loading was performed using a tube furnace type ERO 8/44 KH with a maximum temperature of 1200 °C for the experiments on concretes in the hot state, and a Voetsch oven with the heating capacity up to 750 °C for the experiments on the residual strength of the concrete (Figure 3.7).

Figure 3.7 Heating systems used for the measurement of the hot compressive strength (up) and the cyclic thermal loading regime for the investigation of the residual compressive strength

For concrete characterization in the hot state, cylindric specimens were first heated up at a heating rate of 5 K/min to reach the intended maximum temperature, at which temperature was kept constant for 4 h (temperature homogenization phase), during which the measurements were carried out (Figure 3.8).

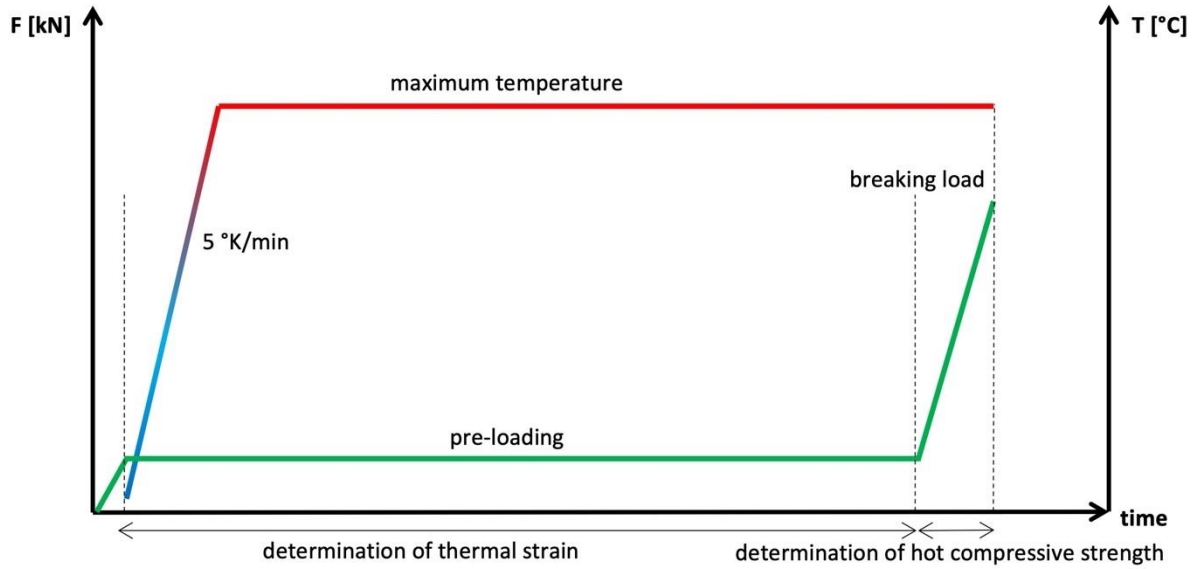

Figure 3.8 Schematic representation of the temperature-time curves (blue-red) and the mechanical stress (green) during the measurement of the hot compressive strength

For concrete characterization in the cooled state, a more elaborate thermal load profile was used (Figure 3.9). As shown in the figure, a temperature increment of 5 K/min was applied in the heating phase (1). Upon reaching the final temperature, the specimens were maintained thereat for 4 h (temperature homogenization phase) (2). As none of the equipment available was capable of actively controlling the cooling phase, numerous preliminary studies were conducted to compare the free cooling curves for different temperature levels in order not only to guarantee a homogenous heating of the specimen, but also a homogenous cooling process (3). To this end, the cooling was fulfilled with a closed oven door, but an open external outlet hood. The specimens reached a temperature span of 20 °C to 40 °C overnight. The samples were then measured at room temperature (4) and if needed exposed to the next cycle (5). Depending on the experiment, specimens were exposed to 1, 5 or 20 thermal cycles.

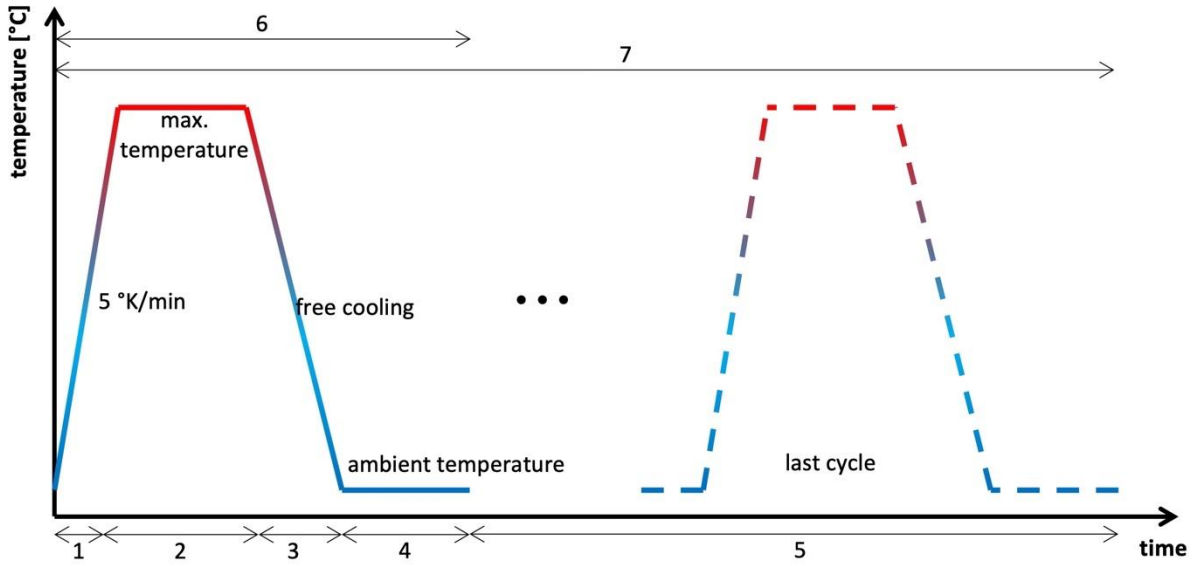

Figure 3.9 Schematic presentation of the theoretical temperature-time regime: 1) heating phase with a rate of 5 K/min, 2) keeping the temperature at the maximum temperature for the duration of 4 h, 3) free cooling phase, 4) measurement in ambient temperature and when needed 5) exposure to further cycles. 6 and 7 schematically represent the total duration of the experiment after one and after more cycles were completed

Figure 3.9 presents a schematic of the theorical temperature-time regime, whereas Figure 3.10 demonstrates the actual temperature-time curves. It is also worth to note that the possibility of temperature layering in the oven was ruled out through various preliminary investigations.

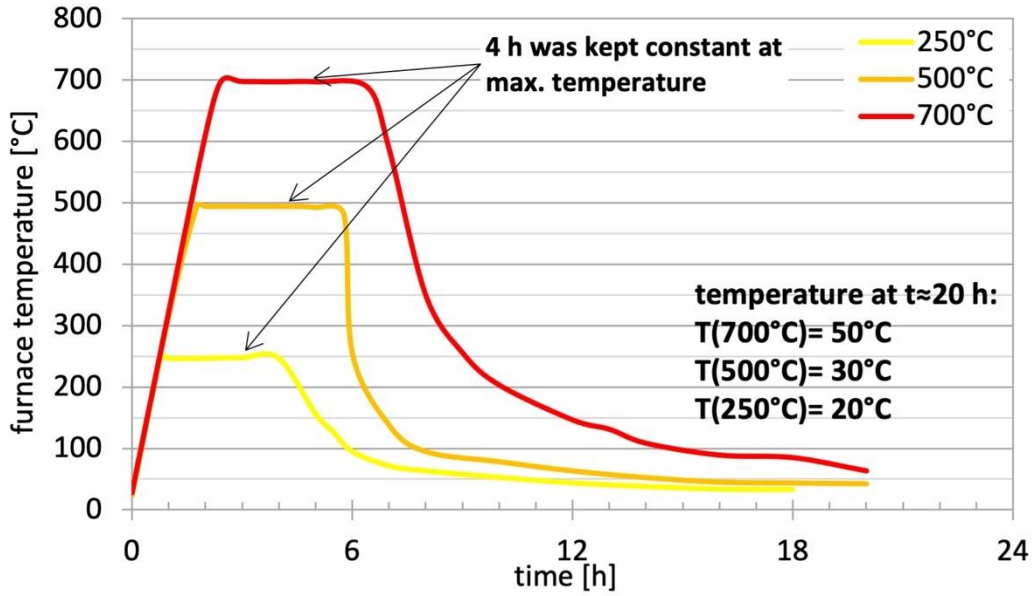

Figure 3.10 Actual temperature-time profile during one complete thermal load (heating and cooling) cycle

3.3.3 Concrete characterization during thermal load exposure

The properties of the concrete during thermal load exposure were examined in terms of the thermal expansion and hot compressive strength.

3.3.3.1 Determination of hot compressive strength and thermal expansion

The hot compressive strength was measured using an electromechanical universal measurement device from MFL Tests Systems with a maximum load of 250 kN (Figure 3.7). Within this context, a methodology based on RILEM [256] was used to enable the simultaneous determination of the hot compressive strength along with the stress-strain curves, and the thermal expansion temperatures over 500 °C.

During the temperature increase and the temperature holding phases, a low mechanical preload of 1 % of the cold compressive strength in force control, i.e. between 1.0 - 1.5 kN, was applied. The goal of the force control was to adjust the thermal expansion of the specimens to keep the load constant. Based on the measured deformation at the end of the holding time, concrete's thermal expansion was calculated using the strain gauge equipment of the electromechanical universal measurement device and based on Equation 3.1. To this end, the measured deformation was corrected by the temperature expansion of the Invar rods used and the remaining deformation was converted into the thermal expansion of the concrete specimen.

$$\Delta L = \propto (T).\ L.\ \Delta T \quad \text{(Equation 3.1)}$$

Where ΔL is the change in length L in mm, ΔT is the change in temperature in K, and α is the linear expansion coefficient in K^{-1}.

It is worth noting that among the used temperature levels of 250 °C, 500 °C and 700 °C, this approach is only effective for those above 500 °C. This is due to the significant change of the thermal expansion coefficient of the invar between 200 °C and 300 °C, resulting in control inaccuracies of the tube furnace, which subsequently leads to inaccuracies in the correction of the deformation measurements.

Following the temperature holding phase, the mechanical stress was increased with a rate of 2.4 kN/s force-controlled according to recommendation of RILEM [256]. Hot compressive strength was measured as the recorded force at the time of the breakage. In parallel, the deformation during the loading was recorded using the strain gauge of the device. These measurements were used to obtain stress-strain curves at maximum temperature. Experiments were carried out on at least two specimens of each concrete type and the mean value and standard deviation were calculated. The actual temperature inside the furnace was documented throughout the experiments.

3.3.4 Concrete characterization after thermal exposure

3.3.4.1 Determination of residual strengths

The residual compressive strength of the concrete specimens was measured based on DIN EN 196-1 [269] using an electromechanical universal measurement device from MFL Tests Systems with a maximum load of 250 kN. The specimens used were standard prisms with the size of 40 x 40 x 160 mm^3. The mechanical stress was increased at a rate of 2.4 kN/s. The residual compressive strength was measured as the recorded force at the time of the specimen breakage.

3.3.4.2 Determination of the dry bulk density

The dry bulk density of the specimens was determined at the age of approximately 46 days based on DIN EN 1015-10 [270] and before conduction of mechanical strengths.

3.3.4.3 Determination of the change of concrete mass

The density of the fresh and hardened concrete differs significantly, and so does that of the concrete before and after exposure to the thermal load. As previously explained, hydration and dehydration of the concrete structure is a crucial determinant of concrete strength. The change in water content of the concrete was simply determined by weighing the specimens at different time points during the pre-curing phase, before exposure to the thermal load, immediately after thermal load exposure, and at certain time points during the post-thermal load storage phase (see section 3.1.1.2). This approach provides the total changes in the concrete water content, i.e. the sum of the physically and chemically bound water in the concrete structure. Given the fact that heating can lead to both water evaporation as well as a shift of the water content from chemically bound to physically entrapped water or vice versa, consideration of the total change in the concrete water content is logical. In higher temperature ranges of 700 - 900 °C, the mass loss can also reflect the decomposition of $CaCO_3$. The mass loss due to high temperature exposure was calculated as the percentual ratio of the specimen mass after thermal exposure (M_w) to the original specimen mass before heating (M_0).

3.3.4.4 Investigation of concrete thermal parameters

To evaluate the effect of different concrete compositions on temperature developing in the specimen cross-sections, the thermal conductivity (λ) was determined. This parameter was measured by heating a representative volume of the samples through the transient hot bridge method using a THB 100 device (Linseis) equipped with a sensor (THB6N). Since the sensor and the device cannot be used during high-temperature exposure, the thermal parameters were measured in the cold state before and after high-temperature exposure. Previous experience has indicated that this measuring technique can be associated with difficulties, in case the specimens exhibit pronounced cracking after exposure to high temperatures. This phenomenon was partly

observed in the case of the specimens containing quartz. Based on extensive preliminary evaluations, the sensor of the device was placed between two prisms of the same series for each measurement. Care was taken to ensure that the measurements before and after thermal exposure were conducted on the exact same prism combinations with the same measuring surface. To ensure sufficient connection of the sensor to the two surfaces, the two prisms were manually pressed together. Furthermore, numerous preliminary measurements were performed to fix the optimal combination of device parameters, such as measuring time, flow intensity, temperature and time interval between two subsequent measurements. The self-configuration of parameters of the device were also studied and compared with optimal combinations. In each configuration, at least 6 measurements with no physical change were performed. Together with at least 3 combinations of prisms in a series, the average value of 18 individual measurements was used for the determination of the thermal parameters.

3.3.5 Concrete characterization during post-storage after thermal exposure

In general, specimens in the cooled state were tested after thermal exposure and once they have cooled down to the ambient temperature. However, some specimens were further stored in standard climate (20 °C, 65 % RH) to study impact of post-storage on the concrete mass and residual compressive strength. Depending on the goal of the experiment, the measurement of compressive strength was carried out after different durations of post-storage. In the majority of the cases, specimens were tested after 28 days of storage under standard climate chamber at 20 °C and 65 % RH. In other cases, tests were also carried out following 7 days of post-storage.

One section of the work was dedicated to the investigation of the influence of the post-storage duration and conditions upon the compressive strength of the concrete specimens after exposure to thermal load. To this end, the compressive strength of the concrete specimens was determined after 28, 56 and 90 days of post-storage under three different conditions; *i)* in dry air with no humidity exchange with the ambient air; *ii)* in standard climate at 20 °C and 65 % RH, and *iii)* under water.

4 Results and Discussion

4.1 Concretes' initial properties before high temperature exposure

The different concretes were characterized in terms of their properties in cold conditions. These characterizations included the initial compressive strength and the initial mass as well as their development over time. The cold compressive strength served as a basis for the calculation of the relative compressive strength values after thermal exposure (see Tables 4.1 and 4.2).

Table 4.1 Cold compressive strength of the prismatic specimens used for the measurement of the residual compressive strength (and mass loss)

a) Cold compressive strength of the specimens used to investigate the effect of slag sand content of the cement and type of the aggregates (normal conditioning)				
Aggregate (0/2 mm/ 2/4 mm)	CEM I	CEM II/B-S	CEM III/A	Unit
Basalt/ Basalt	73.9	74.7	75.4	[N/mm^2]
Quartz/ Quartz	58.4	58.7	65.0	
Slag sand/ BFS	61.3	61.8	63.3	
Quartz/BFS	67.4	71.3	76.6	
Slag sand/Basalt	58.9	56.9	64.1	
b) Cold compressive strength of specimens used to investigate the effect of slag sand and limestone in the cement and as added aggregates (BFS) (shortened conditioning)				
Aggregate (0/2 mm)	CEM I	CEM II/A-LL	CEM III/B	Unit
Quartz	38.9	33.1	33.8	[N/mm^2]
Slag sand	-	-	32.9	
Limestone/Quartz	-	35.7	-	

In addition to the cold compressive strength, the initial mass of the specimens was determined and used for the calculation of the concretes' initial density before exposure to thermal load (see Tables A.2.3 and A.2.4).

Table 4.2 Cold compressive strength of the cylindrical specimens used for the investigation of hot compressive strength

a) Cold compressive strength of specimens used to investigate the effect of slag sand content of the cement and type of the natural aggregates (normal conditioning)				
Aggregate (0/4 mm)	CEM I	CEM II/B-S	CEM III/A	Unit
Basalt	43.5	-	57.4	[N/mm^2]
Quartz	37.4	-	41.2	
Slag	28.6	-	33.3	
b) Cold compressive strength of specimens prepared with laboratory mixed cements used to investigate the effect of slag sand from different sources (normal conditioning)				
Aggregate (0/4 mm)	CEM III/A	CEM III/A (slag 2)	CEM III/A (slag 3)	Unit
Basalt	57.0	42.1	47.5	[N/mm^2]
Slag	33.3	33.2	40.2	
c) Cold compressive strength of specimens used to investigate the effect of non-standard aggregates (normal conditioning)				
Aggregate (0/4 mm)	CEM I	CEM II/B-S	CEM III/A	Unit
Ef-slag 1	45.6	-	59.6	[N/mm^2]
Ef-slag 2	51.2	-	60.2	
LD-slag	45.3	-	59.5	
CU-slag	47.7	-	59.3	

4.2 Concrete strength at hot state

4.2.1 Hot compressive strength

4.2.1.1 Effect of maximum temperature

The effect of the maximum temperature on the hot compressive strength of the concrete mixes composed of CEM I or CEM III/A and three standard aggregates (quartz, basalt and slag; 0/2 and 2/4 mm was investigated. The investigated concretes belonged to cylindrical specimens with the initial properties listed in Table 4.2 and Table A.2.4. Figure 4.1 presents the development of the hot compressive strength as a function of the maximum temperature of exposure. Regardless of the type of cement and aggregate used in the concrete, exposure to 250 °C does not lead to a significant decrease of the concrete strength. This finding is in line with the values reported by Eurocode for normal strength concrete and well as the majority of the reports in the literature summarized by Ma et al. and Kodur et al. [115],[4],. Despite the beginning of the C-S-H phase decomposition around 200 °C and the evaporation of the physically bound water in capillary pores that might promote microcracking, concrete is

maintained or even increased at temperatures below 300 °C in some studies. This has been attributed to the cement paste layers becoming denser [271]. With further increase of the temperature, however, hot compressive strength of the concrete decreases continuously, which can be attributed to the decomposition of $Ca(OH)_2$ (mainly at 460 - 540 °C), C-S-H phase (100 - 500 °C for primary dehydration and 600 - 800 °C for secondary decomposition), and $CaCO_3$ (between 700 - 900 °C, almost completed around 900 °C) as detailed under section 2.1.5 [28],[47]. The reduction rate of concrete hot strength between 250 - 500 °C is lower than that observed between 500 - 700 °C, as the latter temperature range promotes and accelerates concrete decomposition to a higher extent. This is also associated with the higher difference of the thermal expansion between the cement paste and the aggregates at temperatures higher than 500 °C, as the cement paste shrinks and aggregates expand following to high temperatures [169]. In general, the obtained trend for the reduction of the hot compressive strength as a function of temperature is in good accordance with the reports in the literature, particularly those presented by Hertz [62]. Hence, besides the effect of materials used for concrete production, which will be discussed in the next section, the hot compressive strength is highly dependent on maximum temperature of exposure.

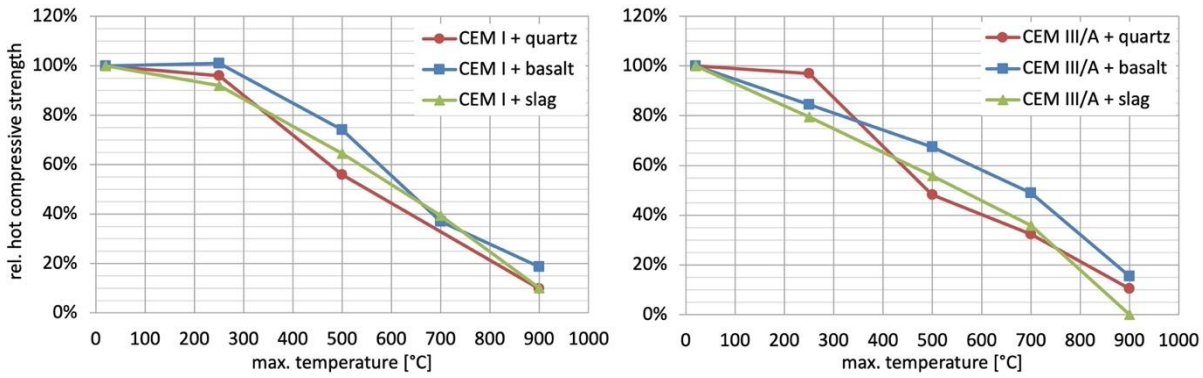

Figure 4.1 Relative hot compressive strength of the specimens made of CEM I (left) and CEM III/A (right) comprising different types of standard aggregates at different temperatures

4.2.1.2 Effect of cement and aggregates

The effect of cement and aggregate type upon the hot compressive strength of the concrete can be also seen in Figure 4.1. A comparison between hot compressive strength of specimens made of CEM I and CEM III/A shows that regardless of the type of aggregates used for concrete production, those containing CEM III/A have a slightly lower hot compressive strength. The only exception is in case of the concrete specimens comprising CEM I and basalt exposed to a maximum temperature of 700 °C. This could be explained based on two different factors; First, as observed in Figure 4.1, the hot compressive strength difference between the specimens made of CEM I and CEM III/A at lower temperatures (about 250 °C) is larger. Up to this temperature, concrete is known to lose the capillary and physically bounded water [28],[47],[115]. Compared to CEM I, CEM III/A is known to have a significantly lower degree of hydration, which is

defined as the fraction of cement, which has thoroughly reacted with water relative to the total amount of cement in the specimen [272]. This means that in case of specimens composed of CEM III/A, the content of the capillary and physically bound water is higher. Accordingly, the evaporation of bound water up to a temperature of 250 °C can lead to the buildup of more steam pressure inside the concrete specimens in case of CEM III/A. As a result, the reduction of the hot compressive strength of specimens at this temperature is more significant. Therefore, up to a temperature of 250 °C, it is expected regarding the mass loss of specimens made of CEM III/A to be larger than those prepared with CEM I.

Second, in case of the specimens containing CEM I, the water is predominantly chemically bound water [37]. While literature holds controversial reports in respect with the exact temperature at which the release of the chemically bound water takes place, the temperature range of 400 - 500 °C is rather critical, as it is associated with the release and evaporation of the water as a result of decomposition of $Ca(OH)_2$ into free lime (CaO) and water [28],[47],[115]. Not surprisingly, the difference between the hot compressive strength of the specimens made of CEM III/A and CEM I at the temperature of 500 °C is smaller. While the difference between the hot compressive strength at 250 °C is around 12 % and 15 %, in case of specimens containing basalt and BFS aggregates, respectively, a significant reduction of this difference at 500 °C is observed. At this temperature, the difference between the relative hot compressive strength of the same specimens is reduced to around 7 % and 8 %, respectively. Despite the reduction of the difference, CEM III/A specimens are still associated with lower hot compressive strength at the temperature of 500 °C. Previous research has solely investigated the residual compressive strength of the CEM III/A-based concrete, and to our best knowledge, no other data on the hot compressive strength of these has been reported. Hence, it is not possible to compare the obtained data with those reported in previous research. However, the slightly lower compressive strength of the specimens with CEM III/A compared to those with CEM I might be explained based on the higher C-S-H to $Ca(OH)_2$ ratio of the CEM III/A hardened cement paste compared to that of CEM I. According to Reiners, this higher ratio means that a higher portion of the cement paste dehydrates at temperatures below 300 °C [61]. This can in turn bring about greater differences between the thermal expansion of the layers at different distances from the heated surface, which promotes more strength loss under hot conditions. On top of that, concrete made out of CEM III/A have a denser microstructure and lower permeability compared to those prepared with CEM I. From the ambient temperature up to 300 °C, physically and chemically bound water are released and evaporated under hot conditions [28],[47],[115]. The denser microstructure and lower permeability of CEM III/A slows down the exit of the evaporated water from the concrete microstructure, leading to the buildup of pore pressure [273]. The increase in pore pressure might promote microcracking in concretes with CEM III/A in this temperature levels, which might in turn lead to the reduction of the hot compressive strength. The temperature range of 460 °C and 540 °C is associated with the decomposition of $Ca(OH)_2$, which is present in CEM I to a higher extent. As a result, the

strength of concretes made of CEM I is more strongly reduced at this temperature range, which decreases the difference between the hot compressive strength of these specimens and those made of CEM III/A. The veracity of this hypothesis, however, needs to be further investigated.

Concerning the effect of aggregates, basalt seems to endow both types of cement with the highest hot compressive strength compared to other aggregate types. While CEM III/A combination with quartz has had the best hot compressive strength at 250 °C, specimens containing both CEM I and CEM III/A along with basalt aggregates have performed superior at all other temperatures. Concretes made of BFS aggregates have been second best in terms of the hot compressive strength, while those with quartz aggregates have been the weakest. In fact, the results show a sudden drop of the hot compressive strength of the latter specimens at 500 °C. This might be due to the higher increase in the thermal expansion of the quartz aggregates between 250 °C and 500 °C, when compare basalt and BFS aggregates [28]. As the aggregates' thermal expansion and cement paste shrinkage contribute to the reduction of the concrete strength, the higher loss of hot compressive strength of the specimens with quartz aggregates is to be expected. The hot compressive strength of the concrete with quartz is further deteriorated as a result of the quartz conversion at 573 °C [57]. Above 500 °C, the growth in thermal expansion of quartz is even more dramatic. As a result of temperature increasing from 500 °C to 700 °C, the thermal expansion of quartz grows from 8 to 16 %, whereas that of basalt and BFS aggregates increases by around 4 % only [28]. Accordingly, regardless of the type of cement, concretes with basalt and BFS aggregates maintain a better compressive strength at high temperatures compared to those with quartzite components.

The tested concretes in this work comprised slag aggregates only. However, Vaidya et al. have demonstrated that the positive influence of the BFS aggregates upon the hot mechanical properties of the concrete is best, when it replaces 20 % of the natural aggregates in concrete formulation. Increase of the replacement ratio to 40 % and 60 % has been shown to negatively influence the compressive strength of the concrete above 600 °C [200]. Hence, that partial replacement of basalt aggregates with BFS might further improve the hot compressive strength of the concrete.

4.2.1.3 Effect of slag source

To investigate whether the obtained results can be extrapolated to cements made with slag sand from other production facilities, and potentially with different reactivities, we compared the hot compressive strength of the specimens made with the commercial CEM III/A and those prepared with two different custom blends containing slag sand from various sources, with basalt and BFS aggregates. As previously elaborated, two different types of slag sands, namely Slag 2 and Slag 3, which fulfill the requirements of DIN EN 15167-1 [141], were used to produce custom laboratory cements with compositions corresponding to CEM III/A according to the requirements of DIN EN 197-1 [146]. The selected slags represent the slag sands typically occurring in Central Europe, and were chosen as previous experience has shown that

they have different reactivity. For the production of the laboratory cements, 60 % of the pure CEM I from the manufacturing plant that provided the industrial cements was replaced by one of the slag sands previously introduced. they were first ground in a 10 kg laboratory ball mill to a typical Blaine fineness of approx. 4200 g/cm². The final composition of the custom blends, except for the type of the used slag sand, was similar to that of the commercial CEM III/A [266]. The prepared specimens were heated up to the temperatures of 500 °C, at which the hot compressive strength was measured. The results are summarized in Figure 4.2. As observed, the relative hot compressive strength of all specimens lays close to one another, with a maximum difference of about 10 % being observed between the specimens made of the commercial CEM III/A and those prepared with the custom CEM III/A blend containing Slag 3.

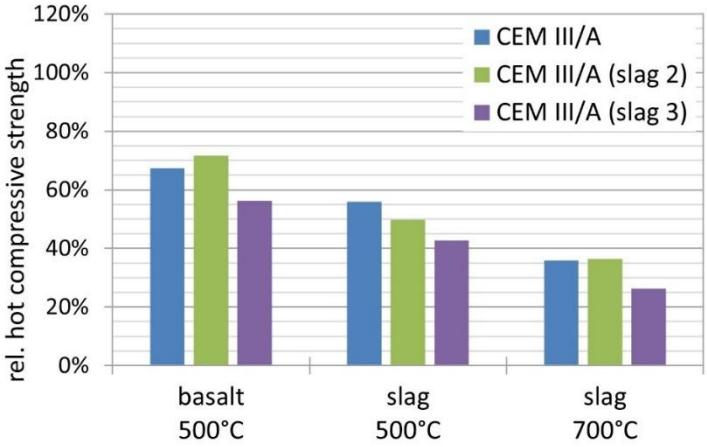

Figure 4.2 Relative hot compressive strength of the specimens made of one industrial and two laboratory CEM III/A containing ground slag (slag 2 and slag 3) sand from various origins at 500 °C (specimens with basalt and BFS aggregates) and 700 °C (specimens with BFS aggregates)

In addition to the relative hot compressive strengths, the stress-strain curves of each specimen were also determined (Figure 4.3). The stress-strain curves have been plotted using the absolute stress values. As Figure 4.3 clearly demonstrates, the main factor determining the shape of the curve, i.e. the elongations on reaching the hot compressive strength and the stiffnesses in the ascending branch is the type of aggregate. Compared to the concrete containing basalt, those prepared with BFS show a more pronounced curvature and lower stiffness. For the concrete made with the same aggregate type, the stress-strain curves for all two laboratory cements lay close to each other.

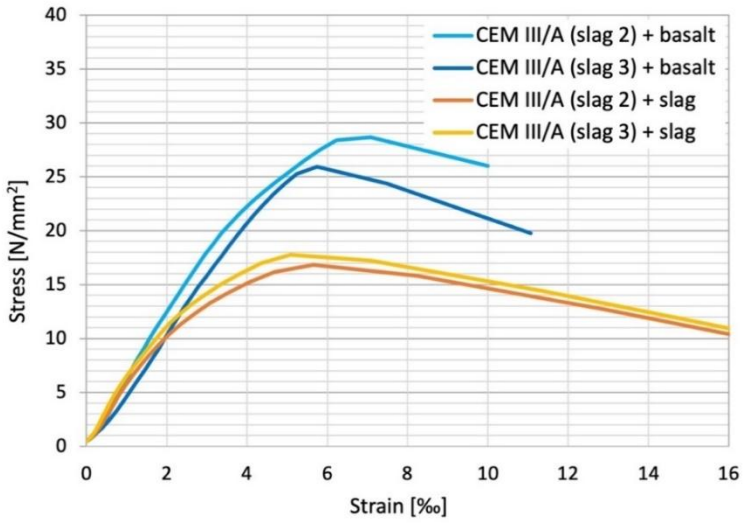

Figure 4.3 Stress-strain curves for specimens made of laboratory CEM III/A containing ground slag sand (slag 2 or slag 3) from various origins with basalt or slag as aggregates measured at 500 °C

4.2.1.4 Effects of non-standard aggregates

The results presented so far covered a wide of aggregates which may be used in concrete according to DIN EN 12620 [169] together with DIN EN 206-1 [274] and DIN 1045-2 [267]. Figure 4.4 compares the effect of various standard and non-standard aggregates on the hot compressive strength of concretes made of CEM I and CEM III/A at 500 °C and CEM III/A at 700 °C. The used non-standard aggregates included the electric arc furnace slag (Ef-slag) from two different sources (Ef-slag 1 and Ef-slag 2), Linz-Donawitz process slag (LD-slag) and copper slag (Cu-slag). Detailed information regarding the composition of the concrete specimens used for these experiments has provided in Table 3.6.c and Table 4.2.c. Based on Figure 4.4, it can be clearly concluded that all standard aggregates, even quartz, perform better to their non-standard counterparts. A comparison of the BFS content of the cement used for concrete production reveals a controversial effect. In case of the specimens made with standard aggregates, those comprising slag sand in the cement (CEM III/A) have lower relative hot compressive strength. For the specimens containing non-standard aggregates, however, the hot compressive strength associated with CEM III/A is the same or higher than the specimens made of pure CEM I. This might pertain to the difference in the thermal expansion of the non-standard aggregates and the standard aggregates, which might in turn impact the difference between the shrinkage of the used cement pastes (CEM I and CEM III/A) and the used aggregates. The measurement of the thermal expansion these aggregates at different temperatures is yet to be investigated and inspires further research.

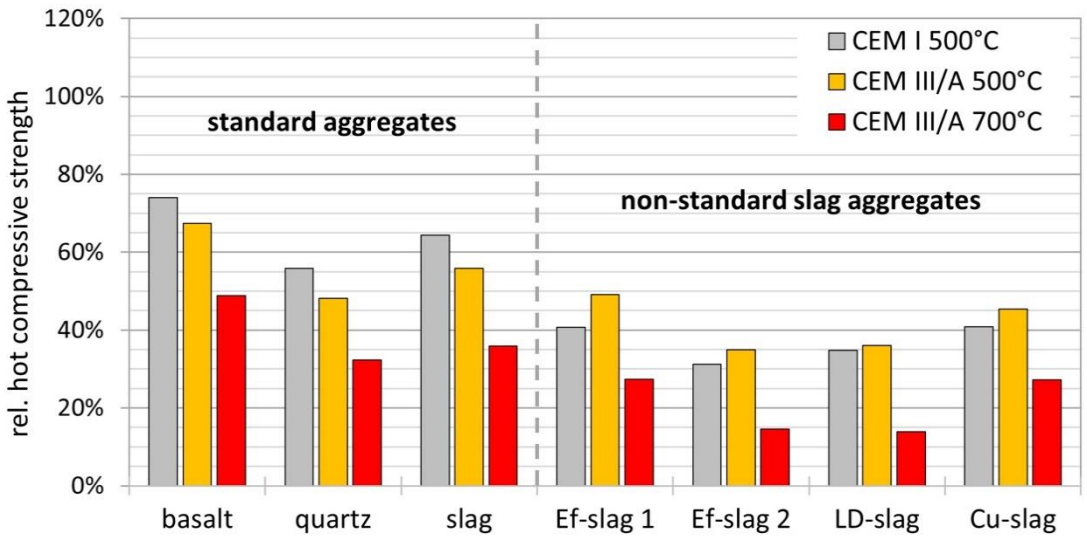

Figure 4.4 Comparison of the hot compressive strength of the specimens made of CEM I or CEM III/A in combination with various standard (basalt, quartz or slag sand/BFS) or non-standard (Ef-salg 1, Ef-slag 2, LD-slag or Cu-slag) aggregates at 500 °C (CEM I and CEM III/A) and 700 °C (CEM III/A)

A generalized statement about the effect of various tested slags, i.e. Ef-slag, LD-slag and Cu-slag is not possible. The comparison of the two electric furnace slags (Ef-slag 1 and Ef-slag 2) shows that even for the same type of industrial aggregate, results can differ based on their origin. The relative hot compressive strengths of the LD-slag and Cu-slag fall in a similar range. Nonetheless, it can be clearly concluded that the hot compressive strength of the concretes prepared with all non-standard aggregates fall below that of the quartz aggregates in most cases. For the use in practice, individual pretesting would be hence necessary.

4.2.1.5 Effect of pre-loading

The tests of hot compressive strength were partially repeated with the same mixtures and thermal load procedure, but with a slight pre-loading of 10 % relative to the initial compressive strength. The goal was to examine the hot compressive strength at hot condition in the presence of an additional one axial load or self-weight load. This phenomenon is often meaningful in fire design of structures under a combination of the mechanical and thermal loads (stressed tests). As observed in Figure 4.5-a, these experiments reflect also the effect of aggregate type, particularly BFS on the mechanical behavior of concrete when exposed to thermal loads. As observed, the results match the findings of thermal loading without the mechanical preload, though the recorded hot compressive strength with the preload is higher. This means that here again, the increase of the maximum temperature to which the concrete has been exposed, leads to more significant reduction of the hot compressive strength of all specimens. A similar trend can be also observed in case of the effect of aggregate type, where compressive strength of the specimens prepared with basalt are higher than that of those prepared with BFA. Specimens with quartz aggregates are associated with the lowest relative hot compressive strengths of all.

The higher measured relative hot compressive strength under mechanical preload can be attributed to the load-mediated densification of the matrix in the concrete structure. This is a simple consequence of the concrete being pressed together as a result of the slight one axial load applied thereto. On the other hand, the preload partially limits the free thermal expansion of the concrete and especially the aggregates, which consequently lead to a lower level of damage to concrete structure. Similar results have been reported in other experiments [275],[276].

The effect of pre-loading is more significant at the temperature of 250 °C compared to 500 °C. This might originate from the relatively high amount of physically bound water which is released in the concrete matrix at 250 °C. The resulting built up steam in the concrete structure creates a resisting force against the mechanical load applied to the concrete structure. As a result, the hot strength overtakes the initial strength of all concrete mixtures at this temperature. While these results are in accordance with the findings of [275], the veracity of the proposed hypothesis should be further investigated and inspires further research.

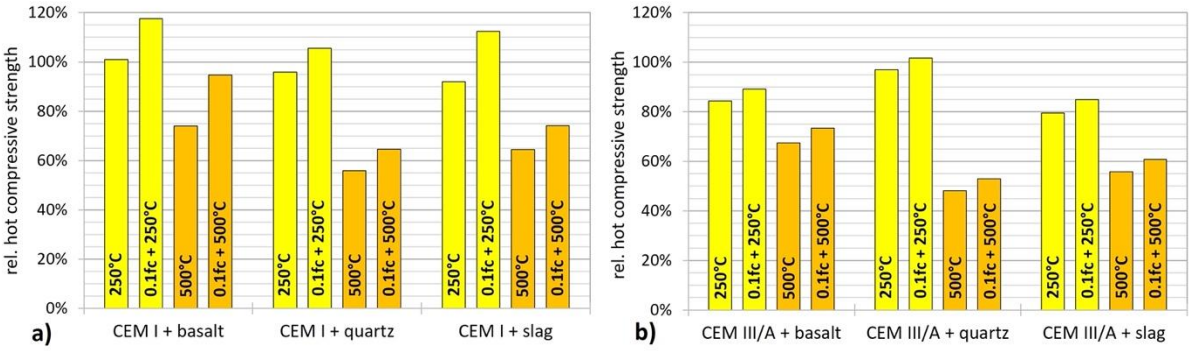

Figure 4.5 Relative hot compressive strength of the specimens made of CEM I (a) and CEM III/A (b) with different standard aggregates at 250 °C and 500 °C in the presence or absence of a pre-load equal to 10 % of the cold compressive strength

The impact of preloading seems to be more dominant for the concretes containing basalt or BFS compared to those with quartzite aggregates (around 15 - 20 %). This can be attributed to the higher thermal expansion of the quartzite aggregates compared to basalt and BFS aggregates [28].

The impact of preloading has been also analyzed for specimens with CEM III/A and the results are demonstrated in Figure 4.5-b. Here again, a similar trend could be observed, though the effect of preloading was less pronounced than in case of specimens made of CEM I. This is to be expected, as concrete made of CEM III/A has in general a much denser microstructure compared to that made of CEM I, which mitigates the effect pre-loading. In all, the positive effect of pre-loading upon the hot compressive strength of the specimens at all tested conditions, at least in the normative and structural planning sense, is to be expected.

4.2.2 Comparison with standards

As discussed in section 4.2.1.2, concretes made of basalt and BFS were associated with higher hot compressive strength when compared to those comprising quartzite aggregates. Within this section, the obtained results in terms of the relative hot compressive strength are compared with the values in European standard DIN EN 1992-1-2 (Figure 4.6) [104], which are the basis of high temperature design for structural components made of reinforced concrete. The standard values were given for reinforced concrete made of CEM I and quartzite (solid blue curve) and calcite (solid red curve) with initial compressive strength in the middle range of normal strength concrete (NPC). For the concrete in range of high-performance concrete (HPC), DIN EN 1992-1-2 considers further strength decrements at lower temperature (blue dashed line) [104]. The three shades of blue refer to the three recommended ranges of class 1 (C55/67 - C60/75), class 2 (C70/85 - C80/95) and class 3 (C90/105 and higher). The initial compressive strength of the cylindrical specimens investigated in terms of hot compressive strength (average 45 N/mm^2), lays within the higher range of the normal strength concrete and beginning of high-performance concrete. Therefore, they can be still compared with these standards without correction.

As shown in Figure 4.6, the hot compressive strength of the investigated concretes containing combination of quartz with both cement types are very close to the solid blue curve, except for the investigations at 500 °C, where the specimens with both cement types lie slightly under. The investigation of concretes containing basalt aggregates are corresponding averagely to the red curve or (concretes with limestone aggregates), or are even higher at the temperatures of 700 °C and 900 °C. This can be attributed to the higher thermal stability of basalt compared to limestone. The hot compressive strength of the specimens containing BFS lays between that of concretes with basaltic and quartzite aggregates, respectively. At 250 °C, the hot compressive strength of the specimens made of CEM III/A falls slightly lower than the solid blue and solid red curves, which are associated with CEM I, and closer to that of class 1 and 2 HPC. As the structure of these specimens is denser than those made of CEM I, these findings seem to be logical. As observed in Figure 4.6, the presented curves for the three classes of HPC show that the initial compressive strength of concrete affects the hot compressive strength, especially at temperatures up to 400 °C, where the loss of strength under hot conditions is higher compared to normal strength concrete. As the initial compressive strength of the concretes investigated in this work was at the higher range of normal strength concrete, and since the microstructure of the concrete made of CEM III/A is much denser, the higher reduction of the hot concrete specimens at 250 °C is to be expected.

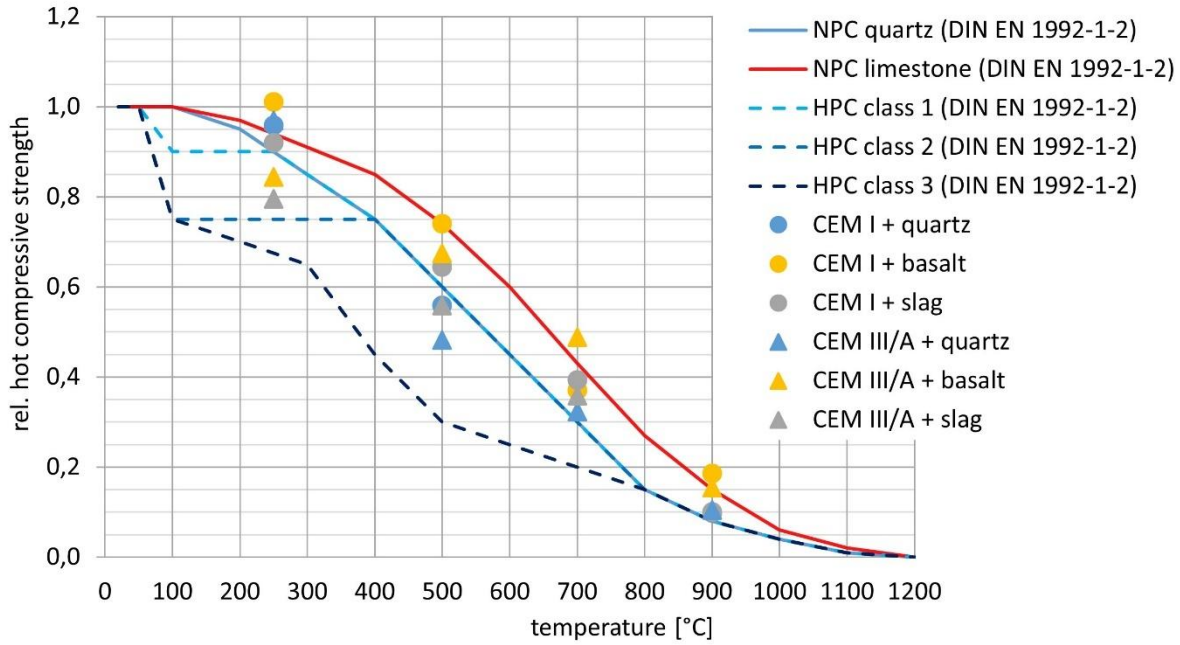

Figure 4.6 Comparison of the relative hot compressive strength of the specimens made of CEM I or CEM III/A in combination with basalt, slag (slag sand/BFS) or quartz aggregates with the standard mixes in range of normal-performance concrete (NPC; CEM I with quartz or limestone aggregates) and high-performance concrete (HPC) class 1, 2 und 3 according to DIN EN 1992-1-2 [104]

The comparison of investigated hot compressive strength reveals that concretes made of both CEM I and CEM III/A show a relatively well accordance with standard values. Hence, the blast furnace slag cement (CEM III/A) is a suitable more sustainable alternative to the conventional CEM I, in regards with the performance and load-bearing capacities at high temperatures.

It is also noteworthy that the substitution of limestone with basalt and quartz with BFS aggregates leads to increase of hot compressive strength, creating more efficient alternatives for the hot design of concrete constructions. These findings inspire further research focusing on the potential of stable aggregates to extend the standards.

Figure 4.7 shows the hot compressive strength of the concretes containing non-standard industrial aggregates in comparison with the concretes prepared with CEM I and the quartzite (blue curve) and calcite (red curve) aggregates within the context of the hot design according to DIN EN 1992-1-2 [104]. It should be noted that at 700 °C, the relative hot compressive strength of Ef-slag 1 and LD-slag as well as Ef-slag 2 and Cu-slag are directly superimposed. The figure clearly indicates that the relative hot compressive strengths of the non-standard slags fall below the common quartz and limestone concretes. The main reason for this phenomenon might be the more pronounced expansion of these industrial aggregates compared to their standard counterparts. At least in case of the steel slag, the problem with expansion is well established. Even at lower temperatures, steel slag is known to react with water and expand as a result. The degree of expansion depends mainly on the amount of free lime in steel slag aggregates [277]. Netinger et al., who investigated the fire resistance of concrete made with steel slag aggregates have reported that despite the good fire resistance of steel slag, it cannot

provide satisfactory thermal performance when combined with CEM I. They have attributed this to the fact that CEM I cannot properly adapt to the expansion of steel slags at high temperatures, which is expected to be high [93]. Ducman et al. have demonstrated that electric arc furnace slag from carbon steel production undergoes a mineralogical change when at temperatures higher than 800 °C, in which of wustite is transformed into magnetite. This transformation leads to significant volumetric expansion, which significantly worsens concrete's mechanical properties [278]. They have reported that firing up steel slag to 1000 °C prior to use will improve the mechanical properties of the concrete product, though it will significantly rise the production costs [278].

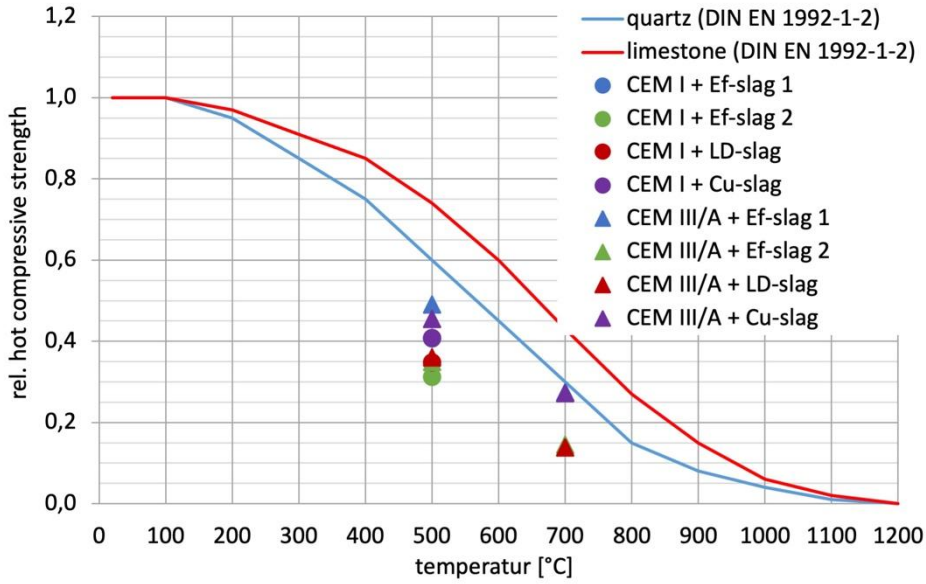

Figure 4.7 Comparison of the relative hot strength of concretes made of CEM I or CEM III/A and non-standard aggregates from steelworks with the standard mixes (CEM I with quartz or limestone aggregates) according to DIN EN 1992-1-2 [104]

4.2.3 Thermal expansion

The thermal expansion coefficients of the specimens following high temperature exposure were primarily determined for the concretes made of laboratory and commercial CEM III/A with BFS and basalt as well as for commercial CEM I or CEM III/A with various non-standard aggregates.

The results are summarized in Figure 4.8, where the thermal expansion of the laboratory and commercial CEM III/A in combination with basalt or slag aggregates is shown on the left and that of the combination of CEM I or CEM III/A with different types of non-standard aggregates is shown on the right. All values are compared with the standard values according to DIN EN 1992-1-2 for thermal expansion [104]. The general rule in the standard is that concretes with quartzite aggregates show greater thermal expansion than concretes with limestone [104]. This, however, becomes more obvious at temperatures above 250 °C, mainly due to the fact

that quartz conversion happens at around 573 °C. It can be concluded based on the Figure 4.8 (left) that laboratory cements made of slag sand from different origins have similar thermal expansion to that of the commercially available CEM III/A. This means that the origin of the slag sand does not influence the thermal expansion of the specimens. Furthermore, the thermal expansion of the specimens made of basalt is smaller than that of the specimens made of slag aggregates. Additionally, both aggregates provide comparable or even smaller thermal expansion compared to limestone. The lower thermal expansion of the specimens in the current work maybe also attributed to their higher cement paste content compared to the norm concrete, which, due to the shrinkage of the cement paste, accounts for a decrease of the total thermal expansion.

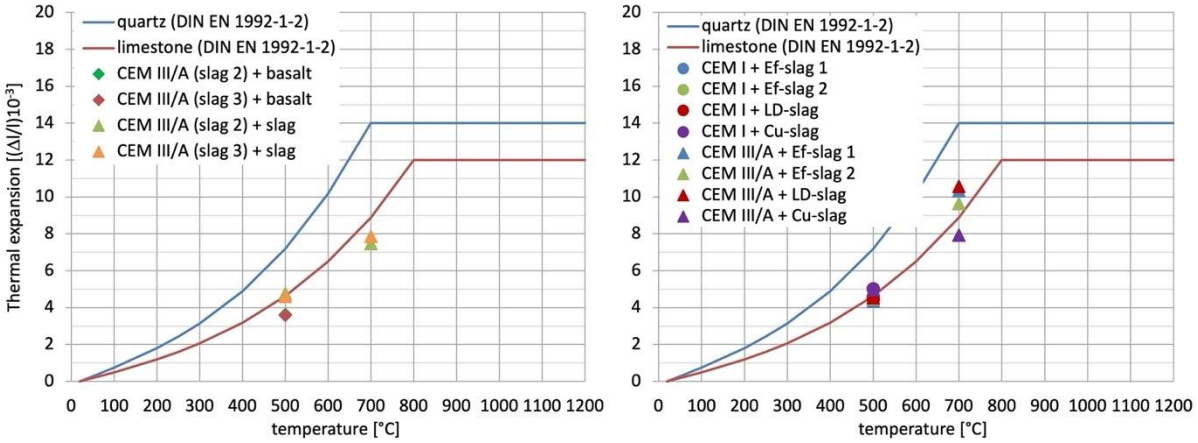

Figure 4.8 Thermal expansion of concretes with heat resistant aggregates (basalt and slag) and laboratory cements made of different ground slag sands as a cement component (slag 2 and slag 3) (left) as well as concretes made of CEM I and CEM III/A and different non-standard aggregates from steel making industry (Ef-slag 1, Ef-slag 2, LD-slag and Cu-slag) (right)

For the non-standard aggregates, the measured thermal expansion at 500 °C corresponds to the thermal expansions of concrete with limestone as given in DIN EN 1992-1-2 [104]. Nevertheless, a higher thermal expansion of concrete with these aggregates was expected, owing to origin of iron particle content. Anyhow, this low thermal expansion is positive considering the design of concretes with relatively good thermal resistance. Even at 700 °C, the measured thermal expansion coefficients are still lower than the thermal expansion of the specimens with quartzite aggregates.

4.3 Residual strength of concrete following cyclic high temperatures

As mentioned before, the residual strength corresponds to the remaining strength within the concrete after exposure to one or more thermal cycles. Cooling of concrete to ambient temperature after the heating phase in each cycle should occur naturally and gradually. Residual strength can be studied by means of several indicators, such as residual compressive strength,

residual flexural strength, residual dynamic module of elasticity, etc. While all of these indicators have been investigated within the context of the current study, only those which have significantly reflected the influence of the concrete components will be debated here. The impact of residual flexural strength or residual module of elasticity were comparatively close to the residual compressive strength. As the results obtained for the flexural residual strength as well as the dynamic module of elasticity followed the same trend as the residual compressive strength, these were not further elaborated in this dissertation. It should be noted that the flexural residual strengths revealed this indicator to have higher sensitivity to the high temperature exposure, as it provides more information regarding the changes in the concrete strength. However, given the similarity of the observed trends, concrete stability in cooled state will be debated solely based on the residual compressive strength. This section presents impacts of the number of thermal cycles and the maximum temperature. Additionally, the effect of concrete post-thermal load storage conditions on the residual compressive strength of concretes with different compositions is debated.

4.3.1 Effect of maximum temperature and number of thermal cycles

Figure 4.9 shows the residual compressive strengths for combinations of CEM I or CEM III/A with basalt, quartz and slag after a single cycle (a), 5 cycles (b) and 20 cycles (c) to maximum temperatures of 250 °C, 500 °C and 700 °C. Again, the results confirm significant reductions of residual strength with an increase of the maximum temperature of the thermal load, which can be obviously seen in Figure 4.9.a. At the maximum temperature of 250 °C, no significant reduction in the residual compressive strength of the specimens is observed, as the thermal expansion of the aggregates at this temperature is rather low. This indeed leads to minimum stress development within the concrete structure. This increase in residual strengths has been reported in other experiments, such as those reported by Boquera at al. [128] and Khan et al. [126],[127]. At higher temperatures a significant reduction of the concrete's residual strength is observed, the magnitude of which is depended on concrete composition [123],[126],[127]. These findings further confirm the concept of "concrete specific critical temperature" suggested by Khoury, which describes a concrete specific temperature below which exposure to a second thermal cycle would not lead to significant damage to concrete's structure [123].

Figures 4.9.b and 4.9.c display the residual compressive strength of specimens made of CEM I or CEM III/A and supplemented with basalt, quartz or slag aggregates after 5 and 20 thermal cycles, respectively. The results clearly show an ongoing reduction of residual compressive strength as the number of the heating cycles increases. Here, the reduction of strength is visible even at the maximum temperature of 250 °C (around 5 - 10 % for all mixtures), though it is more significant for 500 °C and 700 °C. This is attributed to the continuation of dehydration and degradation of the cement paste. The strength reduction is significantly pronounced when the number of cycles is changed from 1 to 5. From 5 to 20 heating cycles, the reduction of the cooled strength still significant, though for some specimens, it not as dramatic as that observed

in the first 5 cycles. The stability of the specimens after 5 thermal cycles depends mostly on the maximum temperature as well as number of heating cycles. Increasing the number of exposed heating cycles from 5 to 20 seems to affect the residual compressive strength depending on cement and aggregate types (will be discussed in detail under 4.3.2). Hence, the number of heating cycles is a vital determinant of the concrete stability mostly at temperature higher than 250 °C, though formulation of the concrete specimens using the appropriate cement and aggregate types can counterbalance the effect of repeated exposure to cycles of the thermal load.

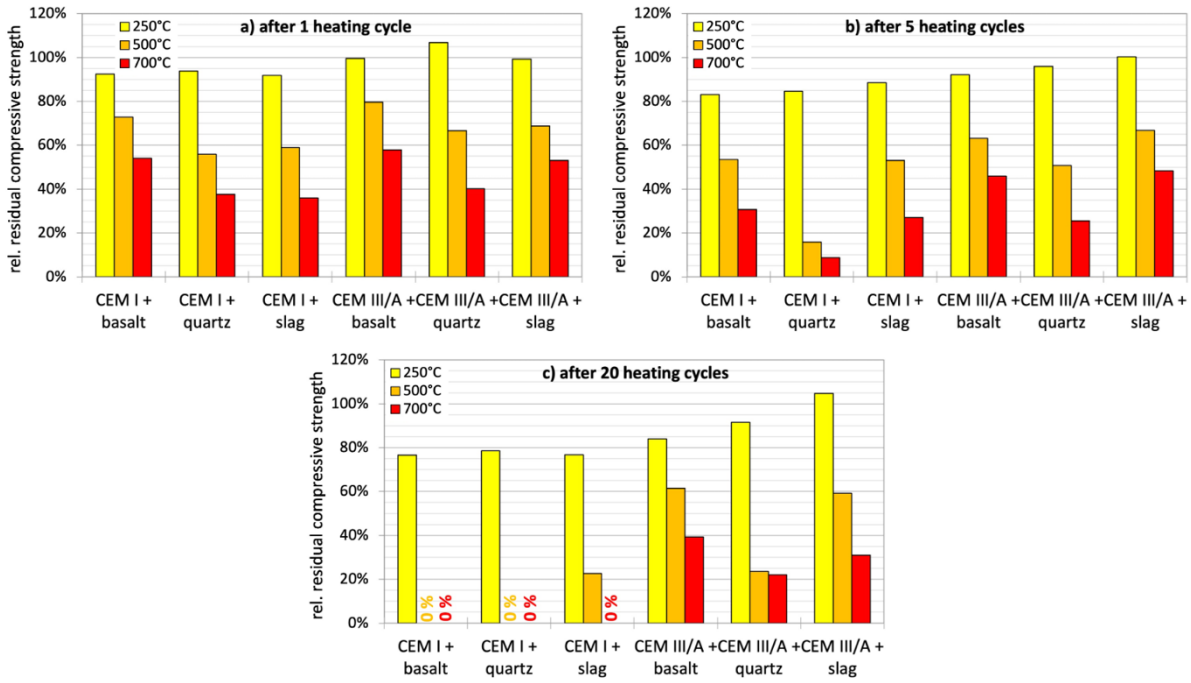

Figure 4.9 Relative residual compressive strength of the aggregates made of CEM I or CEM III/A complemented with basalt, slag or quartz aggregates following exposure to different number of heating cycles with various maximum temperatures

To verify, whether the impact of the maximum temperature and number of heating cycles is similar for other types of cements, additional experiments with specimens made of CEM III/B and CEM II/A-LL and different aggregates (quartz, slag, and limestone/quartz mixtures) were heated up to 3 different end temperatures (250 °C, 500 °C and 900 °C) for 1, 8 and 24 heating cycles. The specimens were then investigated in terms of their residual compressive strength at cooled state. For details about composition and the initial compressive strength of these please see Table 3.6.b and Table 4.1.b, respectively.

Figure 4.10 shows the residual compressive strength of specimens after exposure to one cycle of heating. Interestingly, when heated to 250 °C, the relative residual compressive strength of the specimens does not decrease, but even an increase in the range of 5 - 20 % is observed for all specimens. A similar observation has been reported by Xiao and Falkner and Saravanja et al., who have also measured around 10 % of increase in the residual compressive

strength of the UHPC specimens when heated up to temperatures below 400 °C and 300 °C, respectively [279],[258]. Similar results have been reported by Xu et al. when concrete was heated up to 250 °C for normal strength concrete supplemented by pulverized fly ash [280]. A possible explanation for this slight increase is that the relatively dense structure of the concrete specimens made of CEM III/B and CEM II/A-LL decelerates the escape of water vapor created as a result of the release of the physically bound water up to 250 °C. The resultant increase in pressure together with the created supersaturated atmosphere in the concrete microstructure might lead to a phenomenon similar to autoclave hardening, where the mineralogical changes could lead to compaction or an increase in load-bearing capacity. These changes have been proposed to include the dry hardening of cement paste as a result of further hydration along with hot vapor mediated internal steam curing caused by internal autoclave conditions [51],[64]. This explanation seems to be plausible, since, as previously mentioned, similar results have been found for UHPC, which also has a denser microstructure [258],[279]. Nonetheless, further research should be dedicated to the investigation of the veracity of this hypothesis.

Above 250 °C, the residual strength decreases continuously. Between 250 °C to 500 °C, a decrease of about 20 % is observed. An increase of the peak temperature from 500 °C to 900 °C leads to a reduction of the residual compressive strength by about 70 %. This signifies dramatic thermally induced damages to concrete structure. This is in accordance with the findings of previous studies. In a recent publication, Pasztetnik and Wróblewski have compiled these previous reports and concluded that regardless of the concrete composition and rate and duration of heating, a decrease of the concrete residual strength (normal and high strength concrete) as a result of the increase in the maximum temperature is inevitable [69].

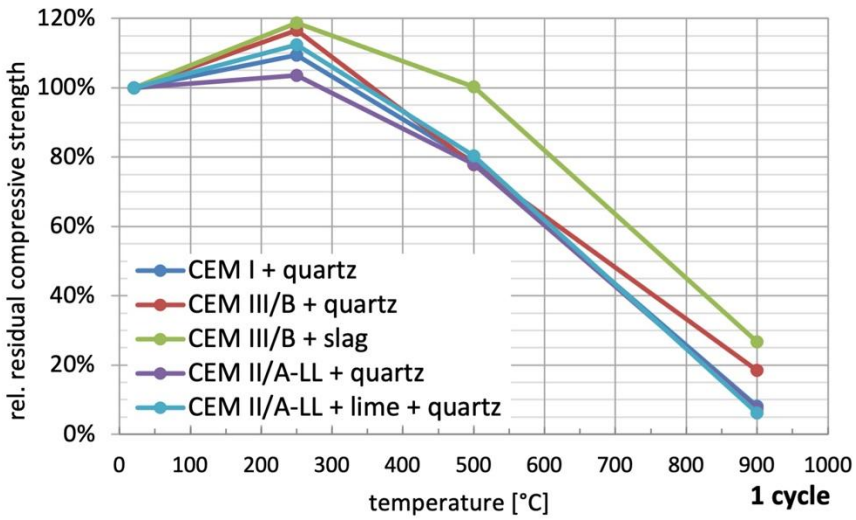

Figure 4.10 Relative residual compressive strength of the specimens made of different cement types (CEM I, CEM III/B or CEM II/A-LL) following exposure to 1 heating cycle with different peak temperatures (250 °C, 500 °C and 900 °C)

In addition to maximum temperature, the influence of the number of heating cycles on the residual strength of the concrete has been presented in Figure 4.11. Here, the residual strengths are depicted against the number heating cycles at 500 °C (left) and at 900 °C (right). The influence of the cement type is obvious within the beginning numbers of heating cycles. For specimens made of CEM I and CEM II/A-LL, an increase of the number of heating cycles up to 8 decreases the residual strength at 500 °C to about 65 - 70 %. No significant loss of strength at cooled state is observed afterwards. At 900 °C, a dramatic reduction of the cooled strength to 5 - 10 % of the reference cold compressive strength occurs after the first heating cycle. A glance at the left diagram of Figure 4.11 reveals that the behavior of concrete specimens containing CEM III/B is partially different. At 500 °C, the exposure to more than one heating cycle and up to 8 cycles does not lead to a significant loss of residual strength. In other words, CEM III/B either with quartz or with BFS aggregates presents more stability over the further 7 cycles of high temperature exposure. This observation provides interesting knowledge regarding the possibility of improved formulation of concrete with CEM III/B that are more stable when subjected to unlimited cyclic thermal loads at temperature range 250 - 500 °C (more details will be given under section 4.3.2). In the right diagram a significant reduction of the residual strength of these specimens at 900 °C can be seen. Yet, the strength of the concrete at this temperature is still about 10 - 20 % higher than specimens made of other cement types. A further decrease 8 % and 13 % is observed between the first and the 5th heating cycle in case of specimens made of CEM III/B combined with slag and quartz aggregates, respectively, following which a plateau is reached. The plateau discussed for the peak temperature 900 °C corresponds to almost complete degradation of the concretes, which in almost all cases occur after exposure to a single heating cycle.

It is worth noting that the change of relative compressive strength of specimens made of quartzic aggregates, regardless of the type of cement, is identical both at 500 °C and 900 °C. This is due to the fact that aggregates constitute the major part of the concrete and have the highest impact upon the thermal behavior thereof.

The results of the second part demonstrate that the dependency of concrete strength loss on the composition can even become visible during exposure to the first numbers of heating cycles, but at temperatures lower than 500 °C. A comparison of the two sets of experiments reveals that while an increase in the number of thermal cycles and the peak temperature can in general deteriorate the concrete stability, concrete formulation using appropriate cement and aggregate types can in help reduce concrete thermal sensitivity at least up to a certain temperature level.

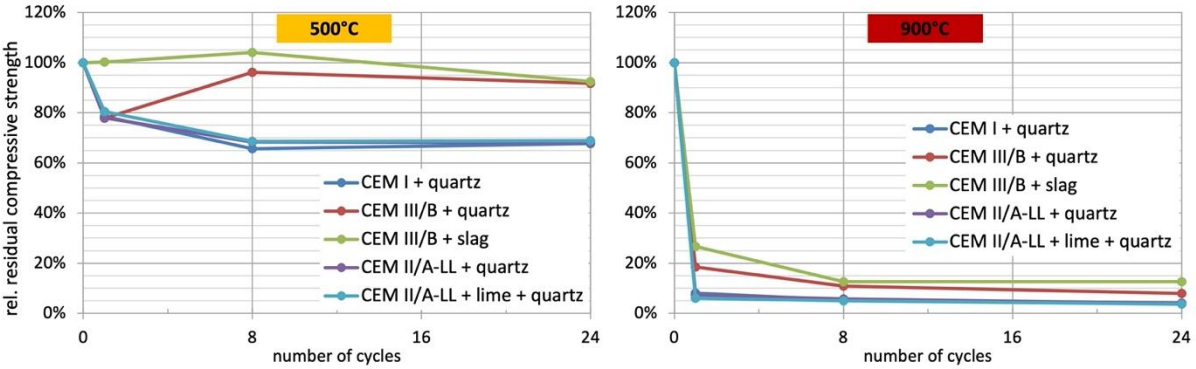

Figure 4.11 Relative residual compressive strength of specimens made of different cement types (CEM I, CEM III/B or CEM II/A-LL) and different types of aggregates following exposure to different number of thermal cycles (1, 8 and 24) with a peak temperature of 500 °C (left) and 900 °C (right). Note that the diagrams of CEM I + quartz, CEM II/A-LL+ quartz and CEM II/A-LL + lime +quartz both at 500 °C and 900 °C superimpose.

4.3.2 Effect of concrete composition

4.3.2.1 Effect of slag content, of the cement and aggregate type

In order to further characterize the effects of different types of cements with various slag sand content, the residual compressive strengths were compared amongst various specimens made of CEM I (0 % slag sand), CEM II/B-S (about 30 % slag sand) and CEM III/A (about 60 % slag sand) in combination with quartz or basalt (natural aggregates), or else BFS aggregates (Figure 4.12). A pronounced decrease in compressive strength is observed for all specimens until the 5th heating cycle, and particularly at 500 °C and 700 °C. At 250 °C, all specimens maintain their stability relatively well, as the aggregates are still stable and have rather low thermal expansion. Exposure to up to 20 thermal cycles at 250 °C decreases the residual compressive strength up to about 20 %. The highest residual strength at 250 °C after every heating cycle belongs the mixes with CEM III/A, followed by CEM II/B-S and CEM I.

A comparison of the three investigated cement types shows a similar trend in the reduction of the residual compressive strength after 1 and 5 heating cycles at 500 °C and 700 °C. This means that specimens containing CEM III/A (about 50 % slag sand) show higher residual strengths compared to CEM II/B-S (about 30 % slag sand), which are in turn associated with higher residual compressive strength compared to specimens made of CEM I. Specimens containing CEM I with quartz shows 10 % and 15 % residual strength after 5 heating cycles at 500 °C and 700 °C, respectively. For CEM I specimens with basalt and slag aggregates, the residual compressive strength after 5 heating cycles at 500 °C and 700 °C are reduced to 50 % and 30 %, and 52 % and 27 %, respectively. Interestingly, all mixes containing CEM I are fully destroyed after 20 heating cycles at 500 °C and 700 °C, where those made of CEM II/B-S and CEM III/A (with the exception of the CEM II/B-S combination with quartz) maintain significantly higher stability.

A review of the results demonstrated in Figure 4.12 clearly demonstrates the significant influence of the slag sand content of the cement upon the residual compressive strength. It can be obviously concluded that the residual compressive strength of the specimens at all temperatures and following exposure to the same number of thermal cycles always follows the order of CEM III/A > CEM II/B-S > CEM I. As previously debated, the main difference among these cement types lays in their slag sand content. Interestingly, the slag content of the specimens follows the same order as the residual compressive strength; which indicates that the amount of the slag sand in the cement is a major determinant of concrete stability in cooled state following exposure to one or more cycles of thermal loading. The fact that cement types containing slag sand can to some extent improve the residual compressive strength of the concrete exposed to one heating cycle has been shown in several investigations [40],[82], [183],[184],[185],[187],[194],[197]. The reports on the temperature at which this positive effect is the highest is rather controversial. Several studies have reported the maximum improvement of the residual compressive strength due to slag addition to be at temperature range of 600 °C - 700 °C. Examples are Andiç-Çakır et al., who reported that when formulated with comparable compositions using siliceous standard sand as aggregates, mortars made of CEM III/A showed significantly superior thermal resistance compared to those made of CEM I, with the highest difference being noticeable at 600 °C [183]. These results have been confirmed by Poon et al. for concretes containing coarse riverbed and granite aggregates [82] and Mandens et al. for concrete specimens made without aggregates [40]. Zemri et al., on the other hand, who investigated concretes and mortars made of CEM I and CEM III/A with sand as fine aggregates observed that both mortars and concretes made of CEM III/A showed higher residual compressive strengths at 300 °C and 400 °C, while no significant difference was observed at 600 °C [184]. In this work, we investigated the results of residual compressive strength at 700 °C (Figure 4.12), which seem to point out that the observed difference is aggregate dependent. As observed, the significant effect of CEM III/A upon the improvement of the residual compressive strength after one thermal cycle at 700 °C is seen in case of the specimens made of BFS but not as much in case of those with quartz and basalt aggregates.

The effect of different slag sand content upon the thermal resistance of concrete has been sought after in several investigations. For instance, Poon et al. compared the residual compressive strength of concretes containing slag sand when heated up to different temperatures ranging from 200 °C to 800 °C. The results showed that the increase in slag sand content from 30 % to 40 % slightly improved the residual compressive strength [82]. Mendes et al. reported an increase in the residual compressive strength when the slag sand content was increased from 35 % to 50 %, which was most pronounced for 600 °C. In case of specimens with 65 % slag sand, however, a significant reduction of the initial compressive strength (around 20 MPa) was observed, which in turn reduced the residual compressive strength at higher temperatures [40]. Sim et al. observed no significant influence of increasing the slag sand content of the concrete from 20 % to 40 % upon the residual compressive strength following exposure to different

temperatures [189]. Comparing concrete specimens made of 20 %, 40 % and 60 % slag sand, Siddique et al. found the substitution ratio of 20 % to have the most positive results upon the residual compressive strength [194]. Aydin has shown that when heated to 900 °C, pumice containing mortars with higher slag sand content, the residual compressive will be higher [188]. It seems that the diversity in the reported results is caused the difference in the concrete and mortar formulation, such as the type and aggregate content, the water to cement ratio, etc., and the initial strength of the concrete [177], [187].

As previously mentioned, our investigations show a positive effect of increasing the slag sand content of the cement (at least up to 50 %) upon the residual compressive strength. Currently, there is no comprehensive explanation as to why this can happen. Mandens et al. have attributed the improved thermal performance to the lowering of the $Ca(OH)_2$ content of the concrete through the substitution of CEM I with higher levels of slag sand. As the decomposition of $Ca(OH)_2$ is a major reason for the reduction of the conventional concretes around 400 - 500 °C, lower strength arising from this component improves the stability of concrete in case of slag sand containing specimens [40]. One potential explanation might be related to the fact that the powdered slag, as a byproduct of reactions at significantly high temperatures, has outstanding thermal stability and can thus reduce the shrinkage of the cement paste and hinder the development of cracks and micro-cracks within the concrete structure. Another possible explanation is a high re-hydration tendency of slag sand through the absorbance of the air moisture between subsequent heating cycles and within the course of the cooling phase, which can reduce the number and intensity of the microcracks. Figure 4.13 shows the development of cracks within the concretes made of CEM III/A, CEM II/B-C and CEM I. A comparison of the specimens clearly demonstrates that the formation of cracks in the concrete specimens following exposure to the thermal load has a reverse relationship with the slag sand content of the cement. A comparison of the results of the residual compressive strength with those related to hot compressive strength reveals that the second explanation seems more plausible. As detailed earlier, the stability of cements made of CEM III/A in hot condition is even lower than that of specimens with CEM I, whereas in the cooled state, the strength of the specimens is in the opposite order. This confirms that the gain in the strength of the specimens made of CEM III/A must be related to the changes during the cooling phase. Nonetheless, the increase in the stability of the concretes made of slag containing cements following storage post-thermal treatment, which will be the subject of discussion under later section 4.4, is a potential confirmation of this hypothesis.

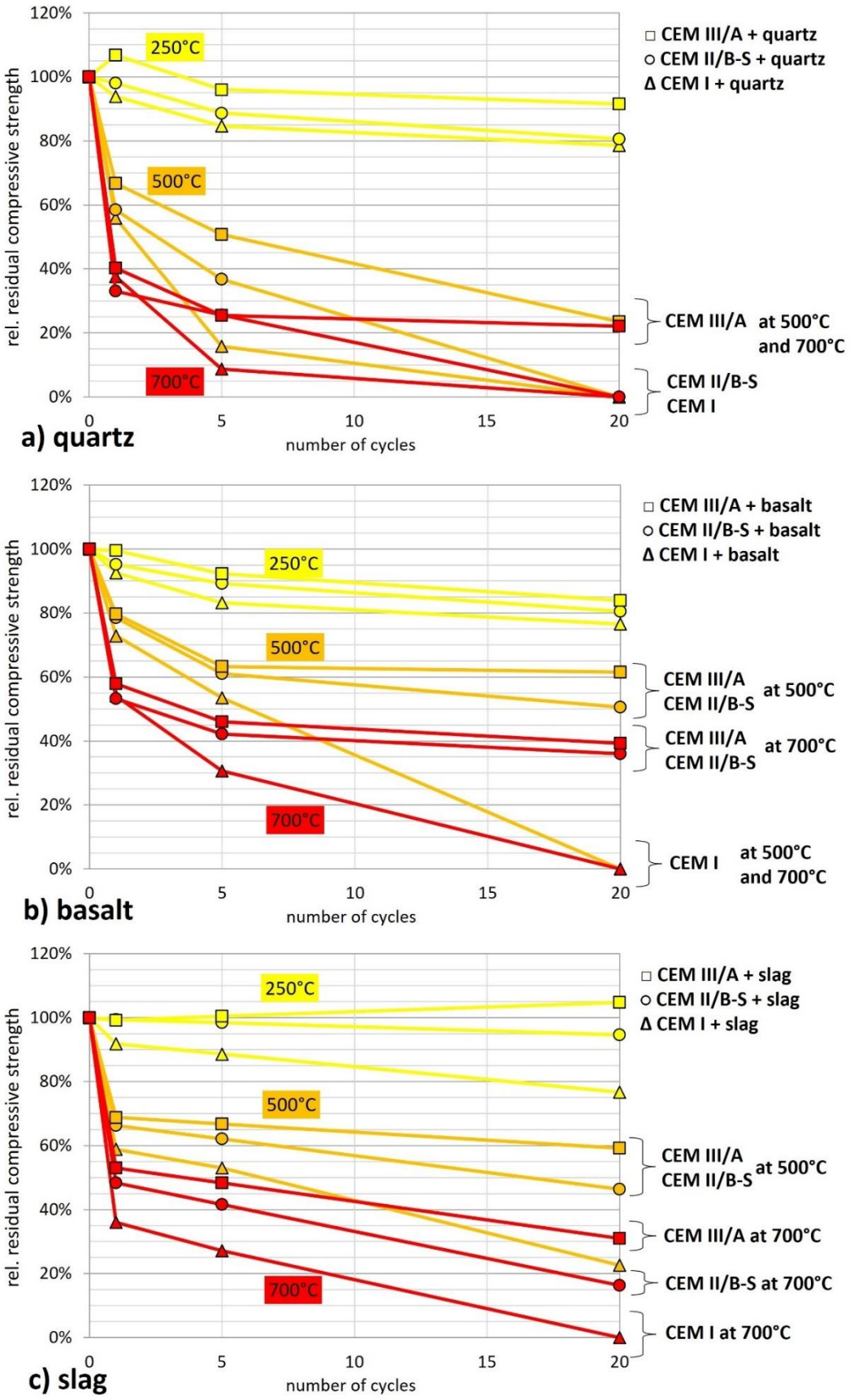

Figure 4.12 Comparison of the relative residual compressive strength of the specimens made of CEM I and CEM III/A complemented with basalt (a), quartz (b) and slag (c) aggregates following exposure to different number of thermal cycles with a maximum temperature of 250 °C, 500 °C and 700 °C [266]

The results also demonstrate the impact of aggregate type upon the residual compressive strength of the concretes made of a certain cement type. As observed in Figure 4.12, specimens with basalt are associated with the highest stability in the cooled state, followed by those made of BFS aggregates, and finally those composed of quartz. This is in accordance with the findings of the previous sections, describing the influence of aggregate type upon the hot compressive strength. Here again, quartzite aggregates have resulted in the lowest concrete stability in the cooled state, as they can create the largest damage to the concrete structure as a result of their significantly larger thermal expansion between 250 °C and 500 °C, followed by the quartz conversion at 573 °C [28]. Basalt and slag aggregates, which play beside cement at high temperatures, however, do not inflict much damage to the concrete structure given their significantly smaller thermal expansions at all investigated temperature levels [28]. Similar to the case of hot compressive strength, basalt aggregates have endowed the concrete better thermal stability compared to the slag aggregates.

The results of our investigations further confirm the presence of a “concrete specific critical temperature” as proposed by Khoury et al. [123]. However, an additional conclusion can be drawn from the data at this point, which is the presence of a temperature-dependent concrete specific "maximum damage threshold“. In combinations of slag sand containing cements with temperature-stable aggregates, the damage appeared to stabilize beyond a certain temperature and number of exposure cycle (Figures 4.12 and 4.13). This suggests the existence of a "temperature-dependent endurance limit," where the concrete's residual strength reaches a plateau despite exposure to further thermal cycles, which is similar to the hypothesis of Khoury et al. [123]. However, we can add that optimization of the concrete composition using thermally stable cements and thermally stable aggregates can increase the “concrete specific critical temperature” described by the authors [123]. This behavior is hypothesized to result from the stabilization of the aggregate-cement matrix interactions and the self-healing effects of certain hydration products at elevated temperatures (see section 4.4).

Figure 4.13 Specimens made of a) CEM I, b) CEM II/B-S (30 % blast furnace slag) and c) CEM III/A (60 % blast furnace slag) complemented with basalt as aggregate after exposure to 20 thermal cycles with a peak temperature of 500 °C

The effect of the slag sand in cement upon the concrete stability in cooled state was further studied in a separate series. Here, specimens made of CEM I, CEM II/A-LL and CEM III/B were investigated. The detailed composition of these specimens is given in Table 3.6.b, while the initial compressive strengths is given in Table 4.1.b. Amongst these, CEM III/B comprised 80 % slag sand, and CEM II/A-LL contained 15 % limestone. The residual compressive strengths of these specimens were compared following exposure to 1, 8 and 24 heating cycles with the maximum temperatures of 250 °C, 500 °C, and 900 °C. The combination of CEM II/A-LL and a maximum heating temperature of 900 °C was primarily selected to illustrate the influence of decarbonization of $CaCO_3$ within the cement at high temperature behavior of concrete, which has the highest rate around 900 °C. Figure 4.14.a shows the relative residual compressive strength of these specimens after 8 heating cycles at different temperature levels. Here again, it can be clearly observed that the presence of a high slag sand content in the cement leads to a significant improvement of the concrete stability in cooled state. Indeed, specimens composed of CEM III/B were associated with the highest residual compressive strengths at all temperatures. Specimens made of CEM I, on the other hand, had the smallest boundary of residual strengths over elevated temperatures. The behavior of concretes made of cements with limestone (CEM II/A-LL) were very similar to the reference concrete with CEM I when exposed to cyclic thermal loads, though specimens made of the former are associated with higher levels of residual strength after exposure to 250 °C.

The effect of the aggregates can be determined by comparing the residual compressive strength of the specimens made of CEM III/B, along with quartz or BFS as aggregates. It is clear from Figure 4.14.a that the residual strength of the specimens with quartz is always below that of the specimens with BFS aggregates. The two curves only superimpose at 900 °C. This highlights the added advantage of using slag not only as a part of the cement, but also as an added aggregate. At 250 °C and 500 °C, the residual strength of the specimens made of CEM III/B and BFS aggregates is about 6 % and 8 % higher that of those comprising CEM III/B and

quartz, respectively. On top of that, BFS aggregates presents more stability against exposure to cyclic elevated temperatures compared to the usual quartz aggregates.

A further investigation was the impact of replacing part of the quartz aggregate within the specimens made of CEM II/A-LL with additional limestone filler. In general, limestone is expected to have better thermal stability, owing to its lower thermal expansion compared to quartz [28]. The results, however, depict no additional benefit of replacing part of the quartz aggregates with limestone. It is probably attributed to the dominant effect of cement type upon the behavior of these concretes at high temperature. As expected, only a small amount of residual strength remains after heating these specimens to 900 °C, highlighting the effect of limestone decarbonation.

In general, the results of both sets of experiments summarized in Figure 4.12 and Figure 4.14 highlight the advantage of using CEM III, in combination with different aggregates, to enhance the residual compressive strength of the concrete post-thermal exposure.

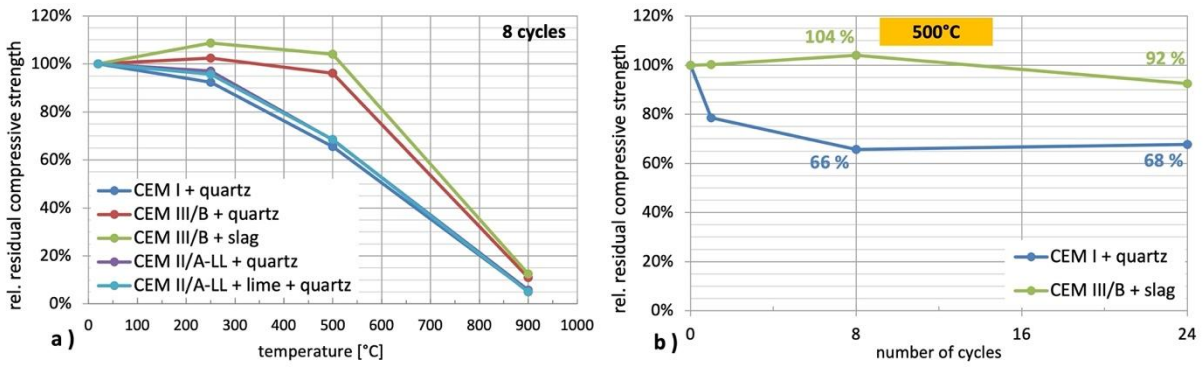

Figure 4.14 a) Comparison of the relative residual compressive strength of specimens made of CEM I, CEM III/B and CEM II/A-LL after exposure to 8 thermal cycles at various peak temperatures (250 °C, 500 °C and 900 °C), b) comparison of the relative residual strength of concrete made of CEM I with quartz aggregates and CEM III/B and BFS aggregates following exposure to 1, 8 and 24 thermal cycles with a peak temperature of 500 °C. Note that the diagrams of CEM II/A-LL+ quartz and CEM II/A-LL + lime +quartz in (a) superimpose.

Figure 4.14.b compares the residual compressive strength of two sets of specimens with the highest and the lowest boundary curves after exposure to different numbers of heating cycles exemplary at a maximum temperature of 500 °C. As evident from the figure, specimens made of the cements containing slag sand in combination with slag as aggregate showed almost no loss of strength when heated up to 500 °C regardless the number of cycles. On the contrary, exposure to the same conditions resulted in an irreversible loss of strength in conventional reference concretes (CEM I with quartz aggregates), even after one cycle of thermal exposure. After 8 and 24 heating cycles at this temperature (500 °C), specimens made of CEM III/B with BFS aggregates have 38 % and 24 % more residual compressive strength compared to those made of CEM I and quartz. This figure perfectly summarizes the positive influence of slag (both

as an SCM and as aggregate) upon the improvement of the concrete stability when exposed to repeated heating and cooling cycles.

In short, both studies highlight the positive role of slag sand as an SMC in improving the residual compressive strength of the concrete. It seems that the higher the slag content of the used cement for concrete production is, the higher the residual compressive strength will be. The results of both studies also highlight the positive impact of BFS and basalt as aggregates upon the thermal stability of the concrete specimens, though the performance of basalt aggregates seems to be superior.

4.3.2.2 Statistical analyses of effect of cement and aggregate mixtures based on the DOE

As elaborated in the methodology section, the influence of cement and aggregate type along with the maximum temperature, number of heating cycles and the post-storage duration upon the residual compressive strength was statistically evaluated through a design of experiments compiled by FEhS. This section primarily focuses on the impact of the cement type and aggregate mixtures, while the impact of post-storage will be elaborated under the related section. The general statistical test plan used for the investigation of the 5 examined aggregate mixtures is shown in Table 3.1 and results are compiled in Table 3.2 in chapter 3. For the statistical evaluation of the test plans, the first step to determine whether the produced concrete came from a homogeneous population. For this purpose, the concrete bulk densities were used as they were the only determined factor at this point. Any outliers that occurred were identified and excluded from further evaluations. Additionally, the normal distribution of concrete raw densities was confirmed. This confirmed a homogeneous concrete production, and hence the possibility of the statistical evaluation of the results.

Specimens with basalt / basalt aggregate mixture

For specimens with basalt as coarse and fine aggregates, the results of the experiments were statistically evaluated in terms of the residual compressive strength using multiple regression analyses. Table 4.3 summarizes the coefficients of determination (R^2) and the standard deviations of the regression as well as the contributions of the significant influencing variables or interactions on the expected result. Due to the binomial nature of the fitting, the squared values of slag sand content of the cement (slag) and maximum temperature of exposure (T) have been evaluated.

Table 4.3 coefficient of determination and contributions of the statistically significant influencing variables and interactions on the relative residual compressive strength [266]

	R^2	σ	Slag	Slag²	T	T²	C	P	T*Slag	T*C	T*P	Slag*C	Slag*P	C*P
	[%]													
$f_{c,HT}$/ $f_{c,45d}$	91	7,5	8	1	57	1	14	1	1	2	0	4	0	1

Abbreviations defined in Table 3.1

For the cases where the regression coefficient was $R^2 \geq 0.50$, the regression equation was evaluated for all combinations of the significant influencing parameters within the previously defined system limits.

Based on the findings presented in Table 4.3, the strong influence of the maximum temperature and the number of thermal stress cycles upon the residual compressive strength of the specimens containing basalt aggregates is once again confirmed. As extensively debated within the previous section, a significant reduction of the concrete residual strengths is observed as the peak temperature increases. There is also a clear decrease in the residual compressive strength of the specimens when the number of the thermal stress cycles increases from 5 to 20 temperature cycles. Although the slag sand content of the cement makes a significantly smaller contribution to the residual compressive strength (compared to the maximum temperature of the load), the detected effect is still highly significant. The positive influence of the slag sand content of the cement upon the concrete strength in cooled state becomes more evident as the number of the heating cycles increases. This means that the thermally induced damage to the concrete specimens with higher slag sand content in the cement is significantly smaller.

Specimens with quartz / quartz aggregate mixtures

For specimens with quartz as coarse and fine aggregates, the results of the experiments were statistically evaluated in terms of the residual compressive strength using multiple regression analyses. Table 4.4 summarizes the coefficients of determination (R^2) and the standard deviations of the regression as well as the contributions of the significant influencing variables or interactions on the expected result. Due to the binomial nature of the fitting, the squared values of slag sand content of the cement (slag) and maximum temperature of exposure (T) have been evaluated.

Table 4.4 Coefficient of determination and contributions of the statistically significant influencing variables and interactions on the relative residual compressive strength [266]

	R^2	σ	Slag	Slag²	T	T²	C	P	T*Slag	T*C	T*P	Slag*C	Slag*P	C*P
	[%]													
$f_{c,HT}/ f_{c,45d}$	95	8,1	-	3	74	5	8	1	0	1	0	0	0	2

- not significant; Abbreviations defined in Table 3.1

Similar to the test plan with basalt as fine and coarse aggregates, regression models with a high degree of determination were calculated. In general, the same significantly influencing parameters identified in the case of specimens with basalt were also found influential in this case. The maximum temperature has an extremely strong influence, with all test specimens being severely damaged or even destroyed at 700 °C. Furthermore, the number of thermal stress cycles as well as the slag sand content of the cement make significant, though smaller, contributions.

Specimens with slag sand / basalt aggregate mixtures

For specimens with slag sand as fine and basalt as coarse aggregates, the results of the experiments were statistically evaluated in terms of the residual compressive strength using multiple regression analyses. Table 4.5 summarizes the coefficients of determination (R^2) and the standard deviations of the regression as well as the contributions of the significant influencing variables or interactions on the expected result. Due to the binomial nature of the fitting, the squared values of slag sand content of the cement (slag) and maximum temperature of exposure (T) have been evaluated.

Table 4.5 . Coefficient of determination and contributions of the statistically significant influencing variables and interactions on the relative residual compressive strength [266]

	R^2	σ	Slag	$Slag^2$	T	T^2	C	P	T*Slag	T*C	T*P	Slag*C	Slag*P	C*P
	[%]													
$f_{c,HT}/ f_{c,45d}$	92	8,1	7	3	67	1	-	-	-	11	-	3	2	0

- not significant; Abbreviations defined in Table 3.1

Here again, the peak temperature has by far the greatest influence on the residual compressive strength of the specimens. In addition, the slag sand content of the cement, the number of temperature cycles and the duration of storage (will be debated separately in section 4.4) also influence the test results.

Specimens with slag sand / BFS aggregate mixtures

For specimens with slag sand as fine and BFS as coarse aggregates, the results of the experiments were statistically evaluated in terms of the residual compressive strength using multiple regression analyses. Table 4.6 summarizes the coefficients of determination (R^2) and the standard deviations of the regression as well as the contributions of the significant influencing variables or interactions on the expected result. Due to the binomial nature of the fitting, the squared values of slag sand content of the cement (slag) and maximum temperature of exposure (T) have been evaluated.

Table 4.6 Coefficient of determination and contributions of the statistically significant influencing variables and interactions on the relative residual compressive strength [266]

	R^2	σ	slag	$slag^2$	T	T^2	C	P	T*Slag	T*C	T*P	Slag*C	Slag*P	C*P
	[%]													
$f_{c,HT}/ f_{c,45d}$	93	8,0	6	1	75	0	-	-	0	8	-	2	1	0

- not significant; Abbreviations defined in Table 3.1

Regression equations with a high degree of certainty and comparatively low standard deviations were also determined for the concretes with slag as fine (slag sand) and coarse (BFS) aggregates. Similar to other concrete specimens, the maximum temperature of the load has an enormous influence on the compressive strength in the cooled state. However, the slag sand

content of the cement and the number of temperature cycles are also significant, though they make a comparatively small contribution to the test results.

Specimens with quartz / BFS aggregate mixtures

For specimens with quartz as fine and BFS as coarse aggregates, the results of the experiments were statistically evaluated in terms of the residual compressive strength using multiple regression analyses. Table 4.7 summarizes the coefficients of determination (R^2) and the standard deviations of the regression as well as the contributions of the significant influencing variables or interactions on the expected result. Due to the binomial nature of the fitting, the squared values of slag sand content of the cement (slag) and maximum temperature of exposure (T) have been evaluated.

Table 4.7 Coefficient of determination and contributions of the statistically significant influencing variables and interactions on the relative residual compressive strength [266]

	R^2	σ	Slag	Slag²	T	T²	C	P	T*Slag	T*C	T*P	Slag*C	Slag*P	C*P
	[%]													
$f_{c,HT}/ f_{c,45d}$	93	8,0	-	1	73	2	7	0	4	4	1	1	-	-

- not significant; Abbreviations defined in Table 3.1

As with all other experiments described above, the maximum temperature during the load exerts a dominant influence on the residual compressive strength of these specimens. Although the influence of the slag sand content in the cement and the duration of the post-thermal stress storage are relatively small, they still make a significant contribution.

Evaluation of the regression equations

To check the regression equations determined from the statistical test plan, additional concrete specimens that were not part of the test plan were produced. The test parameters used were of course within the defined test limits. In Figure 4.15, the residual compressive strengths calculated from the measured values are compared with those that were predicted on the basis of the regression equations. The figure clearly shows that the regression equations can be used to predict the residual compressive strengths with sufficiently good approximation. Thus, the statistical test plans can be interpreted in terms of the significance of the influencing variables.

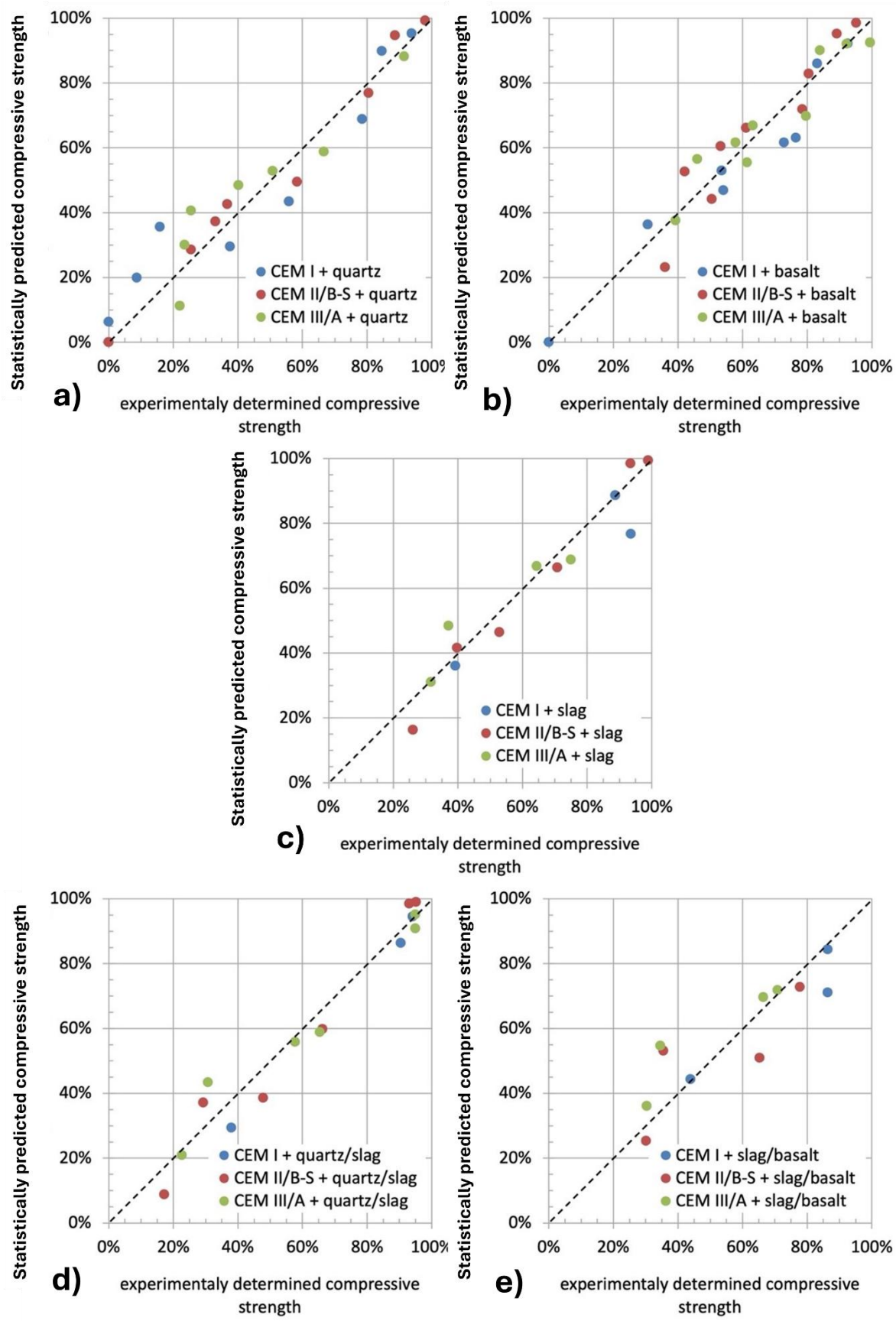

Figure 4.15 Verification of the regression equations through additional trials for all aggregate combinations: a) quartz/quartz, b) basalt/basalt, c) slag (sand)/slag (BFS), d) quartz/slag (BFS) and e) slag (sand)/basalt [266]

Effect of the cement type

The statistical analyses of the mathematical models confirmed that the residual compressive strength following exposure to temperatures are in general higher if CEM I is replaced by cements containing slag sand (CEM III/A and CEM II/B-S). Figure 4.16 shows an example of the change in the residual compressive strength for the concretes with CEM II/B-S and CEM III/A compared to those made of pure CEM I. A detailed discussion of these results have been presented under section 4.3.2. To sum up, an increase in the slag sand content of the cement leads to an improvement of the concrete's relative residual compressive strength, particularly upon exposure to higher peak temperatures and a higher number of the thermal cycles. This applies to concretes that have been produced with temperature-resistant aggregates (i.e. basalt and BFS), but also, to a lower extent, even to specimens containing the non-temperature-resistant quartzite, aggregates. Hence, through the use of slag sand as an SCM, a significant increase in thermal resistance and thermal cycle stability is achieved.

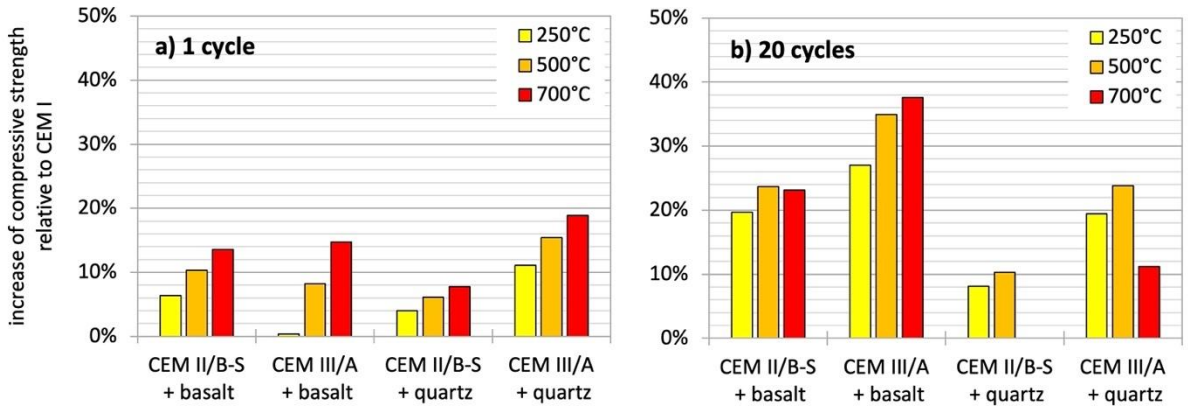

Figure 4.16 Increase in residual compressive strength of the concretes containing cements with slag sand (CEM II/B-S and CEM III/A) compared to those made of CEM I (CEM I) after exposure to thermal loads

Effect of the aggregate type

When exposed to a maximum temperature of 250 °C, the investigated aggregate mixtures do not yet have any significant influence on the residual compressive strength of the specimens (Figure 4.17). This is to be expected, as all aggregates are still stable at this temperature level and the associated thermal expansion is low. Even in case of the quartzite aggregates, the conversion reaction for its inadequate temperature stability occurs at 573 °C [28].

On the contrary, clear differences in terms of residual compressive strength of the specimens can be observed from a peak temperature of 500 °C onwards (Figure 4.18 second and third row). From here on in, concretes with quartzite aggregates in the coarse and fine fraction had significantly lower residual compressive strengths compared to specimens comprising aggregate mixtures containing fine and coarse basalt, and fine and coarse slag (slag sand and BFS). If concretes were produced exclusively with these aggregates, the differences in their residual compressive strength were slight. This means that the combination of the standard,

industrial fine a coarse slag aggregates (slag sand and BFS) endows the concrete adequately high temperature stability comparable to that provided by basalt, which is the most commonly known type of temperature-stable aggregate in the concrete industry.

Another remarkable finding was that replacing the coarse fraction of the quartzite aggregates with BFS accounted for a significant increase in the residual compressive strengths of the specimens. This remarkable improvement was observed both in case of the once time thermal exposure as well as for frequent temperature exposures up to 20 cycles. The positive effect of replacing part of the natural aggregates by BFS coarse aggregates upon the residual compressive strength of the concrete has been shown by Vaidya et al., who found 20 % substitution ratio to bring about superior results compared to 40 % and 60 % [200]. Yu˙ksel et al. showed that substituting part of the natural aggregates by slag sand as fine aggregates could also significantly improve the thermal resistance of the produced concrete when subjected to 800 °C, and that a replacement ratio of 20 % was more beneficial than 10, 30, 40 and 50 % [199].

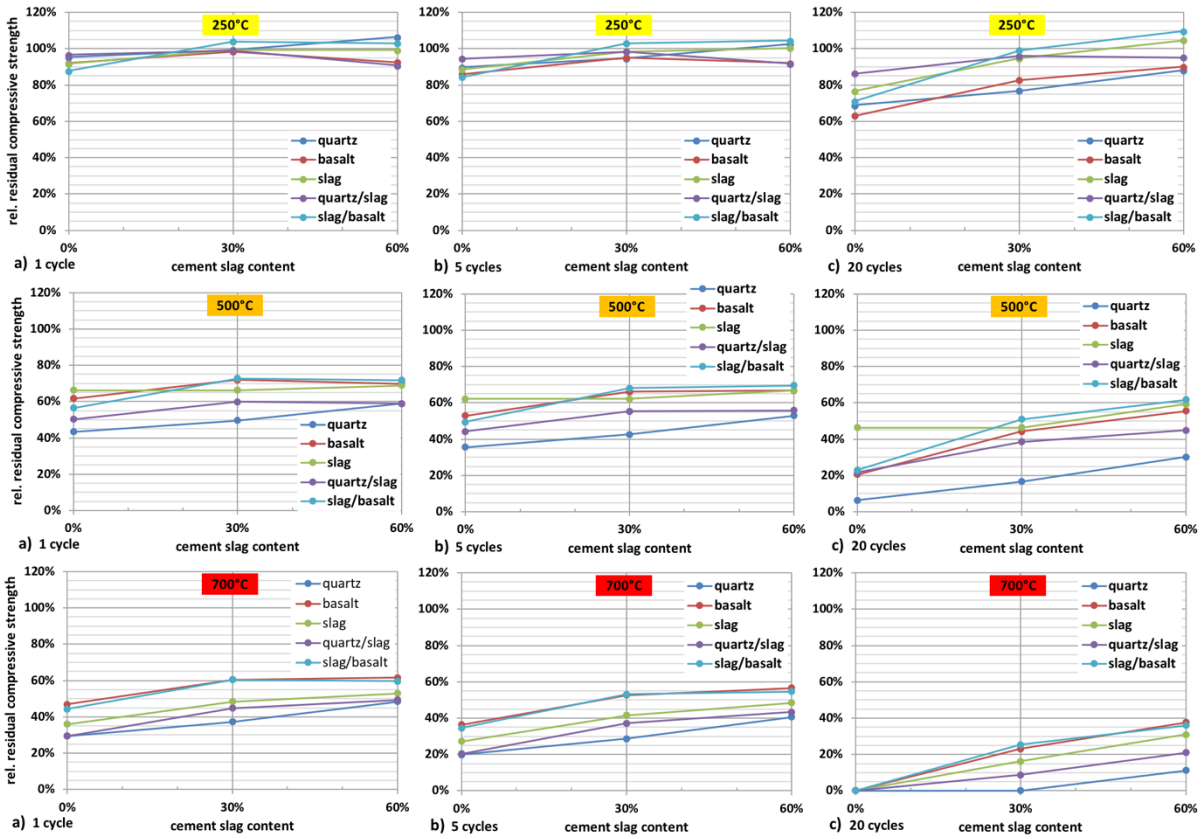

Figure 4.17 Influence of aggregate type on residual compressive strength of concretes after exposure to 1 (a), 5 (b) and 20 (c) thermal cycles at 250 °C (first row), 500 °C (second row) and 700 °C (third row) depending on blast furnace slag content of the cement using the statistical results from DOE analysis [266]

4.3.2.3 Influence of non-standard slag aggregates

Based on the promising results highlighting the positive influence of the slag aggregates (both fine slag sand and coarse BFS aggregates) upon the residual strength of the concrete specimens,

we sought to investigate as to whether other non-standard industrial slag aggregates could potentially provide comparable improvements. As previously debated (section 4.2.1.4 and section 4.2.2), these could not provide a comparable hot condition stability to the standard aggregates. In this section, their influence upon the residual compressive strength of the concrete will be discussed. Detailed information regarding the composition of the concrete specimens used for these experiments has been provided in Table 3.6.c.

Figure 4.18 shows the residual compressive strength of the concrete specimens made of the non-standard slag aggregates (Ef-slag, LD-slag and Cu-slag) following exposure to 5 heating cycles with maximum temperatures of 500 °C and 700 °C. For 500 °C, the results are presented for specimens made of both CEM I and CEM III/A, whereas for 700 °C, only the findings for specimens with CEM III/A are reported. The first result from this figure is the impact of the cement type. By comparing the residual compressive strength of the specimens made of CEM I and CEM III/A, it becomes obvious that the addition of all non-standard industrial aggregates has a significantly better influence upon the growth of the residual strength of specimens made of CEM I. Boquera et al. have reported that compared to silicio- calcareous aggregates, steel slag aggregates led to better cohesion of the components when exposed to high temperatures without forming remarkable cracks, though a notable separation within the bonding of the cement paste matrix and the steel slag aggregate was also observed [238]. A second conclusion is that compared to the findings for the hot compressive strength, the positive impact of the non-standard aggregates upon the improvement of the residual compressive strength of the aggregates is significantly more pronounced. At least when heated to a temperature of 500 °C, the specimens made of non-standard aggregates can in almost all cases provide comparable, if not superior, residual strength compared to reference specimens made of the same cement type but complemented with quartz (non-heat-resistant aggregate). At 700 °C, however, the performance of the non-standard aggregates remains poor, and the values for the residual compressive strength are considerably lower than that obtained for quartzite aggregates.

Additionally, various industrial aggregates show a different influence on the temperature resistance of the concretes made thereof. Following heating, concretes with copper slag have comparable residual strengths to specimens made of slag aggregates. Other aggregates are associated with significantly lower residual compressive strength values. At maximum temperatures of 500 °C, the associated compressive strengths are only in the order of magnitude of concretes with quartzite aggregates. At 700 °C, the results are, as previously mentioned, even poorer. Among various steelwork aggregates, the thermal performance of Ef-slag 2 has been the poorest. Specimens made of Ef-slag 2 have been the only concretes with slightly lower residual compressive strengths compared to those with quartzite aggregates at 500 °C. At 700 °C, these specimens were completely destroyed upon exposure to one thermal cycle, only.

Based on the difference in the function of various steelwork aggregates, a generalization of the results and thus an assessment of the temperature stability of these is not possible. As observed, the Ef-slag from different sources had different performance, which signifies the determining

role of the aggregate source upon the heat stability of the concrete made thereof. While the residual strengths of the concretes with the Ef-slag 1 were in the order of magnitude of those of the concretes with quartz aggregates, much lower residual strength values were measured the concretes made of Ef-slag 2. Further extensive investigations are necessary to determine the reasons behind this different behavior. Hence, the heat resistance of the concrete made of non-standard aggregates is to be verified individually should these be meant to use for concrete production.

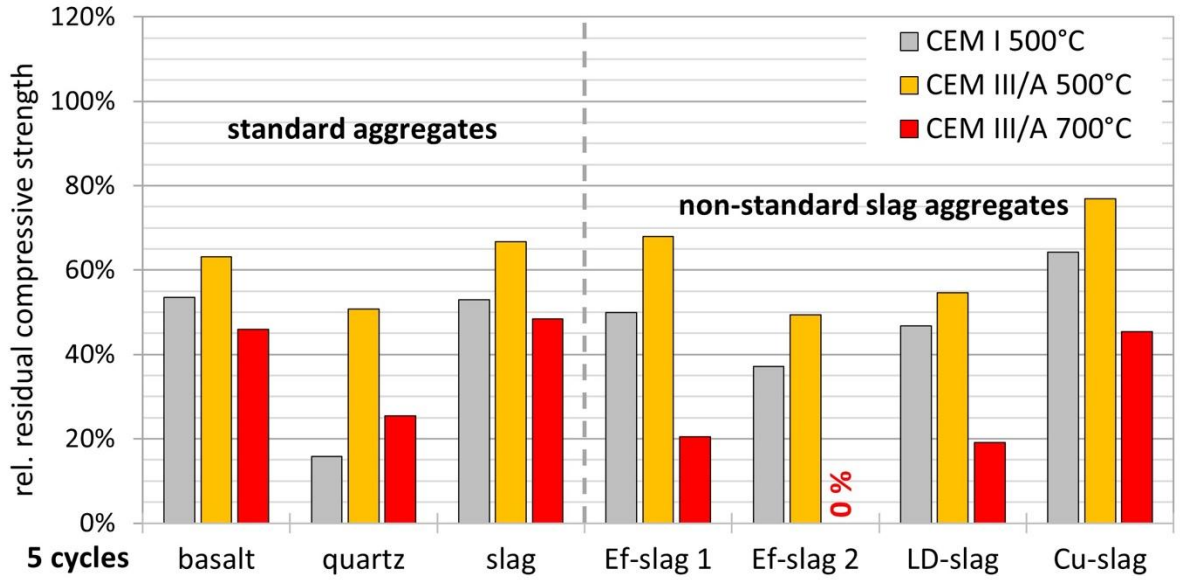

Figure 4.18 Relative residual compressive strength of the specimens made of non-standard aggregates from steelwork in comparison to those made of standard aggregates (basalt, quartz and slag sand/BFS). The results are presented for combination of aggregates with CEM I (500 °C) and CEM III/A (500 °C and 700 °C) after 5 cycles

4.3.2.4 Effect of aggregate size

In addition to the influence of the aggregate type, the effect of the largest grain size of the aggregates upon the residual compressive strength of the concrete specimens was investigated.

As previously debated, the use of basalt as a temperature-stable aggregate and quartz as a thermosensitive aggregate can provide the upper and lower limit of the results for standard aggregates. Accordingly, the investigations into the influence of the largest grain size were limited to these two aggregates. For these experiments, the industrial cement CEM II/B-S was exemplarily used for concrete production. Production, storage, conditioning and testing were carried out as described in section 3.3.1 and Figure 3.6. Detailed information about the concrete compositions were listed in Table 3.6.d and Table A.2.5. The largest aggregate grain size was varied as:

- CEM II/B-S + quartz (0/2, 0/4, 0/8, 0/16 mm)
- CEM II/B-S + basalt (0/2, 0/4, 0/8 mm)

This resulted in a systematic increase of the largest grain size from 2 mm to 16 mm for quartz and to 8 mm for basalt. As the largest grain size of the aggregates used within the rest of the investigations was equal to 4 mm, a such designed experimental setup examined a shift of the largest grain size towards the finer as well as the coarser aggregate variants.

Figure 4.19 demonstrates the residual strength of the specimens made of quartz (left) and basalt (right) aggregates with different largest grain size, when exposed to peak temperature levels of 250 °C and 500 °C. As observed, increasing the largest grain size from 2 mm to 16 mm does not exert any noticeable influence on the residual compressive strength, neither for quartzite nor for basaltic aggregates. The results are qualitatively and quantitatively comparable within the scope of the usual measurement inaccuracies. The residual compressive strength of the specimens made of basalt aggregates with a maximum grain size of 2 mm was only marginally higher than those prepared with other grain sizes of the same aggregate.

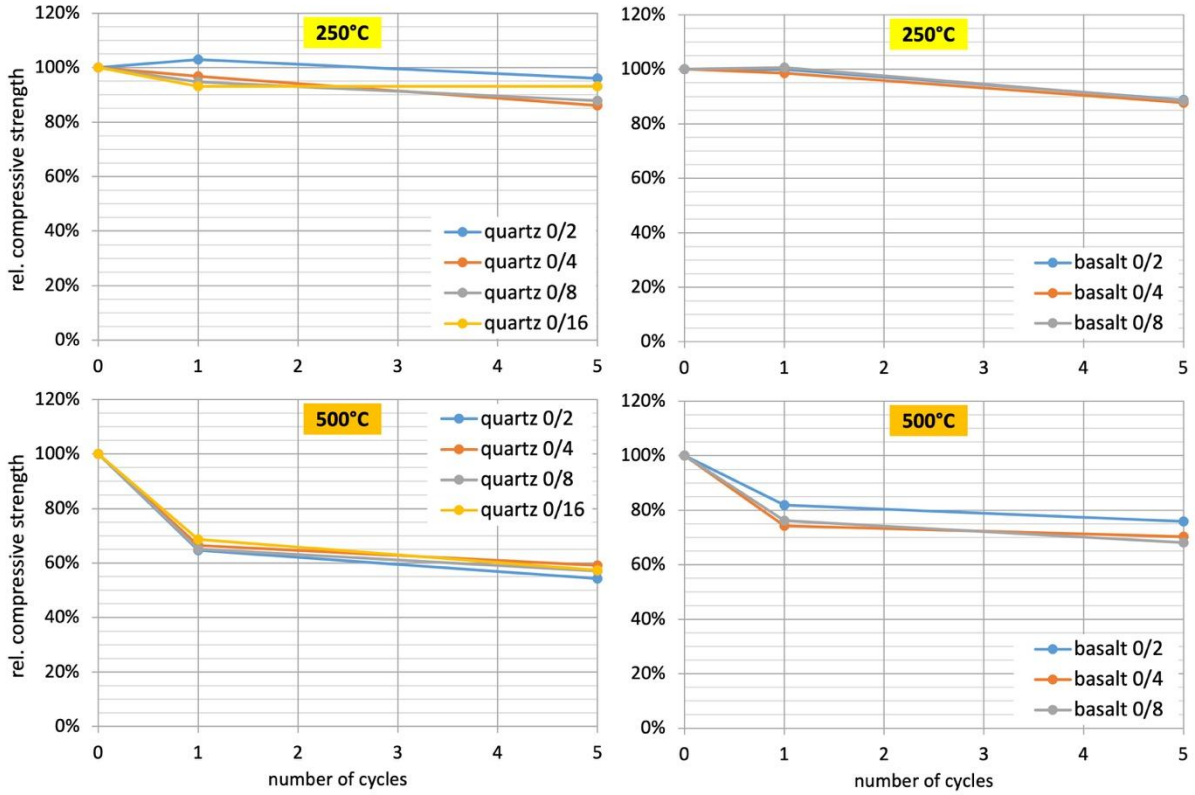

Figure 4.19 Influence of maximum grain size on residual compressive strength for the specimens made of quartz (left) and basalt aggregates (right)

The largest aggregate grain size of quartz aggregates seems to have significant influence on the residual flexural strength of the concrete (Figure 4.20). A recognizable influence of the largest grain can be seen for quartz aggregates following exposure to merely one temperature cycle. In this case, a significant reduction of the residual flexural strength with a growth of the largest aggregate grain size is pronounced. At 250 °C, for instance, the residual flexural strength of the specimens made of quartzite aggregates with a maximum grain size of 2, 4, 8 and 16 mm is equal to ca. 90 %, 90 %, 80 % and 55 %, respectively. This observed decrease is even more pronounced at 500 °C, where an increase of the largest grain size from 2 to 16 mm leads to a

reduction of the residual flexural strength from 90 % to 20 %. Since the lowest fiber is decisive for failure when testing the flexural strength and the transition zone between cement stone and aggregate plays a major role in the flexural tensile area of 16 mm aggregate, the measured effects are plausible.

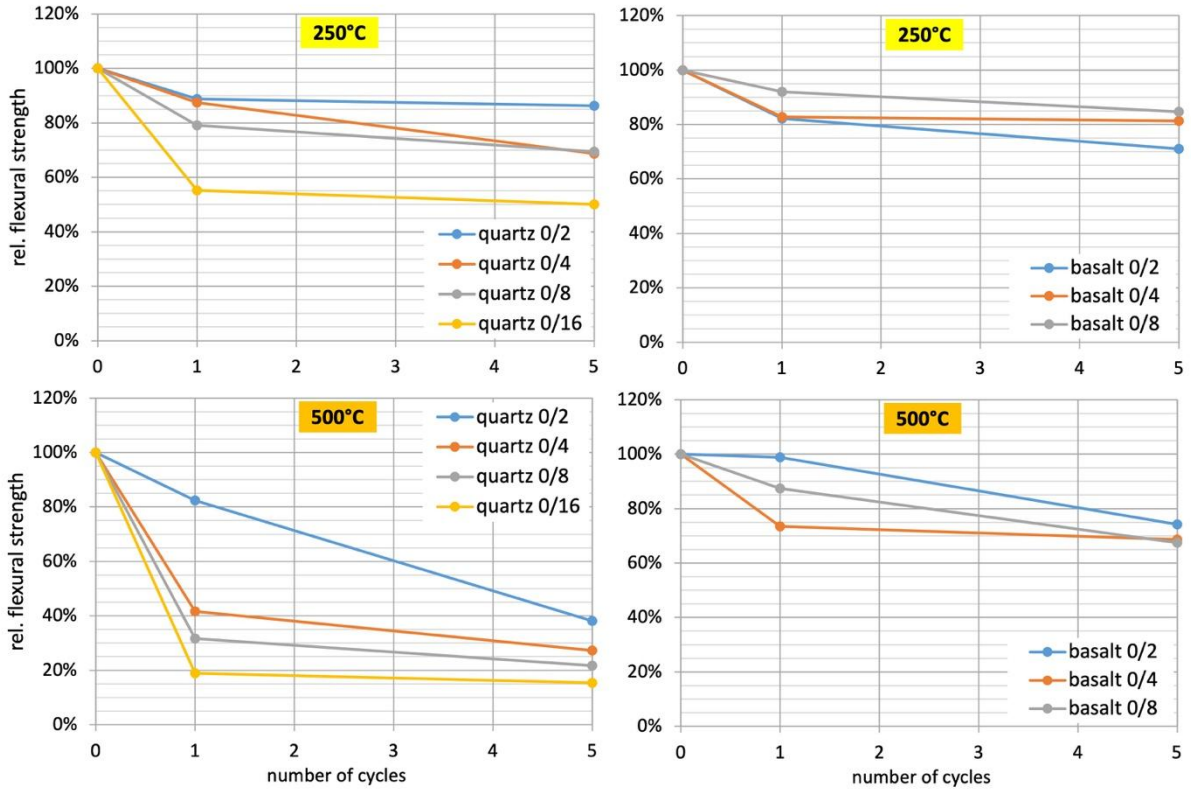

Figure 4.20 Influence of maximum grain size of aggregate on the residual flexural strength (under one point loading) for the specimens made of quartz (left) and basalt aggregates (right)

A similar trend is not observed in case of specimens with basalt aggregates. In this case, the measured flexural compressive strength after one heating cycle at 250 °C is highest for 8 mm basalt aggregates, and similar for those with grain sizes equal to 2 and 4 mm. At 500 °C, the residual flexural strength of the specimens follows the order of 2 mm > 8 mm > 4 mm.

As previously debated, the residual flexural strength reacts faster and more sensitively to thermal damage than the residual compressive strength. As a result, the effect of maximum grain size, which is not visible upon the residual compressive strength of the specimens, is reflected through their influence upon the residual flexural strength.

4.3.3 Comparison of residual compressive strength with standards

DIN EN 1992-1-2 represents no residual compressive strength following temperature exposure for concrete. For the better evaluation of findings of this study, the obtained results for residual compressive strength following exposure to one heating cycle were compared with the residual compressive strength within the approach for consideration of the cooling phase of concrete in

Appendix B of DIN EN 1994-1-2 for fire design of composite steel and concrete structures [114].

The residual compressive strength of investigated concretes containing combination of quartz, basalt and slag with both cement types are shown in Figure 4.21. The standard values are given for concrete with quartzite (blue curve) and calcitic (red curve) aggregates. As observed, the residual compressive strength of investigated concretes containing combination of quartz with both CEM I and CEM III/A, are higher than the blue curve. Regardless of the cement type, concrete with basalt always possesses higher residual compressive strength compared with limestone. Furthermore, the residual compressive strength of the concretes made of a combination of CEM III/A and slag transcends that of the standard limestone curve at all temperatures. Combination of CEM I and slag, on the other hand, yields concretes with residual compressive strength between the standard values for quartz and limestone.

At a thermal load of 250 °C, the measured residual strengths of all tested concretes are between 90 % and 105 % of the cold compressive strength, which is far above that of the standard values for quartz and limestone (approx. 82 % of the cold compressive strength). Furthermore, clear differences are observed at 700 °C. According to DIN EN 1994-1-2, about 30 % and 40 % of the cold compressive strength is expected for standard concretes with quartz and limestone, respectively [114]. The obtained values for CEM I mixes with quartz and slag aggregates as well as CEM III/A mix with quartz are within this range. For concrete mixes comprised of CEM I and basalt, as well as those containing CEM III/A and basalt or slag aggregates, the residual compressive strength values at 700 °C fall within the range of 55 % to 60 % of the cold compressive strength. Accordingly, at these higher temperatures, the influence of the aggregate type and the slag sand in the cement is clearly evident.

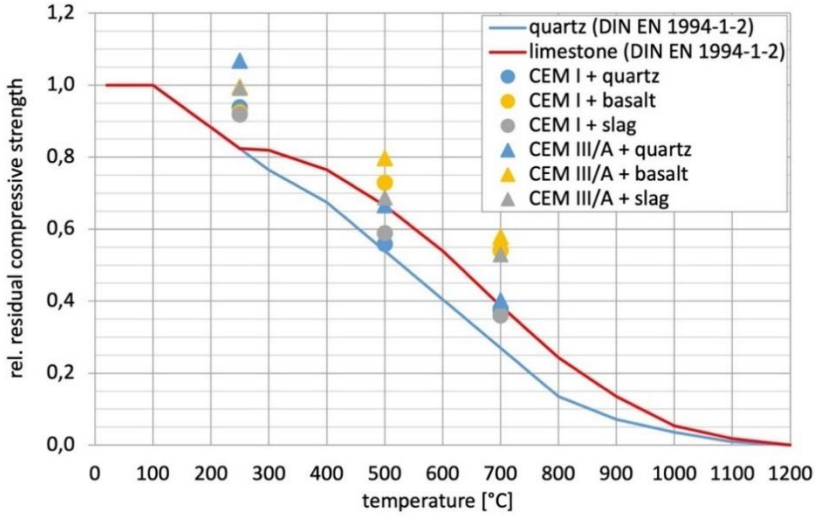

Figure 4.21 Comparison of the relative residual strength of the specimens made of CEM I or CEM III/A in combination with basalt, slag or quartz aggregate with the standard mixes (CEM I with quartz or with limestone aggregates) according to DIN EN 1994-1-2 [114]

4.3.4 Effect of cold compressive strength on the residual compressive strength following high temperature exposure

In this section, the effect of the cold compressive strength of the concrete upon the residual compressive strength following exposure to various numbers of heating cycles is discussed. To this end, two different concrete series with different cold compressive strengths were compared (Table 4.1). The investigated series are compared in Figure 4.22 in terms of their residual compressive strength, where the relative residual strength is depicted against temperature. The diagrams on the left (a, b and c) show the results of concretes with higher cold compressive strength (averagely 65 N/mm^2) exposed various peak temperatures for 1, 5 and 20 thermal cycles, respectively. The curves shown on the right (d, e and f) are obtained for concrete with lower cold compressive strength (35 N/mm^2) with almost similar cement and aggregate types. Unlike the first experimental series whose cold compressive strength was tested approximately on day 46 post-production, the latter specimens were tested after 28 days only, which means that the cold compressive strength of the second test series was significantly lower (almost half; see Table 4.1). The residual compressive strength of the second series is presented after exposure to 1, 8 and 24 heating cycles (Figures 4.22 d, e and f, respectively). The combination of CEM III type A or B with quartz or slag were investigated in both studies. Specimens made of CEM I and quartz have been examined in both experimental series as reference mixture. Combination of CEM III/A with basalt has been added to the first series as a reference for the highest level of temperature resistance (Figures 4.22 a, b and c).

In general, a simple comparison of the two test series reveals that the relative residual compressive strength of the higher cold strength series (Figure 4.22 a, b and c) are smaller than those calculated for the lower cold strength series (Figure 4.22 d, e and f). This difference is in particular more pronounced in case of the specimens made of slag aggregates. At 250 °C, all concretes maintain their compressive strength, or even show a slight increase thereof, which might be related to the evaporation of the released water, entrapped within the concrete matrix. At 500 °C, all the specimens in the second test series with lower cold compressive strength (right diagrams) maintain significantly higher levels of their compressive strength compared to those with higher cold compressive strength (left diagrams). The residual compressive strength of the concretes made of CEM I and quartz heated to a temperature of 500 °C are about 55 %, 15 % and 0 % of the cold compressive strength following exposure to 1, 5 and 20 heating cycles for the specimen series with higher cold compressive strength (left diagrams), respectively. In case of the specimens with the same composition but with lower cold compressive strength (right diagrams), the relative residual compressive strength is reduced to ca. 80 % following exposure to one heating cycle and has then reached a plateau of about 65 % after exposure to 8 thermal cycles. Here, a smaller cold compressive strength seems to signify better thermal stability.

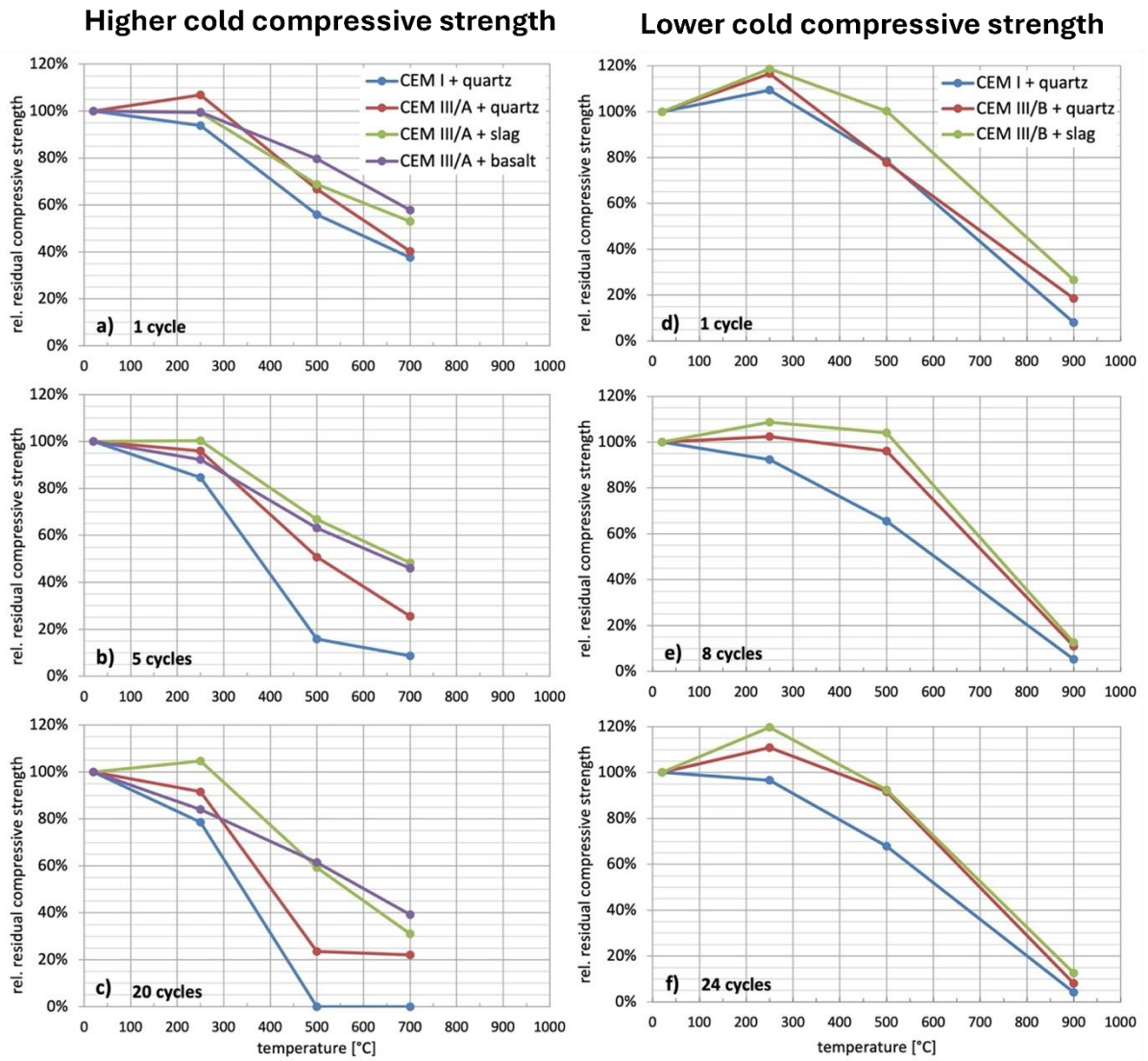

Figure 4.22 Comparison of the relative residual compressive strengths of specimens with higher (a, b and c) and lower (d, e, and f) cold compressive strength following exposure to different numbers of thermal cycles with various maximum temperature

Figure 4.23 compares the a) relative and b) absolute values for the residual compressive strength of the specimens made of CEM I and quartz aggregates in the test series with higher (first specimen series) and lower (second specimen series) cold compressive strength. It can be inferred from the figure that while the relative values for the residual compressive strength of the first specimen series lay far below the second series, the absolute values of the former still transcend that of the latter. Considering the fact that the first series possessed almost double the cold compressive strength, the same level of compressive strength reduction in both series will yield the same values for the relative residual compressive strength, while the absolute residual strength of the former is still higher. This is exactly what we can see in Figure 4.22. Considering the absolute values, we can see that the residual strength of the first series sinks by about 5 N/mm^2 at 250 °C, whereas that of the second series does not change. Though both test series lose significant strength at 500 °C, the loss of strength for the first series (higher cold strength) is much higher (28 N/mm^2 for the first series versus 10 N/mm^2 for the second series). At this

temperature, the absolute values for the residual compressive strength of both specimens is almost the same, with the first series having slightly higher strengths values. At 700 °C, the compressive strength of the second series has not been determined, though a simple extrapolation of the curve based on the obtained values for 500 °C and 900 °C gives us an absolute residual strength of about 18 %, which is still slightly lower than that measured for the first series (about 22 %). The home taking message out of this explanation is that the higher the cold strength of the test specimens is, the more of this strength is lost when the specimens are exposed to high temperatures, particularly around 500 °C.

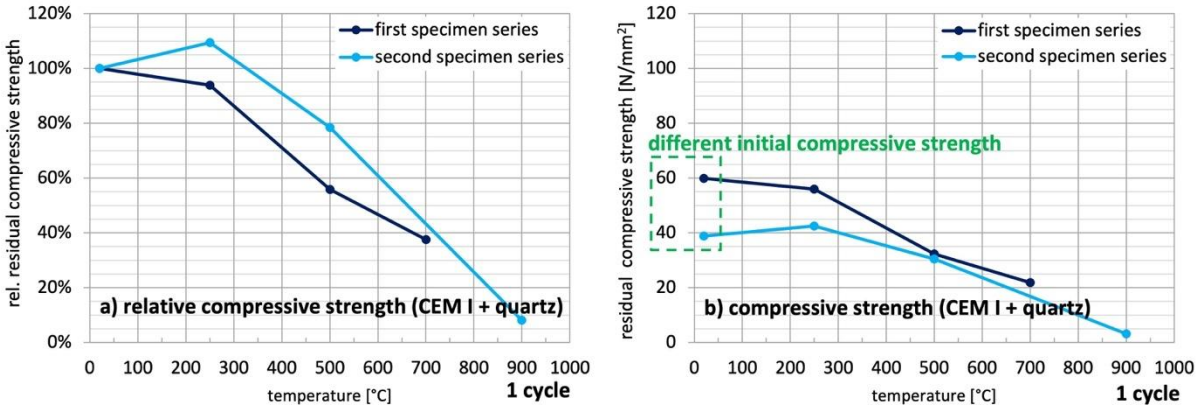

Figure 4.23 Comparison of the relative (a) and absolute (b) values of the residual compressive strength of the specimens made of CEM I and quartz with different cold compressive strengths after exposure to 1 cycle of thermal load with different peak temperatures

To explain the higher reduction of the residual compressive strength in case of the specimens with higher cold compressive strength, we should first heed to how the concrete strength develops over time during the curing phase. This has been introduced in detail under 3.3.1 and Figure 3.6. Curing is related to hydration of cement, which results from the reaction of the cement with water, enabling the concrete to develop from a plastic state to a hardened state while obtaining strength over time. Strength growth is in particular related to the formation of $Ca(OH)_2$ and C-S-H. Which create crystallized structures aggregated with other concrete components to form a dense and bonded network. The rate of hydration is faster during the initial days following concrete placement, and slows down later over time, though it can still go on for years [281]. For the CEM I and quartz mixes used in the current work, the strength of concrete on day 28 has been almost half of that measured on day 48. Hence, it is plausible to assume that this significant growth in the strength is related to the formation of more $Ca(OH)_2$ and C-S-H in the concrete matrix. As the density of both specimens remains similar, the water present in the 28-day-old specimens is more in the form of capillary and physically bound water, whereas the water in the structure of the 48-day-old specimens is to a greater extent consumed for hydration, i.e. for the production of C-S-H. The capillary and physically bound water evaporate at early stages of heating. Given the less dense concrete matrix in specimens with lower cold strength, the released water at this stage can leave the concrete structure more easily,

resulting in less internal stresses. For specimens with higher cold compressive strength the major release of water occurs as a result of the decomposition of $Ca(OH)_2$ at 460 °C - 540 °C, and subsequently C-S-H between 600 °C and 700 °C [28]. Up to 500 °C, the difference in the relative compressive strength between the two test series significantly grows. This temperature corresponds to degradation of $Ca(OH)_2$ and the beginning release of the chemically bound water [28], which is more pronounced in case of 48-day-old specimens (first series). Not only does the strength of the concrete decrease as a result of these decomposition reactions, but also the evaporation of the released water can lead to the formation of steam in the concrete structure. Considering the denser concrete matrix with higher cold compressive strengths, internal pressure might build up as result of the slower release of the entrapped steam, which might contribute to the dramatically reduced residual compressive strength of these specimens.

As mentioned before, DIN EN 1992-1-2 represents no residual compressive strength following temperature exposure for concrete. Hence, the obtained results for residual compressive strength following exposure to one heating cycle were compared with the residual compressive strength within the approach for consideration of the cooling phase of concrete in Appendix C of DIN EN 1994-1-2 [114]. Figure 4.24 shows this curve for quartzite concrete in comparison with the residual compressive concrete for the specimens with higher and lower cold compressive strength, which have been already shown in Figure 4.22. As discussed in the previous section, regardless of the cement and aggregate type, concretes with the lower cold (initial) compressive strength show significantly more residual compressive strength following exposure to 250 °C, 500 °C and 900 °C. The obtained residual compressive strength for both test series still lay above the standard curve from DIN EN 1994-1-2 [114].

As was explained in 4.2.2, Figure 4.6 presents a comparison of hot compressive strength between normal-performance concrete and high-performance concrete according to the DIN EN 1992-1-2 [104]. The figure shows that high-strength concrete loses the hot compressive strength significantly faster than normal-strength concrete, especially in the temperature range below 400 °C. Compared to NPC with quartz aggregate, which has an intermediate cold compressive strength, the HPC class 1 (initial compressive strength class of C55/67) shows 10 % lower hot compressive strength up to 250 °C. For HPC class 2 (initial compressive strength class of C70/85) the hot compressive strength reduces 25 % lower than normal strength concrete with quartz aggregates up to 400 °C. If this statement would be valid for the residual compressive strength, the observed difference in the residual compressive strength of the two concrete series (with lower and higher cold strength) would be plausible. It should be, noted that there are studies in literature that report different results from our findings. For instance, Chan et al. compared the residual compressive strength of CEM I-based normal strength concrete as well as two grades of high strength concrete following exposure to a single thermal cycle at different elevated temperatures. The concretes had similar composition, but different amounts of cement, which altered the water to cement ratio. The 28-day compressive strength were equal to 39 MPa, 76 MPa and 94 MPa for the normal strength, grade 1 and grade

2 HPC, respectively. The results demonstrated that the relative residual compressive strength for the normal strength concrete was lower than both grades of HPC, which showed similar loss of strength post-thermal exposure [282]. In a different experiment, the authors investigated two different grades of normal strength concrete and three grades of HPC. The concretes had similar compositions, though the HPC specimens had more cement content, less sand, and lower water to cement ratio. The 28-day compressive strength of the specimens were equal to 28 MPa and 47 MPa for the two grades of normal strength concrete and 76 MPa, 79 MP and 118 MPa for the three grades of HPC, respectively. The authors found that the loss of strength for different concretes was to some extent temperature dependent. HPC specimens, for instance, underwent a significant strength loss when exposed to 600 °C or higher. Amongst the three grades, grade 3 with the highest cold compressive strength had higher strength loss. The grade 1 NPC with the cold compressive strength of 28 MPa had the highest strength loss throughout, while grade 2 NPC was associated with lower loss of compressive strength post-thermal exposure [283]. In all, the diversity of the reported results necessitates conduction of further in-depth experiments focusing on the effect of cold compressive strength upon the residual strength in cooled state.

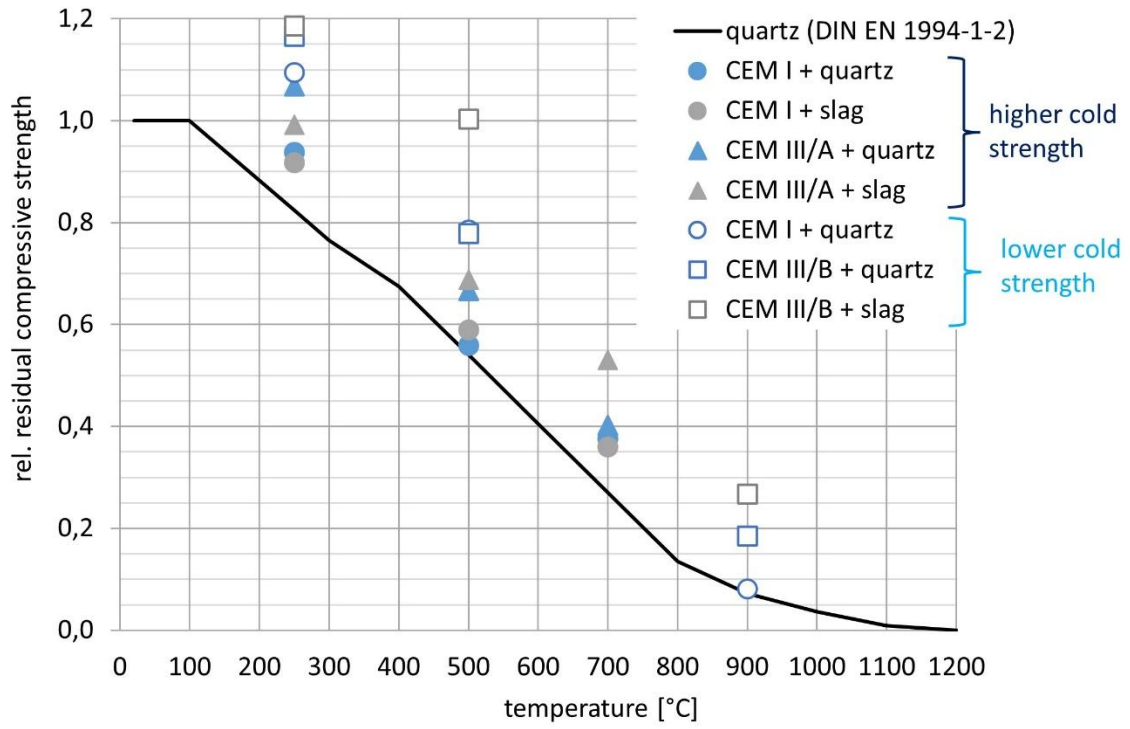

Figure 4.24 Comparison of the relative residual strength of the specimens made of CEM I or CEM III/A in combination with slag or quartz with higher cold compressive strength and the specimens made of CEM I or CEM III/B in combination with quartz or slag with lower cold compressive strength versus the standard mix (CEM I with quartz) according to DIN EN 1994-1-2 [114]

4.4 Post-storage and residual strength

Depending on the temperature, the duration of exposure and the heating and cooling rate, the residual strength of concrete post-thermal exposure is often lower than the initial cold

compressive strength. Under circumstances, the compressive strength of concrete might change with further storage. post-exposure storage duration and environmental conditions might affect the strength of the concrete. In this section, we will explore the effect of post-exposure storage (henceforth referred to as post-storage) humidity and duration upon the compressive strength of concretes subjected to different numbers of thermal cycles with various peak temperatures. The potential of strength re-gain or further damages during post-storage following exposure to thermal loads is a very important material property to ensure the load-bearing capacity of concrete constructions, particularly those exposed to repeated cycles of heating and cooling. As previously debated, the post-storage recovery is highly dependent on the characteristics of thermal load as well as the hygric behavior of concrete during post-storage.

In this section, the impact of post-storage upon the residual compressive strength of the concrete was investigated with respect to the maximum temperature of exposure as well as concrete compositions, with particular focus upon the role of slag sand in the process. The results of these experiments are presented in three parts. In the first section, the residual compressive strength remeasured after 28 days of storage in standard climate (20 °C, 65 % RH), and the influence of post-storage time upon the residual compressive strength is statistically assessed based on the generated DOE. In the second section, the impact of post-storage on a different set of specimens is discussed. In this case, the residual compressive strength of the specimens with different combinations of cement and aggregates was measured after 7 days and 28 days storage under the standard climate. In the third section, the impact of three post-storage conditions (dry, humid in standard chamber, and under water) upon the residual compressive strength of the specimens has been explored. In this case, the duration of post-storage has been significantly longer (up to 90 day).

4.4.1 General effect of post-storage

As a part of the test plan generated by DOE, the impact of a 28-day long post-storage upon the residual compressive strength after high temperature exposure was evaluated. Detailed information regarding the developed mathematical models has been presented under section 4.3.2.2. In Figure 4.25, the mathematically predicted values for the residual compressive strength after heating are compared with the residual compressive strength 28 days post-thermal load exposure, during which concrete specimens were stored in standard climate. The middle line depicts the neutral effect of post-storage, i.e. the case in which the residual compressive strength does not change after the 28-day post-storage in the standard climate. However, as observed, the general trend of the residual compressive strength is closer to the y-axis (the trendline). This means that for concretes, which had a higher residual compressive strength directly after cooling (approximately 80 % - 100 %), the post-storage residual compressive strength has slightly declined. The residual compressive strength of the more-damaged concrete specimens (residual compressive strength of around 30 % - 70 %), however, has not experienced a further decrease during the post-storage. It shows a certain degree of

rehydration in case of the more damaged specimens. This is in parts in line with the findings of Barbhuiya et al., who reported post-storage of light weight concrete being more effective for the strength recovery of the specimens heated to the temperature range of 300 - 500 °C [284]. The temperature range is associated with a strength loss of 30-70 %, which corresponds to the findings presented here.

Additionally, the diagram provides some information about the influence of aggregates. The residual compressive strength for most of concretes containing quartz (red dots) are above the middle line, which statistically shows a further reduction of the compressive strength of these specimens during post-storage. The concretes with basalt (green dots) are located mostly close to middle line for those with lower residual compressive strength and nearly to trendline for those with higher residual compressive strength. This, as previously discussed indicates a slight post-storage reduction of the compressive strength for the less damaged specimens. Many of the gray dots representing the concrete containing quartz as fine sand (0/2 mm) and BFS as coarse aggregate (2/8 mm) are located under the middle line, which shows a benefit on residual strength recovery during the 28-day post-storage. This effect is, however, is not observed for concretes with slag aggregates, only (yellow dots).

Figure 4.25 includes the data obtained for all concretes heated to all maximum temperature (250 °C, 500 °C and 700 °C) for all different numbers of thermal cycles (1, 5 and 20 cycles) collectively for a statistical evaluation. A detailed comparison of residual compressive strength following post-storage in terms of maximum temperature, number of cycles and concrete compositions will be shown in the next section.

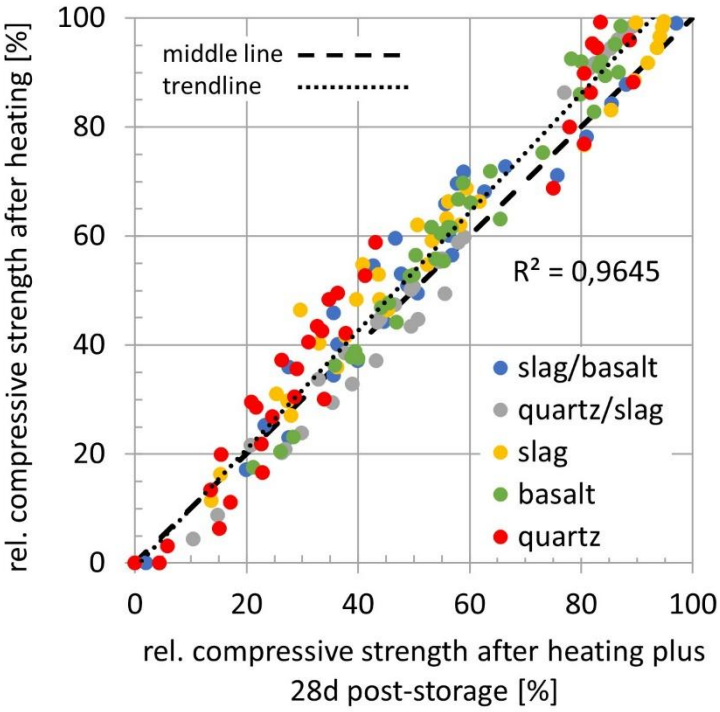

Figure 4.25 Comparison between the predicted relative residual compressive strengths immediately after cooling vs. after 28 days of post-storage under standard climate (20 °C, 65 % RH) [266]

4.4.2 Effect of concrete compositions

The effect of 28 days post-storage under the standard climate (20 °C / 65 % RH) on the residual compressive strength of the specimens is shown in Figure 4.26. Here, the influence of the concrete composition based on the temperature of exposure is highlighted. The residual compressive strength of concrete with different slag sand content of the cement (0 % for CEM I), 30 % for CEM II/B-S and 60 % for CEM III/A) and with various aggregate combinations is shown after one heating cycle at 250 °C, 500 °C and 700 °C (Figure 4.26.a) and after one heating cycle at 250 °C, 500 °C and 700 °C plus 28 days of storage in standard climate (Figure 4.26.b). By comparing the diagrams in a and b, several findings become evident:

i) In general, specimens heated to 250 °C show a slight reduction of compressive strength post-storage, whereas the compressive strength of the specimens subjected to 500 °C has mostly increased. For specimens heated to 700 °C, some degrees of strength recovery are observed for some concrete specimens.

ii) Type of the aggregate is important for strength recovery. For instance, specimens comprising quartzite aggregates, do not show any strength gain, particularly upon exposure to temperatures higher than 500 °C. As a result of quartz conversion within this temperature range, the structure of the concrete is most dramatically damaged, which might account for the remarkable decrease of the residual strength following the post-storage period. Contrary is replacing part of the quartz aggregates by slag dramatically improves the post-storage residual compressive strength of the concretes, especially after exposure at 500 °C and

700 °C. In case of concretes with basalt or slag as aggregates, no significant decrease on residual strength following 28-day post-storage period were observed.

iii) The slag sand content of the cement impacts the initial strength loss during thermal load exposure (Figure 4.26.a). However, it does not have a significant effect on the strength recovery post storage (Figure 4.26.b).

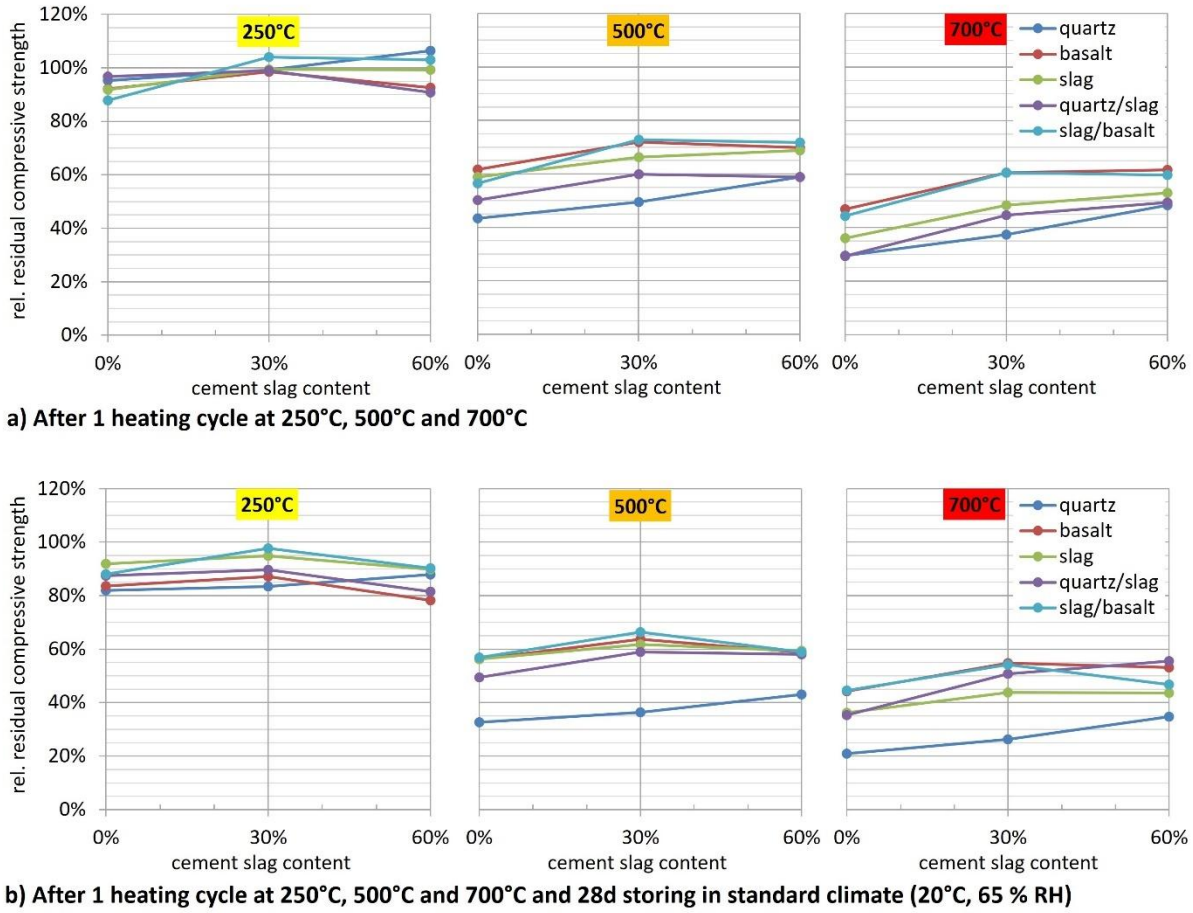

Figure 4.26 Residual compressive strength of the concretes 1 (first row) and 28 (second row) days after exposure to one cycle of the thermal load at 250 °C, 500 °C and 700 °C. The results also depict the influence of the aggregate mixtures and the slag content of the cement

To better evaluate the effect of maximum temperature on the residual compressive strength of concrete during short (7 days) and long (28 days) of post-storage, the specimens with lower cold compressive strength (Table 4.1.b in section 4.1 were investigated. Following exposure to 1, 8 or 24 cycles of heating to 250 °C, 500 °C or 900 °C, the residual strength of the specimens was measured: *i)* directly at the same day as the exposure to the thermal load, once cooled down to room temperature, *ii)* following 7 days of storage under the standard climate (20 °C / 65 % RH), *iii)* following 28 days of storage under the standard climate.

Figure 4.27 summarizes the changes in the residual compressive strength following exposure to one thermal cycles at 250 °C, 500 °C and 900 °C. A comparison of the figures reveals that the post-storage change in the residual compressive strength is different based on the maximum temperature to which the specimens were subjected. For CEM I and quartz heated up to 250 °C,

there is no significant decrease in strength immediately after cooling. Nonetheless, the residual compressive strength continues to sink by day 28 post-storage. Similarly, specimens made of CEM III/B and quartz do not lose their compressive strength immediately after exposure to thermal load, though their residual compressive strength reduces to 88 % on day 7 post-storage. Interestingly, however, an increase of residual compressive strength by 7 % is observed on day 28.

The loss of strength following thermal load at 500 °C follows a similar pattern for the CEM I and quartz specimens. The relative compressive strength decreases from about 80 % as a result of thermal exposure further to about 53 % on day 7 of post-storage. It only slightly decreases from day 7 to day 28. The loss of strength between day 7 and 28 is not observed for specimens with CEM III/B. Here, the relative residual compressive strength that had originally decreased to 76 % immediately after thermal load, continues to decrease to about 61 % on day 7, but increases back to 75 % on day 28. The further decrease of the residual compressive strength of the cooled specimens overtime (particularly up to day 7) demonstrates that the consequences of the thermally induced reactions in the concrete structure with CEM I or CEM III/B continues up to day 7 of post-storage. Once the storing continues from 7 to 28 days, however, the concrete with CEM III/B get the chance to rehydrate and slightly rebuild strength.

When exposed to a maximum temperature of 900 °C, which results in severe damage within the concrete structure, the post-storage change of the residual compressive strength follows a different trend. In case of the reference made of CEM I and quartz, the strength sinks dramatically to lower than 10 % of the cold compressive strength. This value remains unchanged during the 28-day-long post-storage. Substitution of CEM I by CEM III/B improves the thermal stability of the concrete, and the relative residual strength decreases to close to 20 % of the original cold value. This value increases to 25 % and 37 % on days 7 and 28 of storage. This increase of residual compressive strength further confirms the potential of the concretes containing CEM III/B to rebuild strength within the post-storage phase, particularly following exposure to temperatures around 900 °C. The superior post-thermal strength of these concretes might be attributed to the high amount of slag sand in cement and perhaps the renewed activation of the latent hydraulic reaction between the slag sand and the available $Ca(OH)_2$ in the severely damaged concrete structure. The $Ca(OH)_2$ is produced as a result of the reaction of the CaO generated during $CaCO_3$ decarbonization with ambient humidity [28].

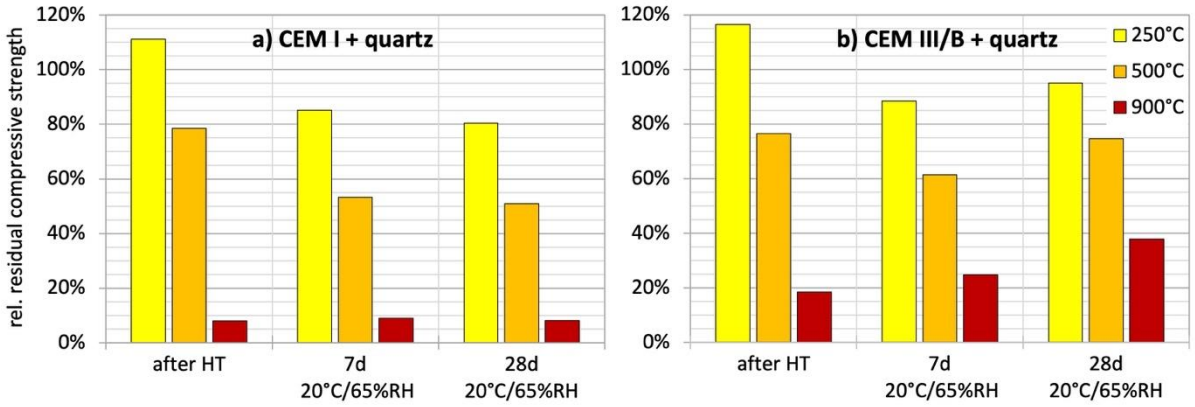

Figure 4.27 Effect of post-storage duration on the residual compressive strength of the specimens made of CEM I (a) or CEM III/B (b) in combination with quartzite aggregates following exposure to one cycle of thermal loading with various peak temperatures (250 °C, 500 °C and 900 °C)

This significant impact of slag sand in the cement upon the strength regain post-storage has not been observed in Figure 4.26.b. This can be attributed to two main factors. First, even for concrete with slag sand, the residual compressive strength after 28 days of storage is lower than that measured immediately after colling. Since Figure 4.26.b only depicts the residual compressive strength after 28 days, the changes of strength in between are not reflected. By measuring the compressive strength on day 7 post-storage, Figure 4.27 shows that the compressive strength initially decreases and then slightly increases for specimens made of CEM III/A. The second factor is that the positive effect of slag sand in the cement is most significant when concretes were heated to 900 °C. This temperature has not been included in Figure 4.26.b. The third factor is the difference between the cold compressive strength of the specimens used for both measurements. The specimens investigated in Figure 4.26.b had significantly higher cold compressive strengths compared to the samples investigated in Figure 4.27. The less dense concrete matrix of the investigated specimens shown in Figure 4.27 might promote higher permeability post-thermal exposure, facilitating the penetration of moisture into the concrete structure and thereby promoting the rehydration reactions.

As already discussed, the post-storage had been shown particularly beneficial for concretes containing slag sand, when subjected to higher temperatures such as 900 °C. To explore the effect of other composite cements, the change of the residual compressive strength of the specimens made of Portland limestone cement (CEM II/A-LL) and complemented with either quartz (Figure 4.28.a) or quartz and limestone powder (Figure 4.28.b) during post-storage was investigated. At 250 °C, no loss of the cold residual compressive strength was observed for these specimens. Compared to the specimens made of only quartz, those containing limestone and quartz had a lower decrease of strength between day 1 and 7 post-storage (approximately 20 % for the latter versus 40 % for the former). Between day 7 and 28 of post-storage, specimens with quartzite aggregates regained about 7 % of their initial strength, whereas those with limestone and quartz lost around 12 % thereof. At 500 °C, the behavior of both specimens was quite similar, with the relative residual strength of the samples immediately after thermal

exposure and on days 7 and 28 being equal to 58 %, 44 % and 43 % for specimens with quartz, and 80 %, 67 % and 71 % for mixes with limestone and quartz. In general, it seems that the addition of limestone powder to the cement has a stabilizing effect up to a temperature of 500 °C. The residual compressive strength directly after exposure at 900 °C was very poor. It reduced to less than 10 % of the cold compressive strength immediately after heating and decreased by about 2 % for the specimens with quartz by day 28. The specimens with limestone powder and quartz aggregates, however, were completely destroyed by day 7. The complete degradation of compressive strength at this temperature can be attributed to the decarbonation of the additional amount of limestone ($CaCO_3 \rightarrow CaO + CO_2$) within these mixtures, which happens at around 850 °C - 900 °C. The resulting calcium oxide (CaO) absorbs the ambient humidity relatively fast and undergoes a chemical reaction to form calcium hydroxide ($CaO + H_2O \rightarrow Ca(OH)_2$). This exothermic reaction results in a significant increase in volume and consequently complete degradation of the specimens [28]. A visual presentation of the state of both concretes 7 days after exposure to different elevated temperatures is shown in Figure 4.29.

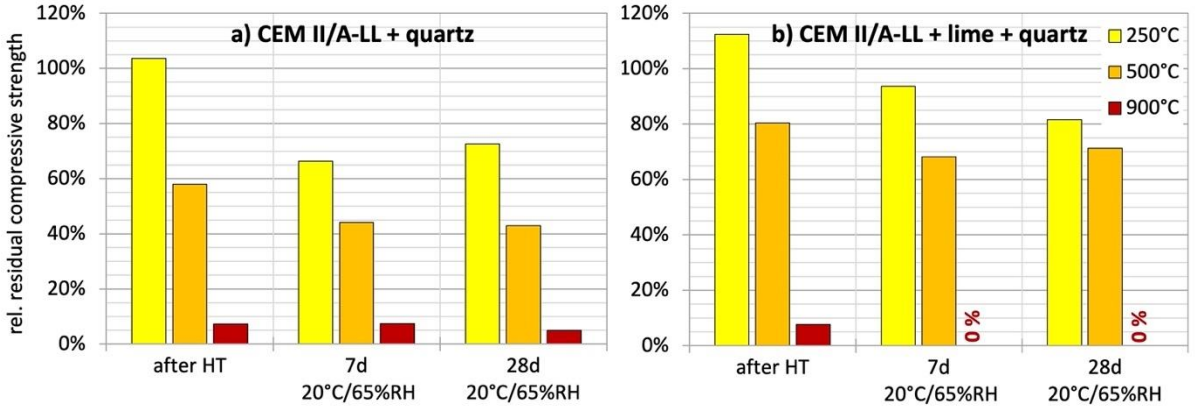

Figure 4.28 Effect of post-storage duration on the residual compressive strength of the specimens made of CEM II/A-LL in combination with quartz (a) or with limestone powder and quartz (b) following exposure to one cycle of thermal load with various peak temperatures (250 °C, 500 °C and 900 °C)

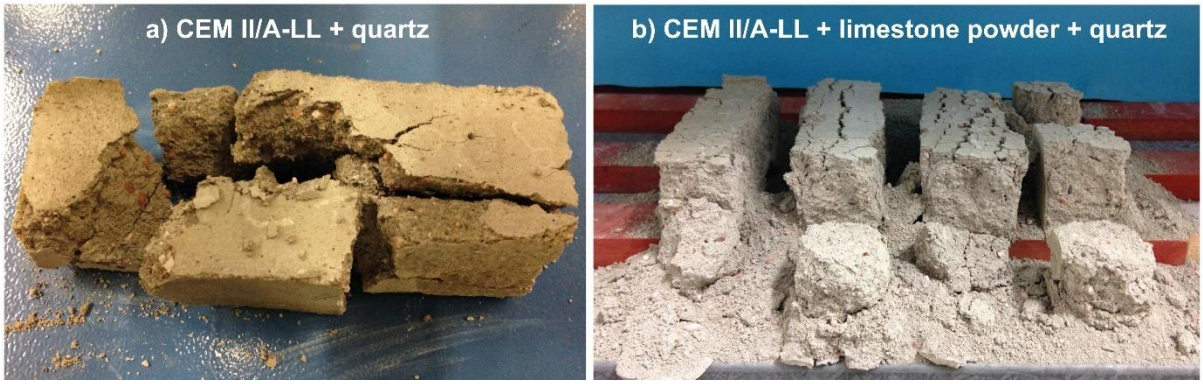

Figure 4.29 Effect of post-storage on concretes containing limestone cements with a) quartz or b) quartz and limestone powder, following exposure to one cycle of 900 °C and after 7 days in 20°C / 65 %RH

To sum up the findings of this section, it can be concluded that concrete composition has a determining impact upon the post-storage rehabilitation. As observed, the presence of slag sand promoted strength recovery, whereas concrete specimens rich in limestone provide poor stability during the post-storage phase. The extent of these effects is more visible when concrete is heated up to 700 °C and higher. The importance of these findings is highlighted when thinking of concrete structures exposed to fire, where the temperature often rises to these levels. Under such circumstances, the load-bearing capacity of the structure most probably containing blast furnace slag will partially regrow after cooling. Yet to this date, a comparable systematic investigation of the residual compressive strength of concrete following exposure to thermal stress, with focus on the main components of the concrete, number of the thermal cycles with various end temperatures up to 900 °C, as well as storage conditions and duration is lacking both on a national and international level. The current study can provide first step stones towards the design and conduction of such large-scale investigations in the future.

4.4.3 Effect of moisture availability during post-storage

The current section sought to investigate the impact of longer post-storage duration as well as the extent of moisture available to the concrete upon the redevelopment of the residual compressive strength post-thermal stress exposure. To this end, some specimens having been subjected to elevated temperatures were stored in water for 5 min and then transferred to standard climate (20 °C/ 65 % RH). On day 7 post-storage, the residual compressive strength of these specimens was compared to those of the samples that have been directly stored under standard climate (without having been submerged in water). The results are shown in Figure 4.30 for specimens made of CEM I or CEM III/B complemented with quartzite aggregates following exposure to a thermal cycle with a peak temperature of 500 °C (left) and 900 °C (right), respectively. As in case of the experiments in last section 4.4.2, following a thermal load of 500 °C, the relative compressive strength of the specimens reduces within the course of the initial 7 days of post-storage. Interestingly, this reduction is significantly lower in case the specimens are provided with additional moisture during the 5-minute-long water immersion treatment. In fact, as a result of the additional moisture provision, the relative residual compressive strength of the specimens made of CEM I and CEM III/B raises by about 12 % and 16 %, respectively. In case of the specimens exposed to 900 °C, the residual strength of both specimens slightly increases within the course of the 7-day storage under standard climate (20 °C / 65% RH). Upon the addition of the 5-minute-long water immersion treatment, the compressive strength of the specimens made of CEM III/B merely rises by 1 %. On the contrary, the strength of the specimens made of CEM I is much more dramatic (about 13 %). These unexpected findings persuaded us to examine the impact of longer post-storage under water upon the strength rebuild of thermally stressed specimens, particularly those made of CEM I.

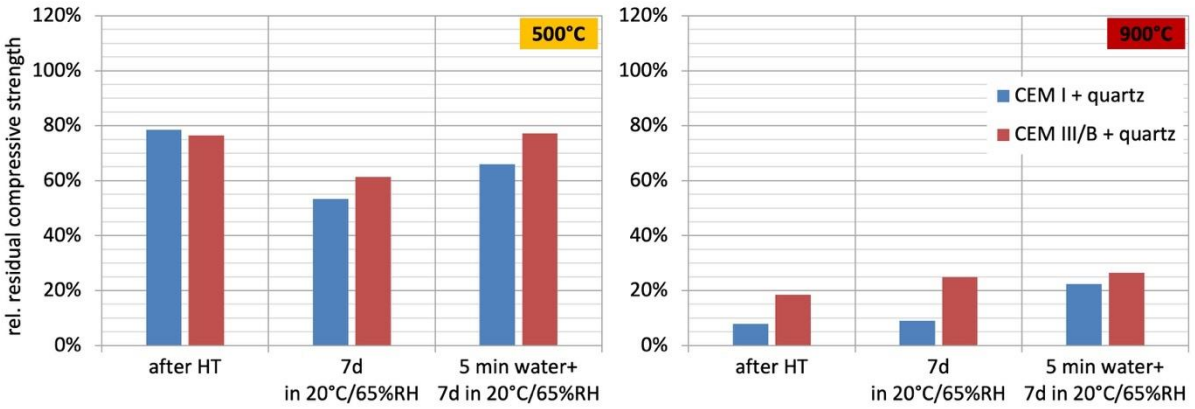

Figure 4.30 Relative residual strength of the specimen made of CEM I and CEM III/B with quartzite aggregates following exposure to one thermal cycle at 500 °C (left) and 900 °C (right). The strength is measured either directly after the heating (HT), or else following 7 days of post-storage under standard climate (20 °C / 65% RH). The impact of a 5-minute-long storage under water immediately after exposure to the thermal stress upon the measured relative compressive strength at day 7 has been presented

To investigate the impact of longer post-storage duration as well as the extent of moisture availability during storage phase, specimens made of CEM I and the heat resistant aggregate basalt were used as reference. These were then compared with two more specimens comprised of CEM III/A complemented with either basalt or slag aggregates. These specimens were selected to provide further information regarding the efficiency of slag sand as an SCM and slag sand/ BFS as fine/ coarse aggregates. Detailed information regarding the composition of these is presented in Table 4.8.

Table 4.8 Composition of the specimens used for the investigation of the effect of post-storage duration and moisture availability on the redevelopment of post-thermal stress residual compressive strength

Composition		CEM I + basalt	CEM III/A + basalt	CEM III/A + slag
Water/ Cement	[-]	0.52	0.52	0.52
Water	[l/m³]	286	286	286
CEM I	[kg/m³]	550	-	-
CEM III/A		-	550	550
Basalt 0/2 mm		1426.5	1426.5	-
Basalt 2/4 mm		107.6	107.6	374.0
slag sand 0/2 mm		-	-	1149.0
Cold compressive strength	[N/mm²]	74.3	76.8	65.2

For these investigations, the specimens were heated up to a temperature of 700 °C or 900 °C, and the residual compressive strength was directly measured in cooled state. The effect of the moisture availability during post-storage was investigated under the following three conditions for up to 90 days; *i)* dry storage in the desiccator (dry storage), *ii)* storage under the standard

climate at 20 °C / 65 % RH (half-wet storage), and *iii)* storage under the water (water storage; only for specimens exposed to 900 °C).

Figure 4.31 summarizes the development of the residual compressive strength for a post-storage period of 28, 56 and 90 days following exposure to high temperatures at 700 °C (a and c) and 900 °C (b, d and e) for the three investigated specimen types. Similar to the findings of the previous sections, the regain of strength during the post-storage is more pronounced when the specimens are exposed to extreme temperatures, i.e. 900 °C. The regrowth of residual compressive strength during the post-storage phase for the specimens exposed to a thermal load at 700 °C is minimal. Furthermore, the amount of moisture provided by the storage environment seems to play a vital part in the rebuilding of compressive strength. Focusing on the diagrams on the right side (b, d and e), where the specimens heated up to 900 °C are portrayed, it becomes clear that no significant change in the residual compressive strength of the specimens under dry storage has been detected up to 90 days post-thermal stress. When stored under standard climate, a minor redevelopment of the residual strength becomes visible at the time points of 28, 56 and 90 days. The strength regain is the most significant for the specimens made of CEM I and basalt (around 10 %), followed by those comprised of CEM III/A and basalt (ca. 6 %) and slag (ca. 5 %). When stored under water, however, the increase in the available moisture leads to a much more remarkable increase in the strength during the subsequent storage period. Nonetheless, the regrowth of strength in the specimens is not identical. Interestingly, with the residual compressive strength growing from ca. 15 % to more than 73 %, the standard specimens made of CEM I and basalt have the highest level of residual compressive strength regain after 90 days of post-storage under water. In case of the specimens made of CEM III/A and basalt, the strength also rises during storage under water, increasing from 19 % to over 46 % on day 90 post-thermal stress. On the last place are the specimens made of CEM III/A and slag, the residual compressive strength of which increases by less than 8 % between day 1 and day 28 and remains constant since day 56 and then increases up to 23 % after 90 days. The reason for the superior strength regains of the specimens made of CEM I is probably the fact that following exposure to extreme temperatures, hydrated cement is completely degraded to re-form the initial clinker phases. As a result of exposure to high amount provided moisture, the CaO available in the cement reacts with water and forms $Ca(OH)_2$, which potentially accounts for the significant growth of residual strength observed [28]. As the amount of clinker in CEM III/A is 60 % lower than CEM I, the strength rebuild is relatively lower. In case of the specimens made of CEM III/A and slag aggregates, a complete degradation of the glass structure of the slag sand occurs at around 850 °C [285]. Accordingly, the slag sand used as fine (0/2 mm) aggregates are in great part irreversibly destroyed due to a peak temperature of 900 °C, which negatively influences the strength recovery (see Figure 4.32).

The conclusions drawn out of these findings are hence summarized as such; First and foremost, an increase in strength by increasing the amount of moisture available through storage under water indicates that the denser matrix of the slag sand containing compositions used here can

have led to a time-delayed strength development due to the slower penetration of moisture into the specimen. This conclusion is also supported by the findings presented under section 4.4.2. Second, the amount of moisture available to the concrete plays a vital part in the redevelopment of concrete strength. When stored dry in the desiccator, the relative residual compressive strengths remain almost unchanged. Storage in a standard climate (20 °C / 65 % RH) leads to a slight increase in the relative residual compressive strength and storage in water largely shows significant post-hardening, provided that the peak temperature stress had been extremely high (i.e. 900 °C). Third, with the investigations that have now been carried out, it is obvious that a remarkable increase in the concrete strength during subsequent storage occurs following exposure to extreme temperatures (mainly 900 °C). Last but not least, when adequate moisture is provided, the increase in strength appears to be faster in concretes containing CEM I compared to the cases, where part of the cement is replaced by slag sand.

To our best of knowledge, the impact of slag sand upon the strength recovery during post-storage in environments with different moisture has not been investigated. However, several studies have explored the strength recovery of CEM I concrete under such conditions. For instance, Suh et al. studied the strength recovery of CEM I-based concrete exposed to different elevated temperatures (200 °C, 500 °C, 800 °C and 1000 °C) under two different conditions; i) storage in standard climate (20 °C/ 60 % RH) for 24 h and ii) storage of hot concrete under water for 24 h. The results indicated that for the concrete exposed to 200 °C, rehydrating the paste at 20 °C/ 60% RH for led to the depolymerization of the silicate in C-S-H paste due to moisture adsorption, and consequently the mechanical degradation of the cement paste. For concrete heated up to 500 °C, rehydration in water could largely restore the mechanical properties of the cement paste. The authors attributed this phenomenon mainly to the increase in the degree of silicate polymerization in the C-S-H phase as well as the reaction between decomposed CaO and the silicate in the cement paste, which leads to the formation of new C-S-H. The authors, however, observed no strength recovery once the specimens heated to 800 °C and 1000 °C were submerged in water for 24 h directly after heating [78]. Our results demonstrate that the rehydration of the cement under such conditions can still occur but requires a significantly longer curing time in water. Li et al. have reported that for specimens made of CEM I (both normal and high strength), which have been exposed to elevated temperatures of 300 °C, 400 °C and 500 °C and cooled through water quenching, 28 day long storage under water and a further 28-62 day storage in standard climate (20 °C/ 60 % RH) could lead to a significant strengthening of bond formation (up to 77 % for NPC and 70 % for HPC) [80]. Similarly, Qian et al. demonstrated the strength recovery of specimens to be highest when stored under water for 14 days, followed by 14-day long storage under dry-wet cycles and finally 14 day long storage in ambient humidity [286]. These reports are also confirmed by the findings of this work.

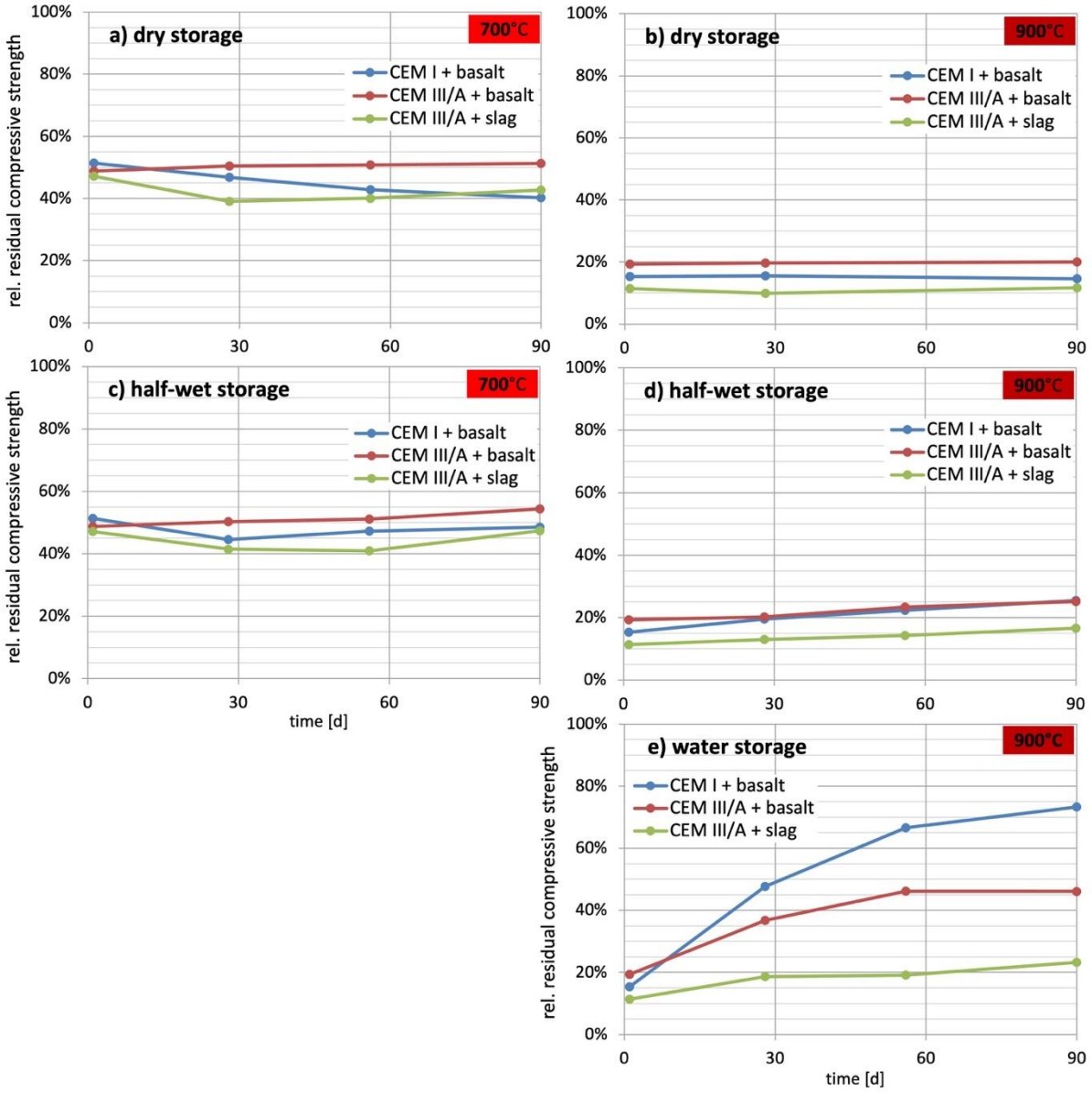

Figure 4.31 Relative residual compressive strength of CEM I and basalt, CEM III/A and basalt and CEM III/A and slag over a period of 90 days post-storage in dried conditions (desiccator), half-wet conditions (standard climate; 20 °C / 65% RH) and under water. Specimens had been exposed to one heating cycle with a maximum temperature of 700 °C (left) and 900 °C (right) prior to post-storage

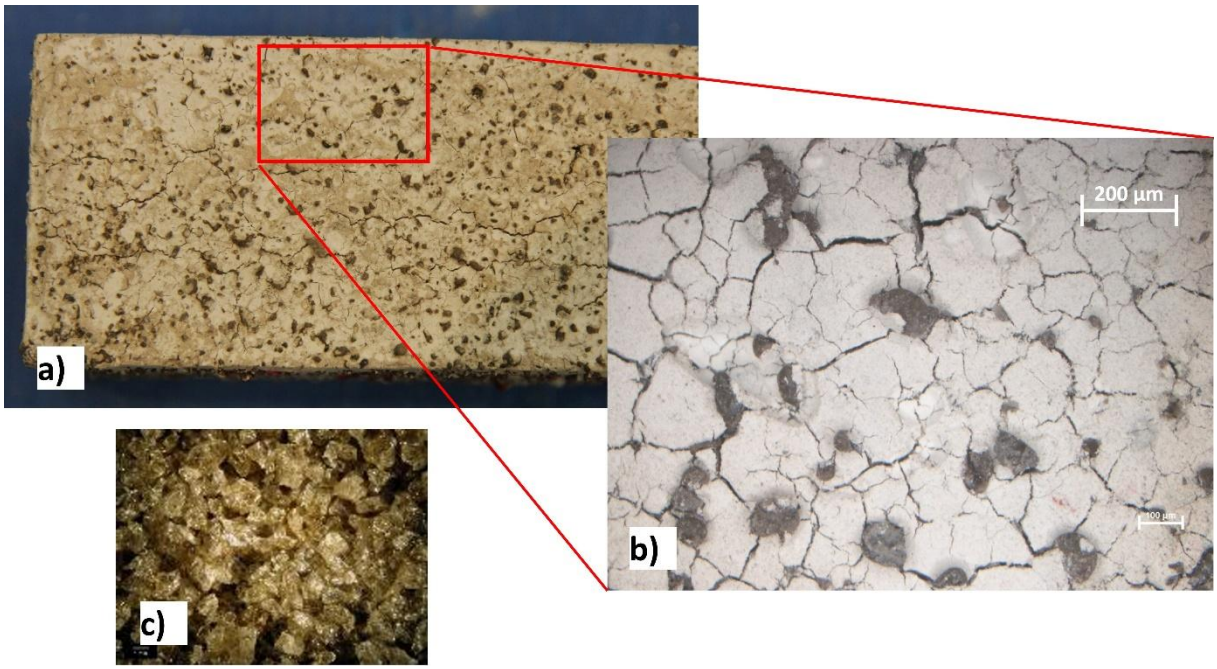

Figure 4.32 Macroscopic (a) and microscopic (b) visualization of the surface of the specimens made of CEM III/A with slag following exposure to one heating cycle with a peak temperature of 900 °C. The structure of the slag aggregates in the heated specimens is shown side by side to that of the natural slag sand (c). The comparison demonstrates complete destruction of the slag glass structure as a result of the extreme thermal load

4.5 Mass loss

As previously explained, the mass measurements were conducted to evaluate the changes, mostly in terms of the water content, within the concrete subjected to high temperatures. The aim was to obtain more information that allowed for the interpretation of the collective impact of hydration or dehydration, in terms of capillary, physically and chemically bound water, upon the change in the compressive strength of the concrete during and after exposure to thermal stress. Hence, mass loss is measured here mostly as an approximate criterion for the change in water content of the specimens. Mass decrement due to decarbonation or other phenomena is not considered, as they occur at temperatures of 800-900 °C, and thus play a relatively minor role in lower temperature ranges.

In this dissertation, the mass loss measurements were carried out in cold condition as well as in cooled state immediately after exposure to high temperatures. In other studies that have not been included in this thesis, however, mass loss had been also monitored during the heating (in hot condition) and the data are available under [106]. As the obtained data in hot conditions showed a comparable behavior as the values in cooled state, the discussion of the hot-state mass loss has not been provided here lest we risk an extremely lengthy and repetitive discussion [106],[107],[287],[288].

The composition of the specimens investigated within this section of the work is presented in Table 3.6.a and 3.6.b. The data were collected simply by weighing the specimens prior to

thermal load as well as before the measurement of the residual strength at various stages. The changes in the concrete mass relative to the concrete weight in cold conditions was calculated. Thus, the change in the concrete mass was documented for specimens with different cement and aggregate types, immediately after exposure to one or repeated cycles of heating with different peak temperature, and at various time points during post-storage at different conditions.

The maximum evaporable water within the concrete was determined separately for each peak temperature as the change in the mass of the specimen following exposure to repetitive thermal cycles until a constant concrete mass is reached. At this point, the concrete is assumed to have lost all water that is evaporable at the tested temperature. This phenomenon can of course influence the physical characteristics of the concrete, as it affects the pore system, crack formation, and permeability of the concrete upon thermal loading [106],[107]. The evaluation of mass changes under a long cyclic exposure could deliver useful knowledge concerning the development of permeability as well as pore pressure balancing, which can help interpret the high temperature behavior of concrete. The composition of the specimens investigated concerning maximum evaporable water is presented in Table 4.9.

4.5.1 Effect of cycle numbers and maximum temperature

To explore the impact of maximum temperature of thermal load on mass loss, the mass loss following exposure to different cyclic temperature levels are exemplarily depicted for concrete specimens made of different cements (CEM I, CEM II/A-LL and CEM III/B) complemented with quartzite aggregates in Figure 4.33. In this Figure, the mass losses at 250 °C, 500 °C and 900 °C are presented over rising numbers of heating cycles. As expected, regardless of the cement type, the maximum temperature has a determining effect on the amount of mass loss. At temperature 250 °C, the maximum mass loss following many repeated heating cycles (24 cycles) was between 3 - 4 % for all specimens. The maximum mass loss at 500 °C, however, is about 5 - 6 % for specimens made of CEM I and CEM III/B, whereas the specimens made of CEM II/A-LL have only lost 4 % of their mass. At 900 °C the maximum mass loss is slightly over 7 % for specimen containing CEM I and CEM II/A-LL, and about 6.5 % in case of specimens made of CEM III/B. Assuming that the mass loss is primarily a product of the water release and evaporation out of the concrete, the increase of mass loss with a rise of the peak temperature can be simply attributed to the temperature dependency of the release and evaporation of the capillary, physically bound and chemically-bound water. This corresponds also to the decrease in the residual strength of the specimens with an increase of the maximum temperature. The significantly enhanced mass loss of the specimen containing CEM II/A-LL at 900 °C, however, is beyond the topic of the water evaporation and is a byproduct of the release of CO_2 due to the decarbonation of cement.

Another finding which is confirmatory of the results of the residual compressive strength is that following the initial dehydration during the thermal load, an increase in the number of the

thermal cycles from 1 to 8 at every temperature level alters the mass loss significantly. In other words, the rate of mass loss within the first 8 cycles is much higher. Further heating cycles (higher than 8), on the other hand do not lead to a significant loss of mass, as the concretes seem to have reached a temperature-specific maximum mass loss. It is concluded, therefore, that the water release and evaporation in the concrete specimens exposed to repetitive cycles of heating is determined within the first heating cycles.

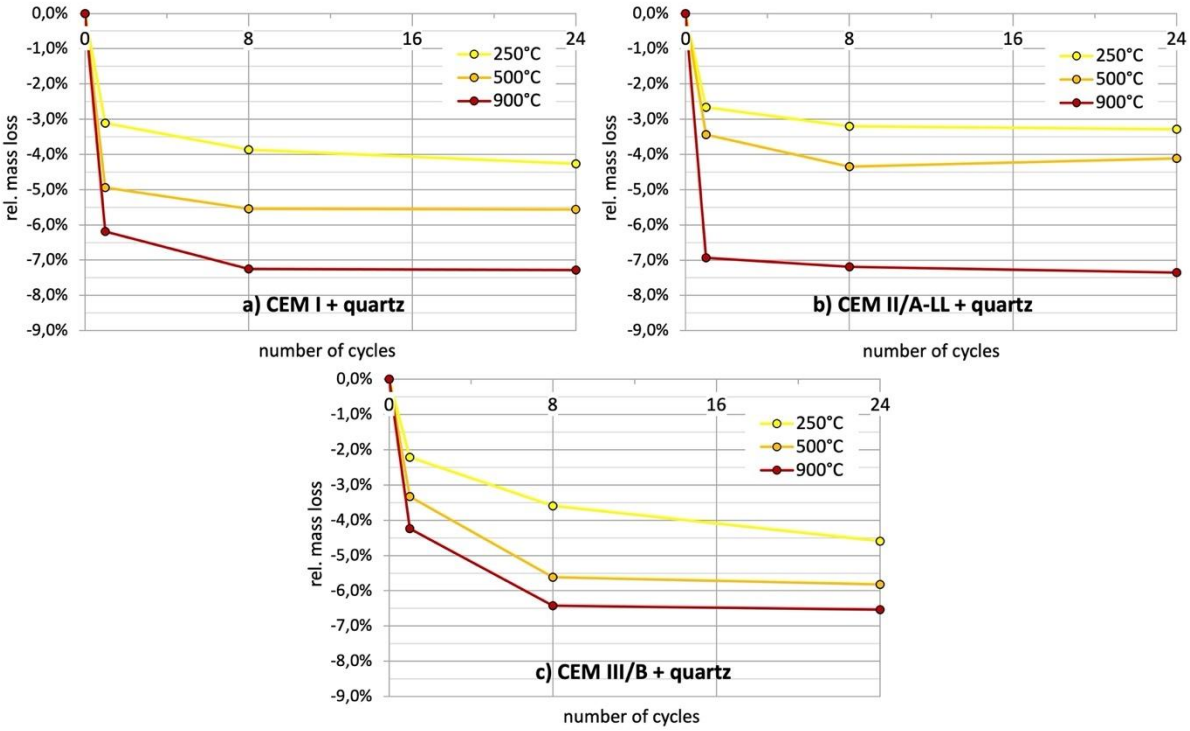

Figure 4.33 Mass loss of the concrete specimens made of a) CEM I, b) CEM II/A-LL and c) CEM III/B with quartic aggregates following exposure to different numbers of thermal cycles with various maximum temperatures

4.5.2 Effect of cement and aggregate types

Here, we first discuss the mass loss of the specimens with the two heat stable aggregates, namely basalt and slag. Figure 4.34 shows the mass loss for concretes with CEM I or CEM III/A in combination of basalt (Figure 4.34.a) and slag (Figure 4.34.b) aggregates, following exposure to different numbers of heating cycles at 250 °C, 500 °C and 700 °C. As expected, the first heating cycle leads to loss of a large amount of water content for all concretes, the mass of which increases with an increase in the maximum temperature. The mass loss of all concretes stays relatively stable upon exposure to further heating cycles (up to 20 cycles). There are minor changes in the mass loss trend depending on the aggregate type. For temperatures of 250 °C, the mass loss of the specimens with basalt significantly increases after the first heating cycle and then stays stable as the number of cycles increases. The significant mass loss after the first heating cycle is also seen for concretes with slag aggregates. However, mass loss continues to

slightly increase with additional heating cycles. At 500 °C, following the initial significant mass loss after the first cycle, the mass loss of specimens with both basalt and slag slightly decreases. This becomes more evident at 700 °C, where the mass loss of specimens with basalt after the 1st cycle and up to the 5th cycle slightly decrease, and then remains stable. For specimens with slag, a continuous slight decrease of mass loss is observed after the 1st cycle and up to the 20th cycle. The extent of decrease in mass loss is more pronounced for specimens made of CEM III/A (and slag aggregates). These findings correspond to the results presented in section 4.4.2, where the concretes containing slag showed a slight re-gain of compressive strength following exposure to highest maximum temperature (700 °C). Based on these results, it seems that the concretes containing slag sand and slag sand/BFS aggregates tend to adsorb humidity from ambient to rebuild part of their structure. This phenomenon was further observed by extending the storage time of the specimens in standard climate.

A comparison of CEM I and CEM III/A with both aggregates shows that specimens containing CEM III/A demonstrate a higher mass loss at all maximum temperatures. This is probably attributed to the higher content of physically bound water in the structure of these concretes, originating from the slower strength development of CEM III/A containing concrete compared to those containing CEM I. Additionally, the type of aggregates influences the extent of mass loss. As observed in Figure 4.34, specimens with basalt always have higher mass loss compared to those with slag aggregates.

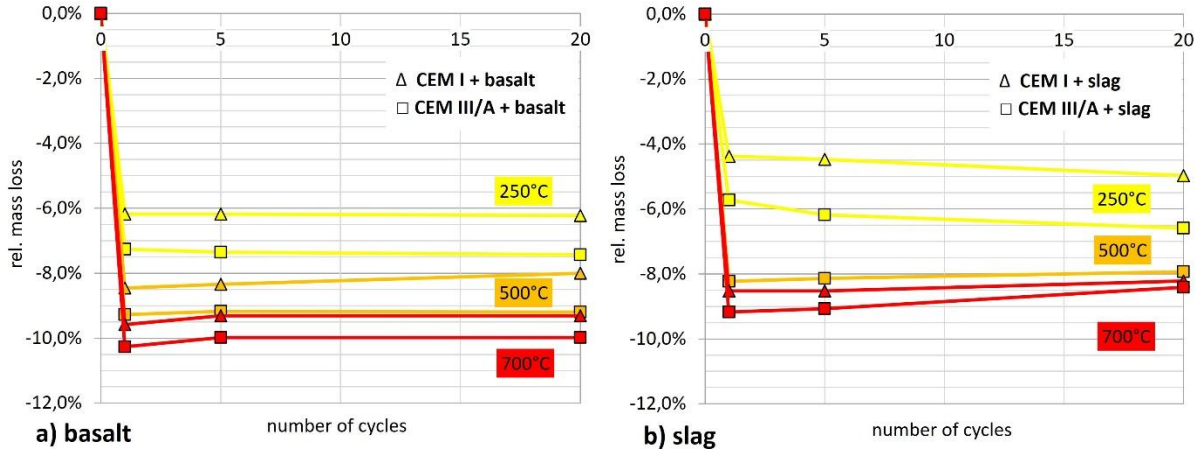

Figure 4.34 Mass loss of the concretes made of CEM I or CEM III/A with a) basalt and b) slag as aggregate following exposure to different numbers of thermal cycles at 250°C, 500°C and 700°C

To study the effect of concrete compositions on mass loss, a further experiment was carried out using CEM I, CEM II/A-LL and CEM III/B with different aggregates. Figure 4.35 (left) demonstrates the amount of mass loss over elevated temperatures after one cycle heating for the investigated specimens. The graph clearly shows that the different combinations of cement and aggregates show various amounts and rate of mass loss at 250 °C, 500 °C and 900 °C.

Figure 4.35 (left) establishes a trend for the mass loss of specimens made with different cement types. In general, up to a temperature of 500 °C, the presence of limestone (CEM II/A-LL) as

well as slag sand (CEM III/B) in the cement seem to reduce the amount of mass loss compared to specimens made of CEM I. A similar effect is observed in case slag and limestone are added as aggregates. In general, however, it seems that limestone has a better ability to reduce the mass loss up to a temperature of 500 °C. The superior performance of limestone relative to slag sand can be concluded based on two factors; *i)* Although the performance of the specimens made of CEM II/A-LL and CEM III/B with quartz seem to be similar within the introduced temperature range, the limestone content within CEM II/A-LL is remarkably lower than the content of slag in CEM III/B (15 - 20 % versus 80 %). *ii)* The addition of limestone aggregates reduces the mass loss much more significantly than the slag aggregates. Above 500 °C, however, the story changes, as the mass loss of CEM II/A-LL dramatically increases and even transcends that of the CEM I specimens. As previously explained, however, this is not related to the release and evaporation of water, but rather the decarbonation of limestone and the release of CO_2 as a gas. Generally, specimens made of CEM III/B demonstrate a smoother and more stable trend from 250 °C to 900 °C compared to other mixes.

Regarding the rate of mass loss, a similar trend is observed for all specimens up to a temperature of 500 °C. Within this context, the rate of mass loss up to 250 °C is always higher than what is observed between 250 °C - 500 °C, as the former range is associated with the evaporation of the capillary water and partially the physically bound water. The temperature range of 250 °C - 500 °C corresponds to the beginning of the release and evaporation of the chemically bound water [28]. Accordingly, the rate of mass loss decreases. Yet here again, there seems to be differences among specimens with different cement types. The rate and amount of mass loss is highest in case of specimens with CEM I, as the decomposition of the $Ca(OH)_2$, which is abundantly present within concretes made of this cement, occurs at this range. As a result of the evaporation of the released water from this reaction, mass loss increases. Between 500 °C and 900 °C, the rate of mass loss in all specimens but those prepared with CEM II/A-LL decreases. Within the context of the latter, the decarbonation of limestone ($CaCO_3$) around 800-900 °C accounts for the significant acceleration of mass loss observed within the diagram [28].

The impact of slag and limestone aggregates upon mass loss can be deduced based on the comparison of the mass loss curves of the CEM III/B specimens with quartz and slag, and the CEM II/A-LL specimens complemented with quartz and limestone and quartz, respectively. With respect to the influence of slag aggregates, the mass loss curves demonstrate a significantly higher rate and amount of mass loss compared to specimens with quartz up 250 °C. Between 250 °C and 500 °C, the rate of mass loss for specimens with slag aggregates decreases. From 500 °C, both quartz and slag specimens show the same mass loss rate. The addition of limestone powder, on the other hand reduces the mass loss of the specimens up to a temperature of 500 °C. This is due to the very fine structure of the limestone both as a part of the cement and as an aggregate, which creates a denser concrete matrix, slowing down the escape of the evaporated water [289]. Above 500 °C, the rate of mass loss in specimens with CEM II/A-LL and limestone overtakes that of their quartzite counterparts, as the hitherto described

decarbonation of limestone is not limited to the cement, but also to the limestone aggregates. The ultimate mass loss for mixes containing CEM III/B are about 4.5 %, whereas for CEM I is about 6.2 % and for CEM II/A-LL mixes are 6.9 % and 8.6 % after one heating cycle.

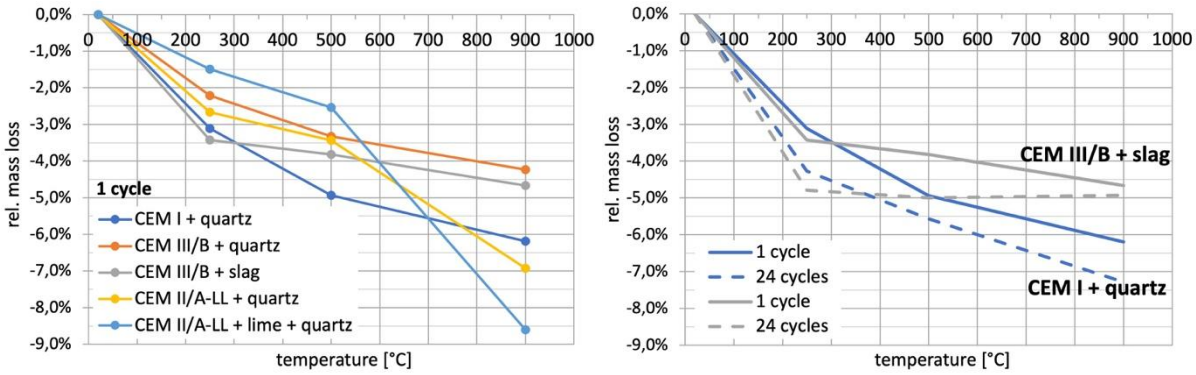

Figure 4.35 Left: Mass loss of the specimens mad of CEM I, CEM II/A-LL or CEM III/B following exposure to one heating cycle with different peak temperatures, Right: comparison of the mass loss of the specimens made of CEM III/B and slag with the reference specimens (CEM I and quartz) after exposure to 1 or 24 thermal cycles with different peak temperatures

To explore the mass loss behavior of CEM III/B and slag, its mass loss after exposure to 1 or 24 heating cycles with various peak temperatures is compared with the reference specimen made of CEM I and slag (Figure 4.35; right). Both after exposure to 1 and 24 heating cycles at 250 °C, the amount and rate of mass loss for both specimens remain very close together, although concrete mixes of CEM III/B with slag show about 0.5 % more mass loss. Above the temperature 250 °C, the mass loss of specimens made of CEM III/B and slag significantly decelerates and reaches a complete plateau following 24 cycles. The mass loss of CEM I and quartz specimens also slows down after 250 °C, though it continues even after exposure to 24 thermal cycles, which means that the concrete still continues to lose water. In temperature range higher than about 300 °C, the amount as well as rate of mass loss for specimens with CEM I are considerably higher than their CEM III/B containing counterparts. At 900 °C, the mass loss of CEM III/A with slag is smaller than that of the reference mix both 1 and 24 cycles, which pertains to their lower $CaCO_3$ content.

4.5.3 Maximum evaporable water at each peak temperature

In this section, the maximum evaporable water of concrete specimens with different cement and aggregate types (Table 4.9) was measured for different peak temperatures of 50 °C, 100 °C, 250 °C, 400 °C and 550 °C [107]. To this end, specimens were heated to the aforementioned peak temperatures (with a constant heating rate of 5 K/min) until a constant mass was achieved. The mass loss at this point was assumed to correspond to the total evaporable water content of the concrete at that given temperature. The results of these measurements for all specimens are presented in accordance with the maximum temperature of the heating, the duration of the heating program required to achieve complete mass loss. The experiments are limited to a

temperature of 550 °C, since higher temperatures are associated with other physicochemical changes within the cement or aggregates that can lead to a loss of mass either directly (e.g. limestone decomposition) or indirectly (e.g. quartz conversion, etc.). Needless to say, the mass loss measured at such temperatures to not correspond to the amount of evaporated water.

Table 4.9 Composition of the specimens used for investigation of the temperature-dependent maximum evaporable water

Composition	Unit	CEM I + Quartz	CEM II/A-LL + Quartz	CEM III/B + Quartz	CEM III/B + Slag	CEM III/B + Basalt
Water/ Cement	[-]	0.52	0.52	0.52	0.52	0.52
Water	[l/m³]	264	264	264	264	264
CEM I	[kg/m³]	510	-	-	-	-
CEM II/A-LL 32.5 N		-	510	-	-	-
CEM III/B 42.5 N		-	-	510	510	510
Quartz 0/2 mm		1468	1461	1461	-	-
Slag sand 0/2 mm		-	-	-	1373	-
basalt 0/2 mm		-	-	-	-	1597

4.5.3.1 Amount and rate of water release at elevated temperatures

The mass loss of the concrete specimens containing combinations of CEM I and quartz is exemplarily presented in Figure 4.36 to provide an overview about the flow of water release behavior at different peak temperatures. As observed, the mass decrement continued throughout the thermal load until an approximate constant value was achieved. At this point, the cumulative mass loss reached a maximum value, unique to that temperature level. This signifies that the concrete had reached its specific temperature dependent dryness, and the experiments were thus terminated after different number of heat cycle repetitions. As expected, higher temperature levels result in an earlier reach of constant mass loss. In fact, the required time for the complete evaporation of the water content was significantly shorter for temperatures higher than 100 °C. For instance, the curves of specimens at 50 °C have a significantly lower gradient compared to 100 °C, where much water evaporates at the early hours. This is even more significant at a temperature of 400 °C, where specimen's maximum mass loss is reached within the first 6 h.

The maximum temperature is also determinant of the amount of mass loss. After 48 h of heating at 50 °C, only about 2.1 % of water content is released. Increase of the temperature up to 100 °C results in up to 4 % loss of the water content. A significant mass loss could be seen in case the tests are run at maximum temperatures between 250 °C (5.1 %) and 550 °C (6.9 %). The increase of mass loss as a function of the temperature level can be attributed to the evaporation of the capillary water and the release of physically bound water (up to around 100 °C), and also the occurrence of dehydration reactions and the subsequent release and evaporation of more water at temperature above 250 °C [28]. The effect of maximum temperature and time is more

important in terms of long-time exposure to elevated temperatures, where a considerable part of water content leaves the concrete in a very short period of time, because of decomposition reaction within concrete. The extreme increase of mass loss at elevated temperatures can further imply the formation of a more porous network within the concrete structure that have facilitated the escape of the evaporated water. While this can reduce the steam pressure build up within the concrete structure, the increased permeability and the formation of the crack networks particularly close to the concrete surface can also reduce the stability of the specimen [47].

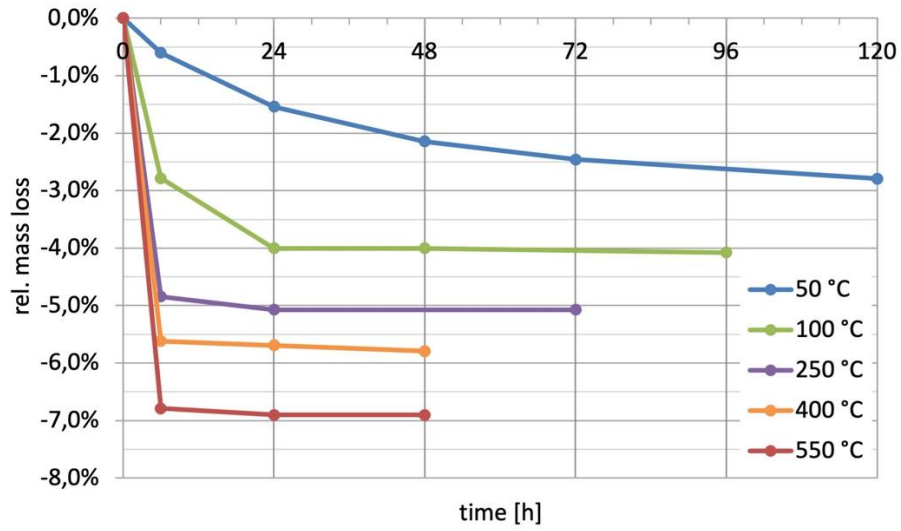

Figure 4.36 Maximum evaporable water mass of the concrete specimens made of CEM I and quartz following heating at different temperatures

4.5.3.2 Maximum water release of various concrete compositions

Figure 4.37 summarizes the maximum mass loss for various concrete mixes over different peak temperatures ranging from 50 °C to 550 °C. The effect of the cement and aggregate types is obvious upon examination of the maximum evaporable water content of concretes over the maximum temperatures of the performed tests. The concrete mixture contains CEM II/A-LL show a lower maximum mass loss almost for all temperatures, given that the calcite content is less prone to decomposition resulting in lower release of free water molecules as well as a denser and more homogenous concrete matrix. The maximum evaporable water for the concretes with CEM II/A-LL and quartz at 550 °C is about 5.5 %.

The maximum evaporable water following the heating at 50 °C and 100 °C, which is mostly considered as free and capillary bound water, has different trends in mixes containing CEM III/B, regardless the aggregate type, compared to CEM I, where CEM I with quartz shows smaller amount and rate of water release. This can be attributed to the higher weakly bound water of mix CEM III/B with quartz, slag or basalt, considering the same curing time as that of CEM I with quartz. A comparison of water release at 100 °C amongst the specimens containing CEM III/B with quartz, slag or basalt aggregates demonstrates a slightly higher water release

for mix with basalt. The behavior of CEM III/B with basalt continues with a variation up to 250 °C compared to the specimens made of CEM III/B either with quartz or with slag aggregates. That is close to water release of CEM II/A-LL and quartz in a smooth manner. It may refer to similar or smooth behavior of limestone and basalt splits at this temperature range in terms of thermal expansion. This results in smaller thermal strain gradient between cement paste and aggregate. At 250 °C the maximum evaporable water of CEM I and quartz reaches a similar value as in CEM III/B either with quartz or with slag (5 %). This value is about 4.5 % and 4.0 % for the specimens containing CEM III/B with basalt and CEM II/A-LL with quartz, respectively.

Temperatures higher than 250 °C accelerate the maximum water release of CEM I and quartz, whereas the specimens made with CEM III/B show a smoother flow of mass loss. A larger value of 7.0 % is observed for the combination of CEM I and quartz at 550 °C. From 250 up to 550 °C, the water release of the specimens containing CEM III/B are mostly similar and reach a maximum value of 5.5 - 6.0 %. At 400 °C, less water release is measured for the specimens containing CEM III/B. A larger water release of CEM I at this temperature range, which occurs due to the decomposition of $Ca(OH)_2$ reveals more initial hydrated products at this specific concrete age [38].

In conclusion, the findings here support the results presented under section 4.4.2. Here again, specimens made of CEM II/A-LL and CEM I have the lowest and highest mass loss at temperature above 250 °C, respectively, whereas specimens made of CEM III/B fall in between. The type of the aggregates (basalt, slag, quartz) seems to minorly impact the maximum evaporable water of the specimens made of CEM III/B, though the specimens with quartz seem to have about 0.5 % less evaporable water at 550 °C.

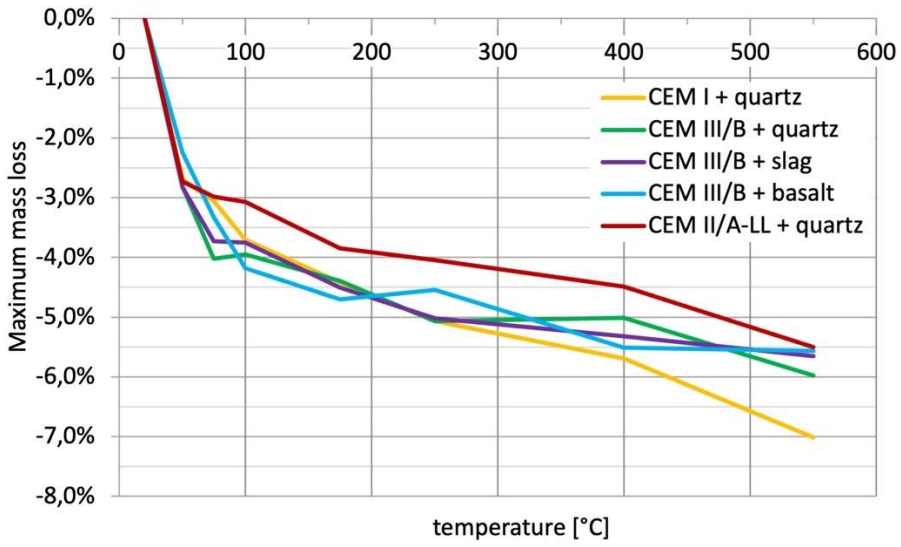

Figure 4.37 Maximum evaporable water content of specimens made of different cement and aggregate types at different temperatures

The role of the cement is also clear when looking at the rate of the water release at various temperatures. Figures 4.38 present the mass loss of specimens containing different cement and aggregate types between from 50 °C to 550 °C over time.

An overall comparison of Figures 4.38.a to 4.38.e shows an interesting outcome concerning the impact of concrete compositions. At 50 °C the water release of different mixes is mostly similar. At 100 °C the specimens with CEM III/B release water faster than those comprising CEM I. As previously mentioned, this can be attributed to the faster hydration of the CEM I during the curing phase, which means that in specimens with the same age, the amount of capillary and physically bound water in CEM I specimens is lower than in specimens made of CEM III/B. At 250 °C, however, CEM I meets the water release level of the mixes containing CEM III/B. At temperatures higher than 250 °C, CEM I specimens overtake the CEM III/B the specimens in terms of the water release, with the difference becoming even more pronounced at 550 °C. This temperature range corresponds to decomposition of $Ca(OH)_2$ and the release of the water as a result of this chemical reaction. It further demonstrates more structure destruction of specimens containing CEM I compared to CEM III/B. Specimens made of CEM II/A-LL are always associated with significantly smaller release of water at temperatures smaller than 550 °C. The impact of aggregate type remains minor.

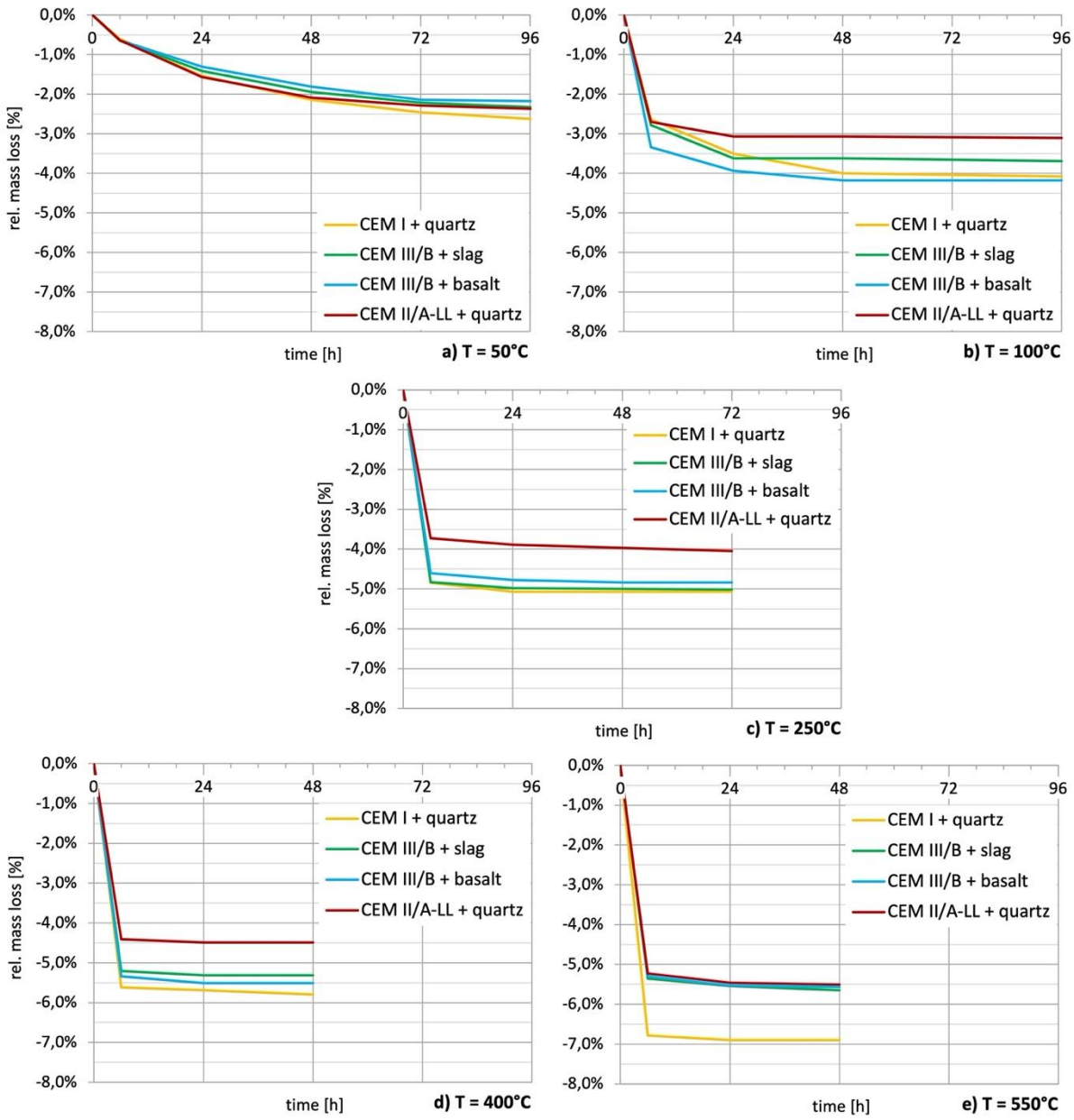

Figure 4.38 maximum evaporable water of the specimens made of different cement and aggregate types at different temperatures over time

4.6 Thermal conductivity

For a better evaluation of concrete subjected to high temperatures, the thermal conductivity of the specimens with different cement and aggregate types was experimentally determined. The thermal conductivity of the concrete is dependent upon both the thermal load and the concrete composition. The change in concrete thermal conductivity alters the temperature penetration inside the concrete, affecting thereby the physical and mechanical properties thereof. The composition of the specimens investigated within this section of the work is presented in Table 3.6.a and 3.6.c.

4.6.1 Concrete with standard aggregates

The thermal conductivity represents an essential parameter when discussing the influence of high temperatures on the construction level and not from the material properties perspective. When focusing on the topic of thermal exposure of structural members, the development of the temperature field within the structure grows in importance. The lower the thermal conductivity of a material is, the lower the temperature-stressed cross-section of the construction element and subsequently the corresponding reduction in its load-bearing capacity will be.

Figure 4.39 shows the thermal conductivity of different concretes before and after exposure to 5 cycles of thermal load at 500 °C. The data are presented for specimens made of cements with various slag sand content (0 %, 30 % and 60 %) and different aggregate mixtures.

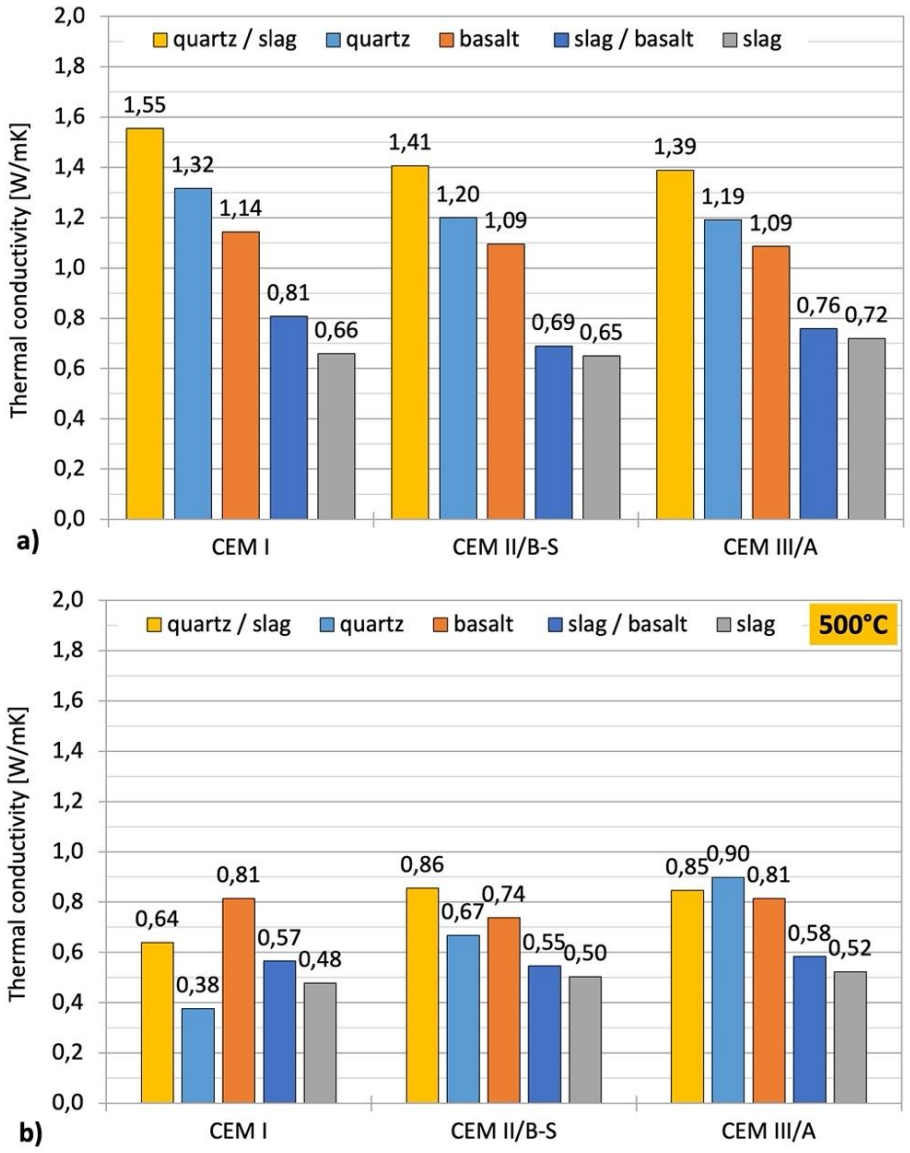

Figure 4.39 Thermal conductivity of the concretes with standard aggregates and different commercial cements before the thermal load loading (a) and after exposure to 5 cycles of thermal loading with a maximum temperature of 500 °C (b)

The results indicate that the type of aggregate has a clearly measurable influence, while the slag content of the cement exerts a minimal impact within the scope of the measurement accuracy except for the combination of quartz and slag aggregates. Within this context, an increase of the slag content of the cement from 0 % (CEM I) to 30 % (CEM II/B-S) and up to 60 % (CEM III/A) affects the thermal conductivity slightly as a result of different hydration development.

The measurements demonstrate that all specimens made of quartz have the highest thermal conductivity. The use of basalt, on the other hand, reduces the thermal conductivity by about 30 %. In case of the specimens with slag sand as fine aggregates, the remaining thermal conductivity will be almost half of the thermal conductivity of the quartz-containing specimens. The fact that the type of fine aggregate has a considerable influence on the thermal conductivity is to be expected, as it makes up the larger volume fraction of the aggregate mixture (see Table 3.6.a).

For the purpose of comparing the thermal conductivities even after high temperature stress, the measured thermal conductivities before and after exposure to 5 cycles of thermal load with a peak temperature of 500 °C are compiled in Figure 4.40. In addition, the standard values according to DIN EN 1992-1-2 for concretes made of CEM I and quartz aggregates are also reported [104]. Overall, the measured thermal conductivities are at the lower limit or, in some cases, well below the values specified in the DIN EN 1992-1-2 [104]. The lower thermal conductivity of specimens at 500 °C compared to the standards is to be expected, as the former were subjected to 5 heating cycles while the reported values for DIN EN 1992-1-2 are following exposure to one thermal cycle only [104]. An increase in the number of thermal cycles leads to more damage to the concrete structure and higher level of crack formation (see section 4.3.1). The difference in thermal conductivity of specimens before thermal loading maybe attributed to the fact that the concretes studied in this section have a higher proportion of binder compared to the normal concrete as well as specific pre-curing conditions, which account for lower thermal conductivities. These values, however, are within the range of the thermal conductivities reported for thermally stressed normal and high-strength concrete in the literature by Lyzwa und Zehfuß, which are shown in Figure 4.40.a [290]. The good agreement with the literature values highlights the plausibility of the obtained results.

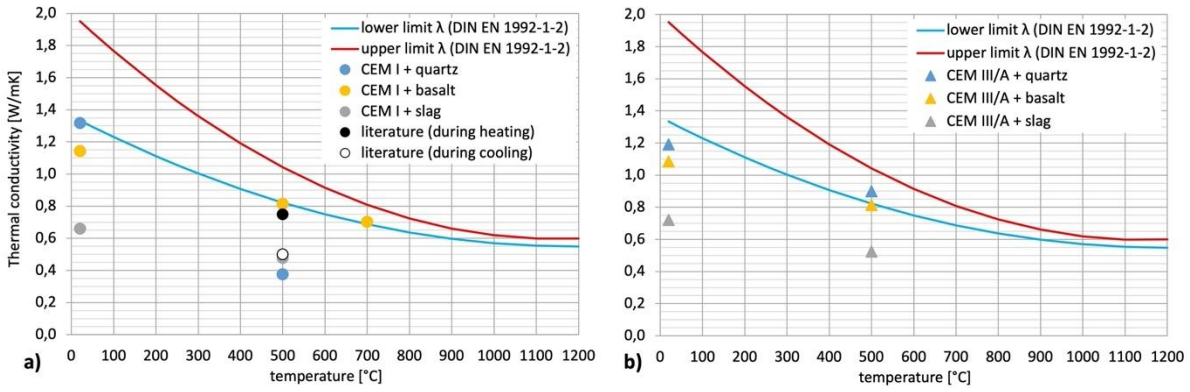

Figure 4.40 Thermal conductivity of specimens made of a) CEM I and b) CEM III/A with standard aggregates before (at 20 °C) and after exposure to thermal stress at 500 °C in comparison to DIN EN 1992-1-2 (upper and lower limits for concretes made of CEM I and quartz aggregates

4.6.2 Concrete with non-standard aggregates

Figure 4.41-a demonstrates the thermal conductivity of the specimens made of CEM I or CEM III/A with different non-standard aggregates from the copper and steel industries before exposure to thermal stress. As observed, both the type of cement and the aggregates only exert a small influence on the thermal conductivity of the specimens before thermal load. Within this context, specimens made of Cu-slag have a slightly higher thermal conductivity, followed by those prepared with Ef-slag and LD-slag. Similarly, the effect of the type of cement in specimens' thermal conductivity is quite small, where the addition of slag sand to the cement decreases the thermal conductivity of specimens relative to those prepared with standard aggregates (Figure 4.40.a). This can be a result of the different hydration development in the specimens made of CEM III/A.

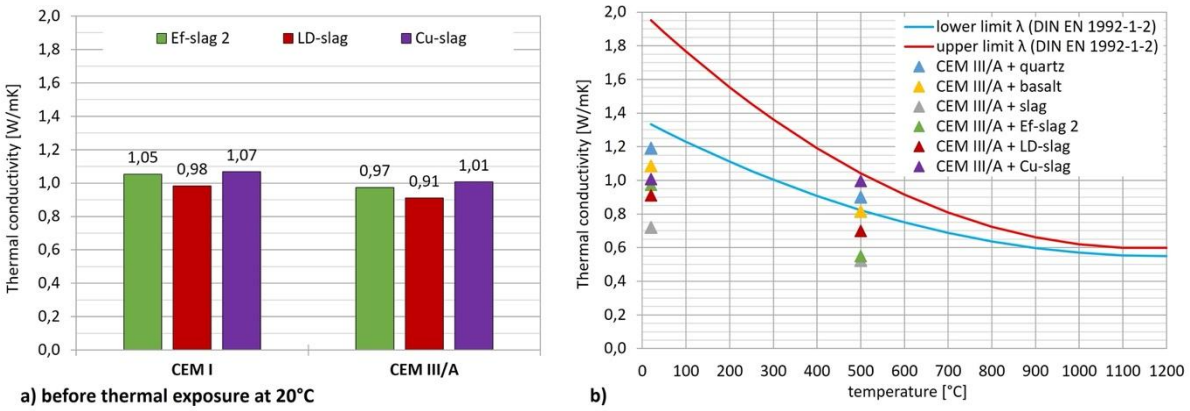

Figure 4.41 a) Thermal conductivity of the specimens with non-standard aggregates and different cements before the thermal stress and b) thermal conductivity of concretes with CEM III/A and standard or non-standard aggregates before (at 20 °C) and after exposure to thermal stress at 500 °C in comparison to DIN EN 1992-1-2 (upper and lower limits for concretes made of CEM I and quartz aggregates) [104]

In Figure 4.41-b, the thermal conductivity of the specimens produced with non-standard aggregates from copper and steel industries are compared with the values from the

DIN EN 1992-1-2 [104] as well as the measured value in specimens containing standard aggregates (quartz, basalt and slag) before and after 5 cycles of thermal exposure at 500 °C. The results show that the thermal conductivities are still lower than the standard for specimens before thermal load, but within the range measured in the specimens with standard aggregates. The thermal conductivity of specimens with Ef-slag, LD-slag or Cu-slag are between values of specimens with slag and specimens either with basalt or quartz. The thermal conductivity of specimens after 5 cycles of thermal load at 500 °C are also comparable with specimens containing standard aggregates. Only in the case of Cu-slag does the thermal conductivity at 500 °C increase. It can be thus concluded that while the type of aggregate (both standard and non-standard) in specimens seems to exert only a small influence on the concrete thermal conductivity in cold conditions, it has a much more significant impact upon the values measured in cooled conditions after exposure to thermal stress.

5 From laboratory to large scale: Transferring the findings to practical application

One of the main goals of the diverse investigations carried out in this dissertation is to formulate a general approach, based on the existing fire structural design, that enables relating the material behavior of both conventional and more sustainable (and stable) concretes in the cooling phase to that of the structural elements, and thus to fill the existing gap with regard to the design of concrete under natural fire exposure as prescribed in the standards. In fire structural design, the load-bearing capacity of components and structures must be verified for the entire duration of the fire, including the cooling phase. This is essential as failure may occur due to delayed heating and/or high tensile forces in the concrete during the cooling phase. The design specifications and material parameters contained in DIN EN 1992-1-2 [104], however, are derived from fire tests using the standard temperature-time profile (ETK) as a thermal load, which measures the maximum time the load-bearing capacity is maintained during the heating phase. The standard takes neither the effect of the inner temperature profile once the heating has stopped nor the material behavior during the cooling phase. According to Schneider [28], the material behavior during the cooling phase is irreversible, and should be thus taken into account for the structural design using natural fire models. It has been also shown that concrete properties can change during post-storage, which can impact the need for repair or the replacement of the structural elements after exposure to high temperatures. Accordingly, in this section of the work, a “simplified” Excel-made model will be introduced, which has been developed with the purpose of simplifying the transfer of the measured values for the hot and residual compressive strengths from the material level to the structural element level. The model is not intended to represent a standard measurement method for the determination of the hot and residual compressive strength of the structural element, but to illustrate the relationship between the high temperature behavior of the concrete, the properties of the used materials and the geometry of the structural element in an exemplary and methodical manner.

5.1.1 Boundary conditions of the developed model

Upon and following exposure to thermal load, the strength of the structure is determined by the temperature profile inside the structural element, which is, in turn, dependent upon the properties of the used materials and the geometry of the structural element. Hence, to enable a proper evaluation of the hot and residual compressive strength of a structural element, the temperature profile inside the element should be also determined in a point-by point manner. The data used for modeling were based on a process with simplified boundary conditions, which results in an increased heat flow into the element, due to overestimated surface temperature of the element, and thereby higher temperatures in different inner layers of the component compared to the standard design in hot conditions. Thus, using this method, the influence of the material properties on the load-bearing capacity of the element will be overestimated. The

calculations based on an exemplary wall with a thickness of 30 cm (Figure 5.1), which is subjected to heating on both sides. The cross section of this wall (across thickness) was divided into 24 individual layers to calculate the transient temperature evolution in each layer. To simulate the thermal loads, a closed temperature-time profile was selected, which combined the heating phase of the standard temperature-time profile (ETK), and the cooling phase based on the RABT-ZTV profile (see under section 2.1.4) [84]. In this temperature-time profile, the temperature first increased to 905 °C based on the standard temperature-time profile within 60 minutes, followed by a linear cooling over a period of 90 min to reach room temperature (20 °C). The surface temperature of the element was regarded equal to the temperature of the oven without considering the heat transfer, which results in higher surface temperatures compared to standard hot measurements. The heat storage capacities and thermal conductivities were averaged for each aggregate combination from the measured values at room temperature and 500 °C and used as constant values. Hence, a slightly higher heat input is estimated for temperatures above 500 °C. When evaluating the hot and residual load-bearing capacity, the hot or residual compressive strength of each layer was assessed separately, and interactions in the form of transferred shear stresses between the layers have not been considered. As a result, thermally damaged layers are recognized with their full hot or residual strength, which they would not achieve due to the overall shortening of the entire column. Thus, a slightly higher load-bearing capacity is calculated in this respect. Due to the small differences in the thermal characteristics of cements with different slag sand contents (see section 4.2.1.2 and section 4.2.1.3), the cement type was not considered in the calculation of the temperature profile. However, considering the significant influence of the slag sand content on the residual strength, the cement type was taken into account in the assessment of the load-bearing capacity, particularly in the cooled state.

5.1.2 Temperature profile

The calculated maximum temperatures reached at different layers of the cross section both during the heating and cooling phases are shown in Figure 5.1 Particularly in the center of the wall section, the temperature at the time of exposure to maximum temperature outside the wall is significantly lower than during cooling. This effect has already been described by Klingsch and Toris [291]. During heating, the heat flow is clearly directed from the surface to the interior of the member. When the fire load is removed and the wall is allowed to cool, the direction of heat flow is partially reversed from the inner volume to the cooling surface. Yet a heat flow towards the interior of the element remains due to the lower temperatures of these layers. This inward heat flow causes an ongoing temperature increase in the inner layers of the cross section, while the outside temperature is already falling. Therefore, the maximum temperature difference between the heating and cooling phases occurs in the center of the component, affecting large parts of the structure during cooling. As seen in Figure 5.1, this difference is around 200 °C regardless of the type of aggregates used in concrete.

The dashed curve in Figure 5.1 shows the inner temperature profile, to which the concrete is exposed during the measurement of the hot compressive strength. Under such circumstances, the center of the model wall made of concrete with quartz aggregates will be exposed to a temperature of around 380 °C, whereas the central temperature of the wall made of concrete with slag sand and BFS aggregates is merely heated up to around 50 °C. In other words, for concrete element made of slag aggregates, only 25 % of the wall cross section is exposed to a temperature of above 500 °C, while for concrete with quartzite aggregates, over 60 % of the element is affected by such high temperatures.

After the cooling phase (shown as solid lines in Figure 5.1), the temperatures in the center of the structural element increases. The extent of this increase is mainly dictated by the aggregate type. For the model wall used in this analysis, a difference of approximately 200 °C is observed between the temperature of the center of the wall during heating to the maximum temperature of 905 °C and during cooling to the room temperature, regardless of the type of aggregate used. Due to the lower thermal conductivity of the concrete made of basalt and slag aggregates, however, the central temperature after cooling remains significantly lower than that observed in case of the concrete made of quartz aggregates, which signifies an overall lower penetration of the temperature into the cross-section of the concrete element made of the former two. As seen in Figure 5.1, the center of the wall made of concretes with slag and basalt aggregates reaches a maximum temperature of 230 °C and 280 °C, respectively during cooling. The inner temperature of the wall made of concrete with quartz aggregates, on the other hand reaches around 590 °C. Consequently, the wall section exposed to a temperature of 500 °C or more increases to 25 % and 28 % for concrete elements with slag or basalt aggregates and to 100 % for concrete element made of quartzite aggregates.

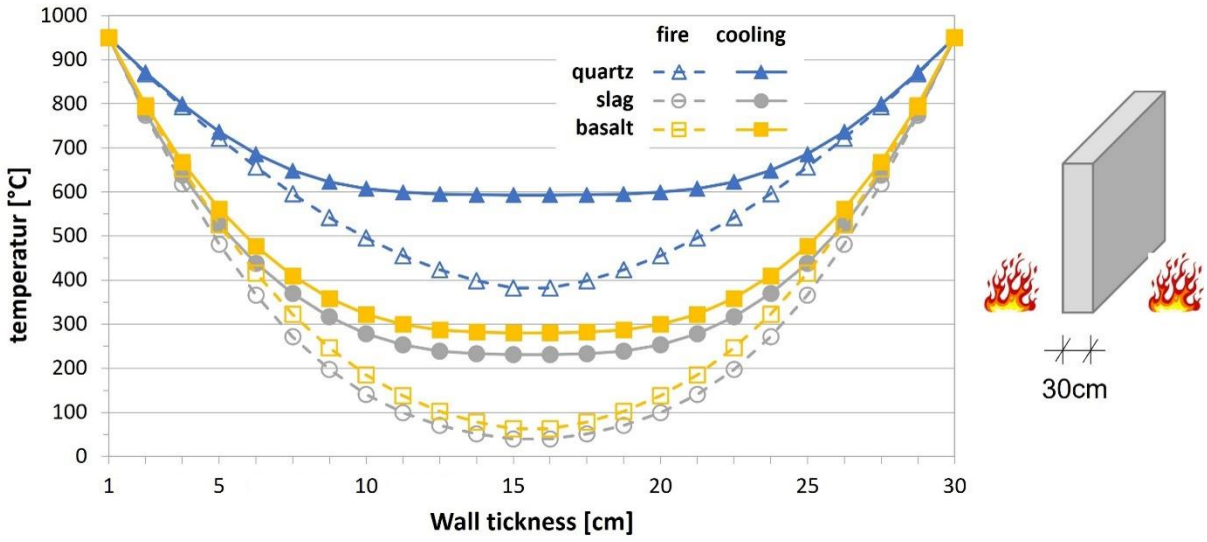

Figure 5.1 Maximum temperatures of the model walls during fire exposure (60 min) and cooling phase (90 min)

The increase in the inner temperature of the element during cooling highlights the necessity of evaluating not only the hot but also the residual compressive strength of the structural elements

exposed to high temperatures. This becomes significantly important to determine the service life of the elements exposed to repeated heating cycles. Due to the increase in the inner temperature, the thermal damage to the concrete element continues even when the thermal load has been apparently removed. Moreover, the concrete element can be further damaged during and post-cooling as a result of cracking and the reformation of $Ca(OH)_2$. On the other hand, partial strength recovery might also occur depending on the concrete composition and the storage conditions. In the next section, we will discuss the influence of the inner temperature profile upon the load-bearing capacity of the structural element under hot and cooled conditions.

At the end, it should be once more highlighted that the developed Excel-made model is to provide a "simplified" overview of the transfer of the measured values for the hot and residual compressive strengths from the material level to the structural element level. The data used for modeling were based on a process with "simplified" boundary conditions, which results in an increased heat flow into the element, due to overestimated surface temperature of the element, and thereby higher temperatures in different inner layers of the component compared to the standard design in hot conditions. In this "simplified model", very small values for specific heat capacity are considered, which contributes to the overestimation of the temperature in different inner layers. Thus, using this method, the influence of the material properties on the load-bearing capacity of the element will be overestimated.

5.1.3 Application of modified material characteristics in structural fire design

As discussed in Chapter 4, concrete specimens made of CEM I and the blast furnace slag cement (CEM III/A) formulated with quartz, basalt and slag aggregates were subjected to thermal loads with different maximum temperatures, following which the hot and residual compressive strength was determined. In this section, the calculated temperature profile for different layers of the wall model was combined with the respective practically determined hot and residual compressive strength for each concrete to determine the overall load-bearing capacity of the wall during the heating and cooling phases (see sections 4.2 and 4.3). The remaining load-bearing capacity in each phase is then divided into the load-bearing capacity before thermal loading and presented as the relative load-bearing capacity of the wall model during the heating phase Figure 5.2.a and during the cooling phase Figure 5.2.b. As observed, aggregate type seems to play a more pronounced role in determining the load-bearing capacity of the structural element in general. However, the effect of the cement type becomes more noticeable in case of the residual load-bearing capacity. As observed in Figure 5.2.a, the load-bearing capacity of the model wall under hot conditions is mainly dependent on aggregate type, where concretes made of CEM I and CEM III/A with quartz and basalt aggregates show the lowest (around 45 %) and highest (around 75 %) relative load-bearing capacity, respectively. In case of concrete made with slag aggregates, the load-bearing capacity of the wall under hot conditions is much higher than concrete with quartz and very close to that of concrete with basalt aggregates (69 %). The relative load-bearing capacity of the wall during cooling,

however, follows a slightly different trend (Figure 5.2.b). First, type of the cement plays a significant role, where concrete walls made of the slag sand containing cement (CEM III/A) are associated with higher load-bearing capacities. Within this context, the relative load bearing capacities of the specimens made of CEM III/A is equal to 45 %, 80 % and 75 % when combined with quartz, slag and basalt aggregates. When formulated using CEM I but with the same three aggregate types, the relative load-bearing capacity is reduced to 26 %, 72 % and 68 %, respectively. The second difference is the effect of aggregate type, where concrete wall made of slag aggregates outperform those made of basalt aggregates in terms of load-bearing capacity during cooling. Thus, the combination of CEM III/A with slag aggregates (slag sand and BFS) are associated with the highest load-bearing capacity of the structural element during cooling.

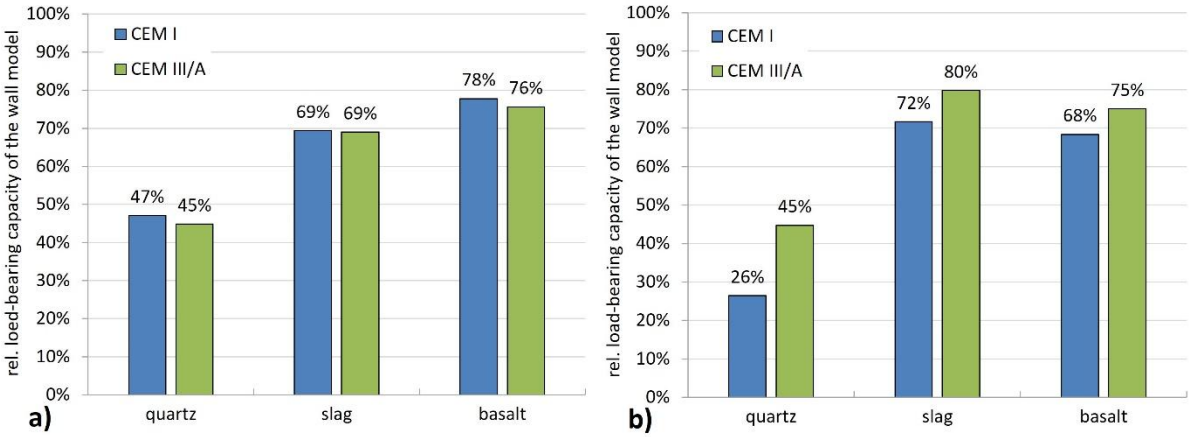

Figure 5.2 Idealized load- bearing capacity of the model wall during exposure to thermal load (a) and during the cooling phase (b)

As observed, combining the inner temperature profile of the structural element with the related hot and residual compressive strength, we have shown that the structural member might have a lower load-bearing capacity after cooling compared to the hot state (e.g. in case of CEM I and quartz aggregate combination). The design of the component according to ISO 834 or equivalent standards, without taking the cooling phase into account, can hence be on the unsafe side. For this reason, it is recommended that the load-bearing capacity of concrete structures should be verified both during exposure to thermal loads and after cooling, preferably with a couple days delay.

5.1.4 Summary of findings related to the model

Based on the findings of this section, it can be concluded that not only the mechanical properties, but also thermal characteristics play a vital part at the structural level. Thermal conductivity plays a key role in load-bearing capacity of the structural elements. This is particularly relevant for the heating phase. The improved load bearing capacity of concrete with slag aggregates (69 %) compared to the concrete with quartz aggregates (47 %) seen in Figure 5.2.a is mainly owing to the lower thermal conductivity of the former as seen in

Figure 4.39). Material properties or concrete composition therefore have a direct effect on load-bearing capacity, especially during and after the cooling phase. The results also showed, perhaps for the first time, that besides the stability of the aggregates, the type of cement also has a significant influence on residual compressive strength. When cement and aggregates with better thermal stability are combined, significant improvement of load-bearing capacity is observed. As seen in Figure 5.2.b, the combination of more thermally stable slag aggregates with the more heat resistant CEM III/A leads to 54 % improvement of the relative load bearing capacity of the model wall, when compared to the standard concrete comprised of CEM I and quartz aggregates.

6 Towards more Sustainable High-Temperature Resistant Concretes: Technological Design Guidelines

6.1 The significance of cold, hot, cooled, and post-storage compressive strength for large scale construction

As abundantly elaborated in this work, as an important indicator of concrete's mechanical properties, compressive strength is the most commonly measured value in laboratory scaled tests for the evaluation of the high temperature resistance. Measurement of compressive strength can be carried out at different stages in the process of testing. Cold compressive strength corresponds to the initial strength before exposure to high service temperatures or fire. It is known that concrete's cold compressive strength impacts its behavior when exposed to thermal loads. In real life, concrete structures that have been used in building structural elements have had specific initial compressive strengths, which might have slightly changed as the concrete aged or has been exposed to different and sometimes extreme environmental conditions. According to the findings of this work, higher cold compressive strength can signify higher decrease in the hot and residual compressive strengths, at least for certain temperature ranges.

The thermal resistance of the concrete can be characterized in terms of hot or residual compressive strength. The main difference in the methodology of hot compressive strength and residual strength is the testing during or after high temperature exposure. In other words, the hot compressive strength is measured immediately at the end of the holding time at maximum temperature, while the residual compressive strength is measured once the specimen is completely cooled down. The rate of cooling process also influences the residual compressive strength, thus the free and slow cooling process was applied in these investigations. To further investigate the impact of curing conditions upon any further strength loss or strength recovery of the concrete not immediately, but long after thermal load exposure, investigation of the residual compressive strength at different time points after exposure to thermal loads and under different storage conditions was also sought after (see Figure 6.1).

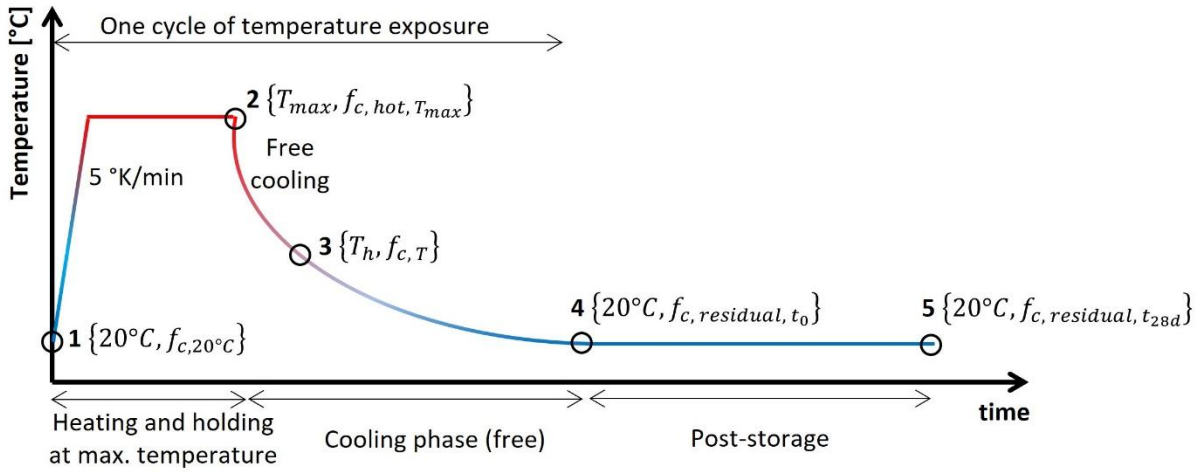

Figure 6.1 Schematic presentation of the theoretical temperature-time regime used in this investigation and the main measurement points for the compressive strength: 1) cold compressive strength measured initially before the heating cycle is applied, 2) measurement of hot compressive strength after the heating phase with a rate of 5 K/min and at the end of the holding time (4 h) at the maximum temperature, 3) free cooling phase, during which no measurement of compressive strength was carried out 4) measurement of the residual compressive strength once the specimen is fully cooled to ambient temperature (after one or more thermal cycles), 5) measurement of the compressive strength after further post storage exemplary shown for storage in standard climate (20 °C, 65 % RH) after 28 days

Figure 6.2 summarizes the values obtained for hot and residual compressive strengths as well as the standards DIN EN 1992-1-2 (EC2; left) [104] and DIN EN 1994-1-2 (EC4; right) [114]. A side-by-side presentation of the two figures, which have been separately presented in sections 4.2.2 and 4.3.4, reveals that the values for the residual compressive strengths are approximately 5 - 10 % lower than those obtained for the compressive strengths in hot conditions. This is mainly due to the fact that the concrete structure is further damaged as a result of further crack systems developed during the shrinkage of the concrete components within the course of the cooling phase. Even more interestingly, the residual compressive strength of the concrete further decreases during the initial days or even weeks after exposure to the thermal load (see section 4.4). This was further confirmed by the modeling of the temperature field inside of a 30 cm-thick wall as a model for a concrete elemental structure. As presented in Chapter 5, the temperature in different inner layers of the structural element continues to rise even during the cooling phase, with the temperature of the innermost layer being about 200 °C higher during cooling when compared to the heating phase. Hence, a continued decrease in the load bearing capacity of the structural element during cooling is to be expected.

At this point it is important to note that so far in practice, concrete strength is in most cases exclusively estimated or measured under hot conditions, which is supposed to simulate the load-bearing capacity, integrity and isolation during fire. The majority of the available building codes apply standards (e.g. ISO 834, ASTM E119, etc.) that prescribe the investigation of the load-bearing capacity of the structure under hot conditions only. Even in case of closed temperature-time curves (such as RABT-ZTV, etc.), which is common for tunnels, few adequate material

models are currently available that allow the evaluation of the load-bearing capacity of the structure in the cooled or re-cooled state. Additionally, existing material properties in available standards are not sufficient to carry out a long-term assessment of the residual load-bearing capacity. Hence, the results presented here highlight the importance of expanding the available concrete load-bearing measurements in practice beyond those conducted at the hot state to include measurements in cooled or re-cooled state, as the strength of concrete might even further decrease once it has reached the supposedly safe cool temperatures. Moreover, most available testing standards do not prescribe compressive strength measurements for concrete structures that are supposed to be subjected to cyclic thermal loads during their service life. Accordingly, the results shown in Figure 6.2. only compare the residual compressive strengths of the specimens with the available standards after exposure to one thermal cycles. However, this work has also investigated the effect of different numbers of thermal cycles upon the residual compressive strength of the concrete, where some further deterioration of the mechanical properties has been detected for some concrete compositions up to a certain number of the thermal cycles. Detailed information on this subject has been presented in section 4.3.2.

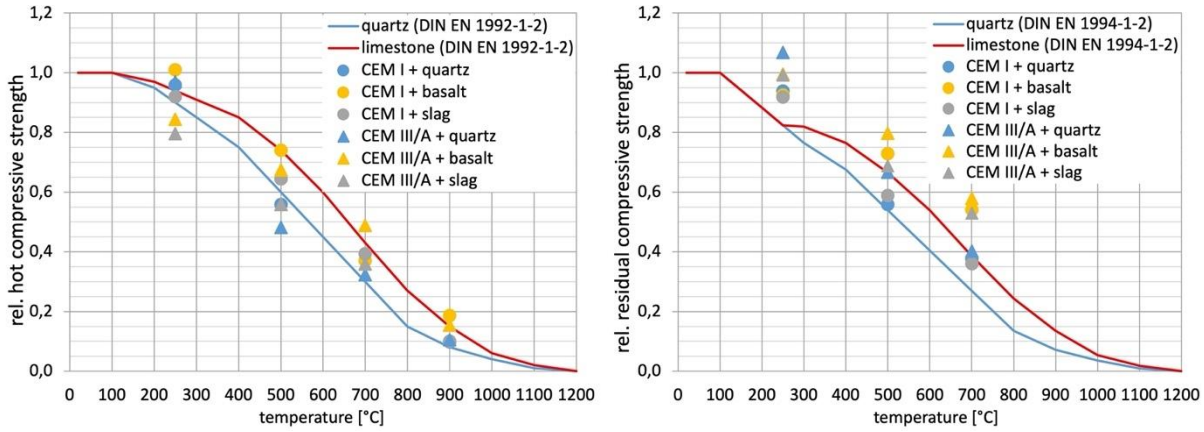

Figure 6.2 Comparison of the results of the hot and residual compressive strength of the specimens investigated in the current work along with the standards presented in DIN EN 1992-1-2 (EC2) [104] and DIN EN 1994-1-2 (EC4) [114]

The significance of the findings for structural design is that hot compressive strength might not be an adequate indicator to reflect the thermal stability of the concrete constructions. Considering the continuation of the concrete strength loss during and after cooling, an adequate hot compressive strength does not necessarily guarantee a sufficient post-cooling stability. As a result, measurement and optimization the compressive strength in cold, hot, cooled and post-storage conditions are required to provide a laboratory-scaled overview of the concrete ability to withstand thermal stresses in real life. This is of particular importance in case of concrete constructions exposed to repetitive cycles of heating and cooling.

Figure 6.3 a) Test of hot compressive strength of concrete in laboratory (self-generated) and b) concrete column after a fire accident in practice [293]

Figure 6.3.a shows the laboratory-based test setup for the measurement of the compressive strength of a cylindrical concrete specimen under hot conditions. In order to be able to use the results for the hot design of reinforced concrete structures, an additional temperature level of 900 °C was introduced, which causes the steel punch to glow at this temperature.

6.2 Design of a temperature resistant sustainable concrete alternative

One of the main objectives of this work was to develop basic knowledge for sustainable and durable alternative to conventional concrete with enhanced thermal resistance. While concrete does not burn, exposure to fire or high temperatures leads to the deterioration of its mechanical properties both due to chemical and mineralogical changes and the thermally induced internal strains. Development of concrete with adequate resistance to heat is both important from a fire safety perspective and industrial serviceability of the structures exposed to repetitive thermal cycles. Here, we sought to investigate the effect of incorporating temperature-resistant sustainable materials, such as blast furnace slag in the cement paste or as fine and coarse aggregates upon the stability of concrete when exposed to a single or repeated thermal load. On one hand, being mostly recycled industrial waste and reducing the required amount of CEM I and natural aggregates in the concrete, the use of these materials can significantly improve sustainability by reducing the CO_2 footprint of the concrete industry and the use of environmental resources. On the other hand, being byproducts of high temperature processes (e.g. in case of slags), or else given their positive impact upon the concrete mechanical properties and strength (e.g. in case of slag sand and limestone), these were expected to improve the thermal resilience of the concrete made thereof. In the next sections, we will provide a summary of the findings of this study with respect to the thermal stability of the aggregates and the sustainable and stable cement types. Since the results point out that compared to the cement type, the thermal stability of the aggregates plays a much more significant part in the heat resistance of the concrete, we will begin the summary focusing on the former.

6.2.1 Stable sustainable aggregates

The choice of aggregates plays a crucial role in determining both the hot and the residual compressive strengths of the concrete, as they comprise the majority of the concrete volume. In general, the compatibility of the aggregates with the cement matrix, e.g. in terms of thermal expansion coefficient at different temperatures, and their ability to withstand thermal stresses exerts a significant effect upon the strength of the concrete both during and after exposure to thermal loads. This study differentiated between conventional natural aggregates, standard industrial aggregates and non-standard aggregates from the steel and copper industries.

The investigation of hot compressive strength of concrete made of different combinations of fine and coarse aggregates showed that aggregates that are byproducts of high temperature processes could improve the thermal performance of the concrete made thereof. These can be naturally occurring aggregates such as basalt, or else industrial aggregates such as slag sand and/or BFS. Compared to traditional natural aggregates such as quartz, these aggregates improved the hot compressive strength of the concretes made thereof. Furthermore, slag sand and BFS as fine and coarse aggregates could provide the concrete with higher thermal resistance compared to limestone. Other industrial slags, e.g. those obtained from the steel and copper industries, however, negatively influenced the thermal stability of the concrete and led to poorer hot compressive strengths even compared to quartz, which is potentially associated with their large thermal expansion at higher temperatures [277].

Thermal stability of the aggregates can also significantly impact the residual compressive strength of the concrete. Aggregates with lower thermal expansion coefficient such as basalt, slag sand and BFS led to higher residual strengths compared to quartz-based aggregates. The low thermal expansion of these aggregates minimizes internal stresses and reduces the risk of thermal cracking within the concrete matrix. While quartz-based aggregates are associated with significantly higher thermal expansion at different temperatures, they also undergo phase transition at approximately 573 °C, which leads to a remarkable volumetric expansion. This leads to significant irreversible microcracking and a substantial loss of strength, which cannot be recovered once the concrete is cooled down to room temperature [28]. Basalt, being highly temperature-resistant, provided superior performance across all temperature ranges tested. Its high melting point and minimal thermal deformation make it particularly suitable for applications involving exposure to extreme heat [28]. Standard sustainable aggregates, namely, slag sand and BFS, provided almost similar results to basalt aggregates, and better results compared to quartz aggregates. Since these are cheaper compared to basalt, and considering their positive impact upon the concrete sustainability, slag sand and BFS provide a valuable, more economical and more sustainable alternative to basalt aggregates for the development of concretes with enhanced thermal performance. These results were further confirmed by the modeling of the load-bearing capacity of a 30 cm-thick wall as a model for concrete structural element. In this case, the role of aggregate type upon the increase of the internal temperature of the concrete element was paramount. Within this context, incorporation of basalt and slag

aggregates in the concrete wall led to comparable temperature profiles in different internal layers of the element, which was significantly lower than that predicted for the concrete structure made of quartz aggregates. As a result, the relative residual load-bearing capacity of the wall comprising basalt and BFS aggregates was significantly higher than that of their quartzite counterpart.

While non-standard industrial aggregates obtained from steel and copper industries had poorer performance in regards with the hot compressive strength of the concrete, they demonstrated better, though varying, effects upon the residual compressive strength. Copper slag aggregates improved the residual compressive strength even more than basalt, slag sand and BFS. It is not clear as to why these aggregates improve the residual mechanical properties of the concrete, when they negatively influence its strength under hot conditions. It seems that unlike quartz, the negative effects associated with copper slag aggregates at hot conditions is reversible once the concrete is cooled down. Slag aggregates obtained from the steel industries provided mixed results, with some samples performing comparable to basalt and slag sand/BFS at moderate temperatures (up to 500 °C). However, when exposed to higher temperatures, these resulted in lower residual strengths, even when compared to concrete made of quartz-based aggregates, likely due to phase changes or internal microstructural instabilities.

The investigations of the concrete thermal dilation showed that concrete made of quartz aggregates suffered from significant thermal expansion (in general and due to the phase transition), leading to irreversible damage to concrete and residual loss of strength. Basalt aggregates exhibited excellent resistance to thermal deformation, enabling the concrete to retain its structural integrity even at temperatures above 700 °C. Concretes made of standard industrial aggregates (slag sand and BFS) demonstrated excellent performance due to their low thermal expansion and compatibility with slag-containing cements, resulting in higher residual compressive strengths. Non-standard slag aggregates obtained from the steel and copper industries showed potential as a sustainable alternative to natural and standard industrial aggregates. Their performance varied, underscoring the need for additional research to optimize their use in high-temperature applications.

6.2.2 Efficient sustainable cement

Partial substitution of the CEM I by slag sand as SCM led to a slight reduction in hot compressive strength of the concrete. Slag sand exhibits slower hydration reactions compared to CEM I, resulting in a microstructure with a relatively higher proportion of unreacted slag particles at early stages. The hydration products of slag sand cements (low-lime C-S-H and secondary phases such as ettringite) dehydrate and decompose faster under high heat conditions, leading to (reversible) microstructural breakdown [61]. This can in turn bring about greater differences between the thermal expansion of the layers at different distances from the heated surface, which may promote more strength loss under hot conditions.

On the other hand, slag sand containing cements, particularly those with higher proportions of slag sand, were found to significantly enhance the residual strength of concrete exposed to high temperatures subsequent cooling. This is observed both in comparison with the concretes made of traditional CEM I and those in which part of the CEM I has been substituted by limestone (PLC). This improvement is attributed to the unique chemical and physical properties of slag sand, which contribute to enhanced microstructural stability, reduced thermal degradation, and improved post-thermal recovery in the concrete matrix. Increasing the slag sand content in the cement enhances both temperature and cycle stability. For instance, CEM III/A cement (with 60 % slag sand content) outperformed CEM II/B-S cement (with 30 % slag sand content) in terms of residual compressive strength following exposure to higher temperatures (500 °C and 700 °C) and an increase in the number of thermal cycles. The superior thermal resistance of slag sand containing cements can be linked to the formation of stable hydration products such as C-S-H with lower Ca/Si ratios, which are less prone to thermal decomposition. Additionally, the latent hydraulic properties of slag sand contribute to ongoing strength development, even after high-temperature exposure in cooled state (post-storage). However, it should be noted that the type of the aggregate seems to influence the performance of the concrete made of slag sand substituted cements. As previously mentioned, the compatibility between the aggregates and the cement paste in terms of thermal expansion at high temperatures is a paramount determinant of concrete thermal stability.

These findings highlight the significant potential of slag sand containing cements for application in structures exposed to high temperatures, refractory linings, and other environments requiring high durability under thermal stress. The ability of slag sand containing cements to retain high residual strength makes them a preferred choice for sustainable and heat resilient construction. By leveraging the benefits of slag sand containing cements, the construction industry can achieve enhanced performance, improved fire safety and thermal resistance, and extended service life for concrete structures, particularly those constantly subjected to extreme thermal conditions.

6.2.3 Interaction between sustainable aggregates and the sustainable cement matrix

The interaction between aggregates and the cement matrix was found to be a critical determinant of the hot and residual compressive strength. Aggregates with higher thermal stability effectively reduced the stress in the cement matrix, enhancing the concrete's ability to withstand thermal cycling and elevated temperatures. The degree of the thermal expansion mismatch between the aggregates and the cement matrix was found as a key factor in temperature induced strength reduction. Aggregates with thermal expansion properties closer to that of the cement paste (e.g., basalt and slag aggregates) minimized cracking and ensured better retention of the strength during and post thermal exposure. The combination of temperature-stable aggregates with slag sand containing cements resulted in the best

improvement of the concrete's residual mechanical properties. This combination proved especially effective under high numbers of thermal cycles and at higher temperature ranges (500 °C and 700 °C). The dense and thermally stable microstructure created by the interaction of slag sand containing cements and temperature-stable aggregates can reduce the propagation of thermally induced microcracks. For example, combinations such as slag sand containing cement with and BFS or basalt aggregates demonstrated the highest thermal stability.

The positive impact of the thermally stable BFS aggregates combined with slag containing cement (CEM III/A) was further confirmed through the temperature dependent prediction of the relative residual load-bearing capacity of the 30 cm-thick concrete wall model. As shown in Figure 5.2, combinations of CEM III/A and BFS aggregates were associated with the highest predicted residual load-bearing capacity, even compared to the model element made with the same cement type, but with basalt aggregates. This highlights the importance of considering cement-aggregate interactions within concrete technological development.

A further finding of this study was the detection of a temperature-dependent "maximum damage threshold" in concrete. In combinations of slag sand containing cements with temperature-stable aggregates, the damage appeared to stabilize beyond a certain temperature and number of exposure cycle. This suggests the existence of a "temperature endurance limit," where the concrete's residual strength reaches a plateau despite exposure to further thermal cycles. This behavior is hypothesized to result from the stabilization of the aggregate-cement matrix interactions and the self-healing effects of certain hydration products at elevated temperatures.

Based on the findings of this work, the use of temperature-stable industrial aggregates, particularly in combination with slag sand containing cements, is highly recommended for structures exposed to high temperatures repeatedly or for prolonged periods of time. This combination offers a sustainable alternative for enhancing the thermal performance of concrete, provided sufficient quality control measures are implemented. The residual compressive strength of concretes made with slag sand containing cements exceeded the normative values specified in standards such as DIN EN 1994-1-2 [114]. This suggests that incorporating slag sand not only meets but surpasses the standard requirements, making these cements particularly suitable for high-performance applications in high-temperature-exposed constructions.

Table 6.1. provides an overview of the findings summarized in this section.

Table 6.1 Summary of the findings regarding the behavior of aggregate and cement type upon the hot and residual (post-cooling or post-storage) compressive strength of the investigated concrete compared to the reference concrete (CEM I + quartz)

Temperature (°C)	Aggregate type	Effect on hot compressive strength	Effect on residual compressive strength		Effect on residual compressive strength post-storage (28 days in 20 °C, 65 % RH)
			One cycle	Repeated cycles	
250 °C	Basalt	-	→ (CEM I) ↑ (CEM III/A)	↑*	↑
	Slag sand/ BFS	-	→ (CEM I) ↑ (CEM III/A) ↑ (CEM II/B-S)	↑*	↑
	Slag/Basalt	-	↓	-	↑*
	Quartz/slag	-	→	-	↑
500 °C	Basalt	↑	↑*	↑*	↑*
	Slag sand/ BFS	↑	↑*	↑*	↑*
	Slag/Basalt	-	↑	-	↑*
	Quartz/slag	-	↑	-	↑*
	Ef-Slag	↓	↑	-	-
	LD-Slag	↓	↑	-	-
	Cu-Slag	↓	↑	-	-
700 °C	Basalt	↑	↑*	↑*	↑*
	Slag sand/ BFS	↑	→ (CEM I) ↑ (CEM III/A)	↑*	↑*
	Slag/Basalt	-	↑*	-	↑*
	Quartz/slag	-	→ (CEM I) ↑ (CEM III/A) ↑ (CEM III/B)	-	↑*
	Ef-Slag	↓	↓	-	-
	LD-Slag	↓	↓	-	-
	Cu-Slag	↓	↑	-	-

*** Specimens made of CEM III/A and CEM III/B have better thermal resistance compared to specimens made of CEM I**

6.3 A performance-based test concept for optimizing concrete composition for high temperature applications

As demonstrated in the preceding sections, well-composed concretes exhibit temperature resistance that is at least comparable to, if not superior to, that of conventional concrete incorporating limestone as aggregate. This finding underscores the importance of optimized material selection and mix design in achieving enhanced thermal performance in concrete structures in high-temperature environments.

The superior thermal resistance of well-composed concretes can be attributed to several key factors. First, the selection of aggregate materials with higher intrinsic thermal stability plays a crucial role. Aggregates such as basalt as well as slag sand and BFS exhibit lower thermal conductivity and reduced susceptibility to thermal degradation compared to limestone. These properties contribute to improved retention of mechanical integrity at elevated temperatures, thereby reducing the likelihood of thermal cracking and structural failure.

Second, the incorporation of SCM, particularly slag sand, can enhance the high-temperature performance of concrete. As pozzolanic materials, SCM refine the microstructure by reducing porosity and increasing the overall density of the concrete matrix. Consequently, well-composed concretes display lower permeability and reduced internal moisture movement, which are critical in mitigating explosive spalling under rapid heating conditions.

Furthermore, the optimization of the water-to-cement ratio and the use of advanced admixtures contribute to the thermal resilience of well-composed concretes. A carefully controlled water-to-cement ratio ensures a dense and durable microstructure, minimizing pathways for heat-induced moisture migration and subsequent internal stresses. High-performance admixtures, including superplasticizers and shrinkage-reducing agents, further enhance the concrete's ability to withstand thermal fluctuations without compromising structural stability.

Experimental studies elaborated on in this dissertation and reported in other studies corroborate these insights, demonstrating that well-composed concretes maintain higher residual compressive strength after exposure to elevated temperatures compared to their limestone-based counterparts. This enhanced resistance is particularly significant in fire-prone environments, where prolonged exposure to high temperatures can severely compromise the structural integrity of conventional concrete. Furthermore, concretes can be specifically engineered for specialized applications, where exposure to defined temperature thresholds, as a one time or recurrent event (i.e. exposure to cyclic high-temperature loads) are critical considerations. The ability to tailor concrete compositions for such scenarios underscores the importance of a holistic approach to material selection. While the role of stable aggregates has been more widely acknowledged, the influence of cement choice has often been underestimated. Different cement types exhibit varying levels of thermal stability, shrinkage behavior, and reactivity with supplementary materials, all of which can significantly impact overall performance in extreme conditions. Consequently, the development of a performance-

based assessment framework is essential to ensure optimal material selection and usage. A structured testing concept for performance-based evaluation is therefore proposed in the following section, offering a systematic methodology to assess and optimize concrete compositions for high-temperature applications.

Before starting on the performance-based audit concept, it is essential to consider whether the concrete's exposure to high temperatures is a one time or a repeated event. In the case of cyclical high-temperature exposure, the resistance of the concrete is the key parameter. In contrast, the heat storage capacity and thermal conductivity are also important in the case of a one time exposure to elevated temperature, e.g. as a result of a fire.

The performance-based testing concept for the design of concrete for high-temperature application involves the following steps:

1) Identification of key performance criteria

Define the essential thermal and mechanical properties for the intended application, including:

- Thermal conductivity and thermal storage capacity
- Maximum exposure temperature
- Hot compressive strength (with specified test levels)
- Residual compressive strength (with test levels, post-storage duration, and conditions)
- Required number of thermal cycles
- Stress-strain relationship and stiffness for structural design (with defined test parameters)

2) Assessment of thermal conductivity and heat storage capacity
   - Establish the maximum operating temperature.
   - Conduct temperature-dependent measurements of thermal conductivity and heat storage capacity during heating.
   - Utilize standardized refractory material testing procedures, as referenced in industry guidelines such as those provided by the German Institute for Refractories and Ceramics [292]

3) Evaluation of residual compressive strength immediately after cooling
   - Define the maximum temperature exposure.
   - Utilize RILEM standard compressive strength testing [256].
   - Conduct residual strength testing using a minimum of three specimens at two or more temperature levels, with one being the maximum exposure temperature.

4) If required: Cyclic thermal stability assessment
   - Establish testing criteria for repeated heating and cooling cycles.
   - Define the maximum exposure temperature and the number of cycles.

- Conduct RILEM-standard compressive strength tests with a minimum of three specimens at defined temperature levels.
- If applicable, specify a “maximum damage level” threshold.

5) If required: Residual strength evaluation after post-storage
   - Define post-exposure conditions, including cooling rates and storage duration.
   - Conduct compressive strength testing using at least three specimens at two or more temperature levels.
   - Ensure compliance with industry standards for post-storage mechanical evaluation.

6) If required: Stress-strain behavior and/or stiffness measurement during or after thermal load exposure
   - Define the maximum exposure temperature.
   - Perform RILEM-compliant stress-strain and stiffness evaluations [256].
   - Conduct testing with a minimum of three specimens during or after thermal exposure, including potential post-storage conditions.

The performance-based testing concept outlined above provides a structured and standardized framework for evaluating the high-temperature resilience of concrete. By incorporating rigorous testing methodologies and industry-recognized standards, this approach ensures reliable assessment of concrete formulations for demanding applications. Future research should focus on refining these protocols, expanding material databases, and integrating predictive modeling techniques to enhance the efficiency and accuracy of high-temperature performance evaluations in industrial and structural applications.

7 Summary and Conclusions

The focus of the dissertation was to investigate the possibility of developing a sustainable alternative to conventional concrete with enhanced thermal resistance. To this end, the effect of cements containing different amounts of slag sand or limestone and the aggregates obtained as byproducts of metal industries at high temperatures, namely unground slag sand (as fine aggregates) and BFS (as coarse aggregate) on the mechanical behavior of concrete during and after exposure to one or more thermal cycles was investigated. The statistical evaluation of the results from more than 1800 data sets showed that the slag sand and BFS aggregates have comparably high temperature stability comparable to that of basalt (and significantly superior to quartz) and improve both the hot and residual compressive strength of the concrete. Thus, it seems that in addition to improving concrete sustainability, industrial aggregates made of slag sand and BFS can be also used as more economical alternatives to temperature-resistant natural aggregates such as basalt. In regards with the cement type, partial replacement of the CEM I by slag sand as SCM was shown to slightly reduce the hot, but significantly improve the residual compressive strength of the concrete, both immediately after cooling and after storage under humid conditions. Within this context, slag sand performed superior to limestone, and increasing the slag sand content of the cement was shown to bring about positive effects upon the concrete residual properties.

The use of slag sand and BFS aggregates and to a lower extent cements containing slag sand as SCM was shown to reduce the thermal conductivity of concrete. This leads to lower temperatures in the internal layers of the structural component made of these materials both during exposure to thermal loads and cooling. As a result, both the temperature-related stress and the size of the regions of the element exposed to temperature-related stress decrease. In fact, the modeling of the residual load-bearing capacity of a 30 cm-thick wall as a model for concrete structural element demonstrated that incorporation of basalt and slag aggregates in the concrete wall led to comparable temperature profiles in different internal layers of the element, which was significantly lower than that predicted for the concrete structure made of quartz aggregates, both during the heating and the cooling phases. As a result, the relative residual load-bearing capacity of the wall comprising basalt and BFS aggregates was significantly higher than that of their quartzite counterpart. Additionally, it was shown that combinations of slag containing cement (CEM III/A) and BFS aggregates were associated with the highest predicted residual load-bearing capacity of the model structural element, even superior to the model element made with the same cement type, but with basalt aggregates. This highlights the importance of considering cement-aggregate interactions within concrete technological development.

Even though a systematic investigation of other industrial by-products, e.g. different types of steel and copper slags, and their influence on the thermal properties of the concrete was out of the scope of this work, some preliminary experiments were done on the subject. The results

indicated that these non-standard industrial aggregates negatively affected the hot compressive strength but mostly improved the residual compressive strength of the concrete, even in some cases in a manner comparable with basalt aggregates. These findings inspire further in-depth research in terms of the thermal properties of these materials and the systematic investigation of their influence on the mechanical properties of the concrete exposed to high temperatures.

Combined, this study successfully managed to introduce a more sustainable alternative to traditional CEM I concrete with superior thermal performance, particularly for constructions that have to endure exposure to repeated heating and cooling cycles during their service life. The findings of this work are interesting both from a fire safety and high temperature serviceability perspective and from the sustainability point of view. We hope that these findings serve as a stepstone, paving the way for the development of more sustainable and at the same time more thermally resilient concrete alternatives for the fields of architecture and civil engineering.

8 Outlook and Perspectives

Neither the standard industrial aggregates such as slag sand and BFS nor the slag aggregates obtained from other industries are currently considered in the fire resistance design of concrete structures according to DIN EN 1992-1-2. The knowledge gained through this work suggests that to treat the standard industrial aggregates (slag sand and BFS) at least similarly to quartzite aggregates might be justifiable. It seems even logical to add these in a new class of concretes with relative hot compressive strengths between those of concrete with limestone and quartz aggregates. In terms of the thermal characteristic values and the thermal expansion, the "favorable properties" curves in the standard could be used. This would allow a normative fire resistance design of concretes with slag sand and BFS as industrial aggregates. Additionally, the preliminary results of this work highlighted the potential of copper slag aggregates, and to some extent the slag aggregates from the steel industries, to improve the residual properties of the concrete exposed to high temperature. This inspires further research focusing on the thermal properties of these aggregates and the potential of using these as standard industrial aggregates in the concrete industry.

For the design of the load-bearing capacity of structures in the cooled state after a fire event, concretes with slag sand and BFS aggregates could be evaluated using the standard curves presented in DIN EN 1994-1-2. The favorable characteristics of the specimens made of these aggregates according to the standard combined with the uncovered positive effect of slag sand containing cements upon the residual mechanical properties of the concrete point out that combination of slag sand containing cements and slag aggregates leads to an increased load-bearing capacity of these structures following exposure to one time or repeated thermal loads. Additionally, the use of further temperature-resistant aggregates such as basalt or limestone (below a temperature of 850 °C) can also provide residual strength values above the standard curve. This is of particular interest for civil engineering projects such as bridges and tunnels, where so-called "closed fire curves" are used for the evaluation of the residual mechanical properties. Furthermore, particularly in line with the detected temperature-dependent "maximum damage threshold" in concrete, similar models can be used to present normative values for the load-bearing capacity of the structures exposed to repeated cycles of heating and cooling.

References

[1] M. Purton, “Cement is a big problem for the environment. Here’s how to make it more sustainable,” World Economic Forum. [Online]. Available: https://www.weforum.org/stories/2024/09/cement-production-sustainable-concrete-co2-emissions/

[2] “Fire Loss in the U.S. 2020: A Synopsis of the NFPA’s Annual Fire Report,” Harrington Group Inc. [Online]. Available: https://www.nfpa.org/-/media/Files/News-and-Research/Fire-statistics-and-reports/Fire-statistics-and-reports.ashx

[3] “EU-Wide data on residential fires,” European Fire Safety Alliance. [Online]. Available: https://www.europeanfiresafetyalliance.org/action-plan/statistics/

[4] V. Kodur, “Properties of Concrete at Elevated Temperatures,” *International Scholarly Research Notices*, vol. 2014, no. 1, p. 468510, 2014, doi: 10.1155/2014/468510.

[5] “DIN EN 1991-1-2:2010-12. Eurocode 1:EN 1991-1-2:2002. Eurocode 1: Actions on structures – Part 1-2: General actions – Actions on structures exposed to fire.” Berlin: Beuth Verlag, 2010.

[6] R. S. Blandon and V. Kodur, “Fire performance of concrete structures,” in *Durability and sustainability of concrete structures*, M. A. Rizkalla&A. S. Nowak (Eds.)., CRC Press, Taylor and Francis Group, 2015, pp. 156–178.

[7] A. M. Neville, *Properties of concrete*, 5th Ed. Prentice Hall, 2012.

[8] L. Y. Siang, F. E. M. Ghazali, N. Y. Zainun, and R. Ali, “General risks for tunnelling projects: An overview,” *AIP Conference Proceedings*, vol. 1892, no. 1, p. 080004, Oct. 2017, doi: 10.1063/1.5005730.

[9] E. Soja, C. Wade, and K. Frank, “4 - Flammability tests for building facades,” in *Flammability Testing of Materials Used in Construction, Transport and Mining (Second Edition)*, V. Apte, Ed., in Woodhead Publishing Series in Civil and Structural Engineering. , Woodhead Publishing, 2022, pp. 89–126. doi: 10.1016/B978-0-08-102801-8.00084-3.

[10] S. Ni and T. Gernay, “Evaluation of expected damage costs from fire in concrete building structures,” presented at the 11th International Conference on Structures in Fire (SiF2020), Brisbane, Australia: The University of Queensland, 2020. doi: https://doi.org/10.14264/04361bb.

[11] M. C. Alonso, J. Guerreiro, and L. Vera, “Potential of concrete as thermal energy storage solid medium exposed to thermal-fatigue cycles,” presented at the 4th International Workshop on Concrete Spalling due to Fire Exposure, Leipzig, Germany, 2015.

[12] J. Emerson, H. Micah, and S. Paneer, “Concrete as thermal storage medium for thermocline solar energy storage systems,” *Solar Energy*, vol. 96, pp. 194–204, 2013, doi: https://doi.org/10.1016/j.solener.2013.06.033.

[13] R. Dvořák, Z. Chobola, I. Plšková, R. Hela, and L. Bodnárová, “Classification of thermally degraded concrete by acoustic resonance method and image analysis via machine learning,” *Materials*, vol. 3, p. 1010, 2023, doi: 10.1016/S0008-8846(01)00781-9.

[14] X. Liu, E. Ma, J. Liu, B. Zhang, D. Niu, and Y. Wang, “Deterioration of an industrial reinforced concrete structure exposed to high temperatures and dry-wet cycles,” *Engineering Failure Analysis*, vol. 135, p. 106150, May 2022, doi: 10.1016/j.engfailanal.2022.106150.

[15] “RILEM TC 129-MHT: Test methods for mechanical properties of concrete at high temperatures,” *Materials and Structures*, vol. 28, pp. 410–414, 1995, doi: https://doi.org/10.1007/BF02473077.

[16] L. Biolzi, S. Cattaneo, and G. Rosati, “Evaluating residual properties of thermally damaged concrete,” *Cement and Concrete Composites*, vol. 30, no. 10, pp. 907–916, Nov. 2008, doi: 10.1016/j.cemconcomp.2008.09.005.

[17] L. T. Phan and N. J. Carino, “Fire performance of high strength concrete: research needs,” in *Proceedings of Advanced Technology in Structural Engineering*, Philadelphia, 2000.

[18] “ISO 834-1:1999: Fire Resistance Tests - Elements of Building Construction - Part 1: General Requirements.” International Organization for Standardization, 1999.

[19] A. Ariyanayagam and M. Mahendran, “Fire safety of buildings based on realistic fire time-temperature curves,” presented at the 19th International CIB World Building Congress, Brisbane, Australia: Construction Society, Queensland University of Technology, 2013, pp. 1–13.

[20] D. Panias, E. Balomenos, and K. Sakkas, “16 - The fire resistance of alkali-activated cement-basedconcrete binders,” in *Handbook of Alkali-Activated Cements, Mortars and Concretes*, F. Pacheco-Torgal, J. A. Labrincha, C. Leonelli, A. Palomo, and P. Chindaprasirt, Eds., Oxford: Woodhead Publishing, 2015, pp. 423–461. doi: 10.1533/9781782422884.3.423.

[21] “DIN EN 1363-2:1999-10: Fire safety tests: Part 2: Alternative and additional procedures.” Berlin: Beuth Verlag, 1999.

[22] M. Gravit, E. Gumerova, A. Bardin, and L. Vitaly, “Increase of fire resistance limits of building structures of oil-and-gas complex under hydrocarbon fire,” in

International Scientific Conference Energy Management of Municipal Transportation Facilities and Transport EMMFT 2017, Springer International Publishing, 2017.

[23] M. Imran, M. Liew, and M. S. Nasif, "Experimental studies on fire for offshore structures and its limitations: a review," *Chemical Engineering Transactions*, vol. 45, pp. 1951–1956, 2015, doi: 10.3303/CET1545326.

[24] Z. Saleheen, R. R. Krishnamoorthy, and A. Nadjai, "A review on behavior, material properties and finite element simulation of concrete tunnel linings under fire," *Tunnelling and Underground Space Technology*, vol. 126, p. 104534, Aug. 2022, doi: 10.1016/j.tust.2022.104534.

[25] N. Taillefer, P. Carlotti, C. Larive, C. Lemerle, R. Avenel, and P. Pimienta, "Ten years of increased hydrocarbon temperature curves in French tunnels," *Fire Technol*, vol. 49, no. 2, pp. 531–549, Apr. 2013, doi: 10.1007/s10694-012-0259-8.

[26] T. Oli, D. Ha, T. Jang, C. Park, G. Kim, and S. Kim, "Temperature distribution curve analysis on concrete through LS-DYNA," *Fire*, vol. 7, no. 1, Art. no. 1, Jan. 2024, doi: 10.3390/fire7010015.

[27] S. Kim, J. Shim, J. Y. Rhee, D. Jung, and C. Park, "Temperature distribution characteristics of concrete during fire occurrence in a tunnel," *Applied Sciences*, vol. 9, no. 22, Art. no. 22, Jan. 2019, doi: 10.3390/app9224740.

[28] U. Schneider, *Verhalten von Beton bei hohen Temperaturen*, Heft 337. Berlin: Verlag von Wilhelm Ernst und Sohn, 1982.

[29] M. Heikal, "Effect of temperature on the physico-mechanical and mineralogical properties of Homra pozzolanic cement pastes," *Cement and Concrete Research*, vol. 30, no. 11, pp. 1835–1839, Nov. 2000, doi: 10.1016/S0008-8846(00)00403-8.

[30] M. Husem, "The effects of high temperature on compressive and flexural strengths of ordinary and high-performance concrete," *Fire Safety Journal*, vol. 41, no. 2, pp. 155–163, Mar. 2006, doi: 10.1016/j.firesaf.2005.12.002.

[31] J. E. van der Merwe, "Evaluation of concrete tensile strength as a function of temperature," *Construction and Building Materials*, vol. 329, p. 127179, Apr. 2022, doi: 10.1016/j.conbuildmat.2022.127179.

[32] W. Khaliq and V. Kodur, "Effect of high temperature on tensile strength of different types of high-strength concrete," *ACI Materials Journal*, vol. 108, no. 4, pp. 394–402, 2011.

[33] Z. Li, H. Shang, S. Xiao, L. Yang, and Z. Li, "Effect of thermal fatigue on mechanical properties and microstructure of concrete in constant ambient humidity," *Construction and Building Materials*, vol. 368, p. 130367, Mar. 2023, doi: 10.1016/j.conbuildmat.2023.130367.

[34] F. M. Nazri, S. Shahidan, N. K. Baharuddin, S. Beddu, and B. H. Abu Bakar, "Effects of heating durations on normal concrete residual properties: compressive strength and mass loss," *IOP Conf. Ser.: Mater. Sci. Eng.*, vol. 271, no. 1, p. 012013, Nov. 2017, doi: 10.1088/1757-899X/271/1/012013.

[35] V. Balagam and S. R. Killamsetti, "Effect of thermal cycles on concrete: an overview," *International Journal for Research in Engineering Application and Management*, vol. 5, no. 3, pp. 6–14, 2019.

[36] C. D. Sa, F. Benboudjema, K. Duong, and J. Sicard, "A meso-scale approach for the modeling of concrete behavior at high temperatures," in *Computational Modelling of Concrete Structures*, CRC Press, 2006.

[37] D. A. Kontogeorgos, G. K. Semitelos, I. D. Mandilaras, and M. A. Founti, "Experimental investigation of the fire resistance of multi-layer drywall systems incorporating vacuum insulation panels and phase change materials," *Fire Safety Journal*, vol. 81, pp. 8–16, Apr. 2016, doi: 10.1016/j.firesaf.2016.01.012.

[38] C. Alonso and L. Fernandez, "Dehydration and rehydration processes of cement paste exposed to high temperature environments," *Journal of Materials Science*, vol. 39, no. 9, pp. 3015–3024, May 2004, doi: 10.1023/B:JMSC.0000025827.65956.18.

[39] G.-F. Peng and Z.-S. Huang, "Change in microstructure of hardened cement paste subjected to elevated temperatures," *Construction and Building Materials*, vol. 22, no. 4, pp. 593–599, Apr. 2008, doi: 10.1016/j.conbuildmat.2006.11.002.

[40] A. Mandes, J. Sanjayan, and F. Collins, "Phase transformations and mechanical strength of OPC/Slag pastes submitted to high temperatures," *Materials and Structures*, vol. 41, pp. 345–350, 2008.

[41] K. R. Rao and T. Tadepalli, "High-temperature behaviour of concrete: a review," in *Low carbon maetrials and technologies for sustainable and resilient infrastructure*, Springer Nature Singapore, 2024, pp. 167–186. Accessed: Apr. 04, 2025. [Online]. Available: https://www.springerprofessional.de/en/high-temperature-behaviour-of-concrete-a-review/26651806

[42] H. Song, Y. Jeong, S. Bae, Y. Jun, S. Yoon, and J. Eun Oh, "A study of thermal decomposition of phases in cementitious systems using HT-XRD and TG," *Construction and Building Materials*, vol. 169, pp. 648–661, Apr. 2018, doi: 10.1016/j.conbuildmat.2018.03.001.

[43] M. Amran, G. Murali, N. Makul, M. Kurpińska, and M. L. Nehdi, "Fire-induced spalling of ultra-high performance concrete: A systematic critical review," *Construction and Building Materials*, vol. 373, p. 130869, Apr. 2023, doi: 10.1016/j.conbuildmat.2023.130869.

[44] F. Lo Monte, R. Felicetti, and C. Rossino, “Fire spalling sensitivity of high-performanceconcrete in heated slabs under biaxial compressive loading,” *Mater Struct*, vol. 52, no. 1, p. 14, Jan. 2019, doi: 10.1617/s11527-019-1318-0.

[45] F. Ali, A. Nadjai, and A. Abu-Tair, “Explosive spalling of normal strength concrete slabs subjected to severe fire,” *Mater Struct*, vol. 44, no. 5, pp. 943–956, Jun. 2011, doi: 10.1617/s11527-010-9678-5.

[46] J. Yang, W. Zhang, D. Hou, G. Zhang, and Q. Ding, “Structure, dynamics and mechanical properties evolution of calcium silicate hydrate induced by dehydration and dehydroxylation,” *Construction and Building Materials*, vol. 291, p. 123327, Jul. 2021, doi: 10.1016/j.conbuildmat.2021.123327.

[47] I. Hager, “Behaviour of cement concrete at high temperature,” *Bulletin of Polish Academy of Sciences, Technical Sciences*, vol. 61, no. 1, 2013, doi: 10.2478/bpasts-2013-0013.

[48] M. Amiri, M. Aryanpour, and F. Porhonar, “Microstructural study of concrete performance after exposure to elevated temperatures via considering C–S–H nanostructure changes,” *High Temperature Materials and Processes*, vol. 41, no. 1, pp. 224–237, Jan. 2022, doi: 10.1515/htmp-2022-0030.

[49] M. Castellote, C. Alonso, C. Andrade, X. Turrillas, and J. Campo, “Composition and microstructural changes of cement pastes upon heating, as studied by neutron diffraction,” *Cement and Concrete Research*, vol. 34, no. 9, pp. 1633–1644, Sep. 2004, doi: 10.1016/S0008-8846(03)00229-1.

[50] Q. Zhou and F. P. Glasser, “Thermal stability and decomposition mechanisms of ettringite at <120°C,” *Cement and Concrete Research*, vol. 31, no. 9, pp. 1333–1339, Sep. 2001, doi: 10.1016/S0008-8846(01)00558-0.

[51] S. Lim, “Effects of elevated temperature exposure on cement-based composite materials,” University of Illinois at Urbana-Champaign, Urbanam Illinois, 2015.

[52] W. Gong, “Mechanical properties and durability performance of concrete subjected to high temperature heatinf,” Tokushima University, Tokushima, Japan, 2018.

[53] S. Shaw, S. M. Clark, and C. M. B. Henderson, “Hydrothermal formation of the calcium silicate hydrates, tobermorite (Ca5Si6O16(OH)2·4H2O) and xonotlite (Ca6Si6O17(OH)2): an in situ synchrotron study,” *Chemical Geology*, vol. 167, no. 1, pp. 129–140, Jun. 2000, doi: 10.1016/S0009-2541(99)00205-3.

[54] E. T. Rodriguez, K. Garbev, D. Merz, L. Black, and I. G. Richardson, “Thermal stability of C-S-H phases and applicability of Richardson and Groves’ and Richardson C-(A)-S-H(I) models to synthetic C-S-H,” *Cement and Concrete Research*, vol. 93, pp. 45–56.

[55] Q. Zhang and G. Ye, “Dehydration kinetics of Portland cement paste at high temperature,” *J Therm Anal Calorim*, vol. 110, no. 1, pp. 153–158, Oct. 2012, doi: 10.1007/s10973-012-2303-9.

[56] G. F. Peng, S. Y. N. Chan, and M. Anson, “Chemical kinetics of C-S-H decomposition in hardened cement paste subjected to elevated temperatures up to 800°C,” *Advances in Cement Research*, vol. 13, no. 2, pp. 47–52, Apr. 2001, doi: 10.1680/adcr.2001.13.2.47.

[57] Z. Xing, A.-L. Beaucour, R. Hebert, A. Noumowe, and B. Ledesert, “Influence of the nature of aggregates on the behaviour of concrete subjected to elevated temperature,” *Cement and Concrete Research*, vol. 41, no. 4, pp. 392–402, Apr. 2011, doi: 10.1016/j.cemconres.2011.01.005.

[58] J. Reiners, J. Zehfuß, F. Dehn, and C. Müller, “The influence of the physical and chemical properties of hardened cement paste on the heat-induced explosive spalling of concrete,” *Civil Engineering Design*, vol. 6, no. 1, pp. 4–21, 2024, doi: 10.1002/cend.202300020.

[59] M. Samtani, D. Dollimore, and K. S. Alexander, “Comparison of dolomite decomposition kinetics with related carbonates and the effect of procedural variables on its kinetic parameters,” *Thermochimica Acta*, vol. 392–393, pp. 135–145, Sep. 2002, doi: 10.1016/S0040-6031(02)00094-1.

[60] X.-G. Li, Y. Lv, B.-G. Ma, W.-Q. Wang, and S.-W. Jian, “Decomposition kinetic characteristics of calcium carbonate containing organic acids by TGA,” *Arabian Journal of Chemistry*, vol. 10, pp. S2534–S2538, May 2017, doi: 10.1016/j.arabjc.2013.09.026.

[61] J. Reiners, “The Influence of the Physical and Chemical Properties of Hardened Cement Paste on the Fire-Induced Spalling of Concrete,” University of Branschweig, 2023.

[62] K. D. Hertz, “Concrete Strength for Fire Safety Design,” *Magazine of Concrete Research*, vol. 57, no. 8, pp. 445-453., 2005, doi: 10.1680/macr.2005.57.8.445.

[63] R. Sarshar and G. A. Khoury, “Material and environmental factors influencing the compressive strength of unsealed cement paste and concrete at high temperatures,” *Magazine of Concrete Research*, vol. 45, no. 162, pp. 51–61, Mar. 1993, doi: 10.1680/macr.1993.45.162.51.

[64] O. E. Babalola, P. O. Awoyera, D.-H. Le, and L. M. Bendezú Romero, “A review of residual strength properties of normal and high strength concrete exposed to elevated temperatures: Impact of materials modification on behaviour of concrete composite,” *Construction and Building Materials*, vol. 296, p. 123448, Aug. 2021, doi: 10.1016/j.conbuildmat.2021.123448.

[65] J. Lee, Y. Xi, and W. Kaspar, “Properties of concrete after high-temperature heating and cooling -,” *ACI Materials Journal*, vol. 105, no. 4, pp. 334–341, 2008.

[66] S. Y. N. Chan, X. Luo, and W. Sun, “Effect of high temperature and cooling regimes on the compressive strength and pore properties of high performance concrete,” *Construction and Building Materials*, vol. 14, no. 5, pp. 261–266, Jul. 2000, doi: 10.1016/S0950-0618(00)00031-3.

[67] L. Xiaoyong and B. Fanjie, “Residual Strength for Concrete after Exposure to High Temperatures,” in *Innovative Computing and Information*, M. Dai, Ed., Berlin, Heidelberg: Springer, 2011, pp. 382–390. doi: 10.1007/978-3-642-23998-4_53.

[68] M. H. Elhussein and A. O. Abd El Halim, “Differential thermal expansion and contraction: a mechanistic approach to adhesion in asphalt concrete,” *Canadian Journal of Engineering*, vol. 20, no. 3, pp. 366–373, 1993.

[69] M. Pasztetnik and R. Wróblewski, “A Literature Review of Concrete Ability to Sustain Strength after Fire Exposure Based on the Heat Accumulation Factor,” *Materials (Basel)*, vol. 14, no. 16, p. 4719, Aug. 2021, doi: 10.3390/ma14164719.

[70] Q. Li, G. Yuan, and Q. Shu, “Effects of heating/cooling on recovery of strength and carbonation resistance of fire-damaged concrete,” *Magazine of Concrete Research*, vol. 66, no. 18, pp. 925–936, Sep. 2014, doi: 10.1680/macr.14.00029.

[71] T. Liu, H. Wang, D. Zou, X. Long, M. J. Miah, and Y. Li, “Strength recovery of thermally damaged high-performance concrete subjected to post-fire carbonation curing,” *Cement and Concrete Composites*, vol. 143, p. 105273, Oct. 2023, doi: 10.1016/j.cemconcomp.2023.105273.

[72] D. Paul Thanaraj *et al.*, “Influence of heating–cooling regime on the engineering properties of structural concrete subjected to elevated Ttemperature,” *Buildings*, vol. 13, no. 2, Art. no. 2, Feb. 2023, doi: 10.3390/buildings13020295.

[73] B. Toumi, M. Resheidat, Z. Guemmadi, and H. Chabil, “Coupled effect of high temperature and heating time on the residual strength of normal and high-strength concretes,” *Jordan Journal of Civil Engineering*, vol. 3, no. 4, 2009, Accessed: Apr. 04, 2025. [Online]. Available: https://www.iiste.org/Journals/index.php/JJCE/article/view/17891

[74] V. Sachin and N. Suresh, “Residual properties of normal-strength concrete subjected to fire and sustained elevated temperatures: A comparative study,” *Journal of Structural Fire Engineering*, vol. 12, no. 1, pp. 1–16, Oct. 2020, doi: 10.1108/JSFE-02-2020-0007.

[75] W. Botte and R. Caspeele, “Post-cooling properties of concrete exposed to fire,” *Fire Safety Journal*, vol. 92, pp. 142–150, Sep. 2017, doi: 10.1016/j.firesaf.2017.06.010.

[76] J. Bi, P. Liu, and F. Gan, “Effects of the cooling treatment on the dynamic behavior of ordinary concrete exposed to high temperatures,” *Construction and Building Materials*, vol. 248, p. 118688, Jul. 2020, doi: 10.1016/j.conbuildmat.2020.118688.

[77] S. Fehérvári, “Effect of cooling methods on the residual properties of concrete exposed to elevated temperature,” *Results in Engineering*, vol. 16, p. 100797, Dec. 2022, doi: 10.1016/j.rineng.2022.100797.

[78] H. Suh *et al.*, “Influences of rehydration conditions on the mechanical and atomic structural recovery characteristics of Portland cement paste exposed to elevated temperatures,” *Construction and Building Materials*, vol. 235, p. 117453, Feb. 2020, doi: 10.1016/j.conbuildmat.2019.117453.

[79] L. Li, P. Jia, J. Dong, L. Shi, G. Zhang, and Q. Wang, “Effects of cement dosage and cooling regimes on the compressive strength of concrete after post-fire-curing from 800 °C,” *Construction and Building Materials*, vol. 142, pp. 208–220, Jul. 2017, doi: 10.1016/j.conbuildmat.2017.03.053.

[80] Z. Li and Y. Ryuda, “Bond Strength Recovery Of Fire-Damaged Concrete After Post-Fire-Curing,” in *Proceedings of International Structural Engineering and Construction*, Sydney, Australia, 2015, pp. 719–724. doi: 10.14455/ISEC.res.2015.63.

[81] C. Wu, J. Pan, W. Zhong, and F. Jin, “Testing of high thermal cycling stability of low strength concrete as a thermal energy storage material,” *Applied Sciences*, vol. 6, no. 10, Art. no. 10, Oct. 2016, doi: 10.3390/app6100271.

[82] C.-S. Poon, S. Azhar, M. Anson, and Y.-L. Wong, “Comparison of the strength and durability performance of normal- and high-strength pozzolanic concretes at elevated temperatures,” *Cement and Concrete Research*, vol. 31, no. 9, pp. 1291–1300, Sep. 2001, doi: 10.1016/S0008-8846(01)00580-4.

[83] X. Cheng *et al.*, “Mechanical and thermal properties of aluminate cement paste with blast furnace slag at high temperatures,” *Construction and Building Materials*, vol. 228, p. 116747, Dec. 2019, doi: 10.1016/j.conbuildmat.2019.116747.

[84] D. Koňáková, E. Vejmelková, V. Pommer, M. Keppert, A. Trník, and R. Černý, “Physical and chemical characteristics of heat resistant materials based on high alumina cement,” *AIP Conference Proceedings*, vol. 2429, no. 1, p. 020004, Nov. 2021, doi: 10.1063/5.0069565.

[85] S. Ramzi and H. Hajiloo, “The effects of supplementary cementitious materials (SCMs) on the residual mechanical properties of concrete after exposure to high temperatures—review,” *Buildings*, vol. 13, no. 1, Art. no. 1, Jan. 2023, doi: 10.3390/buildings13010103.

[86] S. Ramzi, M. J. Moradi, and H. Hajiloo, “The study of the effects of supplementary cementitious materials (SCMs) on concrete compressive strength at high temperatures using artificial neural network model,” *Buildings*, vol. 13, no. 5, Art. no. 5, May 2023, doi: 10.3390/buildings13051337.

[87] A. Behnood and H. Ziari, “Effects of silica fume addition and water to cement ratio on the properties of high-strength concrete after exposure to high temperatures,” *Cement and Concrete Composites*, vol. 30, no. 2, pp. 106–112, Feb. 2008, doi: 10.1016/j.cemconcomp.2007.06.003.

[88] H. Mohammed, H. Ahmed, R. Kurda, R. Alyousef, and A. F. Deifalla, “Heat-induced spalling of concrete: A review of the influencing factors and their importance to the phenomenon,” *Materials*, vol. 15, no. 5, Art. no. 5, Jan. 2022, doi: 10.3390/ma15051693.

[89] Z. Yu, Y. Meng, K. H. Mo, H. Liu, and T.-C. Ling, “Influences of w/c and CO2 curing duration on the high temperature properties of cement pastes,” *Journal of Building Engineering*, vol. 69, p. 106293, Jun. 2023, doi: 10.1016/j.jobe.2023.106293.

[90] M. Yoon, G. Kim, G. C. Choe, Y. Lee, and T. Lee, “Effect of coarse aggregate type and loading level on the high temperature properties of concrete,” *Construction and Building Materials*, vol. 78, pp. 26–33, Mar. 2015, doi: 10.1016/j.conbuildmat.2014.12.096.

[91] V. Hlavička and É. Lublóy, “Concrete cone failure of bonded anchors in thermally damaged concrete,” *Construction and Building Materials*, vol. 171, pp. 588–597, May 2018, doi: 10.1016/j.conbuildmat.2018.03.148.

[92] R. N. R, A.-L. Beaucour, R. Hebert, A. Noumowé, B. Ledésert, and R. Bodet, “Thermal stability of different siliceous and calcareous aggregates subjected to high temperature,” *MATEC Web of Conferences*, vol. 6, p. 07001, 2013, doi: 10.1051/matecconf/20130607001.

[93] I. Netinger, D. Varevac, D. Bjegović, and D. Morić, “Effect of high temperature on properties of steel slag aggregate concrete,” *Fire Safety Journal*, vol. 59, pp. 1–7, Jul. 2013, doi: 10.1016/j.firesaf.2013.03.008.

[94] S. Mirnezami, A. Hassani, and A. Bayat, “Evaluation of the effect of metallurgical aggregates (steel and copper slag) on the thermal conductivity and mechanical properties of concrete in jointed plain concrete pavements (JPCP),”

Construction and Building Materials, vol. 367, p. 129532, Feb. 2023, doi: 10.1016/j.conbuildmat.2022.129532.

[95] Y. El Bitouri, F. Jamin, C. Pélissou, and M. S. El Youssoufi, "Tensile and shear bond strength between cement paste and aggregate subjected to high temperature," *Materials and structures*, vol. 50, no. 6, Dec. 2017, doi: 10.1617/s11527-017-1105-8.

[96] A. Mallat and A. Alliche, "Mechanical investigation of two fiber-reinforced repair mortars and the repaired system," *Construction and Building Materials*, vol. 25, no. 4, pp. 1587–1595, Apr. 2011, doi: 10.1016/j.conbuildmat.2010.10.017.

[97] B. Yumkham, C. Shijagurumaum, and T. Suresh, "Fire resistance of concrete structure-a review," *SAMRIDDHI*, vol. 14, no. 1, pp. 63–68, 2022.

[98] "DIN EN 12664:Thermal performance of building materials and products - Determination of thermal resistance by means of guarded hot plate and heat flow meter methods - Dry and moist products with medium and low thermal resistance; German version EN 12664:2001." Berlin: Beuth Verlag, 2001.

[99] "DIN EN 12667:2001-05:Thermal performance of building materials and products - Determination of thermal resistance by means of guarded hot plate and heat flow meter methods - Products of high and medium thermal resistance; German version EN 12667:2001." Berlin: Beuth Verlag, 2001.

[100] T.-D. Nguyen, D.-T. Pham, and M.-N. Vu, "Thermo-mechanically-induced thermal conductivity change and its effect on the behaviour of concrete," *Construction and Building Materials*, vol. 198, pp. 98–105, Feb. 2019, doi: 10.1016/j.conbuildmat.2018.11.146.

[101] M. Howlader, M. H. Rashid, D. Mallick, and T. Haque, "Effects of aggregate types on thermal properties of concrete," *ARPN Journal of Engineering and Applied Sciences*, vol. 7, no. 7, pp. 900–907, 2012.

[102] T. Z. Harmathy, "Properties of building materials," in *SFPE Handbook of Fire Protection Engineering*, Quincy, Massachusettes, United States: National Fire Protection Association, 2008.

[103] D. K. Hein and P. Eng, "Concrete coefficient of thermal expansion (CTE) and its significance in mechanistic-emperical pavement design," in *Advances in pavement evaulation and instrumentation*, Fredericton, New Bruswick, Canada, 2012.

[104] "DIN EN 1992-1-2:2010-12. Eurocode 2: Design of concrete structures - Part 1-2: General rules - Structural fire design. German version EN 1992-1-2:2004 + AC:2008." Berlin: Beuth Verlag, 2010.

[105] "ASCE Structural Fire Protection." ASCE Committee on Fire Protection, Structural Devision, American Society of Civil Engineers, 1992.

[106] A. Iravani and S. Anders, “Time dependent Mass Loss of UHPC after single and cyclic thermal Exposure,” presented at the 4th International Symposium on Ultra-High Performance Concrete and High Performance Construction Materials, Kassel, Germany, 2016.

[107] A. Iravani and S. Anders, “Effect of cement type, aggregate type and concrete age on the mass loss of concrete exposed to elevated temperature,” presented at the Proceedings of the 5th International Workshop on Concrete Spalling, Borås, Sweden, 2017.

[108] C. Peter, “Tragverhalten von Verkehrstunneln im Brandfall mit einer Innenschale aus PP-Faserbeton,” Bergische Universität Wuppertal, Wuppertal, Germany, 2017.

[109] “DIN EN 12390-3:2019-10 - Testing hardened concrete - Part 3: Compressive strength of test specimens.” Berlin: Beuth Verlag, 2019.

[110] “DIN EN 12390-6:2024-05 - Testing hardened concrete - Part 6: Tensile splitting strength of test specimens.” Berlin: Beuth Verlag, 2024.

[111] “ASTM C39: Standard test method for compressive strength of cylindrical concrete specimens.” American Society for Tesing Materials, 2017.

[112] “ASTM C496: Standard test method for splitting tensile strength of cylindrical concrete specimens.” American Society for Testing and Materials, 2017.

[113] “RILEM TC 200-HTC. Mechanical concrete properties at high temperature - modelling and applications; Recommendation: Part 1: Introduction - general presentation,” *Material and Construction*, vol. 40, pp. 841–853, 2007.

[114] “DIN EN 1994-1-2:2010-12. Eurocode 4: Design of composite steel and concrete structures – Part 1-2: General rules – Structural fire design.” Berlin: Beuth Verlag.

[115] Q. Ma, R. Guo, Z. Zhao, Z. Lin, and K. He, “Mechanical properties of concrete at high temperature—A review,” *Construction and Building Materials*, vol. 93, pp. 371–383, Sep. 2015, doi: 10.1016/j.conbuildmat.2015.05.131.

[116] M. Shahraki, N. Hua, N. Elhami-Khorasani, A. Tessari, and M. Garlock, “Residual compressive strength of concrete after exposure to high temperatures: A review and probabilistic models,” *Fire Safety Journal*, vol. 135, p. 103698, Feb. 2023, doi: 10.1016/j.firesaf.2022.103698.

[117] J. Nilimaa and R. Nilforoush, “A direct tensile strength testing method for concrete from existing structures,” *CivilEng*, vol. 4, no. 1, Art. no. 1, Mar. 2023, doi: 10.3390/civileng4010019.

[118] Mohd. Ahmed, J. Mallick, and Mohd. Abul Hasan, “A study of factors affecting the flexural tensile strength of concrete,” *Journal of King Saud University - Engineering Sciences*, vol. 28, no. 2, pp. 147–156, Jul. 2016, doi: 10.1016/j.jksues.2014.04.001.

[119] A. P. Bennur, C. Kumar, and N. Kumar, “Effect of fly-ash on the mechanical properties and workability of light weight concrete,” *International Advanced Research Journal in Science, Engineering and Technology*, vol. 9, no. 7, pp. 227–235, 2022.

[120] Y. Wang, F. Nejati, S. A. Edalatpanah, and R. Goudarzi Karim, “Experimental study to compare the strength of concrete with different amounts of polypropylene fibers at high temperatures,” *Sci Rep*, vol. 14, no. 1, p. 8566, Apr. 2024, doi: 10.1038/s41598-024-59084-6.

[121] V. K. R. Kodur, S. Banerji, and R. Solhmirzaei, “Test methods for characterizing concrete properties at elevated temperature,” *Fire and Materials*, vol. 44, no. 3, pp. 381–395, 2020, doi: 10.1002/fam.2777.

[122] S. Narayanan, “Elastic modulus of concrete,” *CE&CR*, 2021.

[123] G. A. Khoury, “Strain of heated concrete during two thermal cycles. Part 2: strain during first cooling and subsequent thermal cycle,” *Magazine of Concrete Research*, vol. 58, no. 6, pp. 387–400, Aug. 2006, doi: 10.1680/macr.2006.58.6.387.

[124] H. Zeng *et al.*, “Deterioration of performances and structures of cement pastes under the action of thermal cycling fatigue,” *International Journal of Fatigue*, vol. 165, p. 107181, Dec. 2022, doi: 10.1016/j.ijfatigue.2022.107181.

[125] H. S. Davis, “Aggregate for radiation shielding concrete,” *Materials Research Standards*, vol. 7, no. 11, pp. 494–501, 1967.

[126] M. S. Khan, S. Almutairi, and H. Abbas, “Mechanical properties of concrete subjected to cyclic thermal loading,” *European Journal of Environmental and Civil Engineering*, May 2022, Accessed: Dec. 28, 2024. [Online]. Available: https://www.tandfonline.com/doi/abs/10.1080/19648189.2020.1782771

[127] M. S. Khan and J. Prasad, “Fly ash concrete subjected to thermal cyclic loads,” *Fatigue & Fracture of Engineering Materials & Structures*, vol. 33, no. 5, pp. 276–283, 2010, doi: 10.1111/j.1460-2695.2010.01438.x.

[128] L. Boquera *et al.*, “Thermal and mechanical performance of cement paste under high temperature thermal cycles,” *Solar Energy Materials and Solar Cells*, vol. 231, p. 111333, Oct. 2021, doi: 10.1016/j.solmat.2021.111333.

[129] C. Tao, L. Dong, W. Fan, and T. Yu, “Experimental Study on the Compressive Strength and Fatigue Life of Cement Concrete under Temperature Differential Cycling,” *Materials*, vol. 16, no. 23, Art. no. 23, Jan. 2023, doi: 10.3390/ma16237487.

[130] M. M. Hossain, S. Al-Deen, S. K. Shill, and M. K. Hassan, “Resistance of concrete with various types of coarse aggregate to coupled effects of thermal shocks and chemicals,” *Materials*, vol. 17, no. 4, Art. no. 4, Jan. 2024, doi: 10.3390/ma17040791.

[131] H. Zeng *et al.*, “Performance evolution of low heat cement under thermal cycling fatigue: A comparative study with moderate heat cement and ordinary Portland cement,” *Construction and Building Materials*, vol. 412, p. 134863, Jan. 2024, doi: 10.1016/j.conbuildmat.2024.134863.

[132] S. Hassen and H. Colina, “Effect of a heating–cooling cycle on elastic strain and Young’s modulus of high performance and ordinary concrete,” *Mater Struct*, vol. 45, no. 12, pp. 1861–1875, Dec. 2012, doi: 10.1617/s11527-012-9875-5.

[133] A. C. P. Martins *et al.*, “Steel slags in cement-based composites: An ultimate review on characterization, applications and performance,” *Construction and Building Materials*, vol. 291, p. 123265, Jul. 2021, doi: 10.1016/j.conbuildmat.2021.123265.

[134] J. W. Lim, L. H. Chew, T. S. Choong, C. Tezara, and M. H. Yazdi, “Overview of steel slag application and utilization,” in *MATEC Web of Conferences*, Les Ulis, France: EDP Sciences, 2016. doi: 10.1051/matecconf/20167400026.

[135] “Demand for iron slag to remain high in 2020,” FEHS BUILDING MATERIALS INSTITUTE. [Online]. Available: https://www.zkg.de/en/artikel/zkg_Demand_for_iron_slag_to_remain_high_in_2020_-3697077.html

[136] S. K. Tripathy, J. Dasu, Y. R. Murthy, G. Kapure, A. R. Pal, and L. O. Filippov, “Utilisation perspective on water quenched and air-cooled blast furnace slags,” *Journal of Cleaner Production*, vol. 262, p. 121354, Jul. 2020, doi: 10.1016/j.jclepro.2020.121354.

[137] J. Liao, G. Qing, and B. Zhao, “Phase equilibrium studies of the CaO-MgO-Al2O3-SiO2 system for Iron blast furnace slag: a review,” *Metals*, vol. 13, no. 4, Art. no. 4, Apr. 2023, doi: 10.3390/met13040801.

[138] P. Z. Wang, R. Trettin, and V. Rudert, “Effect of fineness and particle size distribution of granulated blast-furnace slag on the hydraulic reactivity in cement systems,” *Advances in Cancer Research*, vol. 17, no. 4, pp. 161–167, 2005.

[139] Z. Li, S. Zhao, X. Zhao, T. He, and M. Yan, “Selective dissolution and cementitious property evaluation of converter steel slag,” *Mater Struct*, vol. 46, no. 1, pp. 327–336, Jan. 2013, doi: 10.1617/s11527-012-9904-4.

[140] J. I. Escalante, L. Y. Gómez, K. K. Johal, G. Mendoza, H. Mancha, and J. Méndez, “Reactivity of blast-furnace slag in Portland cement blends hydrated under

different conditions," *Cement and Concrete Research*, vol. 31, no. 10, pp. 1403–1409, Oct. 2001, doi: 10.1016/S0008-8846(01)00587-7.

[141] "DIN EN 15167-1:2006-12. Ground granulated blast furnace slag for use in concrete, mortar, and grout – Part 1: Definitions, specifications, and conformity criteria." Berlin: Beuth Verlag, 2006.

[142] "DIN EN 15167-2:2006-12. Ground granulated blast furnace slag for use in concrete, mortar, and grout – Part 2: Conformity evaluation." Berlin: Beuth Verlag, 2006.

[143] A. Klemm, R. Rostami, S. MacLennan, and F. Almeida, "Supplementary cementitious materials and their impact on sustainable construction," 2021. Accessed: Apr. 05, 2025. [Online]. Available: https://www.semanticscholar.org/paper/Supplementary-cementitious-materials-and-their-on-Klemm-Rostami/3cce67d93c907033abc3a2bd125a6e4cd3ae330c

[144] R. Karsten, *Bauchemie: Handbuch für Studium und Praxis*. Karlsrüher, Germany: Verlag C.F. Müller, 1992.

[145] B. Lothenbach, K. Scrivener, and R. D. Hooton, "Supplementary cementitious materials," *Cement and Concrete Research*, vol. 41, no. 12, pp. 1244–1256, Dec. 2011, doi: 10.1016/j.cemconres.2010.12.001.

[146] "DIN EN 197-1:2011-11. Cement – Part 1: Composition, specifications and conformity criteria for common cements." Berlin: Beuth Verlag, 2011.

[147] O. A. Mohamed, "A review of durability and strength characteristics of alkali-activated slag concrete," *Materials*, vol. 12, no. 8, Art. no. 8, Jan. 2019, doi: 10.3390/ma12081198.

[148] Y. Zhang, S. Zhang, Y. Chen, and O. Çopuroğlu, "The effect of slag chemistry on the reactivity of synthetic and commercial slags," *Construction and Building Materials*, vol. 335, p. 127493, Jun. 2022, doi: 10.1016/j.conbuildmat.2022.127493.

[149] W. Czernin, *Zementchemie für Bauingenieure*. Bauverlag, 1997.

[150] O. Henning, D. Knöfel, and D. Stephan, *Baustoffchemie: Eine Einführung für Bauingenieure und Architekten*. DIN e.v., 2013.

[151] S. C. Pal, A. Mukherjee, and S. R. Pathak, "Investigation of hydraulic activity of ground granulated blast furnace slag in concrete," *Cement and Concrete Research*, vol. 33, no. 9, pp. 1481–1486, Sep. 2003, doi: 10.1016/S0008-8846(03)00062-0.

[152] M. Behim, M. Beddar, and P. Clastres, "Reactivity of granulated blast furnace slag," *Slovak Journal of Civil Engineering*, vol. 21, no. 2, pp. 7–14, 2013.

[153] F. Keil, “Slag cements,” presented at the Third International Symposium on the Chemistry of Cements, London, United Kingdom: Cement and Concrete Association, 1952, pp. 530–571.

[154] J. Li *et al.*, “Mechanical activation of medium basicity steel slag under dry condition for carbonation curing,” *Journal of Building Engineering*, vol. 50, p. 104123, Jun. 2022, doi: 10.1016/j.jobe.2022.104123.

[155] William J. Johnson, “The effect of chemical composition of blast-furnace slag on compressive strength and durability properties of mortar specimens,” University of South Florida, Florida, United States, 2017.

[156] S. Kumar *et al.*, “Mechanical activation of granulated blast furnace slag and its effect on the properties and structure of portland slag cement,” *Cement and Concrete Composites*, vol. 30, no. 8, pp. 679–685, Sep. 2008, doi: 10.1016/j.cemconcomp.2008.05.005.

[157] A. Bougara, C. Lynsdale, and N. B. Milestone, “Reactivity and performance of blastfurnace slags of differing origin,” *Cement and Concrete Composites*, vol. 32, no. 4, pp. 319–324, Apr. 2010, doi: 10.1016/j.cemconcomp.2009.12.002.

[158] Y. Zhou and Z. Zhang, “Effect of fineness on the pozzolanic reaction kinetics of slag in composite binders: Experiment and modelling,” *Construction and Building Materials*, vol. 273, p. 121695, Mar. 2021, doi: 10.1016/j.conbuildmat.2020.121695.

[159] J. Dong-geun and S. Lee, “The effect of Pozzolanic reaction under different curing temperatures in strength development of RPC,” presented at the International Conference for Sustainable Building Asia, Bilbao, Spain, 2010.

[160] B. G. Diaz and F. M. Benavides, “Environmental and qualitative benefits of supplementary cementitious materials,” PEC Consulting Group. Accessed: Apr. 06, 2025. [Online]. Available: https://pecconsultinggroup.com/environmental-and-qualitative-benefits-of-supplementary-cementitious-materials/

[161] H. Beushausen, M. Alexander, and Y. Ballim, “Early-age properties, strength development and heat of hydration of concrete containing various South African slags at different replacement ratios,” *Construction and Building Materials*, vol. 29, pp. 533–540, Apr. 2012, doi: 10.1016/j.conbuildmat.2011.06.018.

[162] A. Oner and S. Akyuz, “An experimental study on optimum usage of GGBS for the compressive strength of concrete,” *Cement and Concrete Composites*, vol. 29, no. 6, pp. 505–514, Jul. 2007, doi: 10.1016/j.cemconcomp.2007.01.001.

[163] K. Abdelli, M. Tahlaiti, R. Belarbi, and M. N. Oudjit, “Influence of the pozzolanic reactivity of the Blast Furnace Slag (BFS) and metakaolin on mortars,” *Energy Procedia*, vol. 139, pp. 224–229, Dec. 2017, doi: 10.1016/j.egypro.2017.11.200.

[164] T. Ayano and T. Fujii, “Improvement of concrete properties using granulated blast furnace slag sand,” *Journal of Advanced Concrete Technology*, vol. 19, no. 2, pp. 118–132, Feb. 2021, doi: 10.3151/jact.19.118.

[165] T. V. Reshma, C. Kumar Patnaikuni, H. M. Tanu, and A. Bharath, “Evaluation of strength, durability, and microstructure characteristics of slag-sand-induced concrete,” *Cleaner Materials*, vol. 10, p. 100212, Dec. 2023, doi: 10.1016/j.clema.2023.100212.

[166] H.-S. Lee, X.-Y. Wang, L.-N. Zhang, and K.-T. Koh, “Analysis of the optimum usage of slag for the compressive strength of concrete,” *Materials*, vol. 8, no. 3, Art. no. 3, Mar. 2015, doi: 10.3390/ma8031213.

[167] “Use of air-cooled blast furnace slag as coarse aggregate in concrete pavements.” US Department of Transportation, Federal Highway Adminstration, 2012. [Online]. Available: chrome-extension://efaidnbmnnnibpcajpcglclefindmkaj/https://www.fhwa.dot.gov/pavement/concrete/pubs/hif12031.pdf

[168] T. Mayamoto, T. Koichi, K. Akahane, and S. Hayashiguchi, “Production and use of blast furnace slag aggregate for concrete,” *Nippon Steel and Sumitomo Metal Technical Report*, vol. 109, pp. 102–108, 2015.

[169] “DIN EN 12620:2013-07. Aggregates for concrete.” Berlin: Beuth Verlag, 2013.

[170] P. Panchmatia, J. Olek, and T. Kim, “The influence of air cooled blast furnace slag (ACBFS) aggregate on the concentration of sulfates in concrete’s pore solution,” *Construction and Building Materials*, vol. 168, pp. 394–403, Apr. 2018, doi: 10.1016/j.conbuildmat.2018.02.133.

[171] I. Yuksel, O. Ozkan, and T. Bilir, “Use of granulated blast-furnace slag in concrete as fine aggregate,” *Materials Journal*, vol. 103, no. 3, pp. 203–208, 2006.

[172] T. Ozbakkaloglu, L. Gu, and A. Fallah Pour, “Normal- and high-strength concretes incorporating air-cooled blast furnace slag coarse aggregates: Effect of slag size and content on the behavior,” *Construction and Building Materials*, vol. 126, pp. 138–146, Nov. 2016, doi: 10.1016/j.conbuildmat.2016.09.015.

[173] S. P. Kanniyappan and S. Saravanakumar, “Use of air cooled blast furnace slag as a sustainable material in cement concrete,” *International Journal of Innovative Research and Studies*, vol. 8, no. 4, pp. 545–558, 2018.

[174] Q. Cao, U. Nawaz, X. Jiang, L. Zhang, and W. S. Ansari, “Effect of air-cooled blast furnace slag aggregate on mechanical properties of ultra-high-performance concrete,” *Case Studies in Construction Materials*, vol. 16, p. e01027, Jun. 2022, doi: 10.1016/j.cscm.2022.e01027.

[175] J. Shi, J. Tan, B. Liu, J. Chen, J. Dai, and Z. He, "Experimental study on full-volume slag alkali-activated mortars: Air-cooled blast furnace slag versus machine-made sand as fine aggregates," *Journal of Hazardous Materials*, vol. 403, p. 123983, Feb. 2021, doi: 10.1016/j.jhazmat.2020.123983.

[176] J. D. Ríos, A. Vahí, C. Leiva, A. Martínez-De la Concha, and H. Cifuentes, "Analysis of the utilization of air-cooled blast furnace slag as industrial waste aggregates in self-compacting concrete," *Sustainability*, vol. 11, no. 6, Art. no. 6, Jan. 2019, doi: 10.3390/su11061702.

[177] Z. Li, L. Li, J. Wang, and X. Wu, "Effect of Elevated Temperature on Meso- and Micro-Structure and Compressive Strength of High-Strength Concrete and Mortar Containing Blast-Furnace Slag," *Journal of Advanced Concrete Technology*, vol. 16, no. 10, pp. 498–511, 2018, doi: 10.3151/jact.16.498.

[178] K. Weise, "Reaktivität von Hüttensand," in *Die Reaktivität von Hüttensand als Betonzusatzstoff: Eine thermogravimetrische Systemstudie*, K. Weise, Ed., Wiesbaden: Springer Fachmedien, 2018, pp. 47–82. doi: 10.1007/978-3-658-20492-1_6.

[179] I. G. Richardson, "The nature of the hydration products in hardened cement pastes," *Cement and Concrete Composites*, vol. 22, no. 2, pp. 97–113, Apr. 2000, doi: 10.1016/S0958-9465(99)00036-0.

[180] I. G. Richardson, "The calcium silicate hydrates," *Cement and Concrete Research*, vol. 38, no. 2, pp. 137–158, Feb. 2008, doi: 10.1016/j.cemconres.2007.11.005.

[181] Z. Shui, R. Zhang, W. Chen, and D. Xuan, "Effects of mineral admixtures on the thermal expansion properties of hardened cement paste," *Construction and Building Materials*, vol. 24, no. 9, pp. 1761–1767, Sep. 2010, doi: 10.1016/j.conbuildmat.2010.02.012.

[182] F. Delhomme, J. Ambroise, and A. Limam, "Effects of high temperatures on mortar specimens containing Portland cement and GGBFS," *Mater Struct*, vol. 45, no. 11, pp. 1685–1692, Nov. 2012, doi: 10.1617/s11527-012-9865-7.

[183] Ö. Andiç-Çakır, O. Çopuroğlu, and K. Ramyar, "Effect of High Temperature on Mechanical and Microstructural Properties of Cement Mortar," presented at the 11DBMC International Conference on Durability of Building Materials and Components, Istanbul, Turkey, 2008.

[184] C. Zemri and M. Bachir Bouiadjra, "Comparison between physical–mechanical properties of mortar made with Portland cement (CEMI) and slag cement (CEMIII) subjected to elevated temperature," *Case Studies in Construction Materials*, vol. 12, p. e00339, Jun. 2020, doi: 10.1016/j.cscm.2020.e00339.

[185] I. Hager, T. Tracz, M. Choińska, and K. Mróz, “Effect of cement type on the mechanical behavior and permeability of concrete subjected to high temperatures,” *Materials (Basel)*, vol. 12, no. 18, p. 3021, Sep. 2019, doi: 10.3390/ma12183021.

[186] G. G. Carette, K. E. Painter, and V. M. Malhotra, “Sustained high temperature effect on concretes made with normal Portland cement, normal Portland cement and slag, or normal Portland cement and fly ash,” *Concrete International*, vol. 4, no. 7, p. 16, 1982.

[187] H. Y. Wang, “The effects of elevated temperature on cement paste containing GGBFS,” *Cement and Concrete Composites*, vol. 30, no. 10, pp. 992–999, Nov. 2008, doi: 10.1016/j.cemconcomp.2007.12.003.

[188] S. Aydın, “Development of a high-temperature-resistant mortar by using slag and pumice,” *Fire Safety Journal*, vol. 43, no. 8, pp. 610–617, Nov. 2008, doi: 10.1016/j.firesaf.2008.02.001.

[189] S. Sim, J. H. Rhee, J.-E. Oh, and G. Kim, “Enhancing the durability performance of thermally damaged concrete with ground-granulated blast furnace slag and fly ash,” *Construction and Building Materials*, vol. 407, p. 133538, Dec. 2023, doi: 10.1016/j.conbuildmat.2023.133538.

[190] Hosam. E. H. Seleem, A. M. Rashad, and Tarek. Elsokary, “Effect of elevated temperature on physico-mechanical properties of blended cement concrete,” *Construction and Building Materials*, vol. 25, no. 2, pp. 1009–1017, Feb. 2011, doi: 10.1016/j.conbuildmat.2010.06.078.

[191] Q. Li, G. Yuan, Z. Xu, and T. Dou, “Effect of elevated temperature on the mechanical properties of high-volume GGBS concrete,” *Magazine of Concrete Research*, vol. 66, no. 24, pp. 1277–1285, 2014.

[192] Q. Li, Z. Li, and G. Yuan, “Effects of elevated temperatures on properties of concrete containing ground granulated blast furnace slag as cementitious material,” *Construction and Building Materials*, vol. 35, pp. 687–692, Oct. 2012, doi: 10.1016/j.conbuildmat.2012.04.103.

[193] A. Mendes, J. G. Sanjayan, and F. Collins, “Effects of slag and cooling method on the progressive deterioration of concrete after exposure to elevated temperatures as in a fire event,” *Mater Struct*, vol. 44, no. 3, pp. 709–718, Apr. 2011, doi: 10.1617/s11527-010-9660-2.

[194] R. Siddique and D. Kaur, “Properties of concrete containing ground granulated blast furnace slag (GGBFS) at elevated temperatures,” *Journal of Advanced Research*, vol. 3, no. 1, pp. 45–51, 2012, doi: 10.1016/j.jare.2011.03.004.

[195] H. Singh, A. Kumar Tiwary, and S. Singh, “Experimental investigation on the performance of ground granulated blast furnace slag and nano-silica blended concrete exposed to elevated temperature,” *Construction and Building Materials*, vol. 394, p. 132088, Aug. 2023, doi: 10.1016/j.conbuildmat.2023.132088.

[196] J. Xiao, M. Xie, and Ch. Zhang, “Residual compressive behaviour of pre-heated high-performance concrete with blast–furnace–slag,” *Fire Safety Journal*, vol. 41, no. 2, pp. 91–98, Mar. 2006, doi: 10.1016/j.firesaf.2005.11.001.

[197] P. J. E. Sullivan and R. Sharshar, “The performance of concrete at elevated temperatures (as measured by the reduction in compressive strength),” *Fire Technol*, vol. 28, no. 3, pp. 240–250, Aug. 1992, doi: 10.1007/BF01857693.

[198] V. D. Vaidya, V. Vaghese, and P. K. Morey, “Impact of elevated temperatures on properties of concrete with blast furnace slag as partial replacement of fine aggregate as green building material,” *IOP Conf. Ser.: Earth Environ. Sci.*, vol. 1193, no. 1, p. 012024, Jun. 2023, doi: 10.1088/1755-1315/1193/1/012024.

[199] İ. Yüksel, T. Bilir, and Ö. Özkan, “Durability of concrete incorporating non-ground blast furnace slag and bottom ash as fine aggregate,” *Building and Environment*, vol. 42, no. 7, pp. 2651–2659, Jul. 2007, doi: 10.1016/j.buildenv.2006.07.003.

[200] V. D. Vaidya, A. Badar, V. Varghese, and P. K. Morey, “Enhanced temperature effect on properties of concrete with partial replacement of coarse aggregate by blast furnace slag,” in *API Conference Proceedings*, Berlin, Germany, 2019.

[201] N. Ouffa, M. Benzaazoua, R. Trauchessec, T. Belem, Y. Taha, and C. Diliberto, “Potential reuse of ladle furnace slag as cementitious material: a literature review of generation, characterization, and processing methods,” *Minerals*, vol. 14, no. 12, Art. no. 12, Dec. 2024, doi: 10.3390/min14121204.

[202] D. Fernández-González, J. Prazuch, I. Ruiz-Bustinza, C. González-Gasca, J. Piñuela-Noval, and L. F. Verdeja, “The treatment of Basic Oxygen Furnace (BOF) slag with concentrated solar energy,” *Solar Energy*, vol. 180, pp. 372–382, Mar. 2019, doi: 10.1016/j.solener.2019.01.055.

[203] Q. Zhao, L. Pang, and D. Wang, “Adverse effects of using metallurgical slags as supplementary sementitious materials and aggregate: a review,” *Materials*, vol. 15, no. 11, Art. no. 11, Jan. 2022, doi: 10.3390/ma15113803.

[204] C. Shi, “Steel slag-its production, processing, characteristics, and cementatious properties,” *Journal of Materials in Civil Engineering*, vol. 16, no. 3, doi: https://doi.org/10.1061/(ASCE)0899-1561(2004)16:3(230).

[205] H. Motz and J. Geiseler, “Products of steel slags an opportunity to save natural resources,” *Waste Management*, vol. 21, no. 3, pp. 285–293, Jun. 2001, doi: 10.1016/S0956-053X(00)00102-1.

[206] M. Skaf, J. M. Manso, Á. Aragón, J. A. Fuente-Alonso, and V. Ortega-López, “EAF slag in asphalt mixes: A brief review of its possible re-use,” *Resources, Conservation and Recycling*, vol. 120, pp. 176–185, May 2017, doi: 10.1016/j.resconrec.2016.12.009.

[207] P. Araos, D. Aponte, and M. Barra, “Ladle furnace slag as a new source of supplementary cementitious material: Evaluating long-term performance and environmental impact in Portland cement systems,” *Journal of Building Engineering*, vol. 95, p. 109995, Oct. 2024, doi: 10.1016/j.jobe.2024.109995.

[208] A. Kärnä *et al.*, “Numerical modeling of argon-oxygen decarburization slag cooling,” *steel research international*, vol. 91, no. 11, p. 2000054, 2020, doi: 10.1002/srin.202000054.

[209] L. Jacob, “Ladle furnace slag: synthesis, properties, and applications,” *ChemBioEng Reviews*, vol. 11, no. 1, pp. 60–78, 2024, doi: 10.1002/cben.202300024.

[210] I. Z. Yildirim and M. Prezzi, “Chemical, mineralogical, and morphological properties of steel slag,” *Advances in Civil Engineering*, vol. 2011, no. 1, p. 463638, 2011, doi: 10.1155/2011/463638.

[211] I. Sultana and G. M. S. Islam, “Potential of ladle furnace slag as supplementary cementitious material in concrete,” *Case Studies in Construction Materials*, vol. 18, p. e02141, Jul. 2023, doi: 10.1016/j.cscm.2023.e02141.

[212] A. Santamaria *et al.*, “Ladle furnace slag as cement replacement in mortar mixes,” presented at the Fifth International Conference on Sustainable Construction Materials and Technologies, London, United Kingdom, 2019. Accessed: Apr. 06, 2025. [Online]. Available: https://dsp.tecnalia.com/items/1a3427d0-60a1-4b11-8f73-cf29ba88ed57

[213] M. Bodor, R. Santos, T. Gerven, and M. Vlad, “Recent developments and perspectives on the treatment of industrial wastes by mineral carbonation — a review,” *Open Engineering*, vol. 3, no. 4, pp. 566–584, Dec. 2013, doi: 10.2478/s13531-013-0115-8.

[214] G. Adegoloye, A.-L. Beaucour, S. Ortola, and A. Noumowe, “Mineralogical composition of EAF slag and stabilised AOD slag aggregates and dimensional stability of slag aggregate concretes,” *Construction and Building Materials*, vol. 115, pp. 171–178, Jul. 2016, doi: 10.1016/j.conbuildmat.2016.04.036.

[215] I. Papayianni and E. Anastasiou, “Optimization of ladle furnace slag for use as a supplementary cementing material,” in *Measuring, Monitoring and Modeling Concrete Properties*, M. S. KONSTA-GDOUTOS, Ed., Dordrecht: Springer Netherlands, 2006, pp. 411–417. doi: 10.1007/978-1-4020-5104-3_50.

[216] Z. Ren and D. Li, “Application of steel slag as an aggregate in concrete production: a review,” *Materials*, vol. 16, no. 17, Art. no. 17, Jan. 2023, doi: 10.3390/ma16175841.

[217] E. F. Mariano, G. J. Brigolini, V. A. A. Oliveira, J. L. Calmon, and E. F. Mariano, “Steel slag as a precursor material for alkali-activated binders: a systematic review.,” Oct. 11, 2022, *Preprints*: 2022100137. doi: 10.20944/preprints202210.0137.v1.

[218] M. Tossavainen, F. Engstrom, Q. Yang, N. Menad, M. Lidstrom Larsson, and B. Bjorkman, “Characteristics of steel slag under different cooling conditions,” *Waste Management*, vol. 27, no. 10, pp. 1335–1344, Jan. 2007, doi: 10.1016/j.wasman.2006.08.002.

[219] Q. Wang, P. Yan, J. Yang, and B. Zhang, “Influence of steel slag on mechanical properties and durability of concrete,” *Construction and Building Materials*, vol. 47, pp. 1414–1420, Oct. 2013, doi: 10.1016/j.conbuildmat.2013.06.044.

[220] K. Dhivya, G. Anusha, S. Vinoth, P. R. Shanjai, A. Sreedharan, and V. M. Rahuma, “Steel slag’s effect on concrete mechanical properties and durability,” *Materials Today: Proceedings*, May 2023, doi: 10.1016/j.matpr.2023.05.330.

[221] K. Fang, D. Wang, J. Zhao, and M. Zhang, “Utilization of ladle furnace slag as cement partial replacement: Influences on the hydration and hardening properties of cement,” *Construction and Building Materials*, vol. 299, p. 124265, Sep. 2021, doi: 10.1016/j.conbuildmat.2021.124265.

[222] P. Araos, A. Uribarri, M. Barra, and D. Aponte, “The effect of ladle furnace slag (LFS) content replacement as a supplementary cementitious material in Portland cement-based systems,” in *International RILEM Conference on Synergising Expertise towards Sustainability and Robustness of Cement-based Materials and Concrete Structures*, A. Jędrzejewska, F. Kanavaris, M. Azenha, F. Benboudjema, and D. Schlicke, Eds., Cham: Springer Nature Switzerland, 2023, pp. 76–87. doi: 10.1007/978-3-031-33187-9_8.

[223] Q. Li, B. Li, X. Li, Z. He, and P. Zhang, “Microstructure of pretreated steel slag and its influence on mechanical properties of cement stabilized mixture,” *Construction and Building Materials*, vol. 317, p. 125799, Jan. 2022, doi: 10.1016/j.conbuildmat.2021.125799.

[224] s. P. Palanisamy, G. Maheswaran, M. G. L. Annaamalai, and P. Vennila, “Steel slag to improve the high strength of concrete,” *International Journal of ChemTech Research*, vol. 7, no. 5, pp. 2499–2505, 2015.

[225] B. Yuan, D. Zhao, J. Lei, and S. Song, “Preparation and performance testing of steel slag concrete from steel solid waste,” *Buildings*, vol. 14, no. 8, Art. no. 8, Aug. 2024, doi: 10.3390/buildings14082437.

[226] T. B. Mekonen, T. E. Alene, Y. A. Alem, and W. M. Nebiyu, “Influence of steel slag as a partial replacement of aggregate on performance of reinforced concrete beam,” *Int J Concr Struct Mater*, vol. 18, no. 1, p. 56, Aug. 2024, doi: 10.1186/s40069-024-00698-5.

[227] M. E. Mitwally, A. Elnemr, A. Shash, and A. Babiker, “Utilization of steel slag as partial replacement for coarse aggregate in concrete,” *Innov. Infrastruct. Solut.*, vol. 9, no. 5, p. 175, May 2024, doi: 10.1007/s41062-024-01464-y.

[228] R. Karolina and A. L. A. Putra, “The effect of steel slag as a coarse aggregate and Sinabung volcanic ash a filler on high strength concrete,” *IOP Conf. Ser.: Mater. Sci. Eng.*, vol. 309, no. 1, p. 012009, Feb. 2018, doi: 10.1088/1757-899X/309/1/012009.

[229] D. S. Mahajan and S. Muhammad, “Assessment of the viability of pozzolanic activity of copper slag for use as supplementary cementitious material in ordinary Portland cement,” *Journal of Building Engineering*, vol. 83, p. 108375, Apr. 2024, doi: 10.1016/j.jobe.2023.108375.

[230] M. Penpolcharoen, “Utilization of secondary lead slag as construction material,” *Cement and Concrete Research*, vol. 35, no. 6, pp. 1050–1055, Jun. 2005, doi: 10.1016/j.cemconres.2004.11.001.

[231] Y. He, Q. Chen, Q. Kang, M. Lan, and R. Yang, “Effect of enhanced pozzolanic activity in nickel slag modified with Al2O3 on mechanical properties of cemented fine tailings backfill,” *Construction and Building Materials*, vol. 411, p. 134610, Jan. 2024, doi: 10.1016/j.conbuildmat.2023.134610.

[232] T. Kontan, Ö. F. Özbey, and M. Ardahanli, “Investigation of pozzolanic activity of mortars with waste zinc slag powder admixture for long curing times,” presented at the 8th International Zeugma Conference of Scientific Research, Gaziantep, Turkey, 2022.

[233] A. Gholizadeh Vayghan *et al.*, “Use of treated non-ferrous metallurgical slags as supplementary cementitious materials in cementitious mixtures,” *Applied Sciences*, vol. 11, no. 9, Art. no. 9, Jan. 2021, doi: 10.3390/app11094028.

[234] L. Mussapyrova, R. Nadirov, P. Baláž, M. Rajňák, R. Bureš, and M. Baláž, “Selective room-temperature leaching of copper from mechanically activated copper

smelter slag," *Journal of Materials Research and Technology*, vol. 12, pp. 2011–2025, May 2021, doi: 10.1016/j.jmrt.2021.03.090.

[235] V. Hallet, N. De Belie, and Y. Pontikes, "The impact of slag fineness on the reactivity of blended cements with high-volume non-ferrous metallurgy slag," *Construction and Building Materials*, vol. 257, p. 119400, Oct. 2020, doi: 10.1016/j.conbuildmat.2020.119400.

[236] M. A. Gómez-Casero, S. Bueno-Rodríguez, E. Castro, and D. Eliche Quesada, "Alkaline activated cements obtained from ferrous and non-ferrous slags. Electric arc furnace slag, ladle furnace slag, copper slag and silico-manganese slag," *Cement and Concrete Composites*, vol. 147, p. 105427, Mar. 2024, doi: 10.1016/j.cemconcomp.2023.105427.

[237] I. Sims, J. Lay, and J. Ferrari, "Concrete aggregates," in *Lea's Chemistry of Cement and Concrete (Fifth Edition)*, P. C. Hewlett and M. Liska, Eds., Butterworth-Heinemann, 2019, pp. 699–778. doi: 10.1016/B978-0-08-100773-0.00015-0.

[238] L. Boquera, J. R. Castro, A. G. Fernandez, A. Navarro, A. L. Pisello, and L. F. Cabeza, "Thermo-mechanical stability of concrete containing steel slag as aggregate after high temperature thermal cycles," *Solar Energy*, vol. 239, pp. 59–73, Jun. 2022, doi: 10.1016/j.solener.2022.04.062.

[239] A. K. Saha, P. K. Sarker, and V. Golovanevskiy, "Thermal properties and residual strength after high temperature exposure of cement mortar using ferronickel slag aggregate," *Construction and Building Materials*, vol. 199, pp. 601–612, Feb. 2019, doi: 10.1016/j.conbuildmat.2018.12.068.

[240] T. J. Barrett, H. Sun, T. Nantung, and W. J. Weiss, "Performance of Portland limestone cements," *Transportation Research Record*, vol. 2441, no. 1, pp. 112–120, Jan. 2014, doi: 10.3141/2441-15.

[241] B. Lothenbach, G. Le Saout, E. Gallucci, and K. Scrivener, "Influence of limestone on the hydration of Portland cements," *Cement and Concrete Research*, vol. 38, no. 6, pp. 848–860, Jun. 2008, doi: 10.1016/j.cemconres.2008.01.002.

[242] J. Li, S. Li, M. Aminul Haque, and B. Chen, "Water-resistance performance analysis of Portland composite concrete containing waterproofing liquid membrane," *Journal of Building Engineering*, vol. 76, p. 106889, Oct. 2023, doi: 10.1016/j.jobe.2023.106889.

[243] Ľ. Ježo, T. Ifka, B. Cvopa, J. Škundová, V. Kovár, and M. T. Palou, "Effect of temperature upon the strength development rate and upon the hydration kinetics of cements," *Cermaics-Silikaty*, vol. 54, no. 3, pp. 269–276, 2010.

[244] A. Gardiner, “Portland limestone cement: seven frequently asked questions about the new low-carbon option,” Braun InterTech. [Online]. Available: https://braunintertec.com/insights/portland-limestone-cement-seven-frequently-asked-questions-about-the-new-low-carbon-option/

[245] F. Lollini, E. Redaelli, and L. Bertolini, “Effects of portland cement replacement with limestone on the properties of hardened concrete,” *Cement and Concrete Composites*, vol. 46, pp. 32–40, Feb. 2014, doi: 10.1016/j.cemconcomp.2013.10.016.

[246] “Blended cements and sustainability of concrete construction,” Portland Cement Association. [Online]. Available: https://www.cement.org/a-sustainable-future/reaching-our-goal/blended-cements/#:~:text=For%20portland%2Dlimestone%20cements%20(PLC,portland%20cement%20in%20concrete%20mixtures)

[247] E. Klingsch, A. Frangi, and M. Fontana, “Experimental analysis of concrete strength at high temperatures and after cooling,” *Acta Polytechnica*, vol. 49, no. 1, Art. no. 1, Jan. 2009, doi: 10.14311/1087.

[248] Z. Adel Mohammed, R. Burhan Abdurrahman, and D. Abdul Hakeem Hamed Ahmad, “Influence of limestone powder as partial replacement of cement on concrete and the effect of high temperature on It,” *Al-Rafidain Engineering Journal (AREJ)*, vol. 18, no. 5, pp. 24–34, Oct. 2010, doi: 10.33899/rengj.2010.32863.

[249] A. A. El-Kurdi, A. Abdel-Hakam, and M. M. El-Gohary, “Impact of elevated temperatures on properties of limestone concrete,” *International Journal of Innovative Technology and Exploring Engineering*, vol. 4, no. 4, pp. 1–9, 2014.

[250] T. Uygunoğlu and İ. Bekir Topçu, “Effect of Limestone Powder on High Temperature Resistance of Self-Consolidating Micro-Concrete,” in *ResearchGate*, Kyoto, Japan, 2013. Accessed: Dec. 25, 2024. [Online]. Available: https://www.researchgate.net/publication/262529249_Effect_of_Limestone_Powder_on_High_Temperature_Resistance_of_Self-Consolidating_Micro-Concrete_Tayfun_Uygunoglu_Ilker_Bekir_Topcu_SCMT3_International_Conference_on_Sustainable_Construction_Materials_T

[251] A. E. Ahmed, A. H. Al-Shaikh, and T. I. Afrat, “Residual compressive and bond strengths of limestone aggregate concrete subjected to elevated temperatures,” *Magazine of Concrete Research*, vol. 33, no. 159, pp. 117–125, 1992.

[252] İ. Bekem Kara, “Effects of cooling regimes on limestone rock and concrete with limestone aggregates at elevated temperatures,” *International Journal of Rock Mechanics and Mining Sciences*, vol. 138, p. 104618, Feb. 2021, doi: 10.1016/j.ijrmms.2021.104618.

[253] M. Tufail, S. Khan, B. Gencturk, and J. Wei, “Effect of elevated temperature on mechanical properties of limestone, quartzite and granite concrete,” *International Journal of Concrete Structures and Materials*, vol. 11, pp. 17–28, 2017.

[254] V. M. Roitman, “Consideration of real fire conditions while calculating the fire resistance of building structures on the basis of the kinetic approach,” *Fire Safety Journal*, vol. 16, no. 6, pp. 433–442, Jan. 1990, doi: 10.1016/0379-7112(90)90020-F.

[255] F. Wald, J. Chlouba, A. Uhlíř, P. Kallerová, and M. Štujberová, “Temperatures during fire tests on structure and its prediction according to Eurocodes,” *Fire Safety Journal*, vol. 44, no. 1, pp. 135–146, Jan. 2009, doi: 10.1016/j.firesaf.2008.05.002.

[256] RILEM 129MHT, “Compressive strength for service and accident conditions,” *Materials and Structures*, vol. 28, no. 7, pp. 410–414, Aug. 1995, doi: 10.1007/BF02473077.

[257] S. Anders, “Comparison of Residual Strengths of Concretes with quartzite, limestone and slag sand constituents after cyclic high-temperature exposure,” presented at the International Conference on Concrete Repair, Rehabilitation and Retrofitting, Leipzig, Germany, 2015.

[258] M. Saravanja, W. Klingsch, and S. Anders, “Effects of different Fibre Materials and Quantities on High Temperature Strength and Explosive Spalling of UHPC.,” in *Proceedings of the 2nd International RILEM Workshop on Concrete Spalling due to Fire Exposure*, Delft, The Netherlands, 2011.

[259] O. Arioz, “Retained properties of concrete exposed to high temperatures: Size effect,” *Fire and Materials*, vol. 33, no. 5, pp. 211–222, 2009, doi: 10.1002/fam.996.

[260] M. Malik, S. K. Bhattacharyya, and S. V. Barai, “Thermal and mechanical properties of concrete and its constituents at elevated temperatures: A review,” *Construction and Building Materials*, vol. 270, p. 121398, Feb. 2021, doi: 10.1016/j.conbuildmat.2020.121398.

[261] M. Hafez, M. Kassab, and S. Taha, “Calcination process and kinetic carbonation effect on the hydrated and anhydrate phases of the OPC matrix at early age of hydration,” *HBRC Journal*, Jan. 2021, Accessed: Dec. 25, 2024. [Online]. Available: https://www.tandfonline.com/doi/abs/10.1080/16874048.2021.1944735

[262] I. S. Kishore, L.Mounika, and C. M. Prasad, “Experimental Study on the Use of Basalt Aggregate in Concrete Mixes,” *International Journal of Civil Engineering*, vol. Volume 2, no. 4, pp. 37–40, Jan. 2019, doi: 10.14445/23488352/IJCE-V2I4P107.

[263] “DIN EN 12620:2013-07, Aggregates for concrete; German version EN 12620:2013.” Berlin: Beuth Verlag, 2013.

[264] “DIN 4301:2009-06. Ferrous and non-ferrous metallurgical slag for civil engineering and building construction use.” Berlin: Beuth Verlag, 2009.

[265] “DATAtab: Online statistics calculator,” Full factorial design. [Online]. Available: https://datatab.net

[266] A. Ehrenberg and S. Anders, “Verwendung von Eisenhüttenschlacken zur Steigerung des Hochtemperaturwiderstands zementgebundener Bauprodukte,” Duisburg, Schlussbericht zum IGF-Vorhaben Nr. 20318, 2021.

[267] “DIN 1045-2:2023-08. Concrete, reinforced and prestressed concrete structures – Part 2: Concrete – Specification, properties, production, and conformity.” Berlin: Beuth Verlag, 2023.

[268] “DIN EN 12350:2019-09- Testing fresh concrete.” Berlin: Beuth Verlag, 2019.

[269] “DIN EN 196-1:2016-11. Methods of testing cement – Part 1: Determination of strength.” European Committee for Standardization (CEN), 2016.

[270] “DIN EN 1015-10:2007-05. Methods of test for mortar for masonry – Part 10: Determination of dry bulk density of hardened mortar (includes Amendment A1:2006).” European Committee for Standardization (CEN), 2007.

[271] S. Krishna Priya Rao and T. Tadepalli, “High-Temperature Behaviour of Concrete: A Review,” in *Low Carbon Materials and Technologies for a Sustainable and Resilient Infrastructure*, R. K. Pancharathi, C. K. Y. Leung, and J. M. Chandra Kishen, Eds., Singapore: Springer Nature, 2024, pp. 167–186. doi: 10.1007/978-981-99-7464-1_13.

[272] S. Stephant, L. Chomat, A. Nonat, and T. Charpentier, “Influence of the slag content on the hydration of blended cement,” in *ResearchGate*, Beijing, China, 2015. Accessed: Dec. 26, 2024. [Online]. Available: https://www.researchgate.net/publication/280740798_Influence_of_the_slag_content_on_the_hydration_of_blended_cement

[273] G. J. Osborne, “Durability of Portland blast-furnace slag cement concrete,” *Cement and Concrete Composites*, vol. 21, no. 1, pp. 11–21, Jan. 1999, doi: 10.1016/S0958-9465(98)00032-8.

[274] “DIN EN 206:2021-06-Specification, performance, production and conformity.” Berlin: Beuth Verlag.

[275] L. Shuo, W. Zheng, X. Hou, and Y. Wang, “Research on the residual compressive properties of concrete with preload after sustained high temperatures,” *Structures*, vol. 65, p. 106764, 2024, doi: 10.1016/j.istruc.2024.106764.

[276] S. Liu, W. Zheng, Y. Wang, Z. Yu, H. Zhang, and S. Li, “Comparative study on the compressive performance of NSC and HSC with preload under 24-hour high

temperatures," *Construction and Building Materials*, vol. 443, p. 137658, Sep. 2024, doi: 10.1016/j.conbuildmat.2024.137658.

[277] C. T. Nguyen, P. N. Pham, H. P. Nam, and C. D. Le, "Evaluating potential expansion and strength of compacted steel slag aggregates at different compaction density," *IOP Conf. Ser.: Mater. Sci. Eng.*, vol. 1289, no. 1, p. 012072, Aug. 2023, doi: 10.1088/1757-899X/1289/1/012072.

[278] V. Ducman and A. Mladenovič, "The potential use of steel slag in refractory concrete," *Materials Characterization*, vol. 62, no. 7, pp. 716–723, Jul. 2011, doi: 10.1016/j.matchar.2011.04.016.

[279] J. Xiao and H. Falkner, "On residual strength of high-performance concrete with and without polypropylene fibres at elevated temperatures," *Fire Safety Journal*, vol. 41, no. 2, pp. 115–121, Mar. 2006, doi: 10.1016/j.firesaf.2005.11.004.

[280] Y. Xu, Y. L. Wong, C. S. Poon, and M. Anson, "Impact of high temperature on PFA concrete," *Cement and Concrete Research*, vol. 31, no. 7, pp. 1065–1073, Jul. 2001, doi: 10.1016/S0008-8846(01)00513-0.

[281] Verein Deutscher Zementwerke e.V., *Zement Taschenbuch*, 51st ed. Düsseldorf, Germany: Verlag Bau+ Technik GmbH, 2008.

[282] Y. N. Chan, G. F. Peng, and M. Anson, "Residual strength and pore structure of high-strength concrete and normal strength concrete after exposure to high temperatures," *Cement and Concrete Composites*, vol. 21, no. 1, pp. 23–27, Jan. 1999, doi: 10.1016/S0958-9465(98)00034-1.

[283] S. Y. N. Chan, G. Peng, and J. K. W. Chan, "Comparison between high strength concrete and normal strength concrete subjected to high temperature," *Mat. Struct.*, vol. 29, no. 10, pp. 616–619, Dec. 1996, doi: 10.1007/BF02485969.

[284] S. Barbhuiya, T. Lo, S. Memon, and H. Nikraz, "Strength Recovery of Lightweight Concrete under Elevated Temperature," *Advanced Materials Research*, vol. 905, pp. 300–305, 2014, doi: 10.4028/www.scientific.net/AMR.905.300.

[285] A. Ehrenberg, "Hüttensand - Ein leistungsfähiger Baustoff mit Tradition und Zukunft," *Beton Information 4*, pp. 35–63, 2006.

[286] Y. Qian, D. Yang, M. Liu, Z. Guo, Z. Xiao, and Z. Ma, "Performance recovery of high-temperature damaged ultra-high-performance concrete under different curing environments," *Developments in the Built Environment*, vol. 16, p. 100274, Dec. 2023, doi: 10.1016/j.dibe.2023.100274.

[287] A. Iravani, M. Saravanja, and S. Anders, "Mass Loss and Porosity Development of various Concrete Mixtures at High-Temperatures.," presented at the 4th International Workshop on Concrete Spalling due to Fire Exposure (IWCS), Leipzig, Germany, 2015.

[288] A. Iravani and S. Anders, “Explosive spalling of UHPC - Evaluating spalling risk by mass loss measurement at high temperatures,” in *5th International Workshop on Concrete Spalling (IWCS)*, Borås, Sweden, 2017.

[289] M. Lundgern, “Limestone Filler as Addition in Cement Mortars: Influence on the Early-Age Strength Development at Low Temperature,” *Nordic Concrete Research*, vol. 31, 2004, Accessed: Dec. 29, 2024. [Online]. Available: https://www.researchgate.net/publication/228512666_Limestone_Filler_as_Addition_in_Cement_Mortars_Influence_on_the_Early-Age_Strength_Development_at_Low_Temperature

[290] J. Lyzwa and J. Zehfuß, “Ableitung von thermischen Materialkennwerten für Beton unter Naturbrandbeanspruchung anhand von experimentellen Untersuchungen,” *Beton- und Stahlbetonbau*, vol. 115, no. 5, pp. 392–401, 2020, doi: DOI: 10.1002/best.201900079.

[291] W. Klingsch and D. Toris, “Complete temperature history of structural elements – The key to quantifi-cation of residual safety of concrete structures after fire,” presented at the Advanced Research Workshop “Fire Computer Modeling,” Santander, Spain, 2007.

[292] Industry guidelines: German Institute for Refractories and Ceramics, Deutsches Institut für Feuerfest und Keramik: [Online]. Available: https://www.difk.de/de/unsere-leistungen-in-der-kategorie-hochtemperatur-untersuchungen

[293] Concrete column after a fire accident in practice: [Online]. Available: https://www.sandberg.co.uk/site/inspection/fire-damaged-concrete/

Appendix

The appendix consists of two parts, part A.1 for the tables and figure of chapter 2 and part A.2 for all other chapters.

Appendix A.1

Table A.1.1. Test standards for the evaluation of concrete's thermal and mechanical properties at different temperatures discussed in section 2.1.7

Property		Temperature range	Test Standards
Thermal properties	Thermal conductivity	Ambient temperature to 85 °C	ISO 8302, ASTM C177, ASTM C1363
		Elevated temperatures (up to 1000 °C)	ISO 22007-2
	Specific heat	Ambient temperature to 600 °C	ISO 11357, ASTM E1269
		Elevated temperatures (up to 1000 °C)	ISO 22007-2
	Thermal expansion	Ambient to elevated temperatures (up to 1000 °C)	ISO 11359-2 ASTM E831
	Mass loss	Ambient to elevated temperatures (up to 1000 °C)	ISO 11358382 ASTM E1131
Mechanical properties	Compressive strength	Ambient temperature	DIN EN 12390–3 ASTM C39
		Elevated temperatures (up to 750 °C)	RILEM 200-HTC
	Tensile strength	Ambient temperature	DIN EN 12390–6, ASTM C78, ASTM C1583, ASTM C496
		Elevated temperatures (up to 750 °C)	RILEM 200-HTC

Table A.1.2 Composition and specifications of the specimens used for the investigations discussed in section 2.2.2.1

Type, shape and dimensions	Slag sand content of the cement (%)	w/c ratio	Aggregate type	a/c ratio	Curing time and conditions	Reference
Prismatic mortar specimens 40 × 40 × 160 mm	CEM III/A (45)	0.5	siliceous standard sand aggregates (TS EN196-1)	3	28 days in water + 28 days in air	Andiç-Çakır et al. [183]
Cylindrical concrete or mortar: d = 40 mm and h = 80 mm	CEM III/A (not specified)	0.5	Concrete: No aggregates Mortars: Sand (0/4 mm)	Concrete: No Aggregates Mortars: 1.775	20 °C, 100 % RH for 90 days + 25 °C and 55 % RH for 2 weeks	Zemri and Bachir Bouiadjra [184]
Cubic concrete specimens 150 × 150 × 150 mm and cylindrical concrete specimens d =100 mm and h = 200 mm	CEM III/A (53)	0.3	Quartz sand (0/2 mm)+ river bed gravel or crushed basalt (2/8 and 8/16 mm)	1.5	20 °C and 50 % RH (covered) for 7 days	Hager et al. [185]
Cylindrical hardened cement paste (concrete) d = 20 mm, h = 40 mm	0, 5 , 10 , 20 , 50 , 80 , 100	0.23 0.47 0.71	-	-	>70 % RH + storage at 23 °C for 28 days	Wang [187]
Prismatic pumic mortars 40 × 40 ×160 mm	0 , 20 , 40 , 60 , 80	0.7	-	-	20 °C and 90 % RH for 27 days	Aydin [188]
Prismatic mortars 40 × 40 × 160 mm	0 , 20 , 50 , 80	0.64	Siliceous sand	3.86	Curing in plastic waterproof bags at 20 °C for 28 days + drying at 35 °C for 4 days	Delhomme et al. [182]
Cylindrical hardened cement paste (concrete) d = 100 mm, h = 200 mm	0 , 20 , 40	0.48	Not available	3.65	Moisture curing at 22 °C and 99 % RH for 24 h + curing in lime-saturated water for 28 days + drying at 80 °C	Sim et al. [189]

Type, shape and dimensions	Slag sand content of the cement (%)	w/c ratio	Aggregate type	a/c ratio	Curing time and conditions	Reference
Cubic concrete 150 × 150 × 150 mm	0 , 10 , 20	0.54	Siliceous sand + coarse dolmite aggregates	1.8	Curing in water until testing	El Saleem et al. [190]
Cubic concrete specimens 100 × 100 × 100 mm	0, 50, 60, 70	0.55	River sand (0/5 mm) + crushed stone (0/25 mm)	5.6	Curing in lime saturated water (20 °C) for 28 days	Li et al. [191]
Cylindrical concrete specimens d = 100 mm, h = 200 mm	0, 10, 30, 50	0.41	Sea sand (0/5 mm) and crushed stone (0/25 mm)	4.17	Curing in lime saturated water (20 °C) for 28 days	Li et al [192]
Cylindrical concrete specimens d = 150 mm, h = 300 mm	0, 20, 40, 60	0.45	Natural sand (0/4.75 mm) + coarse selicious aggregates (0/10 mm)	3.38	Ambient temperature (27 °C) for 28 or 57 days	Siddique and Kumar [194]
Cylindrical concrete specimens d = 100 mm, h = 200 mm	0 , 35 , 50	Not available	Old basalt sand + old basalt crushed rock (0/14 mm)	Not available	Curing in lime-saturated water bath at 23 °C for 28 days + drying at 23°C and 50 % RH for 60 days	Mendens et al. [193]

w/c ratio: water to cement ratio, a/c ratio: aggregate to cement ratio

Table A.1.3 Composition and specifications of the specimens used for the investigations discussed in section 2.2.2.2

Type, shape and dimensions	Cement	w/c ratio	Aggregate type	a/c ratio	Curing time and conditions	Reference
Cubic concrete specimens 150 × 150 × 150 mm	OPC	0.45	Fine sand and slag sand (20 %, 40 % or 60 %)+ coarse aggregates not specified (0/20 mm)	4.1	Not specified	Vaidya et al. [198]
Concrete specimens, shape and dimensions not specified	OPC	0.48	River aggregates as coarse (3/7mm) and fine (0/3 mm) aggregates, non-ground granulated BFS, bottom ash or a mixture thereof for the partial substitution of the fine aggregates	5.3	Not specified	Yüksel et al. [199]
Concrete specimens, shape and dimensions not specified	OPC	0.45	River sand (0/4.75 mm) + river aggregates (0/20 mm), BFS for partial substitution of the coarse aggregates (20, 40 or 60 %)	4.1	Not specified	Vaidya et al. [200]

w/c ratio: water to cement ratio, a/c ratio: aggregate to cement ratio

Table A.1.4 Composition and specifications of the specimens used for the investigations discussed in section 2.2.3

Type, shape and dimensions	Cement	w/c ratio	Aggregate type	a/c ratio	Curing time and conditions	Reference
Cubic concrete specimens 100 × 100 × 100 mm	CEM I or calcium aluminum cement	0.45	Silico-calcareous or steel slag aggregates (0/2 mm, 2-4 mm and 6-12 mm)	6.5	28 days in water at 20 °C	Buquera et al [238].
Cylindrical mortar specimens d = 100 mm, h = 200 mm	OPC	0.6	Natural siliceous sand (0/1.18 mm) partially replaced ferronickel slag (0/4.75 mm) aggregates (25, 50, 75 or 100 %)	2.8	Storage at room temperature for 28 days + oven dried at 105 °C for 24 h	Saha et al. [239]

w/c ratio: water to cement ratio, a/c ratio: aggregate to cement ratio

Table A.1.5. Composition and specifications of the specimens used for the investigations discussed in section 2.2.4

Type, shape and dimensions	Cement	w/c ratio	Aggregate type	a/c ratio	Curing time and conditions	Reference
Cylindrical concrete specimens d = 150 mm, h = 300 mm	CEM I or CEM II/A-LL	0.55	Gravel aggregates containing carbonate (57 %) and siliceous (38 %)	Not available	Curing in water or highly humid climate (20 °C, RH > 95 %) + Storage at 23 °C und 50 % RH for 90 days	Klingsch et al. [247]
Cubic concrete specimens 100 × 100 × 100 mm Cylindrical concrete specimens A = 100 mm, h = 200 mm	OPC partially substituted by limestone (0, 10, 15, 20 or 25 %)	0.46	Silico-calcareous or steel slag aggregates (0/4.75 mm and 0/20 mm)	4.65	14 days in water + 14 days in air at 20 °C	Adel Mohammed et al. [248]
Rectangular cubic concrete specimens 100 × 100 × 200 mm	OPC, either partially substituted by limestone, or with the addition of limestone (10 or 15 %)	0.4	Natural siliceous sand + pink limestone	4.4	Storage at 20 °C for 27 days + oven dried at 105 °C for 24 h	El-Kurdi et al. [249]
Prismatic self-conditioning micro-concrete specimens 5 × 5 × 25 mm	OPC, partially substituted by limestone (10, 20 or 30 %)	0.5	Natural sand (0/1 mm)	Not available	Storage at 100 % RH for 24 h + curing in water for 28 days	Uygunoglu et al. [250]
Cylindrical concrete specimens d = 150 mm, h = 300 mm	OPC	0.55	Fine aggregates not specified (0/5 mm) + granite, quartzite or limestone coarse aggregates (5/25 mm)	4.94	Not available	Tofail et al. [253]

w/c ratio: water to cement ratio, a/c ratio: aggregate to cement ratio

Appendix A.2

Table A.2.1. Physical properties of the cements used for concrete production [266]

Parameter		Unit	CEM I 42.5 R	CEM II/B-S 42.5 N	CEM III/A 42.5 N	CEM III/A (Slag 2)	CEM III/A (Slag 3)
Glass content			-	-	-	99.4	99.7
Slag sand content		% (W/W)	0	29	52	-	-
Density		g/cm³				2.928	2.921
Fineness		cm²/g				4290	4100
Grain size distribution (RRSB)	n	-				0.99	0.99
	d‘	µm				15.8	15.3

Results obtained by FEhS-Research Institute for Construction Materials.

Table A.2.2. Chemical analysis of the cements used in the current work [266]

Parameter	Unit	CEM I 42.5 R	CEM II/B-S 42.5 N	CEM III/A 42.5 N	Clinker	CEM III/A (Slag 2)	CEM III/A (Slag 3)
LOI (CO_2+H_2O)	% (w/w)	2.31	2.13	1.02	0.24	0.12	0.12
IR		0.75	0.61	0.23	0.15	0.14	n.d.
Al_2O_3		5.46	7.18	8.23	5.16	10.7	15.1
CaO		63.3	57.3	51.5	66.2	43.1	38.8
f_{CaO}		0.47	0.31	0.44	0.64	n.d.	n.d.
SiO_2		19.7	24.5	26.8	22.1	36.5	33.3
FeO		n.d.	n.d.	n.d.	n.d.	0.78	0.35
Fe_2O_3		2.11	1.78	1.41	2.34	n.d.	n.d.
MgO		1.39	2.94	4.32	1.03	6.85	9.61
Na_2O		0.15	0.16	0.19	0.20	0.26	0.44
K_2O		0.89	0.72	0.69	0.74	0.60	0.59
TiO_2		<0.20	<0.20	<0.20	0.26	0.54	1.33
SO_3		3.19	3.06	3.11	1.02	0.06	0.17
S^{2-}		n.d.	n.d.	n.d.	n.d.	0.79	1.06
Cl^-		0.077	0.084	0.088	n.d.	0.02	0.011
CO_2		1.60	0.99	0.47	0.07	0.11	0.10
H_2O					0.17	0.01	<0.03

LOI: Loss on ignition, IR: Insoluble residue, n.d.: not determined

Results obtained by FEhS-Research Institute for Construction Materials.

Table A.2.3. Initial density of the prismatic specimens used for the measurement of the residual compressive strength (and mass loss)

a) Initial density of the specimens used to investigate the effect of slag sand content of the cement and type of the natural aggregates				
Aggregate	CEM I	CEM II/B-S	CEM III/A	Unit
Basalt	2.353	2.342	2.356	[kg/dm^3]
Quartz	2.183	2.182	2.190	
Slag	2.100	2.107	2.071	
Quartz/BFS	2.055	2.023	2.024	
Slag sand/Basalt	2.186	2.141	2.177	
b) Initial density of the specimens used to investigate the effect of slag sand and limestone in the cement and as added aggregates				
Aggregate	CEM I	CEM II/A-LL	CEM III/B	Unit
Quartz	2.153	2.109	2.110	[kg/dm^3]
Slag	-	-	2.06	
Limestone/ Quartz	-	2.124	-	
c) Initial density of the specimens used for the measurement of the maximum evaporable water				
Aggregate	CEM I	CEM II/A-LL	CEM III/B	Unit
Quartz	2.135	2.032	2.068	[kg/dm^3]
Basalt	-	-	2.137	
Slag	-	-	2.365	

Table A.2.4. Initial density of the cylindrical specimens

a) Initial density of the specimens with industrial cements used to investigate the effect of slag sand content of the cement and type of the natural aggregates				
Aggregate	CEM I	CEM II/B-S	CEM III/A	Unit
Basalt	2.304	-	2.321	[kg/dm^3]
Quartz	2.183	-	2.178	
Slag	2.100	-	2.193	
b) Initial density of the specimens prepared with laboratory mixed cements used to investigate the effect of slag sand from different sources				
Aggregate	CEM III/A	CEM III/A (slag 2)	CEM III/A (slag 3)	Unit
Basalt	2.321	-	2.290	[kg/dm^3]
Slag	2.193	-	2.178	
c) Initial density of the specimens used to investigate the effect of non-standard aggregates				
Aggregate	CEM I	CEM II/B-S	CEM III/A	Unit
Ef-Slag 1	2.881	-	2.906	[kg/dm^3]
Ef-Slag 2	2.853	-	2.840	
LD-Slag	2.810	-	2.687	
Cu-Slag	2.866	-	2.853	

Table A.2.5. Composition of the concretes used for the investigation of the influence of aggregate largest grain size upon the residual compressive strength following exposure to thermal stress

Composition		Quartz 0/2 mm	Quartz 0/4 mm	Quartz 0/8 mm	Quartz 0/16 mm	Basalt 0/2 mm	Basalt 0/4 mm	Basalt 0/8 mm
Water/cement	[-]	0.52	0.52	0.52	0.52	0.52	0.52	0.52
Wasser	[l/m³]	286	286	286	286	286	286	286
Cement CEM II/B-S 42.5 N	[kg/m³]	550	550	550	550	550	550	550
Quartz 0/2 mm		1337.0	865.1	699.3	480.0	-	-	-
Quartz 2/4 mm		-	472.0	-	-	-	-	-
Quartz 2/8 mm		-	-	637.8	435.9	-	-	-
Quartz 8/16 mm		-	-	-	421.2	-	-	-
Basalt 0/2 mm		-	-	-	-	1515.3	1417.2	1094.6
Basalt 2/4 mm		-	-	-	-	-	98.0	-
Basalt 2/5 mm		-	-	-	-	-	-	97.0
Basalt 5/8 mm		-	-	-	-	-	-	324.3
Cold compressive strength	[MPa]	61.4	63.0	61.3	58.2	69.0	73.6	71.7
Cold flexural strength		5.6	8.9	8.2	7.7	9.7	9.4	8.6

Kurzfassung

Der Bausektor ist einer der Hauptverursacher der weltweiten CO2-Emissionen. Um die Klimaziele der EU zu unterstützen, ist die Entwicklung nachhaltiger Betone mit verbesserter Dauerhaftigkeit und reduziertem CO_2-Fußabdruck unerlässlich. Diese Dissertation untersucht die Verwendung von Nebenprodukten aus industriellen Hochtemperaturprozessen, hauptsächlich Hochofenschlacke (BFS) und Hüttensand (slag sand), zur Herstellung von stabilen, thermisch beständigen und nachhaltigen Betonalternativen. Der Schwerpunkt der Studie lag auf der Verbesserung der Dauerhaftigkeit von Beton während und nach einmaliger oder wiederholter thermischer Beanspruchung.

Die Wirkung von Hüttensand als zusätzliches zementartiges Material wurde durch den Vergleich der Heiß- und Restdruckfestigkeit von Betonen untersucht, die mit CEM III/A, CEM III/B sowie herkömmlichem Portlandzement (CEM I) hergestellt wurden und verschiedenen thermischen Belastungen (unterschiedliche Anzahl von Zyklen mit verschiedenen Maximaltemperaturen) ausgesetzt waren. Zudem wurden diese Ergebnisse mit einem kalksteinbasierten Zement (CEM II/A-LL) verglichen. Darüber hinaus wurde die Leistung von BFS, Hüttensand und anderen nicht standardisierten metallurgischen Schlacken als Gesteinskörnung mit konventionellen Gesteinskörnungen wie Quarzit, Basalt und Kalkstein verglichen.

Basierend auf über 1800 experimentellen Datenpunkten konnten BFS und Hüttensand die Restdruckfestigkeit von Beton signifikant verbessern. Während Hüttensand die Druckfestigkeit bei hohen Temperaturen leicht reduzierte, erhöhte er die Restfestigkeit deutlich - insbesondere nach Abkühlung und anschließender Lagerung unter feuchten Bedingungen. Ein höherer Hüttensandanteil im Zement korrelierte mit verbesserten mechanischen Eigenschaften nach thermischer Beanspruchung. Die Modellierung des Temperaturprofils einer 30 cm dicken Wand zeigte, dass Schlacken- und Basaltzuschläge die Innentemperaturen während der Aufheiz- und Abkühlphasen signifikant stärker reduzierten als Quarzit. Die verringerte Wärmeleitfähigkeit und die geringeren thermischen Spannungen führten zu einer höheren geschätzten Resttragfähigkeit, mit leichten Vorteilen für Schlacke gegenüber Basalt während der Abkühlphase. Betone aus schlackenreichen Zementen (CEM III/A) in Kombination mit BFS-Gesteinskörnungen zeigten die besten Resttragfähigkeiten, was die Bedeutung der Zement-Gesteinskörnung-Wechselwirkung unterstreicht. Erste Versuche mit anderen Industrieschlacken zeigten ebenfalls vielversprechende Ergebnisse und weisen auf ein hohes Forschungspotenzial hin. Diese Arbeit liefert ein solides Bewertungsmodell sowie praxisorientierte Ansätze zur Entwicklung langlebiger, thermisch stabiler und umweltfreundlicher Betonlösungen.

Selbstständigkeitserklärung

Hiermit erkläre ich, dass ich die von mir eingereichte Dissertation selbstständig verfasst und keine anderen als die angegebenen Quellen und Hilfsmittel benutzt sowie Stellen der Dissertation, die anderen Werken dem Wortlaut oder Sinn nach entnommen wurden, in jedem Fall unter Angabe der Quelle als Entlehnung kenntlich gemacht habe.

Ein Teil der Ergebnisse dieser Dissertation wurde im Rahmen des von der Arbeitsgemeinschaft industrieller Forschungsvereinigungen e.V. (AiF) und der Organisation "Industrielle Gemeinschaftsforschung (IGF)" des Bundesministeriums für Wirtschaft und Klimaschutz (BMWK) geförderten Forschungsvorhabens Nr. 20318N erarbeitet.

Wuppertal, den 09.04.2025

(Ahmad Iravani)

EINVERSTÄNDNISERKLÄRUNG

Hiermit erkläre ich mich damit einverstanden, dass meine Dissertation wissenschaftlich interessierten Personen oder Institutionen und im Rahmen von externen Qualitätssicherungsmaßnahmen des Studienganges zur Einsichtnahme zur Verfügung gestellt werden kann. Korrektur- oder Bewertungshinweise in meiner Arbeit dürfen nicht zitiert werden.

Wuppertal, den 09.04.2025

(Ahmad Iravani)

Lebenslauf Ahmad Iravani

Persönliche Angaben:

geboren	9. April 1981, Esfahan, Iran
Nationalität	iranisch - deutsch
Familienstand	verheiratet

Studium und Fortbildung:

1995 - 1999	Gymnasium, Vertiefung: Mathematik und Physik, Technischen Universität Isfahan, Iran. Abschluss: Abitur
2000 - 2004	Studium Maschinenbau, Vertiefung: Wärme- und Strömungstechnik, Technischen Universität Shahrekord, Iran. Abschluss: Bachelor of Science
2011 - 2015	Studium Bauingenieurwesen, Vertiefung: Konstruktiver Ingenieurbau, Bergische Universität Wuppertal, Deutschland. Abschluss: Master of Science
2015 - 2025	Promotionsstudent, Bergische Universität Wuppertal, Deutschland.

Berufserfahrungen:

2004 - 2010	Maschinenbau-Ingenieur, Planung, Fertigung, Einbau und Überwachung der Anlagen für Zement- und Stahlwerke, Teif Sepahan EPC-Unternehmen, Esfahan, Iran.
2015 - 2021	Wissenschaftlicher Mitarbeiter Lehrstuhl Werkstoffe im Bauwesen, Fakultät Architektur und Bauingenieurwesen, Bergische Universität Wuppertal, Deutschland.
2022 - jetzt	Leiter Technik und Normung, Geschäftsführer, Bundesverband Leichtbeton e. V., Neuwied, Deutschland.

Curriculum vitae Ahmad Iravani

Personal details:

Date and place of birth	9. April 1981, Esfahan, Iran
Nationality	Iranian - German
Marital status	married

Studies and education:

1995 - 1999	Highschool, in mathematics and physics, Isfahan University of Technology, Iran. Degree: Secondary school certificate
2000 - 2004	Student mechanical engineering, in thermal and fluid mechanics, Shahrekord University of Technology, Iran. Degree: Bachelor of Science
2011 - 2015	Student Civil Engineering, in Structural Engineering, Bergische University of Wuppertal, Germany. Degree: Master of Science
2015 - 2025	PhD-student, Bergische University of Wuppertal, Germany.

Work experience:

2004 - 2010	Mechanical engineer, Planning, manufacturing, installation and supervision of equipment for cement and steel plants, Teif Sepahan EPC Company, Esfahan, Iran.
2015 - 2021	Research and teaching assistant Chair of Materials in Civil Engineering, Faculty of Architecture and Civil Engine, Bergische University of Wuppertal, Germany.
2022 - now	Technical Director, Bundesverband Leichtbeton e. V., Neuwied, Germany.